

**University of Alberta**

**Diagenesis, Burial history, and Reservoir Characterization of the Scollard  
sequence sandstones in Alberta**

by

Ahmed Khidir

A thesis submitted to the Faculty of Graduate Studies and Research  
in partial fulfillment of the requirements for the degree of

Doctor of Philosophy

Department of Earth and Atmospheric Sciences

Ahmed Khidir

Fall 2010

Edmonton, Alberta

Permission is hereby granted to the University of Alberta Libraries to reproduce single copies of this thesis and to lend or sell such copies for private, scholarly or scientific research purposes only. Where the thesis is converted to, or otherwise made available in digital form, the University of Alberta will advise potential users of the thesis of these terms.

The author reserves all other publication and other rights in association with the copyright in the thesis and, except as herein before provided, neither the thesis nor any substantial portion thereof may be printed or otherwise reproduced in any material form whatsoever without the author's prior written permission.

## **Examining Committee**

Octavian Catuneanu, Earth & Atmospheric Sciences

Karlis Muehlenbachs, Earth & Atmospheric Sciences

Jack Lereko, Earth & Atmospheric Sciences

Arie Croitoru, Earth & Atmospheric Sciences

Pamela Willoughby, Anthropology

Kari Strand, University of Oulu Thule Institute

**To my parents:**

**Hadla and Khalaf**

**Thank you very much for help and support**

**I love you both**

## **ABSTRACT**

A detailed laboratory study of sandstone samples from outcrops and conventional core samples from the Maastrichtian-Paleocene Scollard-age fluvial strata in the Western Canada foredeep was undertaken to investigate the reservoir characteristics, burial depth history, and sandstone diagenesis.

The sandstones are predominantly litharenites and sublitharenites, which accumulated in a variety of fluvial environments. The porosity of the sandstones is both syn-depositional and diagenetic in origin. The potential of a sandstone to serve as a reservoir for producible hydrocarbons is strongly related to the sandstone's diagenetic history.

Detailed study of the distribution of authigenic minerals of the Scollard sequence suggests that the diversities in the pattern distribution of authigenic clay minerals in the regions are not random but they coincide with the burial depth of these strata and has a well-defined relation to the sequence stratigraphic framework. The general absence of dickite, coupled with limited conversion of smectite into illite in the Scollard sandstones, suggests crystallization at a depth less than 1.5 km. In contrast, the occurrence of blocky dickite, fibrous illite and chlorite in the Coalspur and Willow Creek sandstones, coupled with albitized feldspars and quartz cement, suggests that sandstones there underwent a maximum burial depth greater than 3 km.

It has been observed that kaolin mineral content increases in sandstones lying below subaerial unconformities, which mark the most significant stratigraphic hiatuses and hence the sequence boundaries in fully fluvial successions.



This study demonstrates the effects of burial depth and paleoclimate on pore-water chemistry, which in turn, influenced the mineralogy and the distributions of authigenic minerals in the sandstones. The  $\delta^{13}\text{C}$  and  $\delta^{18}\text{O}$  compositions of pedogenic carbonate nodules from the Willow Creek Formation associated with the red shale host sediments have been used as a paleoclimate and paleoenvironmental proxy. The isotopic composition of nodules suggests that these formed during drier conditions when C3 vegetation prevailed at the site. The predominance of smectite and illite in fines and the poor floral content point to a low seasonal rainfall in a semi-arid climatic environment.

## **ACKNOWLEDGEMENTS**

I wish to acknowledge all those who helped throughout the course of this study. I thank my supervisor, Dr. Octavian Catuneanu, for his constant support and for shaping my thinking through many discussions. Dr. Catuneanu provided an excellent research environment that significantly improved the quality of my project and also provided a research assistantship during my study and enabling me to finish my thesis and to attend several memorable conferences and field trips. I also thank the other members of my Supervisory Committee Dr. K. Muehlenbachs and Dr. John Lerbekmo for their suggestions about earlier drafts of this thesis. Also, I thank my external examiner,

I thank Dr. K. Muehlenbachs and Dr. N. Banerjee for their assistance with the isotope work and its interpretation, as well as for providing insight into specific questions. Dr. A. R. Sweet from the Geological Survey of Canada also provided many hours of stimulating discussion during the course of this thesis. I thank Hugh Lavalley and Linda Shanks from Encana for their assistance with the earlier drafts of this thesis.

The technical staffs of the Department of Earth and Atmospheric Sciences at the University of Alberta were of great help in completion of this study. G. Braybrook assisted me with the SEM and XRD analyses, and Don Resultay and Mark Labbe helped me to make thin sections. The teaching assistantships provided by the Department of Earth and Atmospheric Sciences, University of Alberta, are also greatly appreciated.

I am grateful to my fellow graduate students for many stimulating and perceptive conversations pertaining to the problems I encountered during the course of this study.

Most of all, I thank my family for its great and enduring support. I thank my wife Nahla without whom I would never have been successful. Nahla, your support is especially unforgettable.

## Table of Contents

Chapter	page
1. INTRODUCTION.....	1
REFERENCES.....	8
2. Reservoir Characterization of Scollard-age Fluvial Sandstones, Alberta foredeep	
INTRODUCTION.....	11
GEOLOGICAL BACKGROUND.....	13
METHODS .....	15
SANDSTONE COMPOSITION AND TEXTURE.....	16
AETHIGENIC MINERALS.....	17
POROSITY OF OUTCROP SAMPLES.....	19
Porosity of the Scollard Sandstones.....	19
Porosity of the Coalspur Sandstones .....	20
Porosity of the Willow Creek Sandstones .....	20
PERMEABILITY IN OUTCROP VERSUS SUBSURFACE.....	21
DIAGENETIC STAGES OF THE SCOLLARD SEQUENCE.....	22
RESERVOIR QUALITY OF THE SCOLLARD SEQUENCE... ..	22
DISCUSSION.....	23
Factors Controlling Reservoir Quality.....	23
Diagenetic Processes and Sandstone Properties.....	24
The Role of Compaction.....	25

Calcite Cementation and Reservoir Properties.....	27
The Role of Clay Minerals .....	28
CONCLUSIONS.....	30
REFERENCES.....	47
3. Basin-scale Distribution of Authigenic Clay Minerals in the Late Maastrichtian - Early Paleocene Fluvial Strata of the Alberta Foredeep: Implications for Burial Depth	
INTRODUCTION .....	53
GEOLOGICAL BACKGROUND .....	54
METHODS.....	56
SANDSTONE COMPOSITION.....	57
AUTHIGENIC MINERALS.....	58
Kaolin.....	58
Dickite.....	59
Smectite.....	60
Illite.....	60
Chlorite.....	61
DISCUSSION: Authigenic Minerals and Maximum Burial Depths.....	62
Kaolinite-dickite transformation.....	62
Illite.....	63
Chlorite.....	64
Quartz overgrowth .....	64

Albitization of feldspar.....	65
SUMMARY OF DISCUSSION .....	66
CONCLUSIONS.....	66
REFERENCES.....	94
4. Predictive diagenetic clay-mineral distribution in siliciclastic rocks as a tool for identifying sequence boundaries in nonmarine successions: the Coalspur Formation, west-central Alberta	
INTRODUCTION .....	106
GEOLOGICAL BACKGROUND .....	107
NONMARINE SEQUENCE STRATIGRAPHY.....	109
METHODS.....	110
RESULTS.....	111
Sandstone petrography.....	111
Authigenic mineral distribution.....	112
Porosity development below the subaerial unconformities.....	113
DISCUSSION.....	114
Position of the sequence boundaries the studied section.....	114
Diagenetic alteration associated with the sequence boundary...	114
Climate control on diagenesis associated with the subaerial unconformity.....	115

Evolution of reservoir quality in the sandstones.....	116
CONCLUSIONS.....	118
REFERENCES.....	126
5. Diagenesis of the Cretaceous-Tertiary Willow Creek Sandstones, Southwestern Region of Alberta	
INTRODUCTION .....	134
GEOLOGICAL BACKGROUND .....	135
TECTONIC AND BURIAL HISTORY.....	136
METHODS.....	137
DETRITAL COMPOSITION.....	138
CLAY MINERALS.....	139
Smectite.....	140
Source of smectite.....	140
Kaolin .....	140
Source of kaolinite.....	141
Illite .....	141
Source of illite .....	142
Chlorite .....	142
Source of Chlorite.....	142
QUARTZ CEMENT.....	143

Source of Quartz Cement.....	143
CALCITE CEMENT.....	144
Source of Calcite Cement.....	144
Isotope Geochemistry of Calcite Cement.....	144
POROSITY AND PERMEABILITY OF THE WILLW CREEK SANDSTONES.....	145
DISCUSSION.....	146
Diagenetic Sequence.....	146
<i>Eodiagenesis</i> .....	147
<i>Mesodiagenesis</i> .....	148
<i>Telodiagenesis</i> .....	151
Diagenetic Control on Reservoir Properties....	151
CONCLUSIONS.....	154
REFERENCES.....	169

5. Petrography and diagenesis of the Paleocene Coalspur sandstones in west-central Alberta: implications for the reservoir properties of fluvial facies

INTRODUCTION .....	183
GEOLOGICAL BACKGROUND .....	184
DATA BASE AND METHODOLOGY.....	185



6. THIN SECTION PETROGRAPHY OF THE UPPET COALSPUR SANDSTONES.....	186
Rock Fragments.....	186
Monocrystalline Quartz .....	187
Feldspar.....	188
AUTHIGENIC MINERALS.....	188
Calcite.....	188
Source of Calcite.....	189
CLAY MINERALS.....	189
Chlorite.....	190
Source of Chlorite.....	190
Chlorite/Smectite(C-S).....	191
Source of Chlorite/Smectite.....	192
Smectite.....	192
Source of Smectite.....	192
Kaolinite and dickite.....	193
Source of Kaolinite .....	193
Illite.....	194
Source of Illite.....	195
QUARTZ.....	195
Influence of grain-coating on silica cement development...	195

Sources of quartz cement.....	196
POROSITY OF THE UPPER COALSPUR SANDSTONES.....	197
STABLE ISOTOPES.....	197
DISCUSSION.....	198
The petrographic composition of sandstones.....	198
Distribution of Authigenic Minerals.....	199
Climatic influence on authigenic clay mineral distribution..	199
Diagenetic Sequence.....	200
Reservoir Heterogeneity.....	201
CONCLUSIONS.....	202
REFERENCES.....	220
7- Concluding remarks.....	232

### List of Tables

Table	Page
2-1 Porosity, permeability (mD), calcite cement .....	45
2-2 Porosity, permeability (mD), calcite cement .....	46
5-1 Detrital mineralogy of the Willow Creek .....	166
5-2 Oxygen and carbon isotopic.....	167
5-3 Porosity and permeability of selected Willow Creek.....	168
6-1 Well location, sample top and sample base .....	218
6-2 Oxygen and carbon isotopic.....	219

## List of Figures

Figure	Page
1-1	Outcrop distribution of the Scollard sequence ..... 6
1-2	Generalized chart of the late Maastrichtian-Paleocene stratigraphy..... 7
2-1	Outcrop distribution of the Scollard ..... 32
2-2	Generalized chart of the late Maastrichtian-Paleocene stratigraphy..... 33
2-3	Classification of the Scollard.... 34
2-4	Thin-section photomicrographs ..... 35
2-5	SEM photomicrographs: (A) – authigenic smectite formed ..... 36
2-6	SEM photomicrographs: (A) – authigenic chlorite, dickite ..... 37
2-7	Thin-section photomicrographs ..... 38
2-8	Contour map showing ..... 39
2-9	Scanning electronic photomicrographs ..... 40
2-10	Photomicrograph of thin section slide ..... 41
2-11	Thin-section photomicrographs..... 42
2-12	Plot showing sandstone grain size ..... 43
2-13	Plot showing sandstone permeability ..... 44
3-1	Outcrop distribution of the Scollard and Coalspur formations ..... 68
3-2	Generalized chart of the late Maastrichtian-Paleocene ..... 69
3-3	Facies types used to describe the sedimentological characteristics ..... 70
3-4	Vertical profile for the Knudsen’s ..... 71
3-5	Vertical profile for the Buffalo Jump Provincial Park locality ..... 72
3-6	Vertical profile for the Ardley locality, upper Scollard Formation ..... 73
3-7	Vertical profile for the Griffith’s Farm locality, lower Scollard. .. 74
3-8	Vertical profile for the Kneehills Creek locality, lower Scollard ..... 75
3-9	Vertical profile for the Hummer Hills locality, lower Scollard ..... 76
3-10	Vertical profile for the Bow River locality, upper Scollard..... 77
3-11	Vertical profile for the Bow River locality, upper Scollard... . 78
3-12	Vertical profile for the Red Deer River Valley section ..... 79
3-13	Vertical profile for the Red Deer River Valley section ..... 80

3-14	Vertical profile for the Coalspur locality, upper Coalspur ..	81
3-15	Vertical profile for the old roadcut near Highway 22.....	82
3-16	Vertical profile for the Oldman River, lower Willow	83
3-17	Vertical profile for the Oldman River Dam Reservoir, lower Willow Creek	84
3-18	Vertical profile for the Oldman River locality, upper .....	85
3-19	Classification of the Scollard, Coalspur, and Willow Creek.....	86
3-20	Authigenic clay mineral association in the Maastrichtian .....	87
3-21	Authigenic clay mineral association in the Paleocene .....	88
3-22	Scanning electronic photomicrographs .....	89
3-23	Scanning electronic photomicrographs .....	90
3-24	Scanning electronic photomicrographs and schematic .....	91
3-25	Contour map of the study area showing the maximum burial .....	92
3-26	Cross-sectional schematic model showing the .....	93
4-1	Outcrop distribution of the Scollard and Coalspur formations .....	120
4-2	Generalized chart of the late Maastrichtian-Paleocene stratigraphy.....	121
4-3	Classification of the upper Coalspur .....	122
4-4	Thin-section photomicrographs .....	123
4-5	SEM photomicrographs: (A) – authigenic .....	124
4-6	Vertical lithologic profile for the.....	125
5-1	Outcrop distribution of the Scollard and Coalspur formations .....	155
5-2	Generalized chart of the late Maastrichtian-Paleocene stratigraphy.....	156
5-3	Vertical profiles for the Oldman River locality.....	157
5-4	Classification of Willow Creek Formation .....	158
5-5	Thin section photomicrographs .....	159
5-6	SEM photomicrograph .....	160
5-7	SEM photomicrographs .....	161
5-8	SEM and thin section photomicrographs.....	162
5-9	Plot showing sandstone permeability .....	163
5-10	Generalized diagenetic sequence for the Willow Creek Formation. ....	164
5-11	SEM and thin section photomicrographs .....	165
6-1	Outcrop distribution of the Scollard and Coalspur formations .....	205

6-2	Generalized chart of the late Maastrichtian-Paleocene .....	206
6-3	Facies types used to describe the sedimentological characteristics .....	207
6-4	Outcrop sketch and vertical profile for the Sundre locality .....	208
6-5	Outcrop sketch and vertical profile for the along Red Deer River .....	209
6-6	Outcrop sketch and vertical profile for the Coal Valley locality .....	210
6-7	Classification of the upper Coalspur Formation sandstones.....	211
6-8	Thin-section photomicrographs .....	212
6-9	Thin-section photomicrographs .....	213
6-10	Thin-section photomicrographs .....	214
6-11	Scanning electronic photomicrographs .....	215
6-12	Scanning electronic photomicrographs .....	216
6-13	Generalized diagenetic sequence.....	217

#### Appendix A

A-1	Latitude and longitude of.....	238
-----	--------------------------------	-----

#### Appendix B

Figure 1	Outcrop distribution of the Willow Creek Formation .....	240
Figure 2	Generalized chart of the late Maastrichtian.....	241
Figure 3	Caliche glaebules from the lower Willow Creek Formation... ..	242
Figure 4	Scanning electronic photomicrographs.....	243
Figure 5	Stratigraphic profile of the lower Willow Creek Formation.....	244

# Chapter 1

## **Introduction**

Late Maastrichtian-Early Paleocene fluvial strata in the Alberta foredeep of the Western Canada Sedimentary Basin are composed of three roughly correlative formations: Scollard, Coalspur, and Willow Creek. The correlation between these formations is based on palynology, fossil mammals and on the position of the Cretaceous-Tertiary boundary (Jerzykiewicz and Sweet, 1988; Sweet et al., 1990). The formations are exposed in a number of areas in Alberta (Fig. 1). In the central Plains region, the Late Maastrichtian - Early Paleocene strata are referred to as the Scollard Formation, which consists of interbedded shale, coaly shale, olive-green mudstone, siltstone, grey-to-buff sandstone, coal, bentonites and tuffs (Gibson, 1977). The Scollard Formation has a well-defined boundary with the Paskapoo Formation above, and the Battle Formation below (Gibson, 1977; Lerbekmo et al., 1990; Dawson et al., 1994; Fig. 2). The thickness of the Scollard Formation in the Red Deer Valley area is about 75 m.

In the central Foothills of Alberta, the Scollard Formation is correlative with the Coalspur Formation. The Coalspur Formation is about 430 m thick and consists of interbedded mudstone, siltstone and fine-to-coarse-grained sandstone (Jerzykiewicz, 1997). At the base of the Coalspur Formation is the Entrance Conglomerate consisting of interbedded conglomerate and sandstone (Jerzykiewicz, 1985b). The Coalspur Formation is overlain by the Paskapoo Formation and overlies the Brazeau Formation (Fig. 2) (Jerzykiewicz and McLean, 1980).

In southwestern Alberta, the Willow Creek Formation is correlative to the Scollard and Coalspur formations and consists of gray, sandy claystones and clayey calcareous sandstones. The Willow Creek Formation is underlain by the St. Mary River Formation and overlain by the Porcupine Hills Formation (Fig. 2). The thickness of the Willow Creek Formation varies from 1006 m close to the axis of the Alberta Syncline (Carrigy, 1971) to about 1375 m on the western limb of the syncline (Tozer, 1956).

The fluvial succession of the Scollard sequence has been the subject of various stratigraphic and coal geology studies, but the work presented in this thesis focuses on aspects that have not previously been addressed. This thesis presents the study of the reservoir properties of the Scollard sequence and diagenetic history of the Coalspur and Willow Creek formations. In addition, this thesis studies in detail the pattern distributions of authigenic minerals as indicator for burial and tectonic history of the strata. This thesis also integrated the diagenesis and sequence stratigraphy in a siliciclastic continental sequence. Additionally, isotope composition of caliche facies from the Willow Creek Formation was used for a paleoclimate and paleoenvironmental study. Composite information has been obtained from thin-section petrography, scanning electronic microscopy, x-ray diffraction, and carbon and oxygen stable isotopes.

The research is presented in six chapters, in a journal publication format. Chapter 2 deals with the reservoir characterization of Scollard-age fluvial sandstones. Basin scale distribution of authigenic clay minerals of the Scollard sequence and their implications for burial depth are discussed in chapter 3. Chapter 4 is study of the

diagenetic clay-mineral distribution in siliciclastic rocks as a tool for identifying sequence boundaries in nonmarine successions. Chapter 5 focuses on the sedimentology and diagenesis of the Willow Creek Sandstones whereas chapter 6 presents the petrography and diagenesis of the Paleocene Coalspur sandstones in west-central Alberta.

Chapters 2, 3, 4, 5, and 6 are independent studies, related to one another by their similar focus. Their similarity stresses the genetic relationship between the Scollard sequences, which are the product of deposition within the same Scollard-age drainage systems. However, chapter 2 investigated reservoir properties (porosity and permeability) of the Scollard-age fluvial sandstones in the Alberta foredeep, and also studied the influence of depositional and post-depositional heterogeneities, such as the variations of authigenic cement and the effect of the aggregate structures of authigenic clay minerals on reservoir quality. Diagenetic processes and their influence on sandstone properties are described as well.

Chapter 3 discusses the variations of authigenic clay mineralogy in the Late Maastrichtian - Early Paleocene successions of the Alberta foredeep across the central Plains and central and southwestern Foothills regions. The objective of this study is to evaluate the origin of authigenic clay minerals, their distribution pattern and diagenetic alteration, and relate the insights of this evaluation to the burial history of the basin.

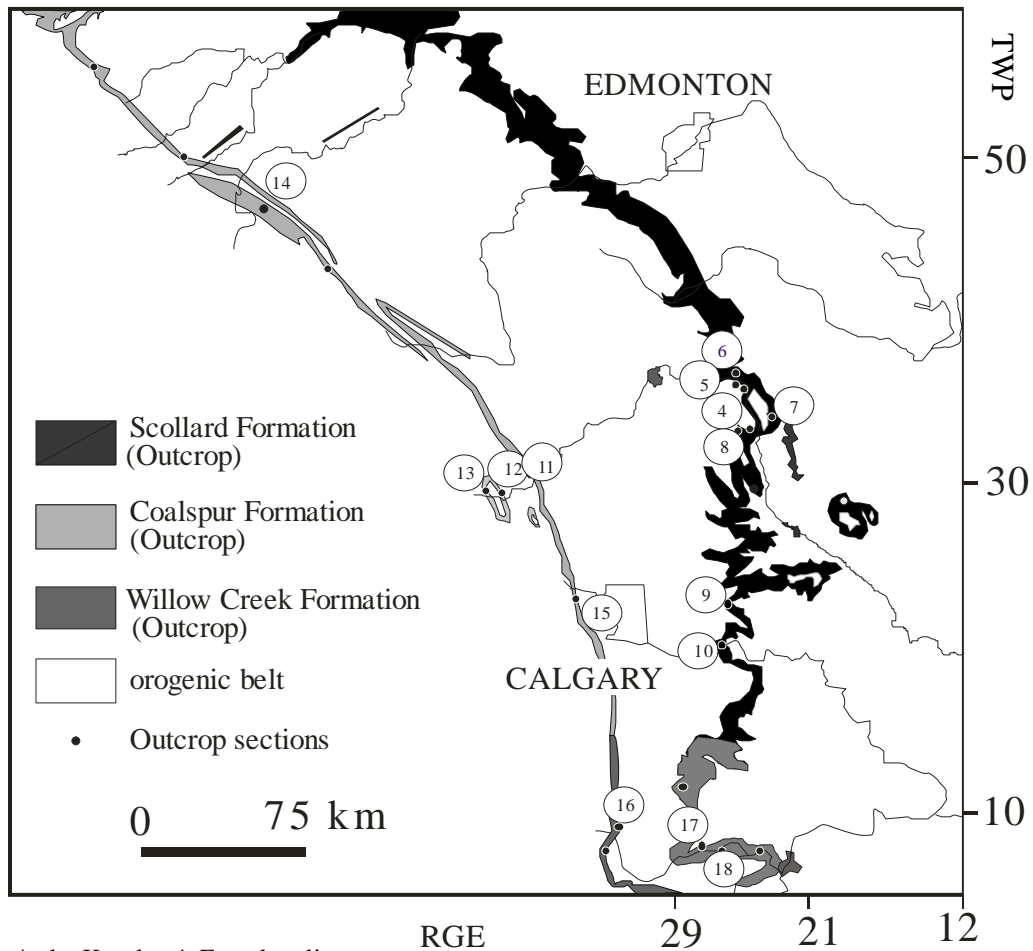
Chapter 4 is a study of authigenic the clay minerals such as kaolinite, dickite, smectite, and non-clay minerals such as quartz overgrowths and calcite cement in sandstones.



These minerals are important from the petroleum geology perspective; they provide a complete picture of diagenetic history, and control reservoir properties such as porosity, permeability and water saturation. The study of this chapter confirms the position of the sequence boundary in the study succession, discusses the role of sequence stratigraphic controls on sandstone diagenesis and, hence, on reservoir properties; and defines a predictive model for the distribution of early diagenetic clay minerals in fluvial sandstones within a sequence stratigraphic framework.

Chapter 5 investigates the diagenetic history of the Willow Creek sandstones and the characteristics of the different diagenetic processes affecting reservoir quality. This chapter suggests that the Willow Creek sandstones in the southern Foothills region of west-central Alberta be classified as sublitharenites and lithic arenites. Three diagenetic stages have been recognized in the Willow Creek sandstones: eodiagenesis, mesodiagenesis, and telodiagenesis. The diagenetic processes that occurred during the progressive burial to various depths, and during uplift, have exerted an important control on reservoir heterogeneity in the predominantly fluvial, upper Cretaceous-lower Tertiary of the Willow Creek sandstones. Generally, the reservoir heterogeneity of the sandstones is attributed to the wide variation in the timing and amounts of calcite cementation, and the illitization and chloritization of the smectite clay coating. The purpose of the present study is to investigate this history of the sandstones and to study the characteristics of the different diagenetic processes affecting reservoir quality. This type of study may be used as analogue for same type of fluvial sandstones in the subsurface reservoir.

Chapter 6 discusses the petrography and diagenesis of the Paleocene Coalspur sandstones in west-central Alberta. This chapter focuses on the upper Coalspur Formation of early Paleocene age. An economically significant amount of high-quality thermal coal associated with floodplain facies occurs within the upper part of the formation (Jerzykiewicz and Mclean, 1980). The upper Coalspur Formation and its coal zones have been described and studied from numerous drillholes, test pits, and other outcrop sections in western Alberta (Kramers and Mellon, 1972; McLean and Jerzykiewicz, 1978; Dawson et al., 1994). To date, however, examinations of the diagenetic history of the sandstones and their reservoir characteristics have received less attention. In this paper we investigate the diagenetic history and reservoir quality of these early Paleocene sandstones of the Coalspur Formation in two main locations, the Red Deer River sections and the Coalspur locality (Fig. 2), through detailed outcrop and laboratory work.



- 4- the Knudsen's Farm locality
- 5- the Buffalo Jump Provincial Park locality
- 6- the Ardley locality
- 7- the Griffith's Farm locality
- 8- the Kneehills Creek locality
- 9- the Hummer Hills locality
- 10- the Bow River locality
- 11- the Sundre locality
- 12- the Red Deer River Valley section1
- 13- the Red Deer River Valley section 2
- 14- the Coalspur locality
- 15- the roadcut near Highway 22
- 16- the Oldman River
- 17- the Oldman River Dam Reservoir
- 18- the Oldman River locality

Figure 1. Outcrop distribution of the Scollard, Coalspur, and Willow Creek formations in Alberta, and the location of the outcrop sections.

Age	Stratigraphic units					
Paleocene	Southern Foothills		Plains		Central Foothills	
	Maastrichtian	Porcupine Hills Formation		Paskapoo Formation		
Willow Creek Formation		upper Willow Creek	Scollard Formation	upper Scollard	Ardley	Val d'Or
Campanian	Lower Willow Creek		lower Scollard		Nevis	Arbour
						Mynheer
						Entrance Member
	St. Mary River Formation		Battle Formation		Brazeau Formation	
			Whitemud Formation			
			Horseshoe Canyon Formation			
	Bearpaw Formation		Bearpaw Formation			
	Belly River Group		Belly River Group			

Figure 2. Generalized chart of the late Campanian to Paleocene stratigraphy of west- central Alberta, showing the position of the Scollard, Coalspur and Willow Creek formations (after Dawson et al., 1994).

## References

Carrigy, M.A. 1971. Lithostratigraphy of the uppermost Cretaceous (Lance) and Paleocene strata of the Alberta plains. Research Council of Alberta Bulletin 27, 161 p.

Dawson, F.M., Evan, C.G., Marsh, R. and Richardson, R. 1994. Uppermost Cretaceous and Tertiary of the Western Canada Sedimentary Basin. In: Geological Atlas of the Western Canada Sedimentary Basin. G. Mossop and I. Shetsen (comps.). Canadian Society of Petroleum Geologists and Alberta Research Council, p. 387-406.

Gibson, D. W. 1977. Upper Cretaceous and Tertiary coal bearing strata in the Drumheller – Ardley region, Red Deer River valley, Alberta. Geological Survey of Canada, Paper 76- 35, p. 1-41.

Jerzykiewicz, T. 1985b. Tectonically deformed pebbles in the Brazeau and Paskapoo Formation, central Alberta Foothills, Canada. *Sedimentary Geology*, v. 42, p. 159-180.

Jerzykiewicz, T. and Mclean, J.R. 1980. Lithostratigraphical and sedimentological framework of coal-bearing Upper Cretaceous and Lower Tertiary strata, Coal Valley area, central Alberta Foothills. Geological Survey of Canada, Paper 79-12, 47 p.

Jerzykiewicz, T. and Sweet, A.R. 1988. Sedimentological and palynological evidence of regional climatic changes in the Campanian to Paleocene sediments of the Rocky Mountain Foothills, Canada. *Sedimentary Geology*, v. 59, p. 29-76.

Jerzykiewicz, T. and McLean, J.R. 1980. Lithostratigraphical and sedimentological framework of coal-bearing Upper Cretaceous and Lower Tertiary strata, Coal Valley area, central Alberta Foothills. Geological Survey of Canada, Paper 79-12, 47 p.

McLean, J.R. and Jerzykiewicz, T. 1978. Cyclicality, tectonics and coal: some aspects of fluvial sedimentology in the Brazeau- Paskapoo Formations. Coal valley area, Alberta, Canada. In: *fluvial Sedimentology*, E. Miall (ed.). Canadian Society of Petroleum Geologists Memoir 5, p. 441-468.

Kramers, J.W. and Mellon, G.B. 1972. Upper Cretaceous-Paleocene coal-bearing strata, northwest central Alberta Plains. In: *Proceedings of the First Geological Conference on Western Canadian Coal*. G.B. Mellon, J.W. Kramers and E.J. Seagel (eds.). Research Council of Alberta, Information Series 60, p. 109-124.

Lerbekmo, J.F., Evans, M.E. and Hoye, G.S. 1990. Magnetostratigraphic evidence bearing on the magnitude of the sub-Paskapoo disconformity in the Scollard Canyon-Ardley area of the Red Deer Valley, Alberta. *Bulletin of Canadian Petroleum Geology*, v. 23, p. 120-124.

Tozer, E.T. 1956. Uppermost Cretaceous and Paleocene nonmarine molluscan faunas of western Alberta. Geological Survey of Canada, Memoir 280, 125 p.

## Chapter 2

*A version of this chapter has been accepted. A. Khidir and O. Catuneanu. 2010. Journal of Marine and Petroleum Geology.*

### **Reservoir characterization of Scollard-age fluvial sandstones, Alberta foredeep**

#### **Introduction**

The predicting of subsurface porosity and permeability is a key challenge for hydrocarbon exploration and development when there is little subsurface data available. Samples from outcrops may provide an important source of data for the study of correlative reservoirs and provide the exploration geoscientists with the opportunity of observing sedimentary structures, lateral facies changes, and three dimensional spatial relationships of correlative subsurface rocks. Outcrop-based samples also help geologists understand the burial history and the role of different diagenetic modification on reservoir properties, which lead to prediction of porosity and permeability of subsurface reservoirs (Tobin, 1997).

The porosity and permeability of reservoir rocks have been shown to depend considerably not only on the sandstones framework mineralogy but also on the authigenic minerals' composition, texture and structure. The presence of authigenic minerals strongly influences and controls sandstone reservoir properties during different stages of diagenetic history (Bjorlykke, 1998). For example, the precipitation of authigenic clay minerals such as pore-lining chlorite and/or illite causes reduction in permeability by



diminishing the size of pore throats hence decreasing reservoir quality (Pittman, 1979). Therefore, the study of authigenic minerals during the different stages of diagenesis can be essential for a precise characterization of reservoir quality.

Despite advantages, the outcrop-based prediction of the subsurface reservoir quality is less direct than those based on the actual subsurface data. Outcrop-exposed sandstones may have undergone a very different tectonic, burial and diagenetic history than their subsurface counterparts (Tobin, 1997). Outcrop weathering may alter the composition and pore system characteristics of reservoir rocks. Therefore, interpretations of reservoir quality from outcrop data present a technical challenge (Tobin, 1997).

The aim of this paper is to examine the reservoir properties (porosity and permeability) of the Scollard-age fluvial sandstones in the Alberta foredeep, and also to study the influence of depositional and post-depositional heterogeneities, such as the variations of authigenic cement and the effect of the aggregate structures of authigenic clay minerals, on reservoir quality. Diagenetic processes and their influence on sandstone properties are described as well. This study shows the importance and limitations of outcrops as a source of data for understanding the characterization of subsurface sandstone reservoirs.

## **Geological Background**

The Scollard sequence consists of nonmarine strata deposited during Late Maastrichtian-Early Paleocene time in the foredeep of the Western Canada Sedimentary Basin. These fluvial strata are composed of three roughly correlative formations: the Scollard, Coalspur, and Willow Creek. Correlation was confirmed with the recognition of the Cretaceous-Tertiary boundary, as well as by palynological studies (e.g., Jerzykiewicz and Sweet, 1988; Sweet et al., 1990).

The upper Maastrichtian-Paleocene strata of the Scollard sequence are exposed in a number of locations in Alberta (Fig. 1). In the central Plains region, the sequence is referred to as the Scollard Formation, which consists of siltstone units interbedded with thin olive-green mudstone beds, thick grey to buff sandstone, and coal. This formation has well-defined boundaries (Fig. 2). The upper contact with the Paskapoo Formation is indicated to be a major unconformity (Lerbekmo et al., 1990). The lower contact is with the lacustrine mudstones of the Battle Formation (Gibson, 1977).

Correlative Foothills strata occur in the Coalspur Formation, which consists of interbedded mudstone, siltstone and fine-grained sandstone, with subordinate coarser-grained sandstone layers and channel lag deposits. The Coalspur Formation is overlain by the Paskapoo Formation and overlies the Brazeau Formation (Fig. 2). The base of the Coalspur Formation, the Entrance Conglomerate, consists of conglomeratic or sandy-conglomeratic units. The contact between the Coalspur and Brazeau formations is usually abrupt and easy to identify in outcrop (Dawson et al., 1994).

Correlative strata in the southern Foothills region, the Willow Creek Formation, consist mainly of soft sandstones, color-banded sandy gray clays, and subordinate clayey calcareous sandstones. The sandstones increase in thickness towards the top of the formation, where the shaly units almost disappear. The St. Mary River Formation underlies the Willow Creek Formation, and the Porcupine Hills Formation overlies it (Fig. 2). The lower contact of the Willow Creek Formation correlates with the sub-Entrance unconformity, and the upper boundary correlates with the sub-Paskapoo unconformity according to Jerzykiewicz (1997).

The first geological examination of the strata now known as the Scollard Formation was by J. B. Tyrrell in 1887 as the upper part of his Edmonton Series (Formation). In 1977, Gibson raised the Scollard member to Formation rank. In 1978, Russell and Singh, on the basis of dinosaur fauna and microflora, concluded that the Cretaceous-Tertiary boundary occurred within the Scollard Formation.

The Coalspur Formation, previously named the “Coalspur beds” by Mackay (1949), was formalized on the basis of its lithologic succession, which consists of interbedded mudstone, siltstone and fine-grained sandstone, with subordinate coarser-grained sandstone layers and channel lag deposits (Jerzykiewicz, 1997).

Early geological studies of the Willow Creek Formation were conducted by Dawson (1883), Williams and Dyer (1930), Hage (1943), Douglas (1950), Tozer (1952), and Carrigy (1971). Dawson (1883) identified the Willow Creek Formation based on its red

coloration. Dawson (1884) also defined the formation on Willow Creek and on the downstream part of the Oldman River. Williams and Dyer (1930) recorded the best exposures on the Oldman River east of Fort Macleod. Douglas (1950) described most of the lower part of the formation. Tozer (1956) described the formation on both sides of the Alberta Syncline. A representative section of the formation on the Crowsnest River near Cowley was described in detail by Jerzykiewicz and Sweet (1986b, 1988) and by Jerzykiewicz (1997).

## **Methods**

A detailed examination of the sandstones from 23 outcrops and 7 cores was carried out by using techniques involving thin sections and a scanning electronic microscope (SEM, JEOL JSM 6400) equipped with an energy-dispersive x-ray analyzer. To verify the modal amount and types of authigenic clay minerals, a grinding technique was used to produce powders free of grains coarser than 20  $\mu\text{m}$ . X-ray diffraction (XRD) was carried out on the bulk samples and on separates finer than 2  $\mu\text{m}$ . The relative abundance of specific clay minerals within the clay fraction was determined using the data obtained on the <2  $\mu\text{m}$  clay fraction. The criteria of Wilson and Pittman (1977) were used to distinguish between detrital and authigenic clay minerals.

The composition and porosity were determined by standard point-count (200 points) analysis after the specimens had been impregnated with blue epoxy resin to highlight their porosity. To quantitatively evaluate the effect of diagenesis on porosity and to determine the effect of cementation on overall sandstone heterogeneity, helium porosity

tests of 53 selected outcrop samples were performed on the same specimens from which the thin sections had been cut (table 1 and table 2). Grain size was estimated to millimeter units, and sorting was estimated by comparison with published sorting comparators (Longiaru, 1987). The permeability of the sandstone samples was measured (Tables 1, 2) by using a Pressure Decay Profile Permeameter. Reservoir variables such as total porosity, mean grain size and cement content were used to estimate reservoir quality.

### **Sandstone Composition and Texture**

The examination of the outcrop-based samples throughout the study area confirms that lithic arenites to sublithic arenites are the dominant sandstone types (Fig. 3).

The essential framework grains, which were used to classify the sandstones in this study, were quartz, feldspar, and rock fragments. The sandstones generally are fine-to-medium grained and well to moderately sorted, according to the definition of Longiaru (1987). The grain shape ranges from subrounded to subangular. The rock samples are also characterized by a general lack of matrix, with an average percentage of 2% (range 0%-4%).

Quartz (mono and polycrystalline) is the dominant framework grain (Fig. 4 A and B) with an average abundance of 45%. Monocrystalline quartz, which is mainly orthoquartzite of sedimentary origin, makes up 25%-70% of the framework grains with an average abundance of 40%, whereas polycrystalline quartz constitutes up to 10%

(average 5%) of the total quartz. About 8% of the quartz grains (mono and polycrystalline) are corroded and replaced by calcite cement (Fig. 4 B).

Rock fragments make up 25%–40% of the framework constituents. Metamorphic, volcanic, and sedimentary rock fragments are present in different percentages. Generally, sedimentary rock fragments such as chert (Fig. 4 B) are more abundant than igneous or metamorphic lithic components (Fig. 4 B and C), probably due to the relative stability of chert when exposed to weathering.

Feldspar makes up about 15% of the framework grains (Fig. 4 D). Ductile grains such as muscovite make up, on the average, about 2% of the framework constituents.

### **Authigenic Minerals**

The proportion of authigenic minerals and their distribution varies within the sandstones. The Scollard sandstones have intermediate-to-abundant smectite and kaolinite followed by smectite/illite (Fig. 5 A, B and C). The Coalspur sandstones have abundant chlorite, smectite, kaolinite, and illite, followed by dickite and chlorite/smectite (Fig. 5 D, E and F), whereas the sandstones of the Willow Creek Formation are dominated by illite, dickite, and smectite, followed by kaolinite, chlorite, and chlorite/smectite (Fig. 6 A and B).

Three major types of cement are present in the sandstones: calcite, hematite and silica (Fig. 7 A, B and C). Calcite, which is the most abundant cement, has an inconsistent

distribution and ranges from 5% to 45% of the rock's entire volume (Fig. 8). The calcite cement has a range of crystal forms, including drusy mosaics in which crystals increase towards the centers of pores, and poikilotopic fabrics, where single large crystals enclose many grains.

Hematite, which occurs as late diagenetic cement formed in the sandstones after burial, is highly variable in abundance, generally averaging 2-7% in outcrop-based samples. No hematite was observed in subsurface core-based samples. Hematite cement also forms as evenly distributed grain coats or a localized batch of drusy coating on the surface of both detrital quartz grains and quartz overgrowths.

Quartz cement in the sandstones occurs mainly as euhedral overgrowths and partly contemporaneous with, and partly prior to, the formation of authigenic clay minerals (Fig. 5 E); moreover, quartz cement is present in amounts ranging from trace to 5% (mean 2%). A relative increase occurs in the amounts of quartz overgrowth in the Coalspur and Willow Creek sandstones, probably due to their higher burial depth. Generally, quartz overgrowths are in the initial stage or absent when the sandstones are extensively cemented by calcite, or when the quartz grains are coated by clay minerals.

Trace to minor amounts of siderite (< 4%) was found in the subsurface core samples as an intergranular cement or partial replacement of detrital grains, especially clay intraclasts.

## **Porosity of Outcrop Samples**

### *Porosity of the Scollard Sandstones*

The porosity is both primary and secondary in origin (Fig. 9 C and D). Secondary porosity may be recognized by using criteria based on petrographic and scanning electronic microscope studies (Schmidt and McDonald, 1979). The point-counted interparticle porosity determined from the thin sections ranges from 1% to 16% and averages 7%. In contrast, conventional, plug-type porosity analysis produced results ranging from 0.2% to 25% and averaging 11.2%. The variation between the point-counted interparticle porosity and conventional, Plug-type porosity analysis is caused by the existence of microporosity in the Scollard sandstones.

The sandstone secondary porosity relates to partial dissolution of soluble constituents (Fig. 9 C); grain moldic porosity produced by the partial dissolution of the feldspar that occurs along the cleavages and twin boundaries of feldspar grains (Fig. 9 D); intra-constituent pores, from the leaching of carbonates and the incomplete replacement of feldspar grains; and the dissolution of intergranular carbonate cement. The fracture porosity in the sandstones is volumetrically insignificant, but can be very effective in increasing the permeability of “tight” sandstones. Most of the secondary porosity is intragranular and was formed by the dissolution of feldspar grains.

The timing of secondary porosity generation is uncertain. The dissolution of unstable detrital grains was most likely a continuous process throughout burial, which led to an increase in secondary porosity. The processes of the dissolution of unstable grains and the



consequent formation of secondary porosity might have started relatively early in diagenesis, shortly after compaction and the formation of clay coatings and rims.

#### *Porosity of the Coalspur Sandstones*

The porosity is both primary and secondary in origin (Fig. 10 E, F, G and H). The secondary porosity includes partial dissolution of soluble constituents (Fig. 10 G); grain moldic porosity produced by the partial dissolution of feldspar along cleavage planes and twin boundaries (Fig. 10 F); corrosion of grains adjacent to pores (Fig. 10 H); and intra-constituent pores, which are generally the result of the incomplete replacement of feldspar grains. Most of the secondary porosity is intergranular and was formed by the dissolution of pore-filling and replacive cements. The porosity determined from thin sections ranges from 1% to 5% and averages 4%. Conventional porosity ranges from 2% to 9% (average 7%).

#### *Porosity of the Willow Creek Sandstones*

The porosity is both primary and secondary in origin (Fig. 11 A and C). The thin section porosity counts range from 2% to 9% and average 5%. Helium porosity ranges from 4% to 11% and averages 9.4%. The solution porosity (secondary porosity) created by the dissolution of calcite cement is considered to account for most of the total volume of secondary sandstone porosity (Fig. 11 A). Moldic porosity due to the dissolution of unstable grains such as feldspar was also observed (Fig. 11 C).

Generally, the porosity of the Scollard sequence sandstones determined by petrographic examination differs significantly from the ‘plug’ laboratory porosity. The frequently much higher plug-sample porosity indicates that the sandstones contain a significant microporosity component, which is not observable in thin sections. Microporosity is most abundant when strata are rich in intergranular and grain-coating clay minerals such as smectite, smectite/chlorite and chlorite. The porosity of both outcrop and core samples is summarized in Tables 1 and 2 respectively. For comparison, the porosity measured in core varies from 3% to 25%, with an average of 17%. This indicates that the reservoir quality tends to be better in the subsurface relative to the outcrop equivalents.

### **Permeability in Outcrop versus Subsurface**

Permeability is one of the dominant controls on fluid flow and solute transport in porous media. The permeability of the Scollard sequence sandstones in outcrop ranges from 0.14 mD to 40 mD and averages 7.8 mD (Table 1; Fig. 12). The permeability of cemented sandstones with less than 5% calcite cement ranges from 1.9 to 8.1 mD (geometric mean = 3 mD). In contrast, sandstones cemented with greater than 5% calcite have a geometric mean permeability of less than 2 mD.

The permeability of the Scollard sequence sandstones measured in core samples ranges from 0.06 mD to 92 mD and averages 40 mD (Table 2). This, once again, indicates that the reservoir quality tends to improve in the subsurface.

### **Diagenetic Stages of the Scollard Sequence**

The study of the diagenetic history of the Scollard sequence was tackled by Khidir and Catuneanu (2009), and it is beyond the scope of this chapter. Based on SEM and thin section photomicrographic observations, three diagenetic stages were recognized: eodiagenesis before effective burial, mesodiagenesis during burial, and telodiagenesis during exposure after burial. These diagenetic stages are adopted from Schmidt and McDonald (1979). Eodiagenesis resulted in mechanical compaction, calcite cementation, kaolinite and smectite formation, and the dissolution of the chemically less stable grains, i.e., feldspar and rock fragments. Mesodiagenesis resulted in chemical compaction, precipitation of calcite cement, quartz overgrowths, chlorite, dickite, and illite formation. Telodiagenesis resulted in kaolinite and mechanically infiltrated smectite formation, and feldspar dissolution.

### **Reservoir Quality of the Scollard Sequence**

Permeability and reservoir quality are a function of how the pore spaces are connected. It also is function of the type and distribution of pores spaces, and the pore and pore throat sizes.

Petrographic and conventional core and outcrop-based sample analysis suggest that the Scollard sequence sandstones are of four types: non-reservoirs, with  $<0.05$  mD; low reservoir quality, with 0.05 to 0.1 mD; moderate to good reservoirs, with 1 to 10 mD; and very good reservoirs, with a permeability in excess of 10 mD. The subsurface data from seven core samples (Table 2) show the sandstones of the Scollard sequence to have a better reservoir quality than their outcrop equivalents (Table 2, Fig. 13). The variation in

the reservoir quality between subsurface core samples and outcrop-based samples is probably due to late sandstone diagenesis and weathering, which resulted in the precipitation of different clay types, including smectite and kaolinite.

## **Discussion**

### **Factors Controlling Reservoir Quality**

Reservoir quality of the fluvial sandstones is a function of both depositional and diagenetic processes. Depositional controls include sandstone grain size, framework composition, sorting and primary fabric. In general, textural parameters such as grain size and sorting have effects on the porosity and permeability of reservoir facies. The finer the sand grain size, the lower the permeability. The better sorted sandstones tend to have higher porosity (Beard and Weyl, 1973). Other parameters such as sandstone composition could also have an influence on reservoir quality. For instance, the higher the quartz content the greater the mechanical stability; hence, less porosity destruction from compaction. Sandstone with abundant unstable grains such as rock fragments and or feldspar grains have more secondary porosity through dissolution.

In the Scollard sequence sandstones, the role of sandstone composition and texture on reservoir quality is overcome by diagenetic processes such as cementation and authigenic clay formation (Fig. 12 A and C). A few parameters such as diagenetic processes and authigenic mineral distribution can be used to explain most of the variations in the porosity and permeability of the lithic arenites of the fluvial strata.

### *Diagenetic Processes and Sandstone Properties*

Diagenetic processes are related to both the environment and burial depth. The most common environment-related diagenetic processes are the formation of calcite and authigenic clay minerals. Both calcite cementation and authigenic clay mineral precipitation play an important role in controlling the reservoir properties of sandstones. Diagenetic processes also control reservoir quality by the interaction of various factors such as differences in burial depth, and the availability and mobility of ions, which may crystallize as cement that is detrimental to the sandstone reservoir properties. The influence of diagenetic processes on porosity and permeability in the Scollard sequence sandstones occurred throughout the diagenetic history. For example, during eodiagenesis, mechanical compaction and early calcite cementation were the main diagenetic processes influencing reservoir quality, as the thin sections, SEM and XRD analyses indicate (Fig. 9 A and B); whereas during mesodiagenesis, the formation of illite, chlorite, smectite-chlorite, calcite, and quartz cement are the major factors that reduced porosity and permeability of the sandstones (Fig. 6 A and B). In contrast, the dissolution of feldspar leads to a significant increase in secondary porosity (Fig. 10 F). Even where primary porosity has been nearly eliminated because of the effect of mechanical and chemical compaction, significant secondary porosity resulting from the dissolution of feldspar may still form (Fig. 10 F).

Telodiagenesis seems to have had less effect on porosity and permeability, even though it resulted in the precipitation of some kaolinite, smectite and partial dissolution of feldspar (Fig. 5 C).

Generally, in the sandstones, three diagenetic related porosity-reducing processes were observed: (1) mechanical compaction, (2) chemical compaction (pressure solution), and (3) authigenic mineral cementation.

### *The Role of Compaction*

In the study area, both mechanical and chemical compaction played a role in reducing the sandstones' primary porosity and permeability. During eodiagenesis the detrital composition of the sandstones exerted an important control on reservoir properties as indicated by the abundance of deformed unstable grains like biotite, muscovite (Fig. 10 D), feldspars, and rock fragments (Kurkijy, 1988) (Fig. 9 A). The deformation of the ductile grains, which are squeezed between and around the closest rigid grains, reduced the primary porosity, as the SEM photomicrographs indicate (Fig. 9 A). During early diagenesis, the mechanical compaction of the Scollard sequence arenites also caused a proportionate reduction of the pore throats and led to a quicker loss of permeability than of porosity.

Compaction involves the reduction in pore space associated with the shortening of a sand column under burial loading. Sandstones respond in two ways to the stress caused by burial depth: a mechanical response to stress (grain slippage, rotation, and fracturing) and a chemical process of pressure dissolution at grain contacts. The mechanical process occurs where the burial depth is less than 1400 m, while the chemical process occurs at a greater depth (>1400m) (Vesic and Clough 1968).

In the Scollard sandstones, the reduction of primary intergranular porosity began soon after burial, as the abundance of deformed ductile grains indicates (Fig. 9 A). This finding suggests that most of the porosity may have been lost rapidly via mechanical compaction before any significant cementation occurred. Mechanical compaction also involved processes of grain rotation and rearrangement. Early calcite cementation affected reservoir quality in some sandstone beds by completely occluding porosity and resulting in “tight” sandstones (Fig. 9 B).

Sediment compaction, mineral cementation, and dissolution are the primary controls on the porosity of the Coalspur sandstones. Separating porosity change caused by compaction from those changes caused by cementation and dissolution is difficult. The primary porosity of the sandstones decreased through the internal slipping of sand grains during the initial compaction, pressure solution, and precipitation of the cement.

Part of the silica cement of the sandstones is derived from pressure solution at the points of contact along which the grains slipped into a denser packing style (Fig. 10 A). Silica dissolution increases when the grains are smaller and when the contacts between grains are steeper. The amount of quartz generally increases with compaction as the contact faces become larger. This finding confirms that mechanical slipping (rearrangement) of the grains occurred before cementation during the initial compaction, whereas the chemical compaction (pressure solution) predominated during the later stages.

### **Calcite Cementation and Reservoir Properties**

Calcite cementation also played an important role in the evolution of the Scollard sequence sandstone porosity and permeability (Fig.12 B and D). SEM and petrographic evidence indicates that the calcite cements formed relatively early in the diagenesis (Khidir and Catuneanu, 2003), were subject to dissolution, and were followed by the precipitation of new calcite cement in later diagenesis. During early diagenesis, calcite cement plays a key role in controlling primary porosity preservation by preserving the porosity in the form of pore fillings. During burial, calcite cementation frequently fills the spaces between the grains (Fig. 10 A and C), resulting in a loss of porosity and permeability. In contrast, the dissolution of the calcite cement, which occurred during different diagenetic stages, resulted in secondary porosity development (Fig. 11 A).

Laboratory analyses confirm that the porosity of the sandstone samples is related to the amount of calcite cement (Fig. 12 B and D). For sandstones cemented with less than 5% calcite, the porosity is higher than 15% (Fig. 12 B and D). In contrast, for sandstones cemented with greater than 5% calcite, the porosity can vary between 4% and 8% and averages 6% (Fig. 12 B and D). The diverse distribution of the calcite cement through sandstone bodies significantly increases the heterogeneity of reservoirs and their quality. Thus, the variability, degree, and timing of calcite cementation are major factors controlling porosity and permeability development and heterogeneity in the Scollard sequence sandstones.



The early calcite cement of the Scollard sandstones interrupted mechanical compaction and prevented the precipitation of other cement types (Fig.9 B). The precipitation of authigenic clay minerals seems to have been less effective than calcite cementation in reducing the porosity of the sandstones.

In the Willow Creek Formation, the reduction of the sandstone porosity is due to the extensive occurrence of calcite (Fig. 11 A), clays and quartz cementation (Fig. 11 B). In some sandstone beds, cementation by calcite was very rapid so that little mechanical compaction occurred.

### **The Role of Clay Minerals**

Authigenic clay minerals are an important control on the permeability and porosity of the sandstones when these minerals' abundance exceeds 15% (Fig. 5 A, B, E, and F). The precipitation of small amounts of authigenic clay changes pore diameter only slightly, yet considerably changes transport properties (Howard, 1992) (Fig. 10 E and H). Smectite is likely the most damaging authigenic mineral to reservoir permeability under different hydrogeochemical conditions (Howard, 1992). The interstitial fibrous structure of smectite causes the pore systems to have a very high surface-area-to-volume ratio (Almon, 1979), which increases turbulence by roughening the pore wall surface (Ives, 1987). Smectite also can absorb water, expand and consequently destroy permeability (Deer et al., 1998). Smectite has a tendency to migrate and then block pore throats during fluid flow in porous sandstones (David et al., 1997). SEM studies have shown that some expandable smectite contains illite interlayers.

Illite, which is produced diagenetically in deeply buried sandstones, occurs as pore-filling and pore-lining cement. In the Scollard sandstones, the illite is characterized by two different texture types: hair-like and radially disposed crystals. These characteristics of illite crystallography result in a decrease in permeability. The permeability reduction with a corresponding increase in the degree of illitization was noted by Guven et al. (1980). Illite also results in a more significant permeability decline than quartz overgrowth cementation. This reduction in permeability is caused by the microporous grain rims, which behave like solid overgrowths as far as fluid flow is concerned. Illite also separates the pore spaces into a large number of very thin channels causing increased tortuosity (Stadler, 1973).

Kaolinite, which is abundant in the Scollard sandstones, also plays a significant role in determining reservoir quality. The various individual kaolinite booklets, which have no preferred orientation relative to one another, consumed a large part of the original pore space, hence affecting the primary porosity. Simultaneously, the distribution of kaolinite in the central pathway of the flow also played an important role in reducing permeability (Howard, 1992).

Chlorite and chlorite/smectite are the most common diagenetic minerals in the Coalspur and Willow Creek sandstones. A progressive cementation by chlorite and chlorite/smectite produces a decline in permeability. At the same time, the microscopic recovery efficiency (microporosity) of chlorite-rich sandstones tends to be higher than in

mixed-layer rich sandstones because the chlorite rims commonly cause no increase in the pore system heterogeneity. The process of grain coating via the precipitation of authigenic clay minerals is also an important diagenetic mechanism controlling the distribution of quartz cementation (Fig. 10 B) and porosity evolution in sandstones (Heald and Larese, 1974). For example, chlorite coating stops the quartz from forming strong bonds with the adjacent grains and results in the inhibition of additional silica cementation (Fig. 10 B), which is considered the most porosity-destructive cement in many deep-buried sandstones. Although clay grain coatings inhibit silica cementation, they also result in a major permeability reduction in the sandstone beds due to the obstruction of the pore throats between the grains (Fig. 10 E).

## **Conclusions**

1. Diagenetic processes that occurred during progressive burial to various depths have resulted in heterogeneous reservoir properties in the predominantly fluvial Upper Cretaceous-Lower Tertiary strata of the Scollard sequence sandstones.
2. The potential of a sandstone to serve as a reservoir for producible hydrocarbons is strongly related to the sandstone's diagenetic history.
3. Calcite cementation is one of the main factors controlling the porosity and heterogeneity of the Scollard sequence when the calcite cement abundance exceeds 5%.
4. The initial clast composition involving a mechanical response is one factor that contributed to the reduction of the sandstone's primary porosity.

5. The clay minerals are an important control on the reservoir properties when clay mineral abundance exceeds 15%.
6. The reservoir quality tends to be better in the subsurface relative to the outcrop equivalents, due to the additional reduction in porosity and permeability caused by exhumation and weathering.

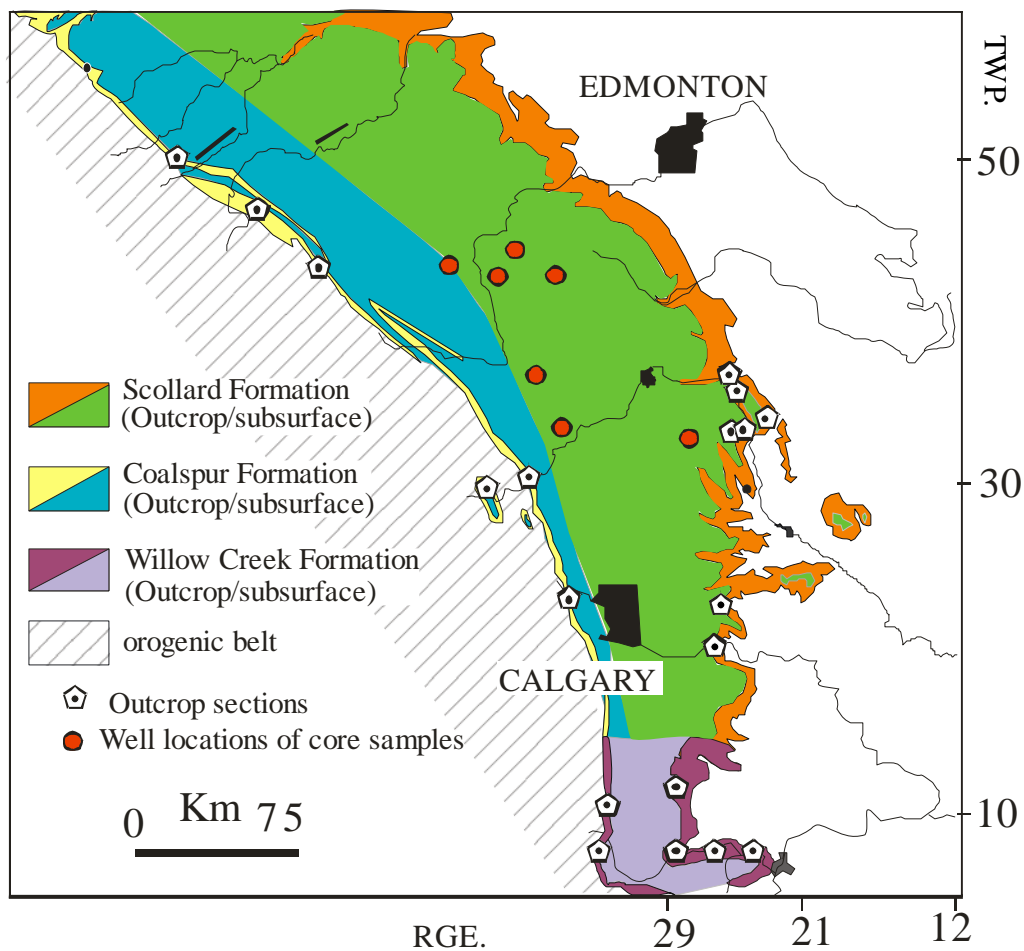


Figure 1. Outcrop distribution of the Scollard, Coalspur and Willow Creek formations in Alberta, and the location of the studied outcrop sections.

Age	Stratigraphic units					
	Southern Foothills		Plains		Central Foothills	
Paleocene	Porcupine Hills Formation		Paskapoo Formation			
	Maastrichtian	Willow Creek Formation	Scollard Formation	upper Scollard	Coalspur Formation	upper Coalspur
lower Willow Creek		lower Scollard		lower Coalspur		Arbour
Maastrichtian	St. Mary River Formation		Battle Formation	Brazeau Formation	Mynheer	
			Whitemud Formation		Entrance Member	
			Horseshoe Canyon Formation			
	Bearpaw Formation	Bearpaw Formation				
Campanian	Belly River Group		Belly River Group			

Figure 2. Generalized chart of the late Campanian to Paleocene stratigraphy of west-central Alberta, showing the position of the Scollard, Coalspur and Willow Creek formations.

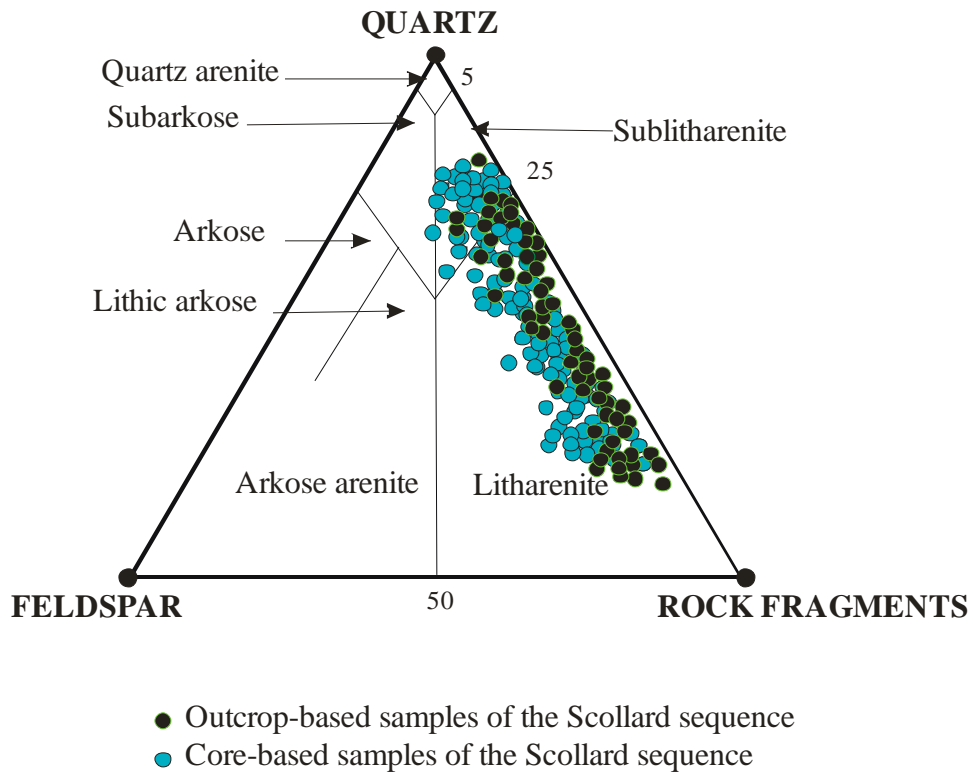


Figure 3. Classification of the Scollard, Coalspur and Willow Creek formation sandstones (after Pettijohn et al., 1987).

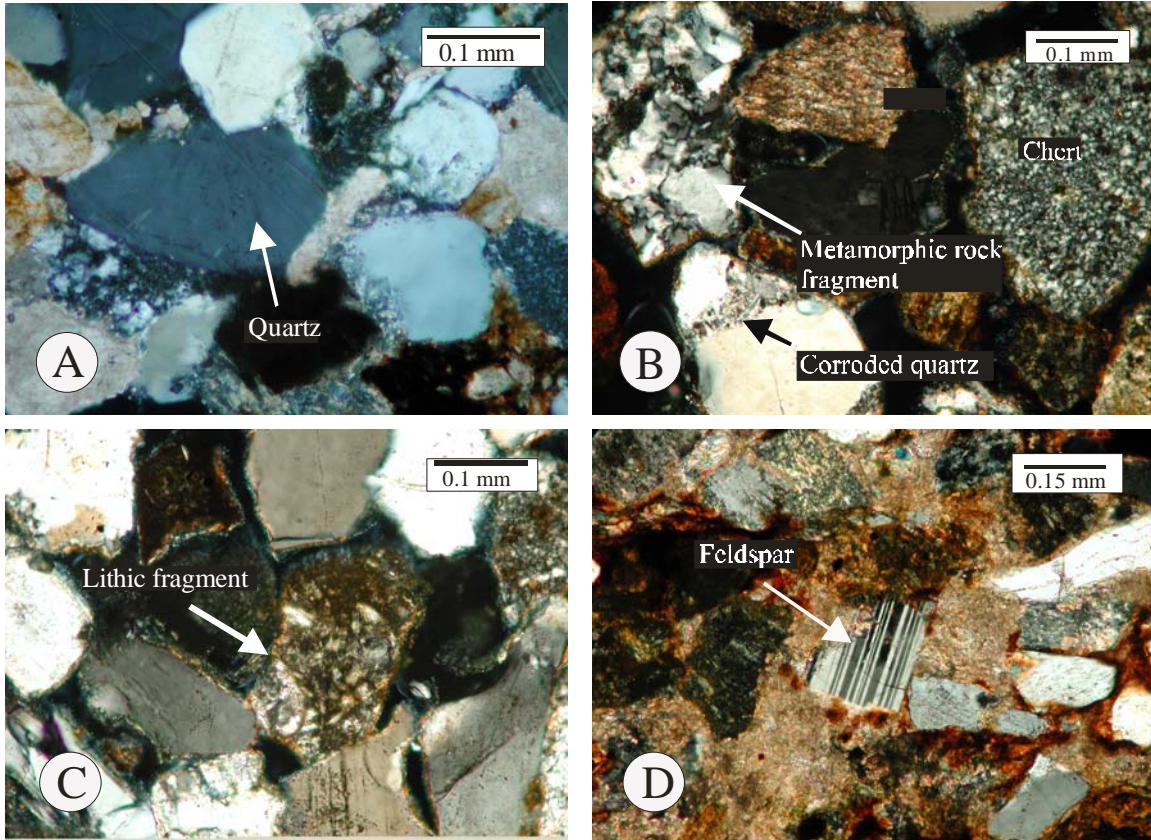


Figure 4. Thin-section photomicrographs: (A) – quartz grains corroded and partially replaced by calcite cement. Note that the calcite cement filling the pores between the quartz grains has reduced porosity (sample 2, upper Coalspur Formation, Sundre locality); (B) – detrital grains of polycrystalline quartz of metamorphic origin and chert grain (sample 3, upper Coalspur Formation, Sundre locality); (C) detrital grain of igneous origin (sample 30, upper Willow Creek Formation, Crowsnest River locality); (D) – feldspar grain corroded and partially replaced by drusy calcite cement (sample 6, lower Willow Creek Formation, Crowsnest River locality).



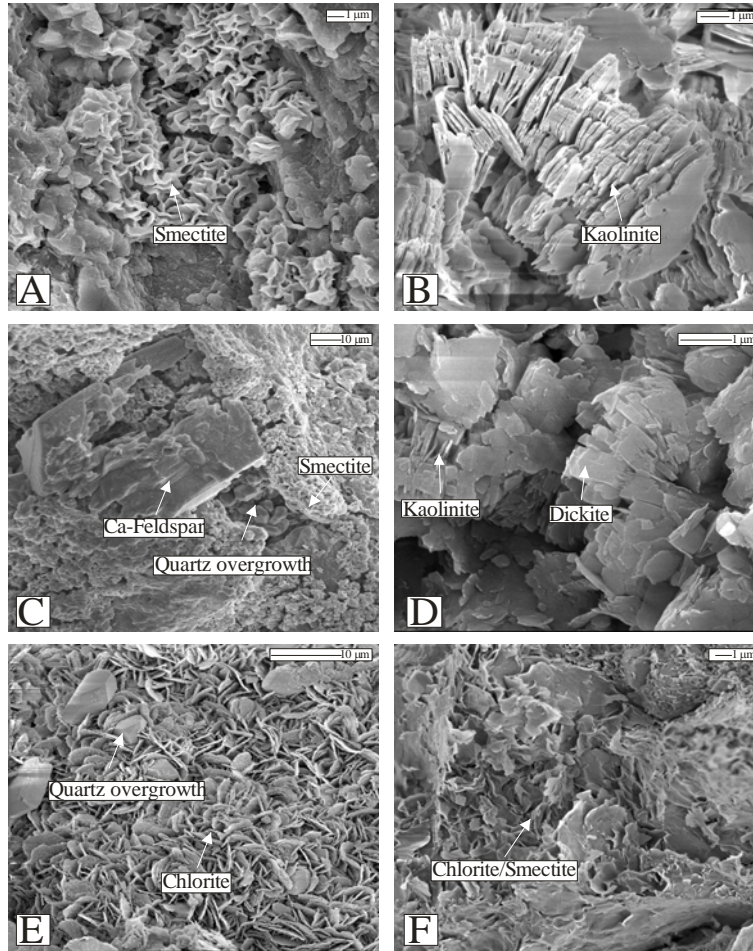


Figure 5. SEM photomicrographs: (A) – authigenic smectite formed as pore lining clay (sample 5, lower Willow Creek Formation, Oldman River locality); (B) – vermicular aggregates of euhedral crystals of authigenic kaolinite formed as pore filling cement (sample T-2, upper Scollard Formation, Buffalo Jump locality); (C) – alteration of Ca-feldspar grain, and the formation of authigenic smectite; note the formation of secondary porosity due to the leaching of feldspar grain (sample kn-5, lower Scollard Formation, Kneehills Creek locality); (D) – authigenic dickite and kaolinite (sample 15 B, upper Willow Creek Formation, Crowsnest River locality); (E) – authigenic chlorite and quartz overgrowth. Note the process of grain coating via authigenic chlorite controlling the distribution of quartz cementation and hence the porosity development in sandstones (sample 3, Entrance Member, lower Coalspur Formation, Highway 22 locality); (F) – authigenic mixed layer chlorite-smectite (sample 25, lower Willow Creek Formation, Crowsnest River locality).

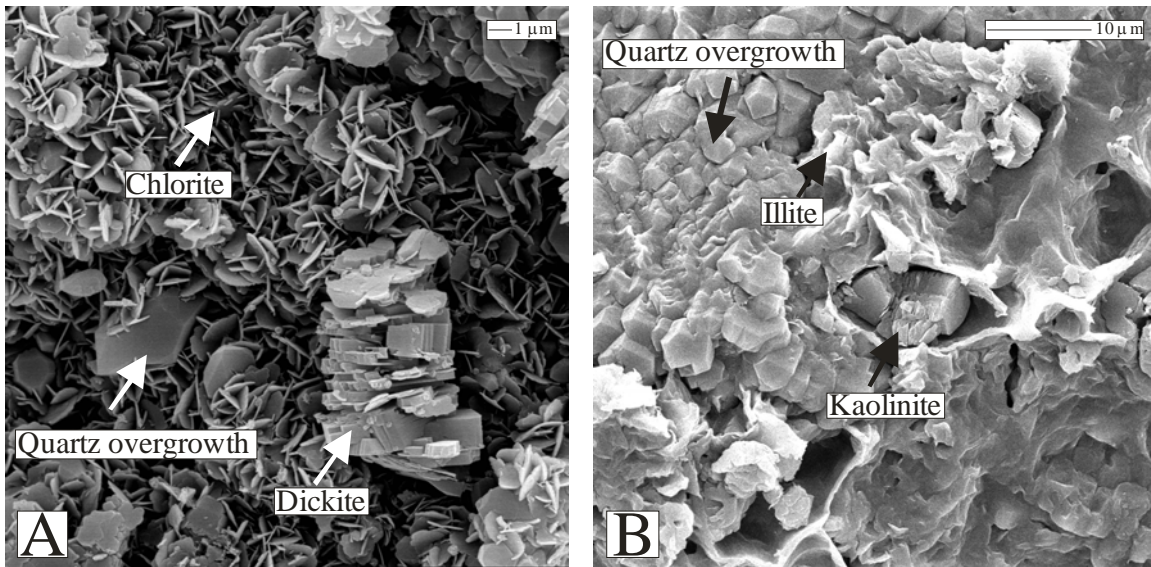


Figure 6. SEM photomicrographs: (A) authigenic chlorite, dickite and quartz overgrowth formed during burial diagenesis (sample 16, upper Willow Creek Formation, Crowsnest River locality); (B) quartz overgrowth coated by illite. Note that the kaolinite formed as a pore-filling clay that reduced porosity (sample 11, upper Willow Creek Formation, Crowsnest River locality).

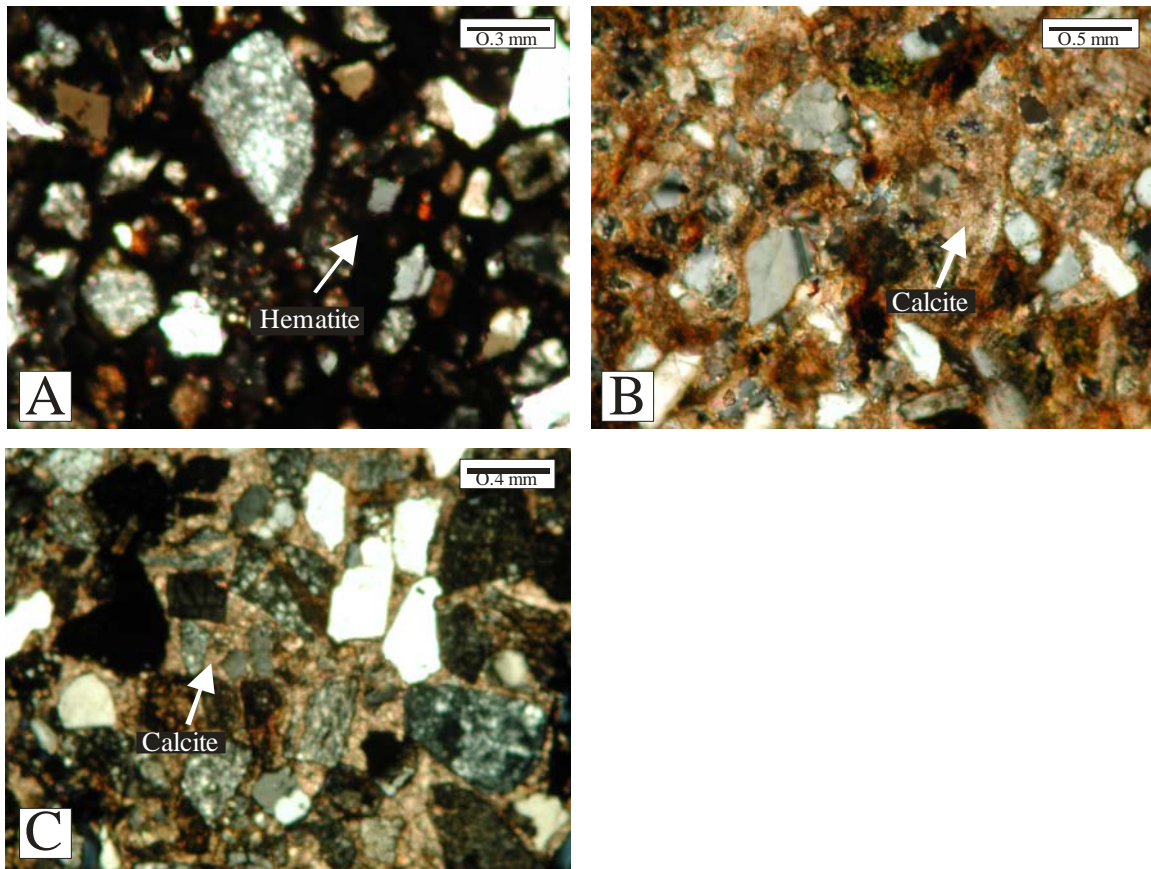


Figure 7. Thin-section photomicrographs: (A) – hematite formed as late diagenetic cement (sample K-5, upper Scollard Formation, Knudsen’s Farm locality); (B) and (C) – sandstone cemented completely by calcite (sample 21, lower Willow Creek Formation, Crowsnest River locality).

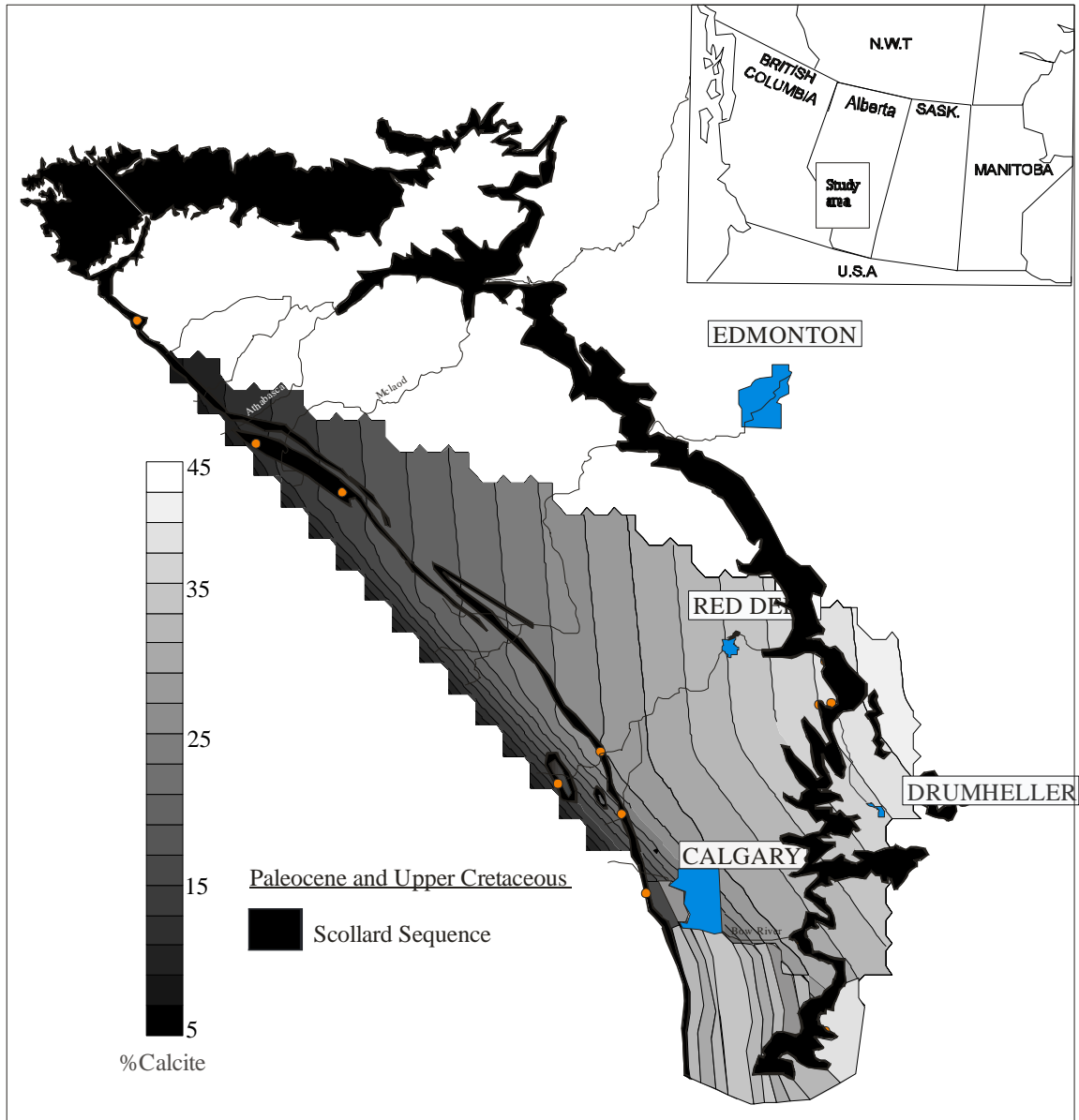


Figure 8. Contour map showing the distributions of the calcite cement in the Scollard, Coalspur and Willow Creek formations in Alberta.



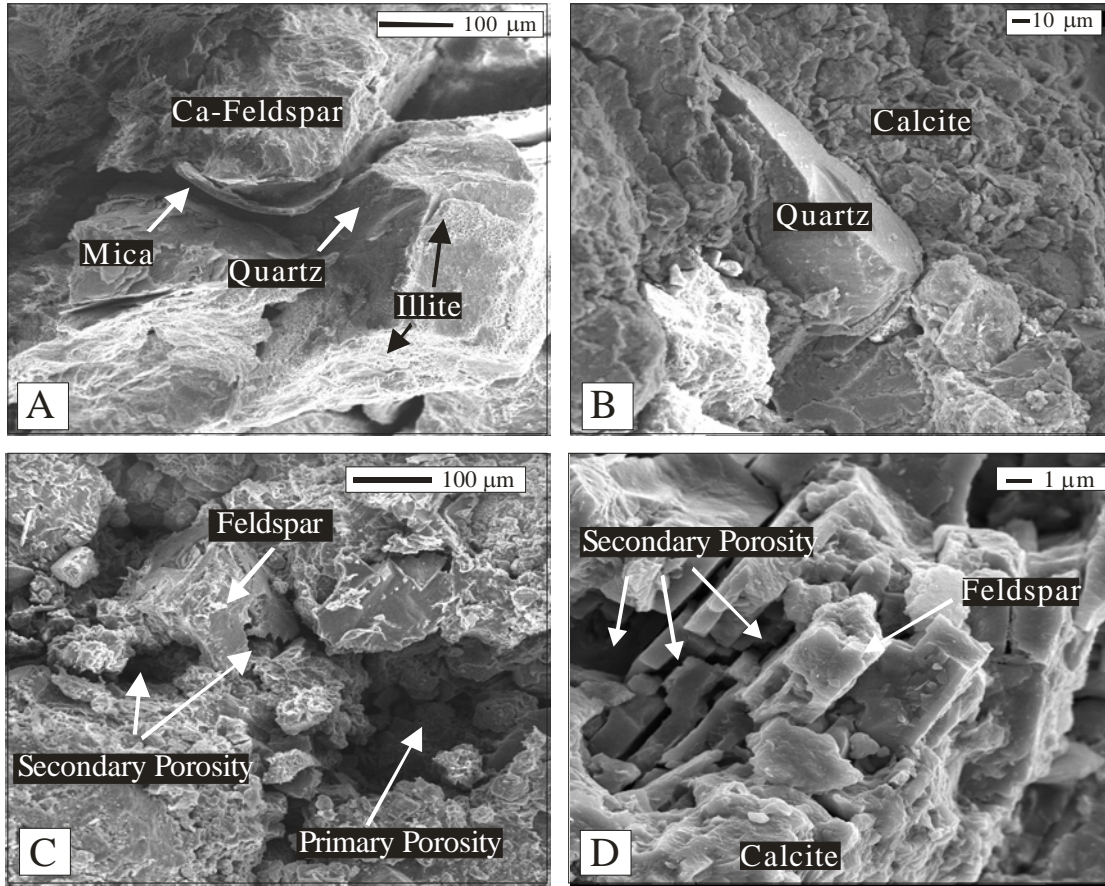


Figure 9. Scanning electronic photomicrographs: (A) ductile mineral (mica) deformation during the early stag of sediment compaction, resulting in decreasing primary porosity ; (sample 35, upper Scollard Formation, Buffalo Jump locality); (B) quartz grain surrounded by extensive calcite cement. Note the role of calcite cement in reducing porosity (sample 25, lower Scollard Formation, Griffith's Farm locality); (C) Secondary porosity developed from partial dissolution of feldspar grain and residual primary porosity (sample T3, upper Scollard Formation, Buffalo Jump locality); (D) Secondary leaching of feldspar and dissolution along the cleavages (sample 37, upper Scollard Formation, Buffalo Jump locality).

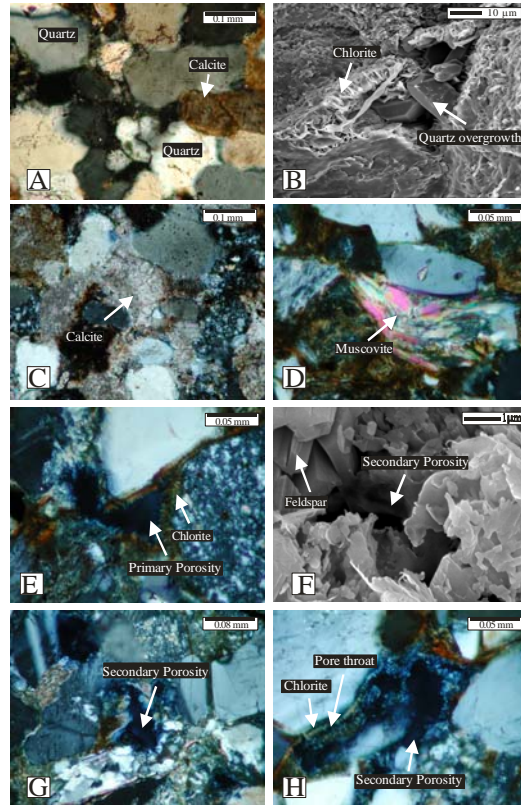


Figure 10. (A) – Photomicrograph of thin section slide showing quartz grains that have slipped into a denser packing style and silica cement (sample 1, upper Coalspur Formation, Sundre locality); (B) – SEM image of authigenic chlorite and quartz overgrowth. Note that the chlorite coating has restrained additional silica cementation (sample E-2, Entrance Member, lower Coalspur Formation, Highway 22 locality); (C) – thin section photomicrograph showing the drusy texture of the calcite cement which limited the primary porosity (sample U-23, upper Willow Creek Formation, Crowsnest River locality); (D) – deformation of muscovite grain by mechanical compaction which resulted in porosity reduction (sample U-15, upper Willow Creek Formation, Crowsnest River locality); (E) and (H) – thin section photomicrograph showing chlorite pore-coating. Note that the chlorite coating has restrained additional silica cementation and caused reduction in the size of pore-throats (sample E-6, Entrance Member, lower Coalspur Formation, Highway 22 locality); (F) – dissolution of porosity (secondary porosity) developed after partial dissolution of feldspar grain (sample E-3, Entrance Member, lower Coalspur Formation, Highway 22 locality).

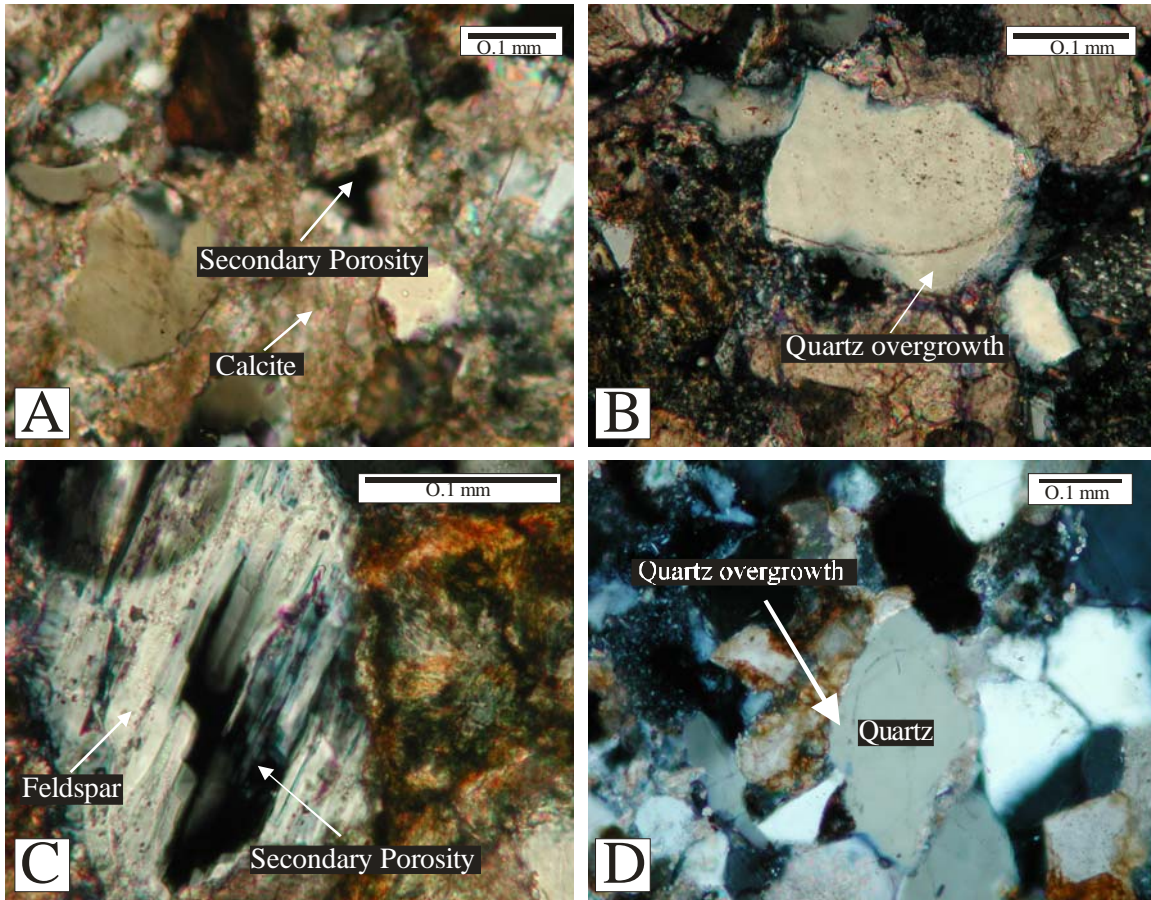


Figure 11. Thin section photomicrograph: (A) – secondary porosity created by the dissolution of calcite cement (sample 22, lower Willow Creek Formation, Crowsnest River locality); (B) – quartz overgrowth on quartz grain (sample 10, lower Willow Creek Formation, Crowsnest River locality); (C) – secondary porosity created by the dissolution of feldspar grain (sample 26, lower Willow Creek Formation, Crowsnest River locality); (D) – quartz overgrowth resulted in reduced permeability (sample 25, lower Willow Creek Formation Crowsnest River locality).



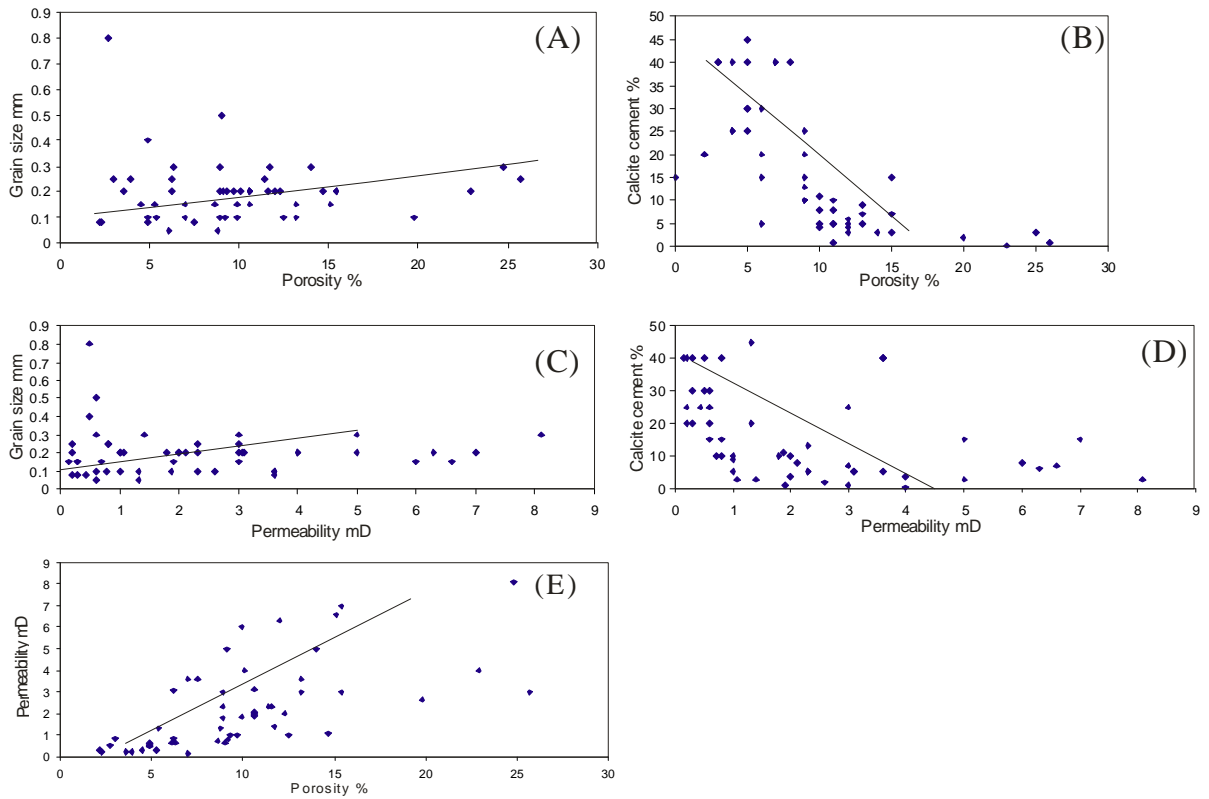
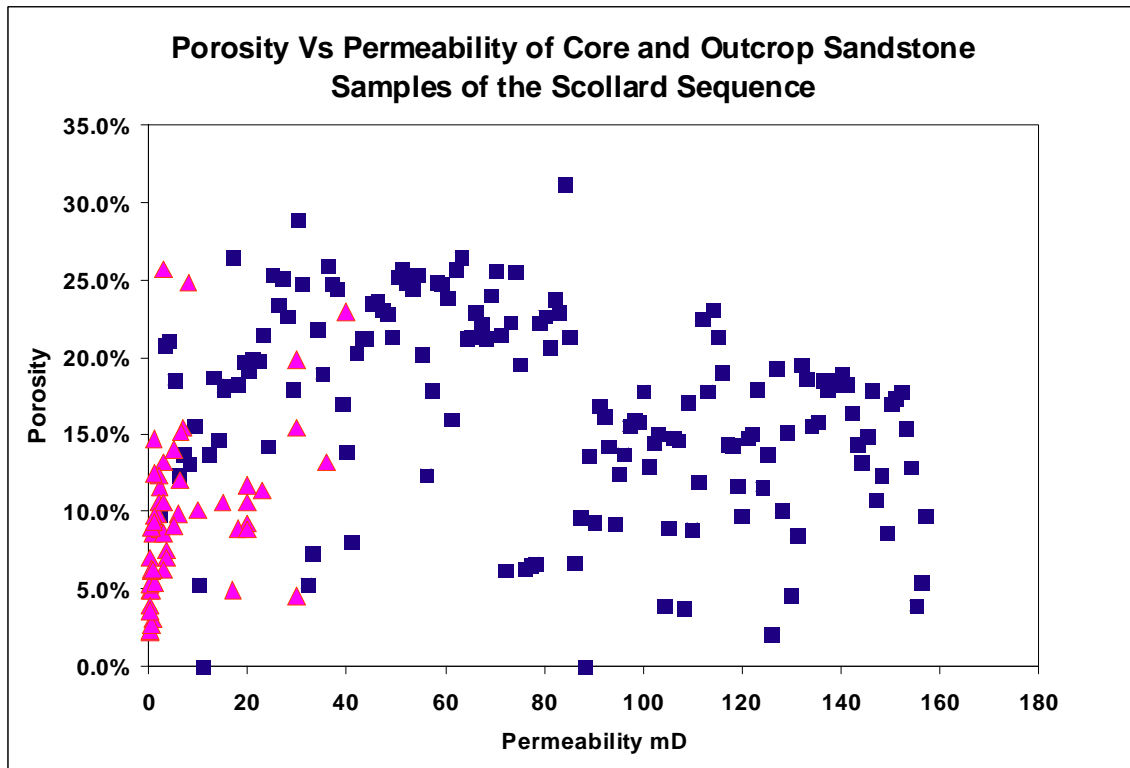


Figure 12. (A) Plot showing sandstone grain size (mm) vs. porosity vol.% of the Scollard sequence sandstones; (B) Plot showing sandstone calcite cement vol.% vs. porosity vol.% of the Scollard sequence sandstones; (C) Plot showing sandstone grain size (mm) vs. permeability mD of the Scollard sequence sandstones; (D) Plot showing calcite cement vol.% vs. permeability of the Scollard sequence sandstones; (E) Plot showing sandstone permeability mD vs. sandstone porosity vol.% of the Scollard age sandstones.





- ▲ Outcrop Samples
- Core Samples

Figure 13. Plot showing sandstone permeability mD vs. sandstone porosity vol.% of the Scollard age sandstones. The plot also shows the difference between the porosity and permeability of the subsurface core data and the porosity and permeability of the outcrop sandstone samples.

Sample #	Formation name	Porosity (%)	Grain Density kg/m3	Permeability mD	Calcite cement %	Grain Size mm
1	Lower Willow Creek	15.4	2620	3	7	0.2
2	Lower Willow Creek	4.9	2690	0.44	25	0.08
3	Lower Willow Creek	9.2	2670	0.79	10	0.1
4	Lower Willow Creek	10.6	2640	2.1	8	0.2
5	Lower Willow Creek	13.2	2640	3	7	0.15
6	Lower Willow Creek	10.1	2640	4	4	0.2
7	Lower Willow Creek	11.4	2640	2.3	5	0.25
8	Lower Willow Creek	11.6	2650	2.3	5	0.2
9	Lower Willow Creek	8.6	2670	0.7	10	0.15
10	Lower Willow Creek	12.3	2640	2	4	0.2
11	Lower Willow Creek	14	2650	5	3	0.3
12	Upper Willow Creek	4.5	2650	0.3	30	0.15
13	Upper Willow Creek	11.7	2590	1.4	3	0.3
14	Upper Willow Creek	10.6	2630	1.9	1	0.15
15	Upper Willow Creek	8.9	2630	1.8	10	0.2
16	Upper Willow Creek	9.9	2630	1.86	11	0.1
17	Upper Willow Creek	9.9	2640	6	8	0.15
18	Upper Willow Creek	8.9	2610	2.3	13	0.1
19	Upper Willow Creek	10.6	2680	3.1	5	0.2
20	Upper Willow Creek	4.9	2690	0.6	25	0.1
21	Upper Willow Creek	7.5	2680	3.6	40	0.08
22	Upper Willow Creek	7	2680	3.6	40	0.1
23	Upper Willow Creek	5.3	2680	0.3	40	0.15
24	Upper Willow Creek	5.4	2670	1.32	45	0.1
25	Lower Scollard	4.9	2730	0.5	30	0.4
26	Lower Scollard	8.8	2630	1.32	20	0.05
27	Lower Scollard	19.8	2630	2.6	2	0.1
28	Lower Scollard	22.9	2600	4	0.2	0.2
29	Lower Scollard	3	2490	0.8	40	0.25
30	Lower Scollard	8.6	2670	3	25	0.3
31	Lower Scollard	24.8	2550	8.1	3	0.3
32	Lower Scollard	25.7	2570	3	1	0.25
33	Lower Scollard	9.1	2650	5	15	0.2
34	Lower Scollard	15.4	2600	7	15	0.2
35	Upper Scollard	9	2620	0.6	15	0.5
36	Upper Scollard	3.9	2550	0.2	40	0.25
37	Upper Scollard	12.5	2630	1	9	0.1
38	Upper Scollard	7	2660	0.14	40	0.15
39	Upper Scollard	13.2	2640	3.6	5	0.1
40	Upper Scollard	6.1	2660	0.6	30	0.05
41	Upper Scollard	15.1	2620	6.6	7	0.15
42	Upper Scollard	2.2	2670	0.3	20	0.08
43	Upper Scollard	2.3	2680	0.2	20	0.08
44	Lower Coalspur	14.7	2660	1.07	3	0.2
45	Lower Coalspur	6.2	2640	3.08	5	0.2
46	Lower Coalspur	12	2660	6.3	6	0.2
47	Lower Coalspur	9.7	2660	1	5	0.2
48	Upper Coalspur	2.7	2890	0.5	40	0.8
49	Upper Coalspur	6.3	2650	0.6	20	0.3
50	Upper Coalspur	6.2	2630	0.8	15	0.25
51	Upper Coalspur	3.6	2650	0.2	25	0.2
52	Upper Coalspur	9.3	2700	1	10	0.2
53	Upper Coalspur	10.6	2620	2	10	0.2

Table 1. Porosity, permeability (mD), calcite cement (%), and average grain-size measurements (mm) of 53 selected outcrop-based samples from Scollard sequence sandstones.

Well Locations	Sample Top (m)	Sample Base (m)	Sample Forms	Permeability (mD)	Porosity (%)	Grain Density (kg/m <sup>3</sup> )	Lithology
0007-25-044-07W5/0	543.5	543.51	Scollard Sequence	0.56	9.8	2680	Very fine grained sandstone with calcite cement
0007-25-044-07W5/0	544.5	544.51	Scollard Sequence	81.9	20.8	2660	Fine to medium Grained sandstone with pyrite
0007-25-044-07W5/0	545.1	545.11	Scollard Sequence	103	21.1	2660	Fine to medium Grained sandstone with pyrite
0007-25-044-07W5/0	545.6	545.61	Scollard Sequence	12.7	18.5	2620	Fine to medium Grained sandstone
0007-25-044-07W5/0	591	591.01	Scollard Sequence	0.42	12.3	2670	Very fine grained sandstone with calcite cement
0007-25-044-07W5/0	594.5	594.51	Scollard Sequence	0.57	13.7	2660	Very fine to fine grained sandstone with calcite cement
0007-25-044-07W5/0	597.5	597.51	Scollard Sequence	1.67	13.1	2670	Fine grained sandstone with calcite cement
0007-25-044-07W5/0	600.5	600.51	Scollard Sequence	2.17	15.6	2650	Very fine to coarse grained sandstone with calcite cement
0007-25-044-07W5/0	602.9	602.91	Scollard Sequence	0.06	5.3	2730	Very fine to medium grained sandstone with calcite and dolomite cement
0007-25-044-07W5/0	603	603.01	Scollard Sequence	0.06	0		NO RECOVERY
0007-25-044-07W5/0	603.4	603.41	Scollard Sequence	0.3	13.7	2690	Very fine to fine grained sandstone with dolomite cement
0007-25-044-07W5/0	604	604.01	Scollard Sequence	4.11	18.7	2660	Very fine to coarse grained sandstone with calcite cement
0007-25-044-07W5/0	604.6	604.61	Scollard Sequence	2.15	14.7	2680	Very fine to coarse grained sandstone with calcite cement
0007-25-044-07W5/0	677	677.01	Scollard Sequence	2.84	18	2670	Very fine to medium grained sandstone with calcite cement
0007-25-044-07W5/0	677.6	677.61	Scollard Sequence	23.9	18.2	2530	Very fine to fine grained sandstone w
0011-21-045-04W5/0	355	355.01	Scollard Sequence		26.5	2670	Very fine to coarse grained sandstone with calcite and siderite cement
0011-21-045-04W5/0	415.2	415.21	Scollard Sequence	43	18.3	2680	Very fine to fine grained sandstone
0011-21-045-04W5/0	415.7	415.71	Scollard Sequence	69.7	19.7	2670	Very fine to medium grained sandstone with siderite cement
0011-21-045-04W5/0	416	416.01	Scollard Sequence	22.4	19.2	2680	Very fine to fine grained sandstone with siderite cement
0011-21-045-04W5/0	416.3	416.31	Scollard Sequence	29.8	19.9	2680	Very fine to fine grained sandstone with siderite cement
0011-21-045-04W5/0	416.8	416.81	Scollard Sequence	99.5	19.8	2670	Very fine to medium grained sandstone with calcite and siderite cement
0011-21-045-04W5/0	460	460.01	Scollard Sequence	115	21.5	2640	Very fine to medium grained sandstone
0011-21-045-04W5/0	461	461.01	Scollard Sequence	2.16	14.2	2680	Very fine to medium grained sandstone with calcite and siderite cement
0011-21-045-04W5/0	495	495.01	Scollard Sequence		25.3	2640	Very fine grained sandstone
0011-21-045-04W5/0	495.5	495.51	Scollard Sequence	350	23.4	2650	Very fine grained sandstone
0011-21-045-04W5/0	519	519.01	Scollard Sequence		25.1	2650	Very fine grained sandstone
0011-21-045-04W5/0	519.5	519.51	Scollard Sequence	93.8	22.7	2640	Very fine grained sandstone
0011-21-045-04W5/0	520.3	520.31	Scollard Sequence	27.5	18	2670	Very fine grained sandstone
0011-21-045-04W5/0	521.1	521.11	Scollard Sequence		28.9	2630	Very fine grained sandstone
0011-21-045-04W5/0	522	522.01	Scollard Sequence	173	24.7	2650	Very fine grained sandstone
0011-21-045-04W5/0	522.9	522.91	Scollard Sequence	0.04	5.3	2680	Very fine to coarse grained sandstone with calcite cement
0011-21-045-04W5/0	523.5	523.51	Scollard Sequence	0.09	7.3	2680	Very fine to coarse grained sandstone with calcite cement
0011-21-045-04W5/0	524.5	524.51	Scollard Sequence	93.4	21.9	2660	Very fine to coarse grained sandstone with calcite cement
0011-21-045-04W5/0	525.2	525.21	Scollard Sequence	20	18.9	2650	Very fine to coarse grained sandstone
0011-21-045-04W5/0	662.8	662.81	Scollard Sequence		25.9	2640	Very fine to coarse grained sandstone
0011-21-045-04W5/0	663	663.01	Scollard Sequence	304	24.7	2640	Very fine to coarse grained sandstone
0011-21-045-04W5/0	664.2	664.21	Scollard Sequence	279	24.4	2630	Very fine to coarse grained sandstone
0011-21-045-04W5/0	723.3	723.31	Scollard Sequence	13.4	17	2660	Very fine to medium grained sandstone with calcite cement
0307-03-044-03W5/0	349.41	349.49	Scollard Sequence	0.13	13.9	2660	Very fine to fine grained sandstone with calcite cement
0307-03-044-03W5/0	349.69	349.93	Scollard Sequence	0.09	8.1	2670	Very fine to fine grained sandstone
0307-03-044-03W5/0	349.93	350.51	Scollard Sequence	4.14	20.3	2670	Very fine to fine grained sandstone
0307-03-044-03W5/0	350.54	351.05	Scollard Sequence	23.4	21.2	2650	Very fine to fine grained sandstone
0307-03-044-03W5/0	351.05	351.36	Scollard Sequence	17.9	21.2	2650	Very fine to fine grained sandstone
0307-03-044-03W5/0	351.36	351.66	Scollard Sequence	17.5	23.5	2680	Very fine to fine grained sandstone
0307-03-044-03W5/0	351.66	351.83	Scollard Sequence	33.1	23.7	2670	Very fine to fine grained sandstone
0307-03-044-03W5/0	351.83	352.04	Scollard Sequence	35.7	23.1	2670	Very fine to fine grained sandstone
0307-03-044-03W5/0	352.04	352.34	Scollard Sequence	99.1	22.8	2650	Very fine to fine grained sandstone
0307-03-044-03W5/0	352.34	352.86	Scollard Sequence	2.81	21.3	2660	Very fine to fine grained sandstone
0307-03-044-03W5/0	352.86	353.01	Scollard Sequence		25.2	2650	Fine to medium grained sandstone
0307-03-044-03W5/0	353.01	353.14	Scollard Sequence		25.7	2650	Very fine to medium grained sandstone
0307-03-044-03W5/0	353.14	353.63	Scollard Sequence	57.9	24.8	2660	Very fine to medium grained sandstone
0307-03-044-03W5/0	353.63	354.16	Scollard Sequence	138	24.4	2660	Very fine to fine grained sandstone
0307-03-044-03W5/0	354.16	354.44	Scollard Sequence	245	25.3	2660	Very fine to medium grained sandstone
0307-03-044-03W5/0	354.44	354.65	Scollard Sequence	55.1	20.2	2670	Very fine to medium grained sandstone
0307-03-044-03W5/0	354.65	354.9	Scollard Sequence	0.92	12.4	2670	Very fine to fine grained sandstone with calcite cement
0307-03-044-03W5/0	357	357.26	Scollard Sequence	28.4	17.9	2660	Very fine to fine grained sandstone with calcite cement
0307-03-044-03W5/0	357.26	357.48	Scollard Sequence	103	24.8	2650	Very fine to fine grained sandstone
0307-03-044-03W5/0	357.48	357.75	Scollard Sequence	214	24.7	2650	Very fine to medium grained sandstone
0307-03-044-03W5/0	357.75	358.06	Scollard Sequence	240	23.9	2670	Very fine to medium grained sandstone
0307-03-044-03W5/0	358.06	358.48	Scollard Sequence	8.01	16	2660	Very fine to fine grained sandstone with calcite cement

Table 2. Permeability (mD), porosity (%), average, grain density and lithology of 156 selected core samples from Scollard sequence sandstones.

## References

Almon, W. R. 1979. Sandstone diagenesis as a factor in stimulation design. Proceedings of the 24<sup>th</sup> Annual Southwest Petroleum Short Course, Lubbock, Texas.

Beard, D.C., and P.K. Weyl, 1973, Influence of texture on porosity and permeability of unconsolidated sand: AAPG Bulletin, vol. 57, no. 2, p. 349-369

.Bjørlykke, K. 1998. Clay mineral diagenesis in sedimentary basins- a key to prediction of rock properties. Examples from the North Sea Basin. Clay Minerals, v 33, p. 15-34.

Carrigy, M.A. 1971. Lithostratigraphy of the Uppermost Cretaceous (Lance) and Paleocene strata of the Alberta Plains. Research Council of Alberta, Bulletin 27, 161 p.

David, C., Wendy, J. and Richard F. 1997. Mineralogical responses of siliciclastic carbonate-cemented reservoirs to steamflood enhanced oil recovery. Applied Geochemistry, v. 13, no. 4, p. 491-507.

Dawson, F.M., Evan, C.G., Marsh, R. and Richardson, R. 1994. Uppermost Cretaceous and Tertiary of the Western Canada Sedimentary Basin. In: Geological Atlas of the Western Canada Sedimentary Basin. G. Mossop and I. Shetsen (comps.). Canadian Society of Petroleum Geologists and Alberta Research Council, p. 387-406.

Dawson, G. M. 1883. Preliminary Report on the Geology of the Bow and Belly

River Region, North West Territory, with Special Reference to the Coal Deposits.  
Geological Survey of Canada, Rept. of Prog. 1880-82, pt. B.

Dawson, G. M. 1884. Report on the region in the Vicinity of the Bow and Belly Rivers,  
North West Territory; Geological Survey of Canada, Rept. of Prog. 1882-83-84, pt. C.

Deer, W.A., Howie, R.A. and Zussman, J. 1998. An introduction to the rock forming  
minerals. Longman, Harlow, 528 p.

Douglas, R.I.W. 1950. Callum Creek, Longford Creek, and Gap map-areas, Alberta.  
Geological Survey of Canada, Memoir 255. Geological Survey of Canada Rept. of Prog.  
1880-82, pt. B.

Gibson, D. W. 1977. Upper Cretaceous and Tertiary coal bearing strata in the Drumheller  
– Ardley region, Red Deer River valley, Alberta. Geological Survey of Canada, Paper 76-  
35, p. 1-41.

Guyen, N., Hower, W.F. and Davies, D. K. 1980. Nature of authigenic illites in sandstone  
reservoirs. *Journal of Sedimentary Petrology*, v. 50, p 761- 766.

Hage, C.O. 1943. Cowley map-area, Alberta. Geology Survey of Canada, Paper 43-1.

Heald, M. and Larese, R. 1974. Influence of coatings on quartz cementation. *Journal of  
Sedimentary Petrology*, v. 44, no. 4, p. 1269-1274.

Howard, J. 1992. Influence of Authigenic-clay minerals on permeability. Society for Sedimentary Geology Special Publication, no.47, p. 257-264.

Ives, K. 1987. Filtration of clay suspensions through sand. Clay Minerals, v. 22, p. 49-61.

Jerzykiewicz, T. 1997. Stratigraphic framework of the upper Cretaceous to Paleocene strata of the Alberta Basin. Geological Survey of Canada Bulletin 510, 121p.

Jerzykiewicz, T. and Sweet, A.R. 1988. Sedimentological and palynological evidence of regional climatic changes in the Campanian to Paleocene sediments of the Rocky Mountain Foothills, Canada. Sedimentary Geology, v. 59, p. 29-76.

Jerzykiewicz, T. and Sweet, A.R. 1986b. Caliche and associated impoverished palynological assemblages: an innovative line of paleoclimate research onto the uppermost Cretaceous and Paleocene of southern Alberta. In: Current Research, Part B. Geological Survey of Canada, Paper 86-1B, p. 653-663.

Khidir, A. and Catuneanu, O. 2003. Sedimentology and diagenesis of the Scollard sandstones in the Red Deer Valley area, central Alberta. Bulletin of Canadian Petroleum Geology, v. 51, no. 1, p. 45-69.

Khidir, A. and Catuneanu, O. (2009). Basin-scale distribution of authigenic clay minerals in the Late Maastrichtian–Early Paleocene fluvial strata of the Alberta foredeep:

implications for burial depth. *Bulletin of Canadian Petroleum Geology*. v. 57. no. 3. P. 251-274.

Kurkju, K.A. 1988. Experimental compaction studies of lithic sands. M.S. thesis, Rosensteil School of Marine and Atmospheric Sciences, University of Miami, 101p.

Lerbekmo, J.F., Evans, M.E. and Hoye, G.S. 1990. Magnetostratigraphic evidence bearing on the magnitude of the subPaskapoo disconformity in the Scollard Canyon-Ardley area of the Red Deer Valley, Alberta. *Bulletin of Canadian Petroleum Geology*, v. 23, p. 120-124.

Longiaru, S. 1987. Visual comparators for estimating the degree of sorting from plane and thin section. *Journal of Sedimentary Petrology*, v. 57, p. 791-794.

Mackay, B.R. 1949. Coal areas of Alberta. Geological survey of Canada, Atlas, to accompany estimate of coal reserve prepared for the Royal Commission on Coal.

Pettijohn, F.J., Potter, P.E. and Siever, R. 1987, *Sand and sandstone*, 2nd Edition. Springer-Verlag, New York, 553 p.

Pittman, E.F., 1979, Porosity , diagenesis and productive capability of sandstone reservoirs. *Society of Economic. Paleontologists and Mineralogists Special Publication*. v. 26, p. 159-173.

Russell, D.A. and Singh, C. 1978. The Cretaceous-Tertiary boundary in south-central Alberta- a reappraisal based on dinosaurian and microfloral extinctions. *Canadian Journal of Earth Sciences*, v. 15, p. 284-292.

Schmidt, V. and McDonald D. A. 1979. The role of secondary porosity generation in the course of sandstones diagenesis. In: *Aspects of diagenesis*. P. A. Scholle and P. R. Schluger, (eds.). Society of Sedimentary Geology, Special Publication 26, p. 175-207.

Stadler, P. 1973. Influence of crystallographic habit and aggregate structure of authigenic clay minerals on sandstones permeability: *Geologie en Mijnbouw*, v. 52, p. 217-220.

Sweet, A. R. Braman, D. R. and Lerbekmo, J. F. 1990. Palynofloral response to K/ T boundary events; a transitory interruption within a dynamic system. *Geological Society of America, Special Paper*, v. 247, p. 457-469.

Tobin, R.C. 1997. Porosity prediction in frontier basins: a systematic approach to estimating subsurface reservoir quality from outcrop samples. In: *Reservoir quality prediction in sandstones and carbonate*. J.A. Kupecz, J. Gluyas, and S. Bloch, (eds.). American Association of Petroleum Geologists Memoir 69, p. 1-18.

Tozer, E. T. 1952. The St. Mary River–Willow Creek Contact on Oldman River, Alberta. *Geological Survey of Canada, Paper* 52-3. 9P.



Tozer, E. T. 1956. Uppermost Cretaceous and Paleocene nonmarine molluscan faunas of western Alberta. Geological Survey of Canada, Memoir 280, 125p.

Tyrrell, J.B. 1887. Report on a part of northern Alberta, and portions of adjacent districts of Assiniboia and Saskatchewan. Geological Survey of Canada, 1886 Summary Report Part E.

Vesic, A.S. and Clough, G.W. 1968. Behavior of granular material under high stresses. Journal of Soil Mechanics Foundation Division, v. 94, p. 661-688.

Williams, M. Y. and Dyer, W. S. 1930. Geology of Southern Alberta and Southwestern Saskatchewan. Geological Survey of Canada, Memoir 163.

Wilson, M.D. and Pittman, E.D. 1977. Authigenic clays in sandstones: recognition and influence on reservoir properties and paleoenvironmental analysis. Journal of Sedimentary Petrology, v. 47, p. 3-31.

## **Chapter 3**

*A version of this chapter has been published. Khidir, A. and Catuneanu, O. 2009. Bulletin of Canadian Petroleum Geology Vol.57, No.3. P. 251-274*

### **Basin-scale distribution of authigenic clay minerals in the Late Maastrichtian - Early Paleocene fluvial strata of the Alberta foredeep: Implications for burial depth**

#### **Introduction**

The distribution and diagenesis of authigenic clay minerals in sedimentary basins can be used as a geothermometer to explain the relationship between diagenetic grade and the burial history of sandstone strata (Hoffman and Hower, 1979; Ehrenberg et al., 1993; Wiebel, 1999). Such studies are significant in terms of understanding and predicting changes in sandstone reservoir quality, and for reconstructing subsidence patterns in different areas of a sedimentary basin. While the paleotemperature history across the Western Canada Sedimentary Basin has been investigated on the basis of apatite fission track analysis (Issler et al., 1999), the relationship between the distribution of authigenic minerals and the burial history of the basin has received less attention.

In this paper we discuss authigenic clay mineralogical variations in the Late Maastrichtian - Early Paleocene successions of the Alberta foredeep across the central Plains and central and southwestern Foothills regions. The objective of this study is to evaluate the origin of authigenic clay minerals, their distribution pattern and diagenetic alteration, and relate the insights of this evaluation to the burial history of the basin.

## **Geological background**

Late Maastrichtian-Early Paleocene fluvial strata in the Alberta foredeep of the Western Canada Sedimentary Basin are composed of three roughly correlative formations: Scollard, Coalspur, and Willow Creek. The correlation between these formations is based on palynology, fossil mammals and on the position of the Cretaceous-Tertiary boundary (Jerzykiewicz and Sweet, 1988; Sweet et al., 1990). The formations are exposed in a number of areas in Alberta (Fig. 1). In the central Plains region, the Late Maastrichtian - Early Paleocene strata are referred to as the Scollard Formation, which consists of interbedded shale, coaly shale, olive-green mudstone, siltstone, grey-to-buff sandstone, coal, bentonites and tuffs (Gibson, 1977). The Scollard Formation has a well-defined boundary with the Paskapoo Formation above and the Battle Formation below (Gibson, 1977; Lerbekmo et al., 1990; Dawson et al., 1994; Fig. 2). The thickness of the Scollard Formation in the Red Deer Valley area is about 75 m.

In the central Foothills of Alberta, the Scollard Formation is correlative with the Coalspur Formation. The Coalspur Formation is about 430 m thick and consists of interbedded mudstone, siltstone and fine-to-coarse-grained sandstone (Jerzykiewicz, 1997). At the base of the Coalspur Formation is the Entrance Conglomerate consisting of interbedded conglomerate and sandstone (Jerzykiewicz, 1985b). The Coalspur Formation is overlain by the Paskapoo Formation and overlies the Brazeau Formation (Fig. 2) (Jerzykiewicz and McLean, 1980).

In southwestern Alberta, the Willow Creek Formation is correlative to the Scollard and Coalspur formations and consists of gray, sandy claystones and clayey calcareous sandstones. The Willow Creek Formation is underlain by the St. Mary River Formation and overlain by the Porcupine Hills Formation (Fig. 2). The thickness of the Willow Creek Formation varies from 1006 m close to the axis of the Alberta Syncline (Carrigy, 1971) to about 1375 m on the western limb of the syncline (Tozer, 1956).

Late Maastrichtian - Early Paleocene fluvial deposition in the Alberta foredeep corresponds to a stage of loading in the thrust-fold belt which generated accommodation by means of flexural subsidence (Catuneanu and Sweet, 1999). Thrusting in the Cordillera resulted in differential subsidence across the foredeep with higher rates towards the thrust-fold belt and also to the South towards the center of loading (Catuneanu et al., 2000). This subsidence pattern explains the observed change in the thickness of the three age-equivalent fluvial formations. Differential subsidence along dip resulted in a shallowing of the topographic gradient during the deposition of the late Maastrichtian to lower Paleocene fluvial systems (Gibson, 1977; Eberth and O'Connell, 1995; Catuneanu and Sweet, 1999; Catuneanu et al., 2000). The gradual shallowing of the topographic gradient during orogenic loading resulted in a shift in the fluvial facies from braided channels during the late Maastrichtian to meander channels during the Paleocene time. Following deposition of the fluvial sequence, post-Paleocene regional tectonic uplift and isostatic rebound resulted in the erosion of more than 1000 m of foreland basin sediments (Hacquebard, 1977; Nurkowski, 1984; Bustin, 1992; Issler et al., 1999).

## **Methods**

Fieldwork was carried out in southwestern Alberta, the central Foothills of Alberta and the Plains region. Standard outcrop logging techniques were applied to each exposure, including thickness measurements, facies description, and sampling for laboratory work. Figure 3 illustrates the facies codes used for the description of all outcrop sections (Figs. 4 to 18). The localities studied in the Plains region include Knudsen's Farm (Fig. 4), Buffalo Jump Provincial Park (Fig. 5), the Ardley locality (Fig. 6), Griffith's Farm (Fig. 7), the Kneehills Creek locality (Fig. 8), Hummer Hills (Fig. 9), and the Bow River locality (Fig. 10). Localities that have been studied in the Foothills of central Alberta include Sundre (Fig. 11), the Red Deer River sections 1 (Fig. 12) and 2 (Fig. 13), the Coalspur locality (Fig. 14), and the road cut near Highway 22 (Fig. 15). The localities studied in southwestern Alberta include the Oldman River (Fig. 16), the Oldman Dam Reservoir (Fig. 17), and the Oldman River locality (Fig. 18).

Representative fractions of 129 samples were used for mineralogical study of bulk sediments, and a separate fraction was used for the extraction and analysis of clay minerals. Optical microscope examination was performed on 60 sandstone thin sections with a 400-point count of mineralogy from each sample for the identification of the composition of framework constituents of the sandstones.

In order to distinguish authigenic minerals and to verify the paragenesis of the sandstones, 129 samples were studied by scanning electron microscope (SEM, JEOL JSM 6400) equipped with an energy-dispersive x-ray analyzer. To determine the modal amount and

types of authigenic clay minerals, a grinding technique was used to produce powders free of grains coarser than 20  $\mu\text{m}$ . X-ray diffraction (XRD) was carried out on the bulk samples and on separates finer than 2  $\mu\text{m}$ . Diffraction data was acquired using a Phillips XRG3100 X-Ray Diffraction System. The resulting diffraction data was then analyzed using the industry standard MDI Jade software and the CDD PDF-2 powder diffraction database. Two equivalent fractions of each sample were selected for (1) bulk analysis and (2) for the analysis of the less than 2  $\mu\text{m}$  glycolated fraction. The fraction selected for bulk analysis was manually ground to a fine powder. The resulting powder was packed into a glass sample holder to present a flat powder-packed surface for powder diffraction analysis. Glycolated clay samples were prepared from a separate fraction of each powder sample. Following centrifugal separation, the resulting clay slurries were pipetted onto frosted glass slides and allowed to dry. Diffraction data on the resulting clay slides were acquired. The relative abundance of specific clay minerals within the clay fraction was determined using the data obtained on the  $<2$   $\mu\text{m}$  clay fraction. The criteria of Wilson and Pittman (1977) were used to distinguish between detrital and authigenic clay minerals.

### **Sandstone composition**

The dominant types of outcrop sandstones are lithic arenites and sublithic arenites (Fig. 19). The framework grains used to classify the sandstones are quartz, feldspar, and rock fragments. The sandstones consist typically of well-to-moderately sorted monocrystalline quartz and feldspar along with a mixture of volcanic, sedimentary and metamorphic rock fragments. The sandstones are fine-to-medium grained and

subrounded to subangular. The samples are characterized by a general lack of matrix, with an average estimate of 2% (range 0-4%), based on thin-section observations. The lack of matrix and the good sorting of most of the sandstone samples suggest that the original primary porosity and permeability were relatively high.

### **Authigenic minerals**

The distribution of authigenic clay minerals in the sandstones is highly variable (Figs. 20 and 21). The Maastrichtian samples of the Plains region are dominated by smectite followed by kaolinite; the Paleocene samples of the same region are dominated by kaolinite. In the Foothills, the Maastrichtian samples are dominated by chlorite followed by illite. Dickite and chlorite-smectite are the dominant authigenic clays of the Paleocene samples in the Foothills. The dominant authigenic clays in the Scollard sandstones include smectite and kaolinite followed by smectite/illite (Fig. 22 a, b), whereas the Coalspur and Willow Creek sandstones are dominated by dickite, chlorite, chlorite/smectite, smectite and kaolinite followed by illite/smectite (Figs. 22 c, d, e, f). Other authigenic minerals such as albite and quartz overgrowths are also observed in some of the Coalspur and Willow Creek sandstones (Fig. 23 a, b).

### *Kaolin*

Two types of authigenic kaolin were recognized in the sandstones: kaolinite and dickite. Kaolinite occurs as pore-filling cement and is one of the most important diagenetic clay minerals in the sandstones of the Plains and Foothills regions. Kaolinite is formed authigenically in the sandstones as indicated by vermicular stacks of pseudohexagonal

crystals (Fig. 22 b). Kaolinite forms in fluvial sandstones from the dissolution or alteration of aluminosilicate minerals such as feldspar aided by the action of low-pH meteoric water discharged at a shallow depth (Sieffermann et al., 1968; Chamely, 1968; Bjørlykke and Aagaard, 1992).

A precise determination of the timing of kaolinitization is difficult due to the complex burial history of the sandstones. Kaolinitization in the sandstones may have occurred during eodiagenesis and teleodiagenesis that followed Tertiary uplift. During burial diagenesis, most of the kaolinite may alter to illite or change to well-ordered kaolinite and blocky dickite through dissolution and reprecipitation, as indicated by the SEM and XRD data (Fig. 22). Lanson et al. (2002) showed that kaolinite and dickite are genetically linked and that kaolinite progressively converts to coarse and blocky dickite as burial depth and temperature increase. Thus, dickite is commonly interpreted as the stable kaolin polytype in deeply buried sandstones (Zotov et al., 1998).

### *Dickite*

The relative proportion of dickite is highly variable. In the Willow Creek sandstones, dickite is abundant (Figs. 20, 21). In the Coalspur sandstones, dickite is found in all localities except the Red Deer River Valley Section 2 and the roadcut near Highway 22, probably due to the influence of different types of fluid chemistry on the sandstones.

In the Coalspur sandstones, most of the dickite, which is observed above the coal zone, formed during deep burial from progressive conversion of early kaolinite. The formation of early diagenetic kaolinite is probably due to the invasion of organic acid into the



sandstones during coalification (Bjørkum et al., 1990; Ehrenberg et al., 1993; Ganor et al., 1995; Beaufort et al., 1998; Cassagnabère et al., 1999).

### *Smectite*

Smectite forms in non-marine settings at a lower temperature and shallower burial depth than dickite, either under arid climatic conditions or in sandstones with a relatively high volcanoclastic content (Velde, 1985). Smectite is the dominant clay mineral in the Scollard sandstones and is highly crenulated with interlocking crystals. The crystals have an irregular, wavy, plate or sheet-like architecture (Fig. 22 a) and occur as authigenic pore-lining minerals (Lerbekmo, 1957). Smectite is also observed to a lesser abundance in the Coalspur and Willow Creek sandstones (Figs. 20, 21). Most of the smectite rims exhibit a preferred orientation perpendicular to the grain surface, or as flakes curling up from an attachment zone on the detrital sand grain surface, indicating an authigenic origin (Wilson and Pittman, 1977). During progressive burial, most of the smectite changes into illite and/or chlorite via mixed layers of illite/smectite or chlorite/smectite (Fig. 22 d). Burst (1969) and Perry and Hower (1970) have also suggested that increased burial temperatures transform smectite to illite or chlorite.

### *Illite*

Illite occurs as flakes, filaments or hair-like crystals (Fig. 22 f) and typically begins to form during burial at temperatures exceeding 70°C (Bjørlykke, 1994). The SEM images show that authigenic illite growth is closely associated with smectite (Fig. 22 f). The rate of illitization of smectite depends on the supply of potassium (K) (Hower et

al., 1976) and requires a relatively high temperature (Bjørlykke, 1989; Ehrenberg, 1990). As indicated by the SEM images, the source of potassium for illite formation is probably K-feldspar and smectite (Fig. 23 c). The presence of the honeycomb texture of illitic phases supports the conclusion that the illitization of early authigenic smectite involved an intermediate stage of mixed-layer illite/smectite (Fig. 22 f).

The Scollard sandstones contain a smaller amount of authigenic illite compared with the Coalspur and Willow Creek sandstones (Khidir and Catuneanu, 2003; Figs. 22 f, 23 e). The increased proportion of illite in the Coalspur and Willow Creek formations is probably the result of greater subsidence and corresponding burial depth along the proximal side of the Alberta foredeep.

### *Chlorite*

Authigenic chlorite occurs as grain-coating and/or pore-filling cement in the Coalspur and Willow Creek sandstones. Grain-coating chlorite occurs as interlocking crystals perpendicular to grain surfaces, whereas pore-filling chlorite cement consists of a cluster of rosettes of variable sizes (Fig. 22 c). The chlorite cement in the Coalspur sandstone consists generally of crystals thicker than 2  $\mu\text{m}$ , up to 10-15  $\mu\text{m}$  across. The development of chlorite grain-coating cements may be related to the abundant volcanic material in the sandstones and the increased burial depth and temperature (Hillier, 1994). Volcanic glass is metastable and transforms rapidly into smectite. During deep burial diagenesis most of the smectite transforms into chlorite rather than illite, as indicated by the presence of mixed layer chlorite/smectite (Fig. 22 d). A number of authors studying

different sedimentary basins have described the transformation of smectite into chlorite via a chlorite-smectite phase (Dunoyer de Segonzac, 1970; Helmold and Van De Kamp, 1984; Humphreys et al., 1993).

## **Discussion:**

### **Authigenic Minerals and Maximum Burial Depths**

#### *Kaolinite-dickite transformation*

The kaolinite-dickite transition has long been recognized as being related to increasing depth of burial in sedimentary successions (Smithson, 1954; Dunoyer de Segonzac, 1970). In recent years, more studies on the details of this process have been published (Scotchman et al., 1989; Harris, 1992; Ehrenberg et al., 1993; Macaulay et al., 1993; Stewart et al., 1994; Beaufort et al., 1998). The kaolinite-dickite transformation is often interpreted as a dissolution-precipitation reaction that appears to be temperature-dependent (Ehrenberg et al., 1993). A clear modification of the morphology of kaolinite occurs with a progressive increase in burial depth and temperature from vermicular, low-temperature forms of kaolinite to the higher-temperature form, blocky dickite (Beaufort et al., 1998). Dickite progressively replaces kaolinite at a burial depth of 2 to 3 km corresponding to 70 to 90° C (Beaufort et al., 1998). At a burial depth between 3.0 and 4.5 km (90 to 130° C) most of the early kaolinite is subject to dissolution and precipitation as blocky dickite (Worden and Morad, 2003). Lanson et al. (2002) suggested that the presence of blocky crystals between stacks of partly dissolved kaolin plates is more frequent as the burial depth reaches ~3500 m. At a burial depth >4.5 km (>130°C), dickite transforms into more isometric blocky crystals (Beaufort et al., 1998).

The wide spread development of dickite (Fig. 23 d) in the Coalspur and Willow Creek sandstones is interpreted to suggest that the maximum burial depth of the sandstones in the Foothills region and in southwestern Alberta prior to Tertiary uplift and erosion was greater than in the Plains region of central Alberta (Fig. 24). The distribution of kaolin clay minerals (dickite and kaolinite) throughout the study area reveals a pattern of decreasing maximum burial from the thrust front toward the more distal part of the foreland basin. The paleogeothermal gradient for the present-day Foothills region is approximated to have been about 30°C/km (Hitchon, 1984; Bachu and Burwash, 1991); thus, the maximum burial depth needed for dickite formation ranges from 3 to 4 km (Fig. 24).

#### *Illite*

Illite begins to form from the dissolution of smectite during burial via mixed layers of illite/smectite at temperatures estimated by various authors as: >70° C (Bjørlykke, 1998), ~95° C (Perry and Hower, 1970), 90–110° C (Chang et al., 1986), or 100–110° C (Pearson and Small, 1988). Illite formation strongly increases in sandstones buried deeper than 3.8 - 4 km, corresponding to 120–140° C (Bjorkum and Gjelsvik, 1988; Ehrenberg and Nadeau, 1989; Bjørlykke and Aagaard, 1992; Ehrenberg, 1990; Giles et al., 1992).

The occurrence of fibrous illite (Fig. 23 e) in the Coalspur and Willow Creek sandstones confirms a late diagenetic origin and is taken to suggest that illite was exposed to a maximum burial temperature of more than 105° C (Wiebel, 1999). In contrast, the limited conversion of smectite into illite in the Scollard sandstones (Khidir and Catuneanu,

2003) suggests that the maximum burial depth in the Plains region was less than 1.5 km, corresponding to about 50° C.

### *Chlorite*

Hillier (1994) and Worden and Morad (2003) suggest a deep burial origin for chlorite. These researchers indicated that a complete transformation of Mg-rich clay minerals to chlorite by way of a mixed layer of chlorite-smectite occurs at a depth greater than 3 km during deep burial diagenesis. Thus, the presence of completely transformed chlorite in the Coalspur and Willow Creek sandstones (Fig. 23 f) suggests that the sandstones were buried deeper than 3 km (Hillier, 1994; Worden and Morad, 2003). Chlorite formation during deep burial is also indicated by the high crystallinity of the thick rim of chlorite crystals, which was observed in the Coalspur sandstones (Fig. 23 f). In the upper Coalspur sandstones of Sundre and Coalspur localities, chlorite is not present probably due to the absence of a source of Fe and Mg ions that are needed for chlorite formation or due to the instability of chlorite in acidic environments.

### *Quartz overgrowth*

Generally, quartz cement (Fig. 23 b) is more abundant in the Coalspur and Willow Creek sandstones than in the Scollard sandstones, probably due to increased burial temperatures. Quartz cement commonly occurs where sandstones are buried deeper than 3 km, corresponding to >70° C (McBride, 1989; Giles et al., 1992; Worden and Morad, 2000; Salem et al., 2000). Therefore, the occurrence of silica cementation in the Coalspur

and Willow Creek formations suggests that the sandstones were buried deeper than 3 km, corresponding to  $>70^{\circ}\text{C}$  (McBride, 1989; Giles et al., 1992).

#### *Albitization of feldspar*

The K-feldspar grains in the Scollard sandstones are only slightly albitized (Khidir and Catuneanu, 2003), whereas the sandstones of the Coalspur and Willow Creek formations are strongly albitized (Fig. 23 a). Although the process of formation of albite cements (i.e., albitization) may occur during both early and late diagenesis, a deeper burial diagenetic origin of albite in the sandstones is supported by the growth of euhedral albite on numerous sites of the host feldspar and by the continued growth of replacement albite into adjacent pores (Fig. 23 a) (Lerbekmo, 1963; Chowdhury and Noble, 1993). The Willow Creek and Coalspur formations are interpreted to have entered a deep-burial environment based on the presence of euhedral albite, which forms at temperatures higher than  $100^{\circ}\text{C}$  (Walker, 1984; Morad et al., 1990; Bjorkum et al., 1993; De Ros, 1998). This observation is in agreement with the diagenetic development of the other authigenic clay minerals that have been studied and discussed above. Reconstructed overburden and burial depth of Cretaceous and Tertiary Plains Coal of Alberta by Nurkowski (1984) indicated erosion had removed between 900 and 1.900 m of sediment, with greatest amount of removal occurring in west-southwest direction. This finding is well matched with our finding.

### *Summary of Discussion*

The morphological changes recorded by the kaolin minerals and the progressive transformation of smectite to fibrous illite or chlorite via mixed-layers (I/S) or (C/S), suggest that the sandstones of the Coalspur and Willow Creek formations were subject to a maximum burial depth of 2 to 4 km, corresponding to a temperature of 70–140° C. The Scollard sandstones were subject to a shallower burial depth, of less than 1.5 km, with a corresponding temperature of <80° C (Figs. 25, 26). This is in agreement with results published by other authors from the study of burial histories in a variety of sedimentary basins (Bjorlykke and Aagaard, 1992; Ehrenberg et al., 1993; Beaufort et al., 1998, Lanson et al., 2002). The current outcrop distribution of authigenic minerals in the Alberta foreland basin indicates that about 1 to 1.5 km of sediments have been eroded from the Plains region, and 3 to 3.5 km of strata have been removed from the Foothills region (Fig. 26). The study of coal quality and its relation to reconstructed overburden and burial depth of Cretaceous and Tertiary Plains Coal of Alberta by Nurkowski (1984) had indicated that erosion had removed between 900 and 1,900 m of sediment, with greatest amount of removal occurring in west-southwest direction. This result is comparable with our finding.

### **Conclusions**

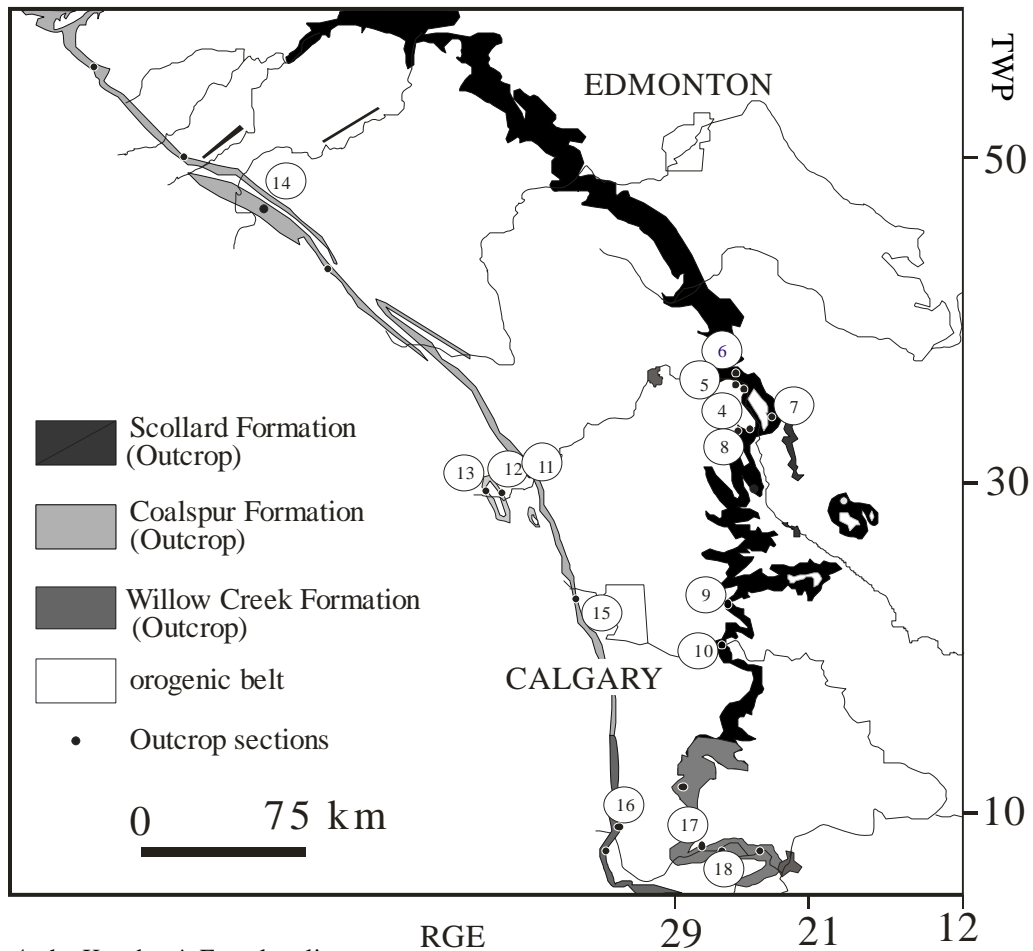
1. The distribution of authigenic clay minerals, as well as the degree and history of diagenetic alteration within the late Maastrichtian-early Paleocene sandstones vary with the geographic location across the Alberta foredeep. In the Scollard Formation, the authigenic clay minerals are represented mainly by smectite and kaolinite. In contrast, the

Coalspur and Willow Creek formations display a wider range of authigenic clays, including smectite, kaolinite, dickite, chlorite, chlorite/smectite, illite and illite/smectite.

2. The Scollard sandstones were buried to a depth of less than 1.5 km, corresponding to a burial temperature of no more than 70° C. This conclusion is supported by the limited conversion of smectite to illite; the absence of authigenic dickite; and the weak albitization of K-feldspar coupled with limited precipitation of silica cements.

3. The abundance of blocky dickite, illite and chlorite suggest that the Willow Creek and Coalspur sandstones were buried deeper than 3 km. The morphological characteristics of dickite, chlorite, and illite crystals suggest a maximum burial depth of approximately 3 – 4 km, corresponding to 90 – 120° C. This conclusion is also supported by the albitization of K-feldspar and by the development quartz overgrowths within the sandstones.





- 4- the Knudsen's Farm locality
- 5- the Buffalo Jump Provincial Park locality
- 6- the Ardley locality
- 7- the Griffith's Farm locality
- 8- the Kneehills Creek locality
- 9- the Hummer Hills locality
- 10- the Bow River locality
- 11- the Sundre locality
- 12- the Red Deer River Valley section1
- 13- the Red Deer River Valley section 2
- 14- the Coalspur locality
- 15- the roadcut near Highway 22
- 16- the Oldman River
- 17- the Oldman River Dam Reservoir
- 18- the Oldman River locality

Figure 1. Outcrop distribution of the Scollard, Coalspur, and Willow Creek formations in Alberta, and the location of the outcrop sections.

Age	Stratigraphic units						
Paleocene	Southern Foothills		Plains		Central Foothills		
	Porcupine Hills Formation		Paskapoo Formation				
Maastrichtian	Willow Creek Formation	upper Willow Creek	Scollard Formation	upper Scollard	Coalspur Formation	Val d'Or	
		lower Willow Creek		lower Scollard		lower Coalspur	Arbour
Campanian	St. Mary River Formation			Ardley	Coalspur Formation	Mynheer	
				Nevis		Entrance Member	
	Bearpaw Formation		Battle Formation				
			Whitemud Formation				
Belly River Group		Horseshoe Canyon Formation				Brazeau Formation	
		Bearpaw Formation					
		Belly River Group					

Figure 2. Generalized chart of the late Campanian to Paleocene stratigraphy of west-central Alberta, showing the position of the Scollard, Coalspur and Willow Creek formations (after Dawson et al., 1994).

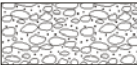
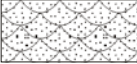
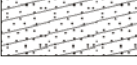



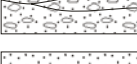

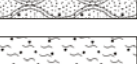


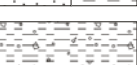





Facies	Facies code and symbol	Sedimentary structures	
Gh		Clast-supported, crudely bedded gravel	Horizontal bedding, imbrication
St		Sandstone, fine to very coarse, may be pebbly	Solitary or grouped trough cross-beds
Sp		Sandstone, fine to very coarse, may be pebbly	Solitary or grouped planar cross-beds
Sr		Sandstone, very fine to coarse	Ripple cross-lamination
Sh		Sandstone, very fine to coarse, may be pebbly	Horizontal lamination, parting or streaming lineation
Sl		Sandstone, very fine to coarse, may be pebbly	Low-angle (<15°) cross-beds
Ss		Sandstone, fine to very coarse, may be pebbly	Broad, shallow scours
Sm		Sandstone, fine to coarse	Massive or faint lamination
Sb		Sandstone, fine to very coarse, may be pebbly	Ball-and-pillow structure, may show internal lamination
Sf		Sandstone, fine to coarse with mud	Massive, may be laminated
Fl		Sandstone, siltstone, mudstone	Fine lamination, very small ripples
Fsm		Siltstone, mudstone	Massive
Fp		Mudstone with pebbles	Vague laminated mudstone with floating, isolated clasts
Fs		Mudstone with sand, fine to coarse	Massive, may be laminated
Fb		Mudstone, siltstone	Ball-and-pillow structure, may show internal lamination
Fm		Mudstone, siltstone	Massive, desiccation cracks
C		Coal, carbonaceous mudstone	Plant, mudstone films

Figure 3. Facies codes used to describe the sedimentological characteristics of the studied outcrop sections (Figs. 4-18).

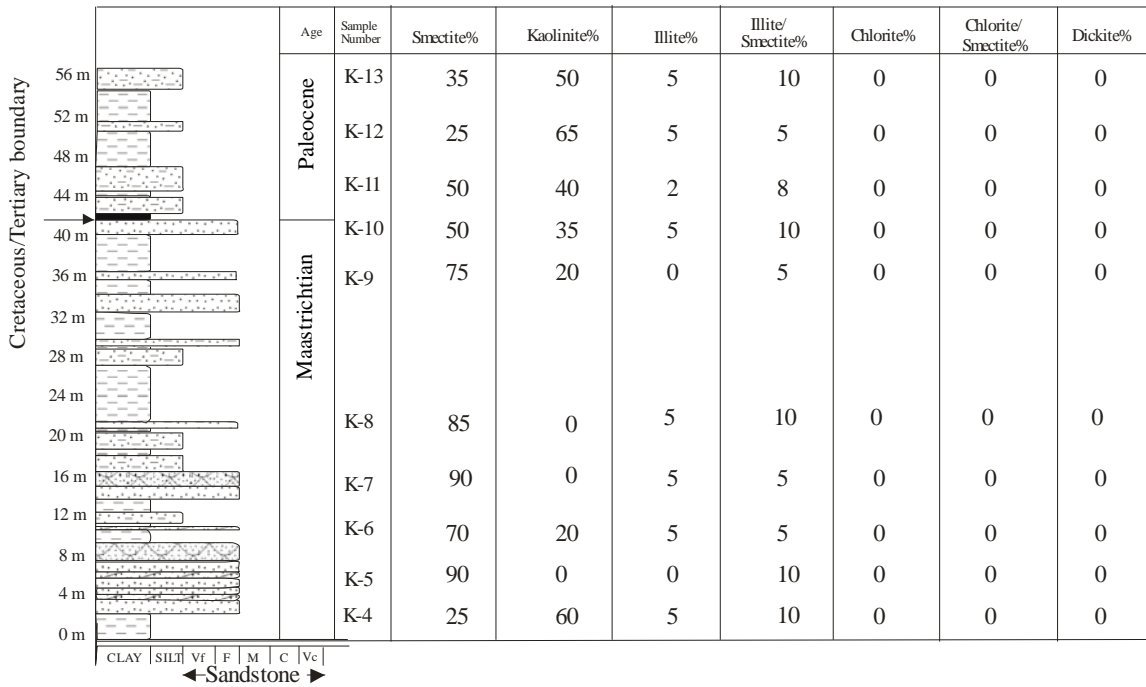


Figure 4. Vertical profile for the Knudsen's Farm locality, Scollard Formation. The table shows the sandstone composition in terms of relative percentages of the main authigenic clay minerals.

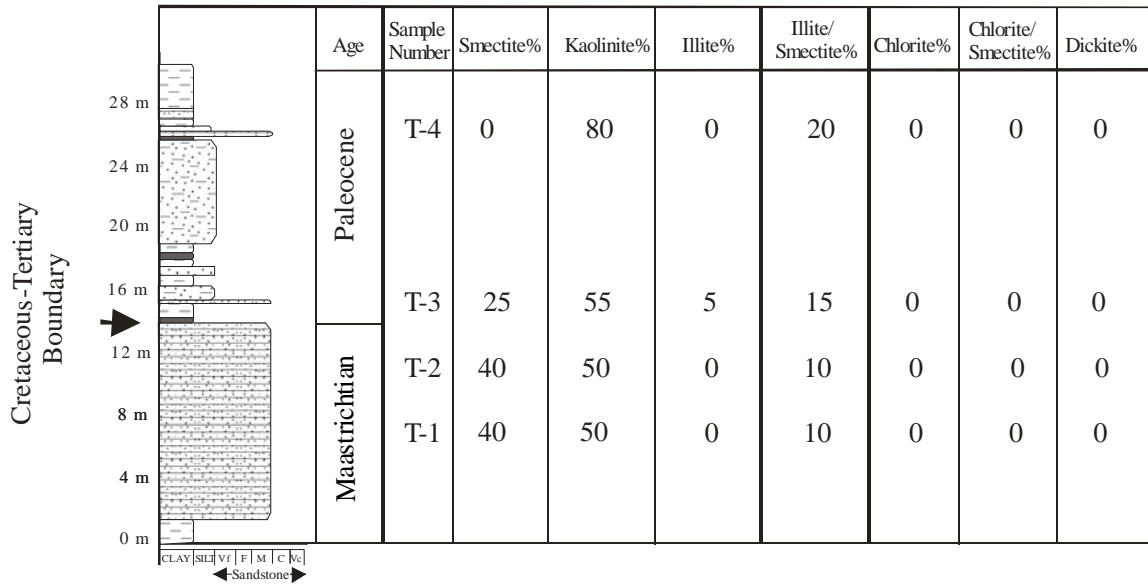


Figure 5. Vertical profile for the Buffalo Jump Provincial Park locality, Scollard Formation. The table shows the sandstone composition in terms of relative percentages of the main authigenic clay minerals.

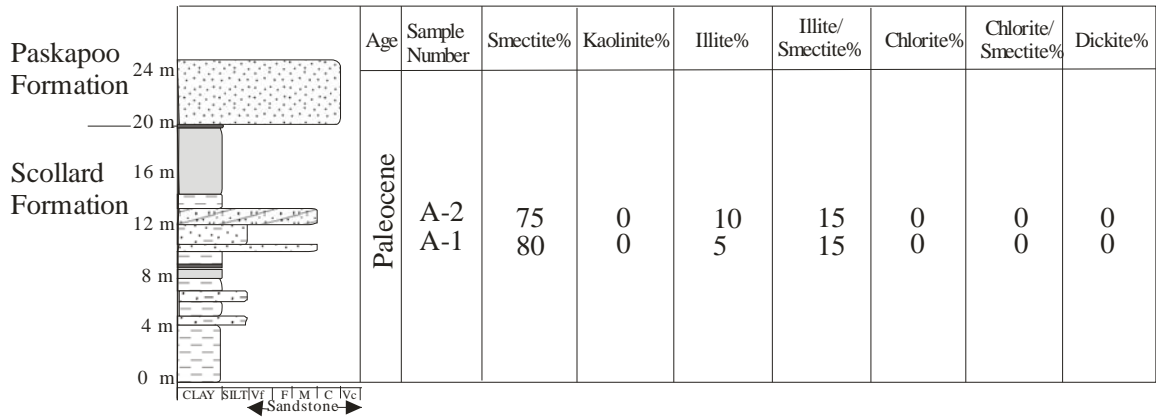


Figure 6. Vertical profile for the Ardley locality, upper Scollard Formation. The table shows the sandstone composition in terms of relative percentages of the main authigenic clay minerals.

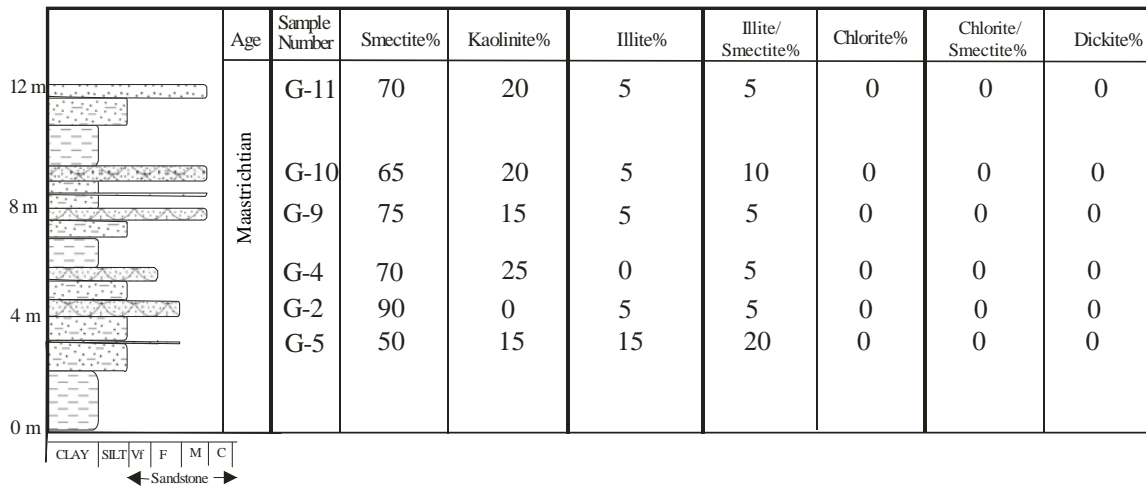


Figure 7. Vertical profile for the Griffith's Farm locality, lower Scollard Formation. The table shows the sandstone composition in terms of relative percentages of the main authigenic clay minerals. Zero datum is the base of the outcrop section which is the Maastrichtian part of the lower Scollard Formation.

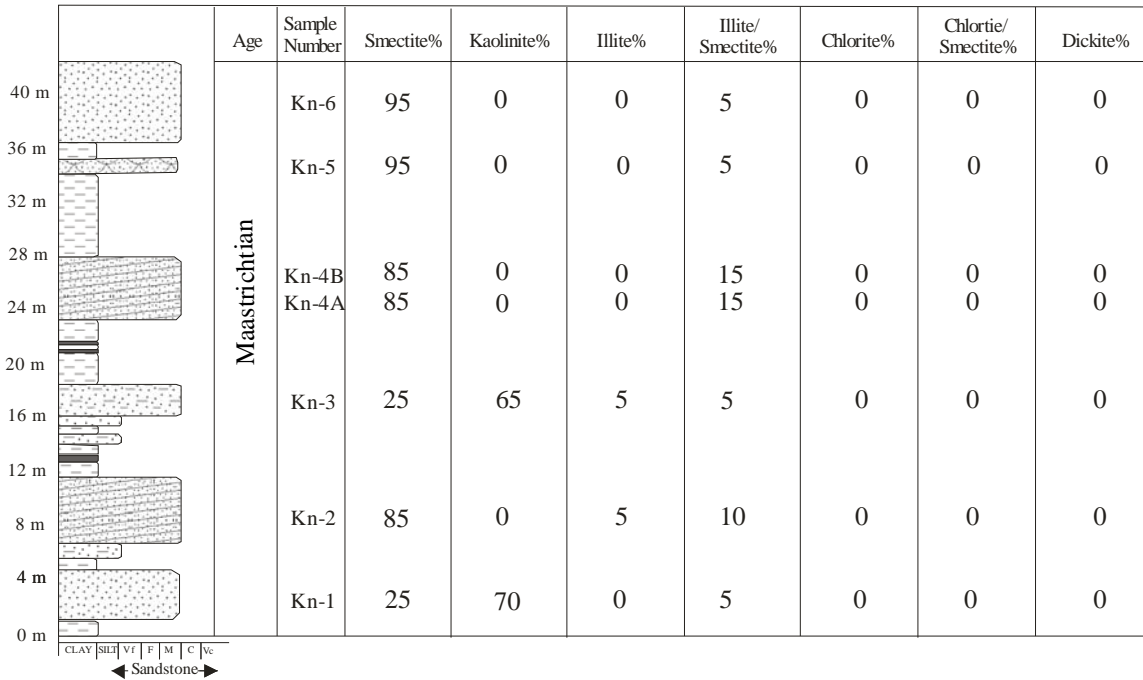


Figure 8. Vertical profile for the Kneehills Creek locality, Lower Scollard Formation. The table shows the sandstone composition in terms of relative percentages of the main authigenic clay minerals. Zero datum is the base of the outcrop section in the study area which is the Maastrichtian part of the Scollard Formation.



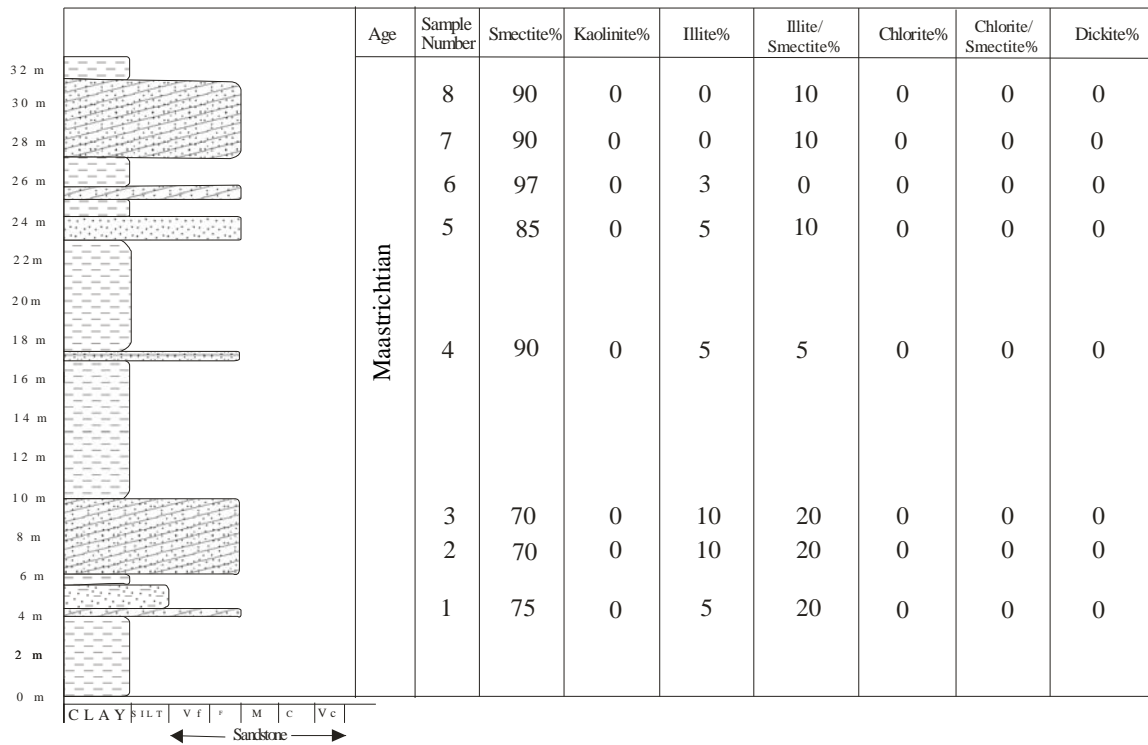


Figure 9. Vertical profile for the Hummer Hills locality, lower Scollard Formation. The table shows the sandstone composition in terms of relative percentages of the main authigenic clay minerals. Zero datum is the base of the outcrop section in the study area which is the Maastrichtian part of the Scollard Formation.

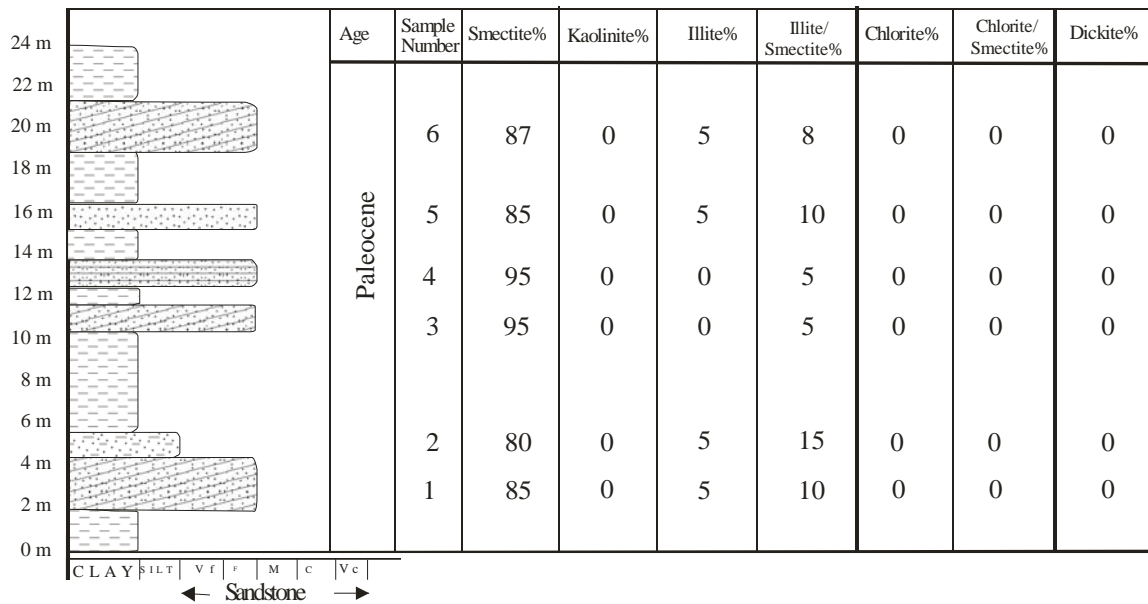


Figure 10. Vertical profile for the Bow River locality, upper Scollard Formation. The table shows the sandstone composition in terms of relative percentages of the main authigenic clay minerals. Zero datum is the base of the outcrop section in the study area which is the upper, Paleocene part of the Scollard Formation.

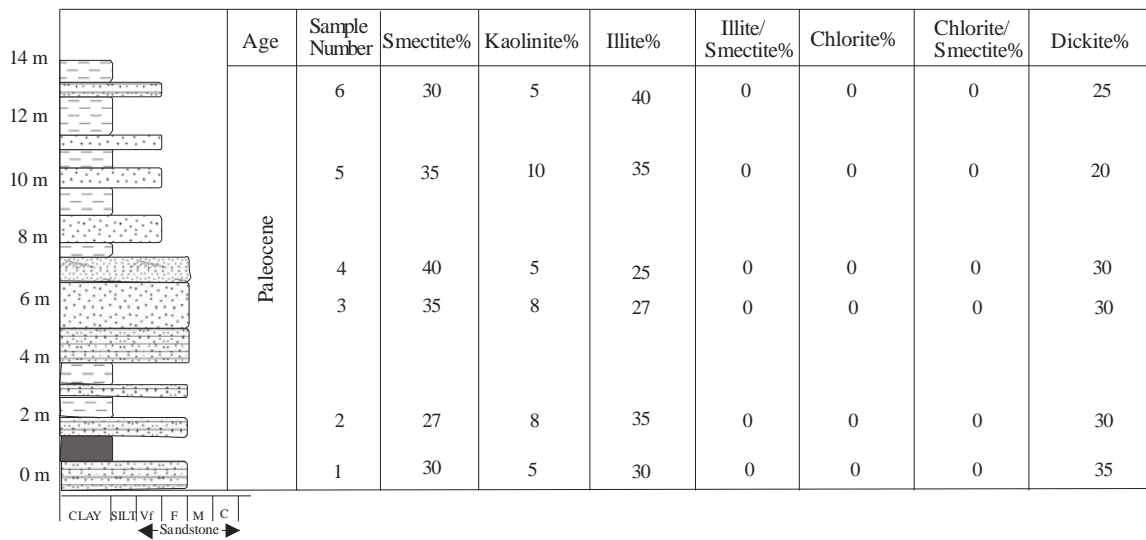


Figure 11. Vertical profile for the Sundre locality, upper Coalspur Formation. The table shows the sandstone composition in terms of relative percentages of the main authigenic clay minerals. Zero datum is the base of the outcrop section in the study area which is the upper, Paleocene part of the Coalspur Formation.

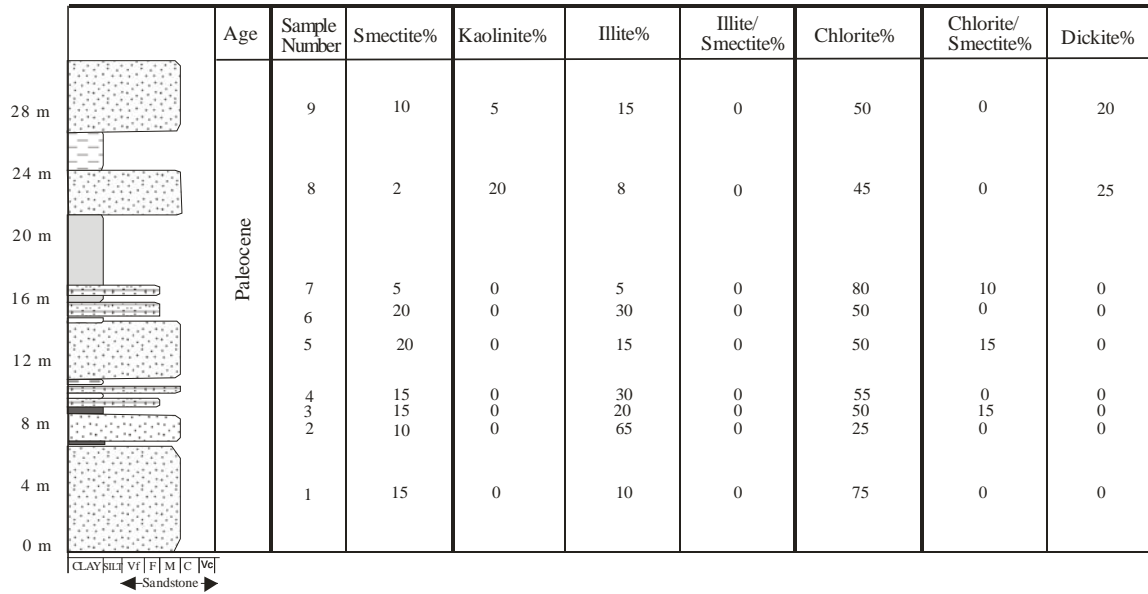


Figure 12. Vertical profile for the Red Deer River Valley section 1, upper Coalspur Formation. The table shows the sandstone composition in terms of relative percentages of the main authigenic clay minerals. Zero datum is the base of the outcrop section in the study area which is the upper, Paleocene part of the Coalspur Formation.

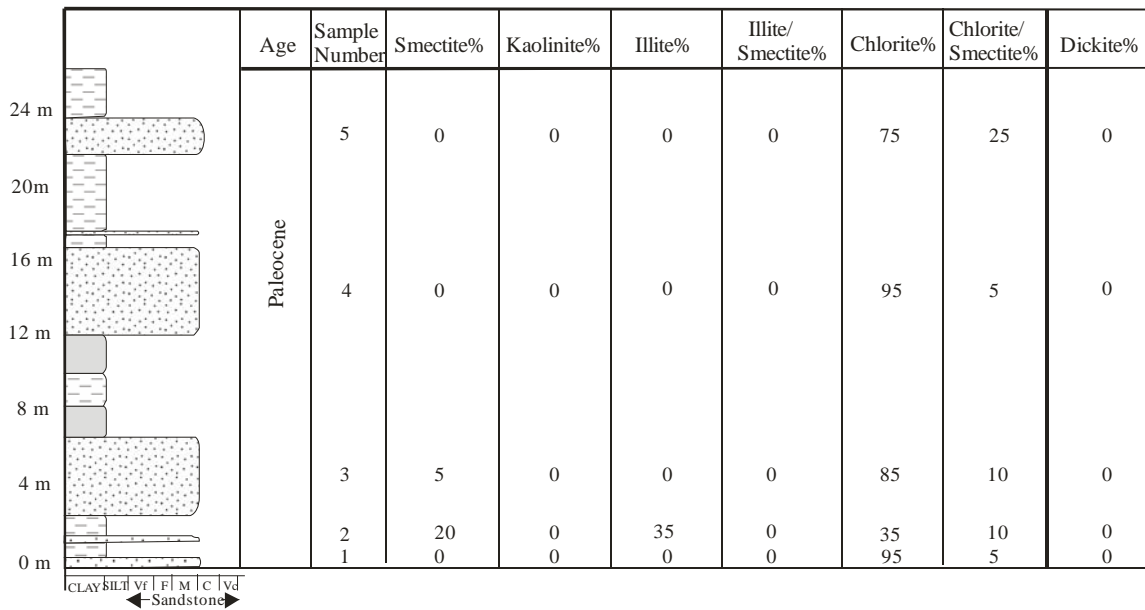


Figure 13. Vertical profile for the Red Deer River Valley section 2, upper Coalspur Formation. The table shows the sandstone composition in terms of relative percentages of the main authigenic clay minerals. Zero datum is the base of the outcrop section in the study area which is the upper, Paleocene part of the Coalspur Formation.

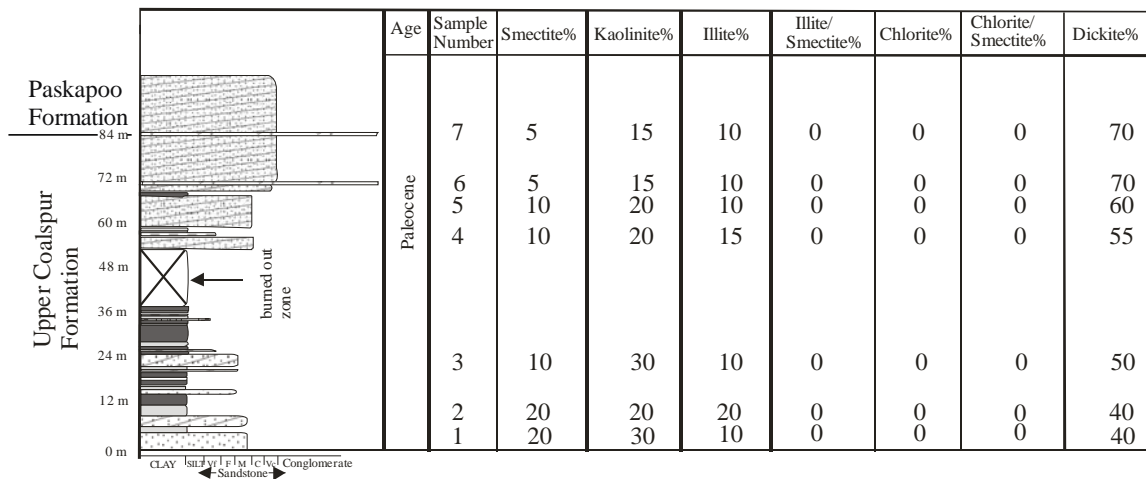


Figure 14. Vertical profile for the Coalspur locality, upper Coalspur Formation. The table shows the sandstone composition in terms of relative percentages of the main authigenic clay minerals.

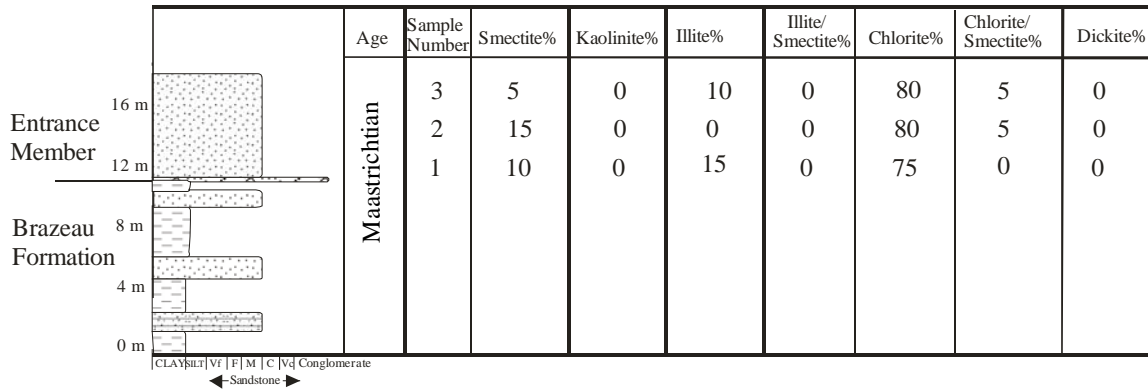


Figure 15. Vertical profile for the old roadcut near Highway 22, lower Coalspur Formation. The table shows the sandstone composition in terms of relative percentages of the main authigenic clay minerals. Zero datum is the base of the outcrop section in the study area.

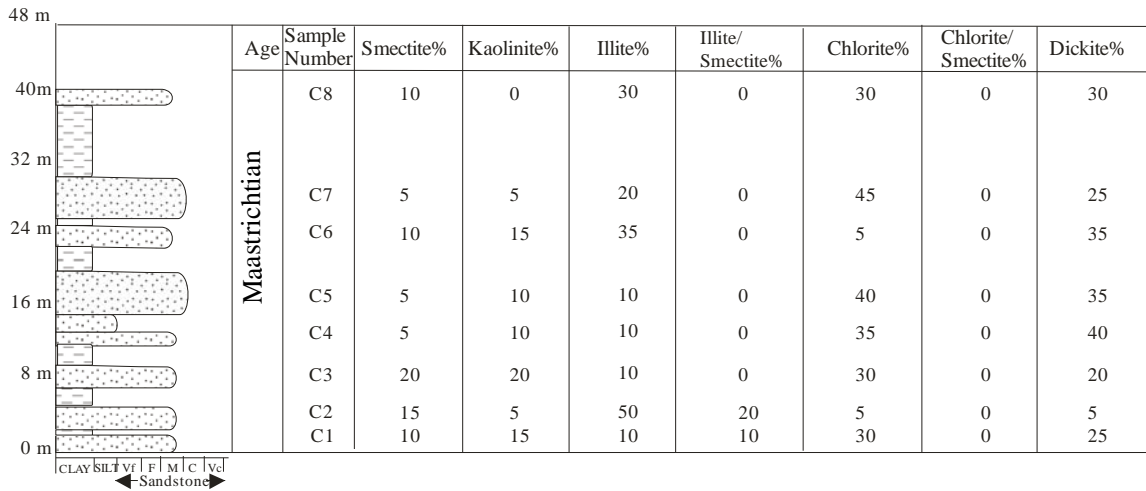


Figure 16. Vertical profile for the Oldman River, lower Willow Creek Formation. The table shows the sandstone composition in terms of relative percentages of the main authigenic clay minerals. Zero datum is the base of the outcrop section in the study area which is the lower, Maastrichtian part of the Willow Creek Formation.



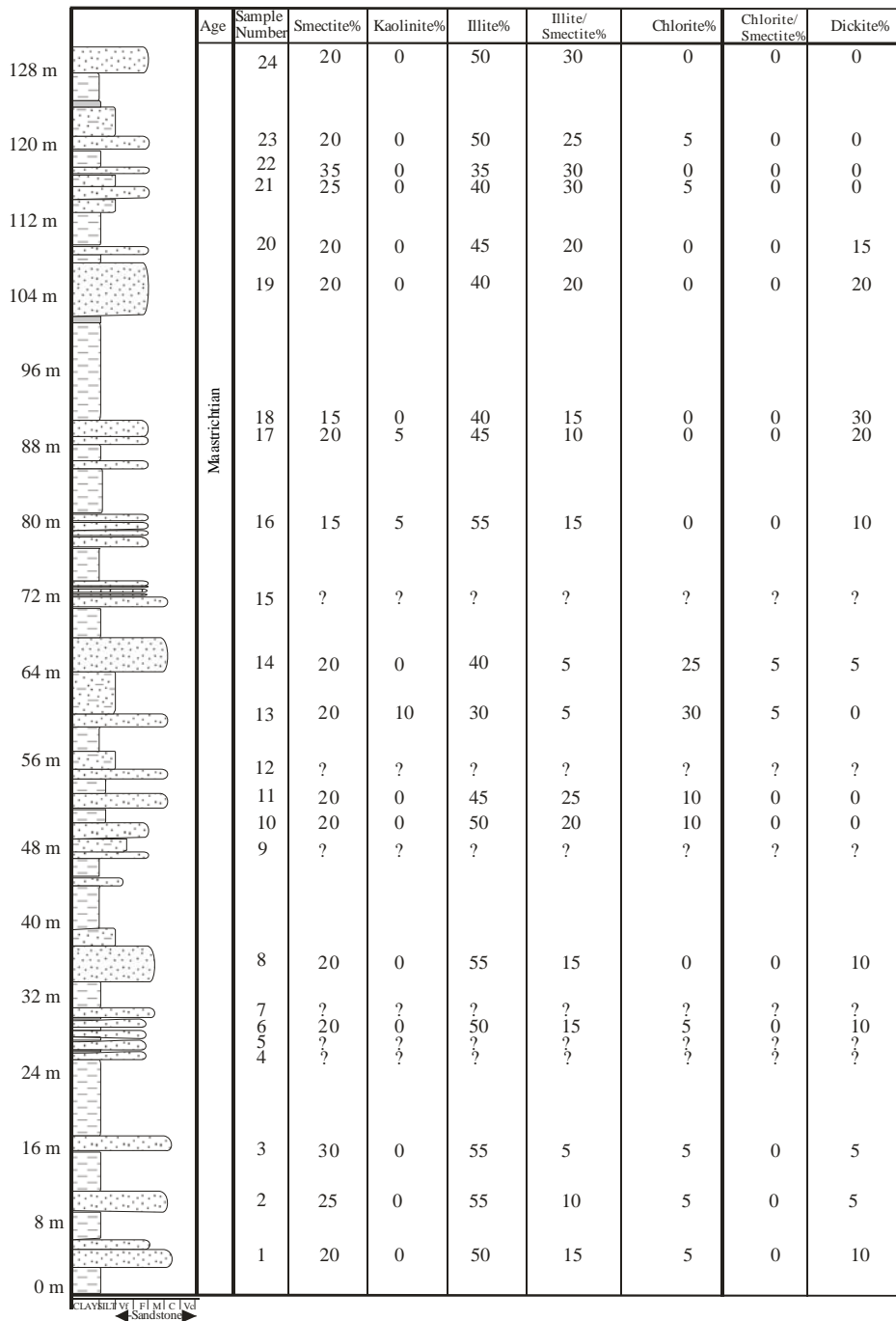


Figure 17. Vertical profile for the Oldman River Dam Reservoir, lower Willow Creek Formation (Maastrichtian). The table shows the sandstone composition in terms of relative percentages of the main authigenic clay minerals. Zero datum is the base of the outcrop section.

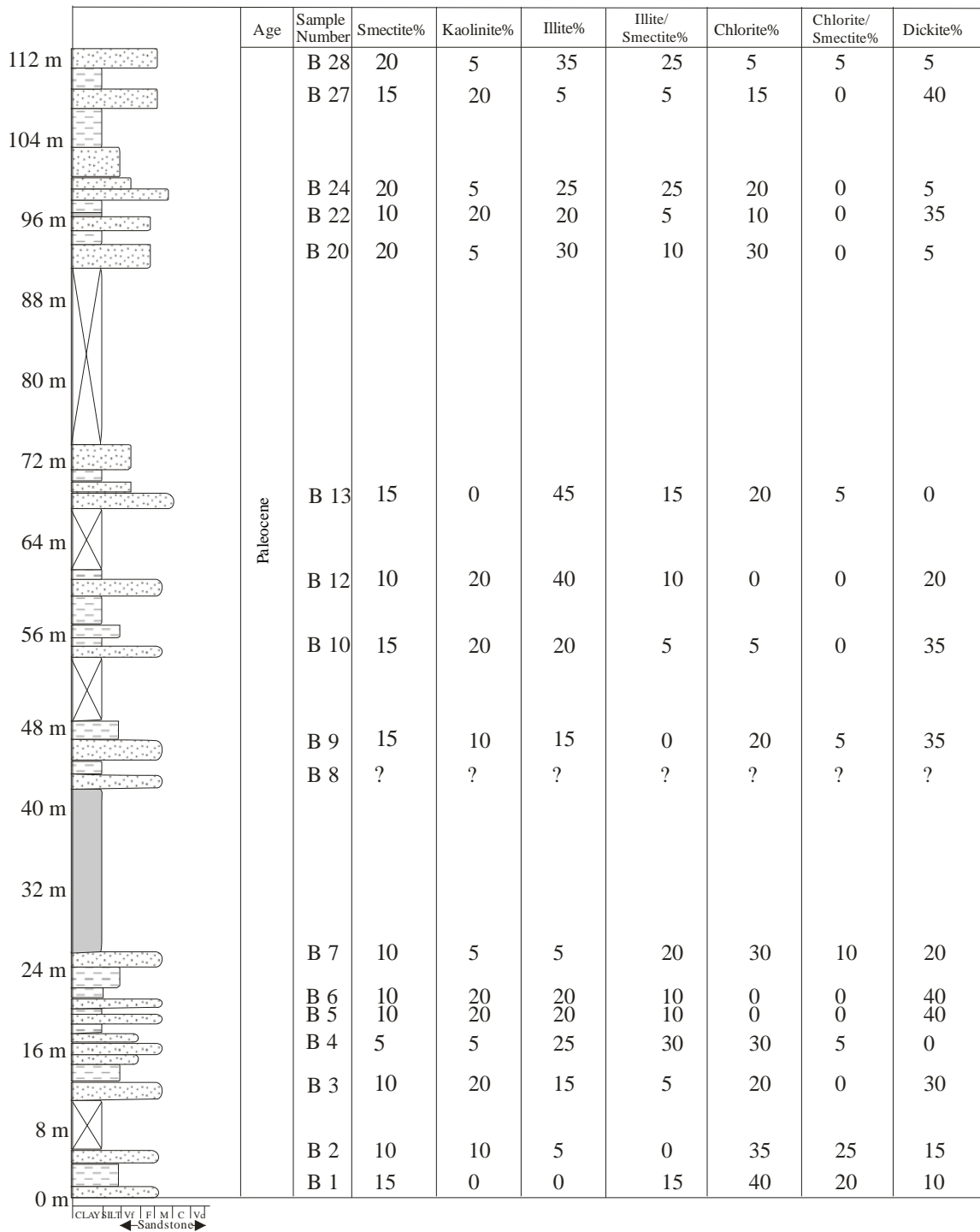


Figure 18. Vertical profile for the Oldman River locality, upper Willow Creek Formation (Paleocene). The table shows the sandstone composition in terms of relative percentages of the main authigenic clay minerals. Zero datum is the base of the outcrop section.

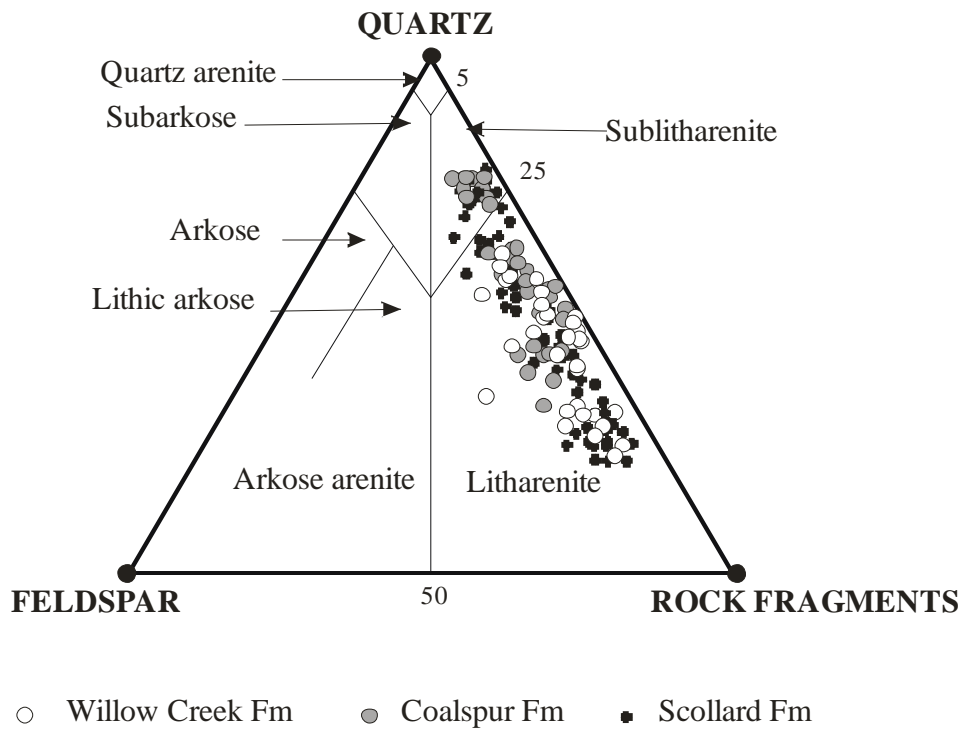


Figure 19. Classification of the Scollard, Coalspur, and Willow Creek sandstones (after Pettijohn et al., 1987).

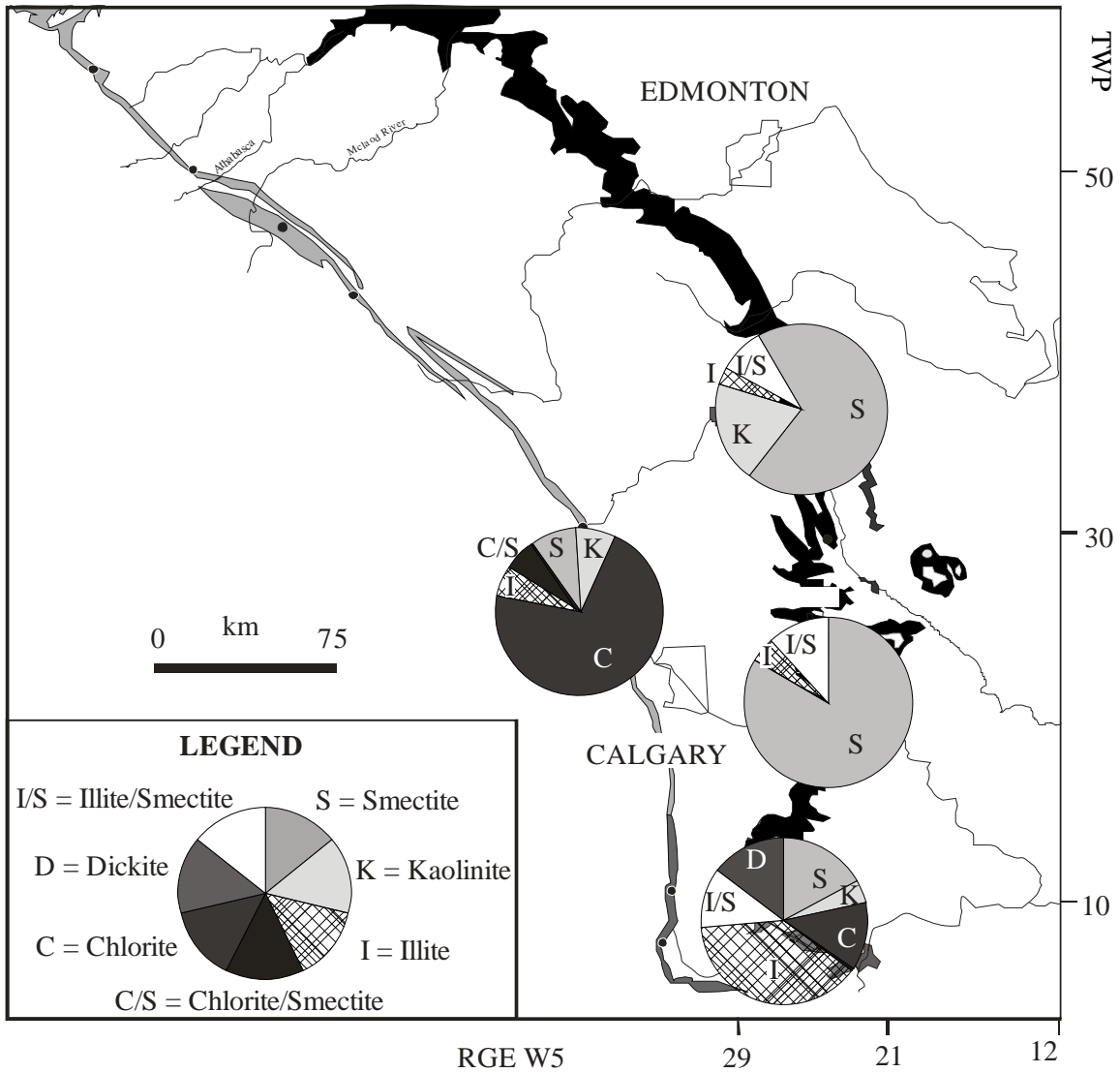


Figure 20. Authigenic clay mineral association in the Maastrichtian part of the Scollard, Coalspur and, Willow Creek formations. The pie charts show the average clay mineralogy in all investigated samples from each outcrop.

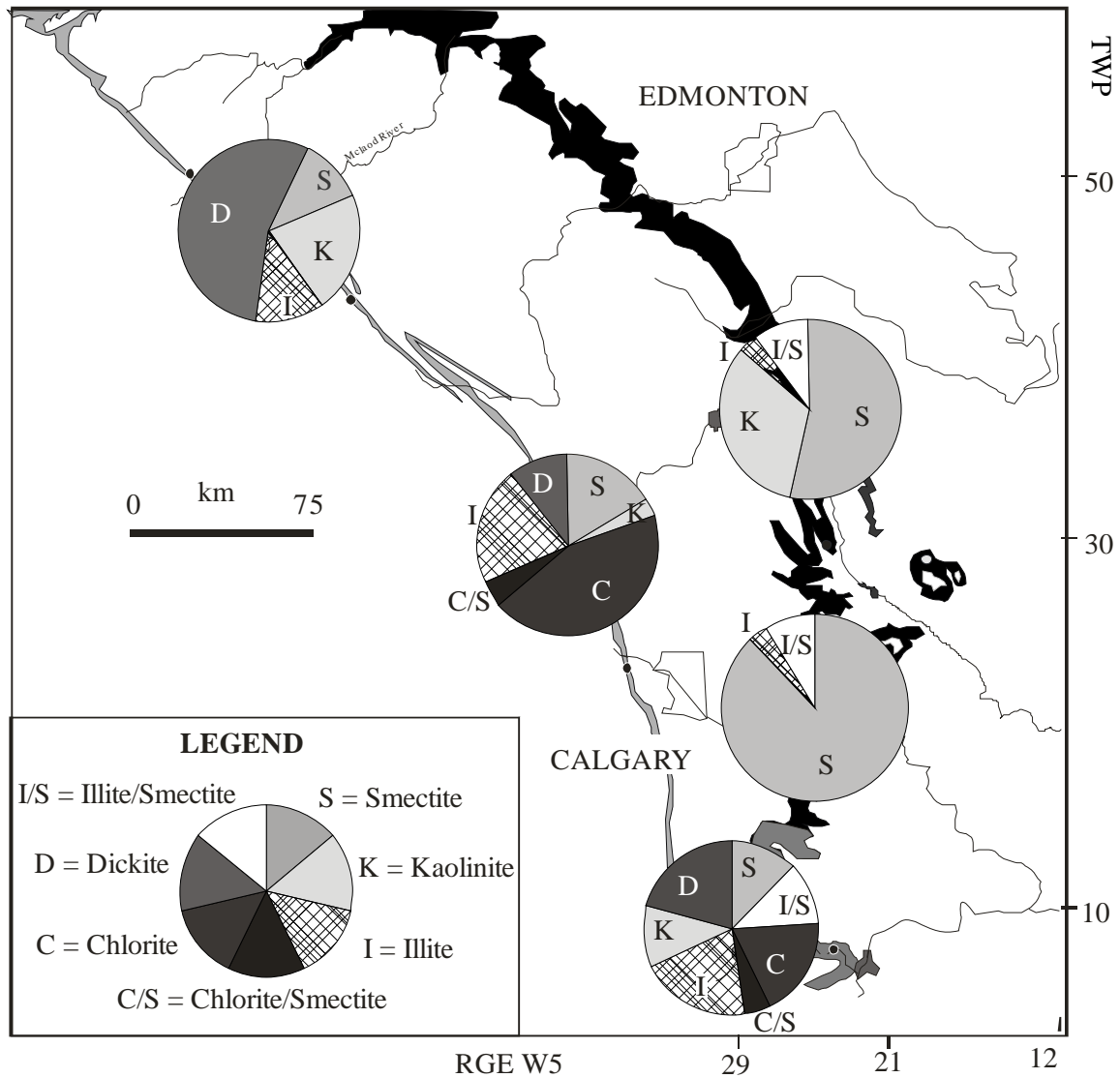


Figure 21. Authigenic clay mineral association in the Paleocene part of the Scollard, Coalspur, and Willow Creek formations. The pie charts show the average clay mineralogy in all investigated samples from each outcrop.

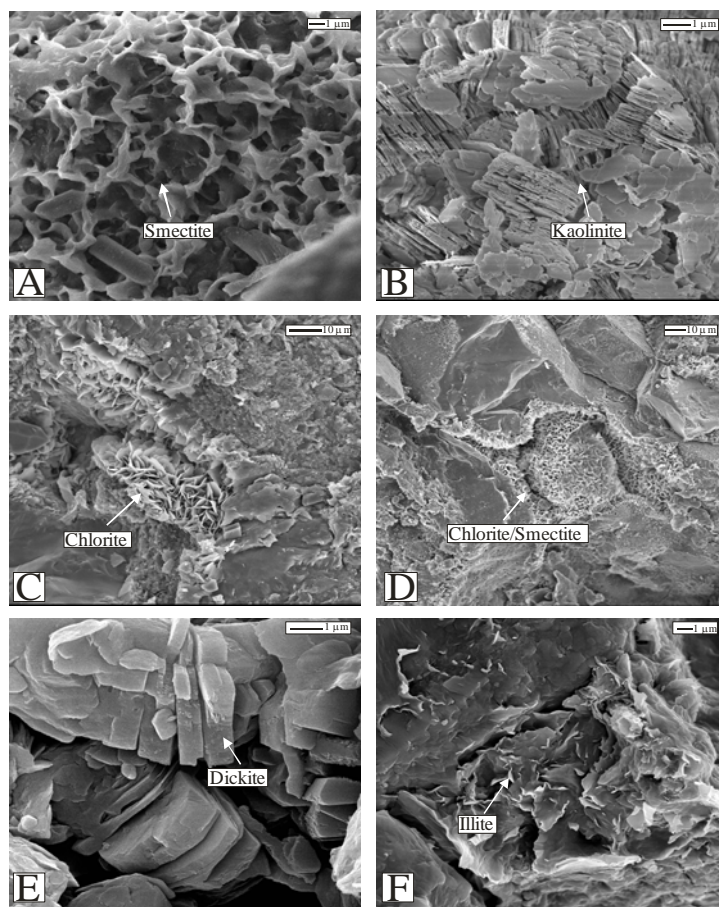


Figure 22. Scanning electron photomicrographs: (A) – authigenic pore-lining smectite; (sample Kn-5, lower Scollard Formation, Kneehills Creek locality); (B) – vermicular authigenic kaolinite (sample Kn-3, lower Scollard Formation, Kneehills Creek locality); (C) – late diagenetic chlorite (sample 7, upper Coalspur Formation, Red Deer River locality); (D) – authigenic chlorite/smectite clay (sample 8, upper Coalspur Formation, Red Deer River locality); (E) – Dickite formation during deep burial (sample C-2, lower Willow Creek Formation, Crowsnest River locality); (F) – authigenic illite formed as a late diagenetic clay (sample 7, upper Willow Creek Formation, Oldman Dam Reservoir locality).

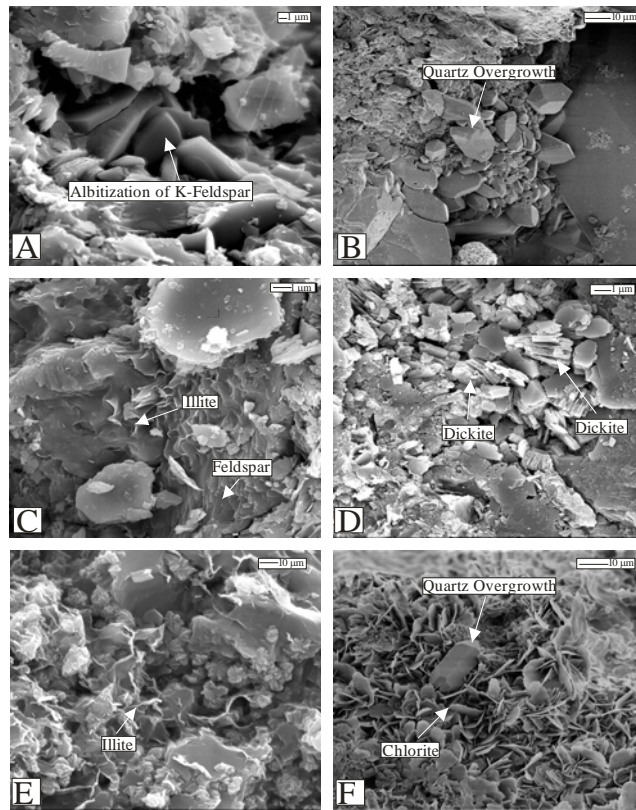


Figure 23. Scanning electron photomicrographs: (A) – euhedral growth of authigenic albite (sample D-1, lower Willow Creek Formation, Crowsnest River locality); (B) – euhedral growth of authigenic quartz (sample 14, upper Scollard Formation, Red Deer River section 1); (C) – intercalation of dickite crystals between stacks of partly dissolved kaolin plates which suggests that the sandstones underwent 3 to 4 Km of burial depth (Lanson, et al., 2002); (sample A-3, lower Willow Creek Formation, Oldman Reservoir Dam locality); (D) – fibrous authigenic illite on corroded feldspar grains (sample F-3, upper Willow Creek Formation, Oldman Dam Reservoir locality); (E) – authigenic illite. Note the fibrous nature of the authigenic illite (sample G-2, Willow Creek Formation, Crowsnest River locality); (F) – complete conversions of authigenic smectite to chlorite and euhedral quartz overgrowth (sample 10, upper Coalspur Formation, Red Deer River locality).

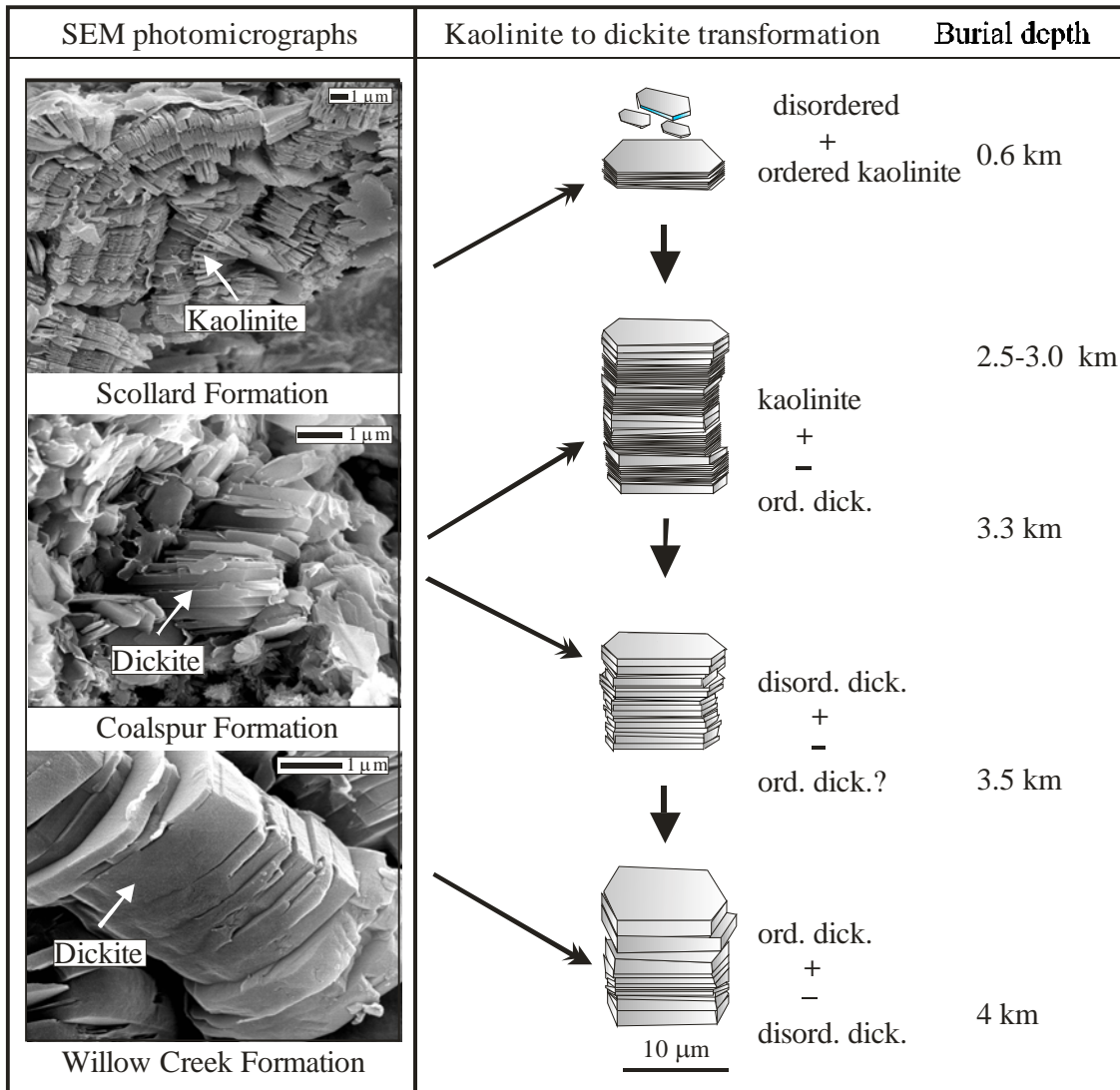


Figure 24. SEM photomicrographs and schematic model of kaolinite-to-dickite transformation showing the relationship to the maximum burial depth within the Scollard, Coalspur, and Willow Creek formations (modified from Beaufort et al., 1998).



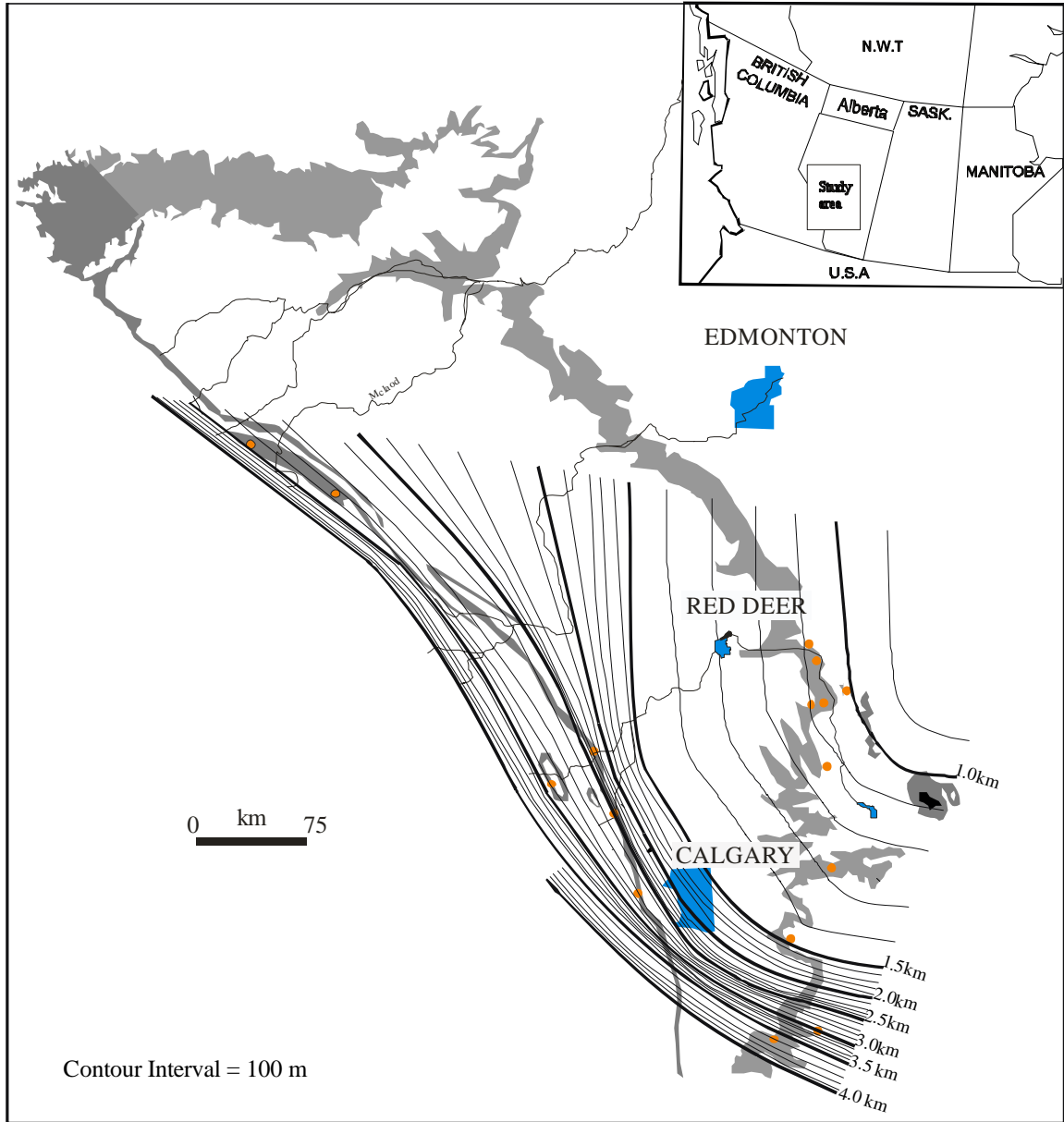


Figure 25. Contour map of the study area showing the maximum burial depth of the Scollard, Coalspur, and Willow Creek sandstones. This map is constructed based on relative abundance of authigenic minerals in the sandstones as a function of burial depth.

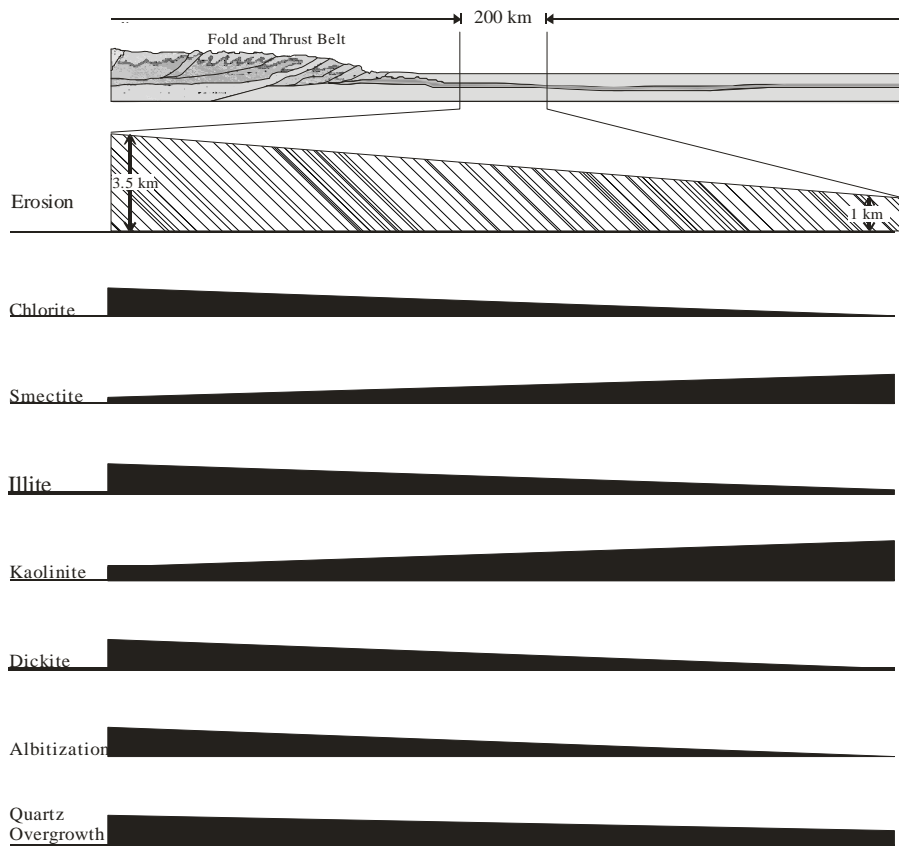


Figure 26. Schematic model showing the relative abundance of authigenic minerals in the Scollard sequence sandstones of west-central Alberta, and the amount of erosion that affected the Plains and the Foothills regions following the onset of isostatic rebound in the Tertiary.

## References

Bachu, S. and Burwash, R.A. 1991. Regional-scale analysis of the geothermal regime in the Western Canada Sedimentary Basin. *Geothermics*, v. 20(5/6), p. 387-407.

Beaufort, D., A. Cassagnabère, S. Petit, B. Lanson, G. Berger, J. C. Lachapagne, and Johansen, H. 1998. Kaolinite-to-dickite reaction in sandstone reservoirs, *Clay Minerals*, v. 33, p. 297-316.

Bjorkum, P.A. and Gjelsvik, N. 1988. An isochemical model for formation of authigenic kaolinite, k-feldspar, and illite in sediments. *Journal of Sedimentary Petrology*, v. 58, p. 506-511.

Bjorkum, P.A., Mjos, R., Walderhaug, O., and Hurst, A. 1990. The role of the late Cimmerian unconformity in controlling the distribution of kaolinite in the Gullfakes Field northern North Sea. *Journal of Sedimentology*, Volume 37, p. 395-406.

Bjorkum, P.A., Walderhaug, O., and Aase, N.E. 1993. A model for the effect of illitization on porosity and quartz cementation of sandstones. *Journal of Sedimentary Petrology*, v. 63, p. 1089–1091.

Bjørlykke, K. 1989. *Sedimentology and Petroleum Geology*. Springer-Verlag, Berlin. 363 pp.

Bjørlykke, K., 1994, Fluid-flow processes and diagenesis in sedimentary basins, In Parnell, J., ed., *Geofluids: Origin, Migration and Evolution of Fluids in Sedimentary Basins*: Geological Society of London, Special Publication 78, p. 127-140.

Bjørlykke, K. 1998. Clay mineral diagenesis in sedimentary basins- a key to prediction of rock properties. Examples from the North Sea Basin. *Clay Minerals*, v 33, p. 15-34.

Bjørlykke, K. and Aagaard, P. 1992. Clay minerals in North Sea sandstones. In: *Origin, diagenesis, and petrophysics of clay minerals in sandstone* (Houseknecht, D.W. and Pittman, E.D. (eds.), SEPM Special Publication 47, p. 65-80.

Burst, J.F. Jr. 1969. Diagenesis of Gulf Coast clayey sediments and its possible relation to petroleum migration, *American Association of Petroleum Geologist Bulletin*, v. 53, p. 73-93.

Bustin, R.M. 1992. Organic maturation of the Western Canadian Sedimentary Basin. *International Journal of Coal Geology*, v. 19, p. 319-358.

Carrigy, M.A. 1971. Lithostratigraphy of the uppermost Cretaceous (Lance) and Paleocene strata of the Alberta plains. *Research Council of Alberta Bulletin* 27, 161 p.

Cassagnabère A., Iden I.K., Johansen H., Lacharpagne J.-C. & Beaufort D. (1999) Kaolinite and dickite in Frøy and Rind sandstone hydrocarbon reservoirs of the Brent

Formation (Norwegian Continental Shelf). Pp. 97–102 in: Clays for our Future: Proceedings of the 11th International Clay Conference (H. Kodama et al., editors). ICC97 Organizing Committee, Ottawa.

Catuneanu, O. and Sweet, A.R. 1999. Maastrichtian-Paleocene foreland basin stratigraphies, Western Canada: A reciprocal sequence architecture. *Canadian Journal of Earth Sciences*, v. 36, p. 685-703.

Catuneanu, O., Sweet, A.R. and Miall, A.D. 2000. Reciprocal stratigraphy of the Campanian-Paleocene Western Interior of North America. *Sedimentary Geology*, v. 134, p. 235-255.

Chamely, H. 1968. La sédimentation argileuse actuelle en Méditerranée nord-occidentale. *Bulletin Société Géologique du France*, v. 10, p. 75-88.

Chang, H., Mackenzie, F.T. and Schoonmark, J. 1986. Comparisons between the diagenesis of dioctahedral and trioctahedral smectite, Brazilian offshore basins. *Clays and Clay Minerals*, v. 34, p. 407-423.

Chowdhury, A and Noble, J. 1993. Feldspar albitization and feldspar cementation in the Albert Formation reservoir sandstones, New Brunswick, Canada, *Marine and Petroleum Geology*, v. 10, p. 394-402.

Dawson, F.M., Evan, C.G., Marsh, R. and Richardson, R. 1994. Uppermost Cretaceous and Tertiary of the Western Canada Sedimentary Basin. In: Geological Atlas of the Western Canada Sedimentary Basin. G. Mossop and I. Shetsen (comps.). Canadian Society of Petroleum Geologists and Alberta Research Council, p. 387-406.

De Ros, L.F. 1998. Heterogeneous generation and evolution of diagenetic quartzarenites in the Silurian–Devonian Furnas Formation of the Parana Basin, southern Brazil. *Sedimentary Geology*, v. 116, p. 99–128.

Dunoyer de Segonzac, G. 1970. The transformation of clay minerals during diagenesis and low-grade metamorphism: a review. *Sedimentology*, v. 15, p. 281-326.

Eberth, D. and O'Connell, A. 1995. Note on changing paleoenvironments across the Cretaceous-Tertiary boundary (Scollard Formation) in the Red Deer River valley of southern Alberta. *Bulletin of Canadian Petroleum Geology*, v. 43. no. 1, p. 44-53.

Ehrenberg, S.N. 1990. Relation between diagenesis and reservoir quality in sandstone. *Bulletin of American Association of Petroleum Geologists*. v. 74, p. 1538-1559.

Ehrenberg, S.N. and Nadeau P.H. 1989. Formation of diagenetic illite in sandstones of the Garn formation, Haltenbanken area, mid-Norwegian continental shelf. *Clay Minerals*, v. 24, p. 233 253.

Ehrenberg, S.M., Aagaard, P., Wilson, M.J., Fraser, A. R. and Duthie, D.M.L. 1993. Depth-dependent transformation of kaolinite to dickite in sandstones of Norwegian continental shelf. *Clay Minerals*. v. 28, p. 325-352.

Ganor J., Mogollon J.L. & Lasaga A. 1995 The effect of pH on kaolinite dissolution rates and on activation energy. *Geochim. Cosmochim. Acta*, v. 59, p. 1037-1052.

Gibson, D. W. 1977. Upper Cretaceous and Tertiary coal bearing strata in the Drumheller – Ardley region, Red Deer River valley, Alberta. *Geological Survey of Canada, Paper 76- 35*, p. 1-41.

Giles, M. R., Syevenson, S., Martin, S. V., Cannon, S.J. C., Hamilton, P.J., Marshall, J.D. and Samways, G.M. 1992. The reservoir properties and diagenesis of Brent Group: a regional perspective. In: *Geology of Brent Group*, Morton, A.C., Haszeldine, R.S., Giles, M.R. and Brown, S. (eds.), *Geological Society Special Publication 61*, p. 289-327.

Hacquebard, P.A. 1977. Rank of coal as index of organic metamorphism for oil and gas in Alberta, Canada. *American Association of Petroleum Geologists Bulletin* 61, v. 5, p. 791.

Harris, N.B. 1992. Burial diagenesis of Brent sandstones: a study of Staffjord, Hutton and Lyell fields. In: *Geology of the Brent Group*, A. C. Morton, R. S. Haszeldine, M. R. Giles and S. Brown (eds.). *Geological Society, London*, p. 351-376.

Helmold, K.P. and Van De Kamp, P.C. 1984. Diagenesis mineralogy and controls on albitization and laumontite formation in Paleogene arkoses, Santa Ynez Mountains California. In: *Clastic diagenesis*. D.A. McDonald and D.C. Surdan (eds.). American Association of Petroleum Geologist Memoir 37, p. 239-276.

Hillier, S. 1994. Pore-lining chlorite in siliciclastic reservoir sandstones: electron microprobe SEM and XRD data, and implications for their origin. *Clay Minerals*, v. 29, p. 664-679.

Hitchon, B. 1984. Geothermal Gradient, hydrodynamics, and hydrocarbon occurrences, Alberta, Canada. *Bulletin of the American Association of Petroleum Geologist*, v. 68, p. 713-743.

Hoffman, J. and Hower, J. 1979. Clay mineral assemblages as low grade metamorphic geothermometers: application to the thrust faulted disturbed belt of Montana, U.S.A. *SEPM Special Publication*, no. 26, p. 55-79.

Hower, J., Eslinger E.V. and Perry, E.A. 1976. Mechanism of burial metamorphism of argillaceous sediments: mineralogical and geochemical evidence. *Geological Society of America*, v. 87, p. 725-737.

Humphreys, B., Kemp, S.J., Lott, G.K., Bermanto, Dharmayanti, D.A. and Samsori, I. 1993. Origin of grain-coating chlorite by smectite transformation: An example from



Miocene sandstones, North Sumatra Back-Arch Basin, Indonesia. *Clay minerals*, v. 29, p. 681-692.

Issler, D.R., Willett, S.D., Beaumont, C., Donelick, R.A. and Williams-Jones, A.E. 1999. Paleotemperature history of two transects across the Western Canada Sedimentary Basin: Constrains from apatite fission track analysis. *Bulletin of Canadian Petroleum Geology*, v. 47, no. 4, p. 475-486.

Jerzykiewicz, T. 1985b. Tectonically deformed pebbles in the Brazeau and Paskapoo Formation, central Alberta Foothills, Canada. *Sedimentary Geology*, v. 42, p. 159-180.

Jerzykiewicz, T. 1997. Stratigraphic framework of the upper Cretaceous to Paleocene strata of the Alberta Basin. *Geological Survey of Canada Bulletin 510*, 121 p.

Jerzykiewicz, T. and McLean, J.R. 1980. Lithostratigraphical and sedimentological framework of coal-bearing Upper Cretaceous and Lower Tertiary strata, Coal Valley area, central Alberta Foothills. *Geological Survey of Canada, Paper 79-12*, 47 p.

Jerzykiewicz, T. and Sweet, A.R. 1988. Sedimentological and palynological evidence of regional climatic changes in the Campanian to Paleocene sediments of the Rocky Mountain Foothills, Canada. *Sedimentary Geology*, v. 59, p. 29-76.

Khidir, A. and Catuneanu, O. 2003. Sedimentology and diagenesis of the Scollard sandstones in the Red Deer Valley area, central Alberta. *Bulletin of Canadian Petroleum Geology*, v. 51, no. 1, p. 45-69.

Lanson, B., Beaufort, D., Berger, G., Bauer, A., Cassagnabère, A. and Meunier, A. 2002. Authigenic kaolin and illitic minerals during burial diagenesis of sandstones: a review. *Clay Minerals*, v. 37, p. 1–22.

Lerbekmo, J.F. 1963. Petrology of the Belly River Formation, southern Alberta Foothills. *Sedimentology*, v. 2, p. 54-86.

Lerbekmo, J.F. 1957. Authigenic Montmorillonoid cement in Andesitic sandstones of central California. *Sedimentary Petrology*, v. 27, No. 3, p. 298-305.

Lerbekmo, J.F., Evans, M.E. and Hoye, G.S. 1990. Magnetostratigraphic evidence bearing on the magnitude of the sub-Paskapoo disconformity in the Scollard Canyon-Ardley area of the Red Deer Valley, Alberta. *Bulletin of Canadian Petroleum Geology*, v. 23, p. 120-124.

Macaulay, C.I., Fallick, A.E. and Haszeldine, R.S. 1993. Textural and isotopic variations in diagenetic kaolinite from the Magnus oilfield sandstones. *Clay Minerals*, v. 28, p. 625-639.

- McBride, E. F. 1989. Quartz cementation in sandstones: a review, *Earth Science Reviews*, v. 26, p. 69-112.
- Morad, S., Bergan, M., Knarud, R., and Nystuen, J.P. 1990. Albitization of detrital plagioclase in Triassic reservoir sandstones from the Snorre Field, Norwegian North Sea. *Journal of Sedimentary Petrology*, v. 60, p. 411–425.
- Nurkowski, J.R. 1984. Coal quality, coal rank variation and its relation to reconstructed overburden, Upper Cretaceous and Tertiary plains coals, Alberta, Canada. *American Association of Petroleum Geologists Bulletin*, v. 68, p. 285-295.
- Pearson, M.J. and Small, J.S. 1988. Illite-smectite diagenesis and palaeotemperatures in northern North Sea Quaternary to Mesozoic shale sequences. *Clay Minerals*, v. 23, p. 109-139.
- Perry, E. and Hower, J. 1970. Burial diagenesis in Gulf Coast pelitic sediments. *Clays and Clay Minerals*, v. 18, p. 165-177.
- Pettijohn, F. J., Potter, P.E. and Siever, R. 1987, *Sand and sandstone*, 2nd (ed.). Springer-Verlag, New York, 553 pp.
- Salem, M. A., Morad, S., Mato, F. L. and Al-Asam, I. S. 2000. Diagenesis and reservoir-quality of fluvial sandstones during progressive burial and uplift: Evidence from the

Upper Jurassic Biopeda Member, Recôncavo Basin, Northeastern Brazil. *Bulletin of American Association of Petroleum Geologists*, v. 84, no. 7, p. 1015-1040.

Scotchman, I.C., Johnes, L.H. and Miller R.S. 1989. Clay diagenesis and oil migration in Brent Group sandstones of NW Hutton field, UK North Sea. *Clay Minerals*, v. 24, p. 339-374.

Sieffermann, G., Jehl, G., Millot, G. 1968. Allophanes et minéraux argileux des alterations récentes des basaltes du Mount Cameroun. *Bulletin du Groupe d' Argiles de France*, v. 20, p.109-129.

Smithson, F. 1954. The petrography of dickite sandstones in North Wales and Northern England. *Geol. Magazine*, v. 91, p. 177-188.

Stewart, R.N.T., Fallick, A.E. and Haszeldine, R.S. 1994. Kaolinite growth during pore-water mixing: isotopic data from Paleocene sands, North Sea, U.K. *Clay Minerals*, v. 29, p. 627-636.

Sweet, A.R., Braman, D.R. and Lerbekmo, J.F. 1990. Palynofloral response to K/T boundary events: A transitory interruption within a dynamic system. In: *Global catastrophes in Earth history*, V.L. Sharpton and P.D. Ward (eds.). Geological Society of America, Special Paper 247, p. 457-469.

Tozer, E.T. 1956. Uppermost Cretaceous and Paleocene nonmarine molluscan faunas of western Alberta. Geological Survey of Canada, Memoir 280, 125 p.

Velde, B. 1985. Clay minerals, a physico-chemical explanation of their occurrence: Developments in Sedimentology, v. 4, New York, Elsevier, 427 p.

Walker, T.R. 1984. Diagenetic albitization of potassium feldspar in arkosic sandstones: 1984 presidential address of the Society of Economic Palaeontologists and Mineralogists. Journal of Sedimentary Petrology, v. 54, p. 3–6.

Wiebel, R. 1999. Effect of burial on the clay assemblages in the Triassic Shagerrak Formation, Denmark. Clay Minerals, v. 34, p. 619-635.

Wilson, M.D. and Pittman, E.D. 1977. Authigenic clays in sandstones: recognition and influence on reservoir properties and paleoenvironmental analysis. Journal of Sedimentary Petrology, v. 47, p. 3-31.

Worden, R. H. and Morad, S. 2000. Quartz cementation in oil field sandstones: a review of the key controversies. In: Quartz cementation in sandstones: Special Publication of the International Association of Sedimentologists. R.H. Worden and S. Morad (eds.), v. 29, p. 1-20.

Worden, R.H. and Morad, S. 2003. Clay minerals in sandstones: controls on formation, distribution and evolution. International Association of sedimentologists Special

Publication. In: Clay mineral cement in sandstones, R. Worden and S. Morad (eds.).  
Blackwell, v. 34, p. 3-41,

Zotov, A., Mukhamet-Galeev A. and Schott J. 1998. An experimental study of kaolinite  
and dickite relative stability at 150-300 degrees C and the thermodynamic properties of  
dickite. American Mineralogist, v. 83, p. 516-524.

## Chapter 4

A version of this chapter has been published. Khidir, A. and Catuneanu, O. 2009. *Geologos*, 15 (3–4): P. 169–180.

### **Predictive diagenetic clay-mineral distribution in siliciclastic rocks as a tool for identifying sequence boundaries in nonmarine successions: the Coalspur Formation, west-central Alberta**

#### **Introduction**

The application of sequence stratigraphy to a continental setting results in an improved understanding of the variation in the facies architecture of fluvial deposits; in turn, this implies a better prediction of the development of hydrocarbon fluvial reservoirs. Many studies have demonstrated the close association between fluvial stratigraphic traps and sequence boundaries that are surfaces of subaerial erosion (Wu, et al., 1998; Luebking et al., 2001). Various authors have also examined and described the characteristics of diagenesis in the vicinity of unconformities, with emphasis on reservoir properties (Garcia, 2000; Csoma et al., 2004).

The relation between sequence stratigraphy and the distribution of authigenic cement in sandstone is predictable because changes in the detrital composition and pore water chemistry often occur at sequence stratigraphic surfaces (Morad et al., 2000; Ketzer et al., 2002, 2003a). Thus, knowledge of sequence stratigraphy and sequence stratigraphic surfaces in particular can provide useful information on parameters controlling near-surface diagenesis. Integrating sequence stratigraphy and diagenesis can help improve the

prediction of the distribution of diagenetic minerals in sandstones and, hence, the evolution of reservoir quality (Morad et al., 2000; Ketzer et al., 2002, 2003b).

Authigenic clay minerals such as kaolinite, dickite, smectite, and non-clay minerals such as quartz overgrowths and calcite cement in sandstones are studied in this present paper. These minerals are important from the petroleum geology perspective; they provide a complete picture of diagenetic history, and control reservoir properties such as porosity, permeability and water saturation. Authigenic minerals may also provide indications of the paleo-environmental and paleoclimatic conditions that prevailed during the development of unconformities. The aim of the current paper is to: (1) confirm the position of the sequence boundary in the study succession; (2) discuss the role of sequence stratigraphic controls on sandstone diagenesis and, hence, on reservoir properties; and (3) define a predictive model for the distribution of early diagenetic clay minerals in fluvial sandstones within a sequence stratigraphic framework.

### **Geological background**

Late Maastrichtian - Early Paleocene strata of the Coalspur Formation in the Western Canada foredeep (Fig. 1) form a fully nonmarine depositional sequence bounded by regional subaerial unconformities (Fig. 2). The Coalspur Formation overlies the Brazeau Formation and is overlain by the Paskapoo Formation (Fig. 2). Jerzykiewicz and McLean (1980) and Jerzykiewicz (1997) suggested that the upper unconformable boundary be placed at the base of the lowest major sandstone bed above the highest thick coal seam (Val d'Or) of the Coalspur coal zone. Magneto-biostratigraphic studies of Lerbekmo and



Sweet, 2008 also concluded the most likely position of the Coalspur/Paskapoo sequence boundary was directly above the top of the Val d'Or coal seam, and at the base of the lowest sandstone directly above the "burned zone" (Fig. 2).

The lower unconformable boundary occurs at the sub-Entrance conglomerate unconformity (Fig. 2). On the basis of palynology and an iridium anomaly, the Cretaceous-Tertiary boundary was defined within the Coalspur Formation at the base of the Mynheer coal seam (Jerzykiewicz et al., 1984; Jerzykiewicz and Sweet, 1986).

Coalspur Formation correlates with the Scollard Formation of the Plains region and the Willow Creek Formation in southwestern Alberta. This correlation is constrained in part by the occurrence of the Cretaceous-Tertiary boundary, which divides these formations into upper and lower parts. The depositional environment of the Coalspur Formation was dominated by fluvial systems sourced from the adjacent Cordilleran belt, with additional sedimentation in lacustrine and swamp environments.

The Coalspur Formation was defined and mapped in the central Foothills between the Athabasca River and the Coal Valley (Jerzykiewicz and Sweet, 1986) (Fig. 1). The upper part of the formation in the vicinity of the Coalspur section, from the McPherson coal seam up to the upper unconformable contact with the Paskapoo Formation (Fig. 2) was also described and studied by Jerzykiewicz and Maclean (1980), Jerzykiewicz and Langenberg, (1983), and Jerzykiewicz and Sweet (1986, 1988). The Coalspur Formation accumulated in a predominantly fluvial and lacustrine environments. Deposition of the Coalspur Formation in the Alberta foredeep corresponds to a period of loading in the

thrust-fold belt which created accommodation (Catuneanu and Sweet, 1999). Sedimentation continued until the beginning of Eocene time. At the beginning of the Eocene epoch, subsidence of the foreland basin was replaced by isostatic uplift resulting in the erosion of more than 1000 m of post-Paleocene sediments from the foreland basin (Nurkowski, 1984; Dawson, et. al., 1994). Thus, the Coalspur Formation was subject to deep burial followed by significant uplifting and the formation was probably buried deeper than 2 km prior to Paleocene time.

### **Nonmarine sequence stratigraphy**

Sequence stratigraphy is a genetic approach to the subdivision of the stratigraphic record into sequences based on how depositional systems respond to changes in the space available for sediment accumulation that is termed “accommodation” (Posamentier et al., 1988). Fluvial accommodation may be modified by downstream controls (i.e., base-level change) and upstream controls (i.e., source area tectonism and climate) (e.g., Aitken and Flint, 1995; Miall, 1997; McCarthy and Plint, 1998; Catuneanu, 2006). Lowering of the fluvial equilibrium (graded) profile (i.e., negative fluvial accommodation) leads to fluvial channel incision, which results in the development of a regional unconformity termed a “sequence boundary” (Posamentier and Vail, 1988; Shanley and McCabe, 1994).

Fluvial accommodation during the deposition of the Coalspur Formation was modified by upstream controls, primarily flexural tectonism (Catuneanu and Sweet, 1999; Catuneanu et al., 2000). Differential subsidence across the foredeep of the Alberta basin, with higher subsidence rates towards the thrust-fold belt, generated a gradual shallowing of the topographic gradient during orogenic loading, and resulted in a shift in fluvial

depositional elements from braided channels (lower Coalspur) to isolated meandering channels, crevasse splays and overbank fines (upper Coalspur). Regional isostatic rebound during stages of orogenic quiescence has been proposed as the cause for the formation of fluvial sequence boundaries within the Alberta foredeep (Catuneanu and Sweet, 1999; Catuneanu et al., 2000). Based on the ratio between fluvial depositional elements, the Coalspur Formation may be subdivided into two fluvial systems tracts, which are the (channel-dominated) low-accommodation systems tract of the lower Coalspur Formation, and the (low-energy fluvial and lacustrine-dominated) high-accommodation systems tract of the upper Coalspur Formation.

## **Methods**

Fieldwork was carried out in west-central Alberta in the Coalspur locality and outcrop section was studied in detail (Fig. 1). Standard logging techniques were applied, including thickness measurements, facies analysis, and sampling for laboratory work. Twenty-five sandstone samples were impregnated with blue epoxy resin to highlight porosity before preparing the thin-section slides. Representative thin-sections were point-counted (250 points) to calculate the relative amounts of detrital framework grains, interstitial minerals, and porosity. The grain size was estimated in millimetre units, and sorting was estimated by comparison with published sorting comparators (Longiaru, 1987).

To identify clay minerals, porosity, and to determine paragenesis, selected samples were studied and examined by scanning electron microscope (SEM, JEOL JSM 6400) equipped

with an energy-dispersive x-ray analyzer. To determine the modal amount and types of authigenic clay minerals, a grinding technique was used to produce powders free of grains coarser than 20  $\mu\text{m}$ . X-ray diffraction (XRD) was performed on the bulk samples and on samples finer than 2  $\mu\text{m}$ . The resulting diffraction data was then analyzed using the industry standard MDI Jade software and the CDD PDF-2 powder diffraction database. Two equal fractions of each sample were selected for bulk analysis and for the analysis of the less than 2  $\mu\text{m}$  fraction. Diffraction data on the resulting clay slides were acquired. The relative abundance of specific clay minerals within the clay fraction was determined using the data obtained on the  $<2$   $\mu\text{m}$  clay fraction. The criteria of Wilson and Pittman (1977) were used to differentiate between detrital and authigenic clay minerals.

## **Results**

### *Sandstone petrography*

The sandstones consist mainly of quartz and rock fragments with small amounts of feldspar grains. Monocrystalline quartz averages 50% of the framework grains (Fig. 3A), whereas rock fragments, which are of igneous (Fig. 3A), metamorphic (Fig. 3B), and sedimentary origin (Fig. 3C), make up 45% of the framework grains. Feldspar has less abundance (Fig. 3D) and averages 5% of the framework grains. Accessory minerals such as muscovite also occur (Fig. 3C). The sandstones range from fine- to medium-grained and display moderate sorting. Based on Pettijohn et al.'s (1987) classification, the sandstones of the Coalspur locality are defined as litharenites to sublitharenites (Fig. 4) and characterized by a general lack of matrix.

### *Authigenic mineral distribution*

The dominant authigenic minerals in the sandstones are the kaolin minerals (i.e., kaolinite and dickite; Fig. 6), with subordinate quartz overgrowth, calcite, smectite, and mixed layer illite/smectite (Figs. 3E and 5C and D).

Kaolinite and dickite are the most widespread authigenic clay minerals in the sandstones (Fig. 5A and B). Kaolinite generally formed at low temperatures (<120 °C) during weathering and diagenetic processes, and occurs as pore filling pseudo-hexagonal crystals with booklet and vermicular shapes (Fig. 5A). The kaolinite in the sandstones may have precipitated during the Tertiary uplift due to abundant groundwater flow through the porous sandstones. Dickite, which reflects an increase in burial temperature and pressure (Shutov et al., 1970; Ehrenberg et al., 1993), occurs as blocky pseudo-hexagonal crystals (Fig. 5B). The aggregation of dickite crystals increases significantly in the sandstones below the first conglomerate bed above the last coal zone of the Coalspur Formation (Fig. 6).

An insignificant amount of authigenic smectite is found in the sandstones (Fig. 6). Trivial mixed layer illite-smectite was observed as well (Fig. 5D).

Authigenic non-clayey minerals in sandstones are quartz overgrowths (Fig. 5C) and calcite cement (Fig. 3E). The quartz overgrowths in the sandstones show no distinct distribution pattern related to the sequence boundary. The calcite cement in the sandstones ranges from patchy to uniform (Fig. 3E). The detailed chemistry of calcite precipitation is beyond the scope of this paper.

The occurrence of quartz overgrowths (Fig. 5C) may be attributed to the influx of meteoric (acidic) water into the sandstones. The mixing of the meteoric water with alkaline pore water would increase the acidity of the pore water, resulting in a decrease in the solubility of silica and alumina and precipitation of quartz overgrowths, and possibly kaolinite, in the pore systems.

The precipitation of the late diagenetic calcite cement, typically associated with unconformity surfaces, was probably caused by the enrichment of the pore solutions with  $\text{Ca}^{2+}$  and  $\text{HCO}_3^-$  through the dissolution of Ca-feldspar grains. Carbonate rock fragments another possible source of calcite cement in the upper Coalspur sandstones, were probably derived from sedimentary strata in the Rocky Mountain Front Ranges. The presence of calcite cement in the Coalspur sandstones preferentially below the top unconformity (sequence boundary) may have occurred during subaerial exposure related to isostatic rebound.

#### *Porosity development below the subaerial unconformities*

The sandstone porosity of the outcrop-derived samples determined from thin sections ranges from 3% to 13% and averages 10%. The present porosity is secondary in origin. The secondary porosity includes grain moldic porosity produced by the partial dissolution of feldspar along cleavage planes and twin boundaries (Fig. 5E), corrosion of grains adjacent to pores, which are generally the result of the incomplete replacement of feldspar grains.

## **Discussion**

### *Position of the sequence boundary at the studied section*

Feldspar leaching and the associated production of abundant kaolinite can be used to infer the past interaction of meteoric water with sandstone and, more generally, that kaolinite is indicative of unconformities (Tardy, 1971; Emery et al., 1990). In this context, the relative abundance of authigenic kaolinite/dickite may be used as an indicator of an unconformity.

By examining the authigenic clay mineral trend in the sandstones (Fig. 6) we observed a systematic increase in the abundance of authigenic dickite toward the erosional base of the conglomerate bed above the upper coal zone (Fig. 6). The possible scenario that explains the clay-mineralogy trends is that meteoric flushing, which was accompanied by the dissolution of unstable minerals (e.g., feldspar), and consequent authigenic kaolinite precipitation occurred when the Coalspur Formation was subaerially exposed. During subsequent burial diagenesis most of the kaolinite below the unconformity altered to dickite. Thus, the increase in kaolinite/dickite mineral abundance may be taken as a proxy to locate subaerial unconformities, and in this particular case study, the upper boundary of the fluvial Coalspur sequence.

### *Diagenetic alteration associated with the sequence boundary*

Kaolinite formation, which requires intensive weathering and high rates of water percolation (Weaver, 1989; Robert and Chamley, 1991), is the main diagenetic alteration related to the sequence boundary in the sandstones of the upper Coalspur Formation. The

flushing of meteoric water in the sandstones resulted in a thick zone of intense kaolinitization below the sequence boundary (Fig. 5B). During burial diagenesis most of the kaolinite that formed in the time of subaerial exposure is transformed to dickite. The thick dickite zone suggests significant time of subaerial exposure, and hence stratigraphic hiatus associated with the top-Coalspur unconformity. The thickness of dickite zone may also depend on the porosity of the sandstone, grain size and climate.

In addition to the role of the sequence boundary in controlling the distribution of authigenic kaolinite in the sandstones, the initial permeability of the sandstones and the acidity of the pore water chemistry also play a role in kaolinite precipitation. The initial permeability controls water circulation and, consequently, influences the precipitation of kaolinite, whereas the influx of meteoric water and acidic fluids, some of which may have derived from the coalification of organic matter, caused an increase in the acidity of the pore solutions and enhanced kaolinite precipitation (Grim, 1953). This kind of environment could explain the increase of diagenetic kaolinite concentration near the sandstone-coal contacts.

*Climate control on diagenesis associated with the subaerial unconformity*

Unconformities in the rock record correspond to periods of non-deposition or erosion during considerable time intervals. During the formation of unconformities, sediments may be subject to erosion, dissolution, and the formation of early authigenic cement. The nature of the early cement below the unconformity is a function of the groundwater chemistry, which in turn may be controlled by climate (Suttner and Dutta, 1986). Cation-



rich clays such as smectite form when the climatic condition is relatively arid, and the resultant ionic concentration in the groundwater is high (Velde, 1985). During high humidity and relatively wet climatic conditions, authigenic kaolinite and quartz cements are abundant (Dutta, 1992).

In the sandstones of the upper Coalspur Formation, the occurrence of authigenic kaolin minerals may be interpreted to reflect the influence of humid climatic conditions on the ground water chemistry. Humid climate conditions during the accumulation of the upper Coalspur sediments are also indicated by the presence of thick coal seams.

The occurrence of smectite probably resulted from the alteration of volcanic rock fragments (Fig. 3A), and may also reflect warm climatic conditions, possibly seasonal. The conversion of smectite to mixed-layered illite-smectite may indicate an increase in the depth of burial, accompanied by an increase in paleotemperature gradient.

#### *Evolution of reservoir quality in the sandstones*

Weathering may enhance porosity below unconformities, allowing sandstones to act as hydrocarbon reservoirs and pathways of fluid migration (Shanmugam and Higgins, 1988; Shanmugam, 1990). The influx of meteoric acidic water into the sandstones below the sequence boundary may result in an increase in intergranular porosity and permeability of the sandstones by the dissolution of feldspar; at the same time, this process may also result in the formation of authigenic minerals such as kaolinite and silica cement (Bjørlykke, 1984; Emery et al., 1990). The development of authigenic pore-filling kaolinite modifies the amounts of available porosity and permeability. The stacked, book-

shaped, pseudo-hexagonal kaolin minerals that occur as pore-fillings and coatings act as small particles plugging the pore-throats (especially during production), thereby reducing permeability. The presence of other authigenic minerals such as quartz overgrowths further reduces porosity and permeability.

In the upper Coalspur sandstones, determination of precise reservoir quality evolution below the sequence boundary is difficult, partly due to the complicated diagenetic history and involvement of other parameters such grain size, nature and extent of initial diagenesis, climate, and duration of subaerial exposure. Most of the secondary porosity is interpreted to be formed as a result of feldspar leaching (Fig. 5E) during subaerial exposure from meteoric pore-water circulation associated with formation of kaolinite (Fig. 5A and B). Feldspar leaching and dissolution during transportation and during different stages of diagenesis could also explain the low feldspar abundance in the sandstones. Most of the secondary porosity that was created during early diagenesis by leaching of unstable grains was filled by calcite cement during later burial diagenesis. Another important control on reservoir quality of the Coalspur sandstones is the occurrence of kaolin minerals. Generally, the high abundance of kaolin clay minerals below the sequence boundary (Fig. 6) played a strong role in controlling the reservoir quality of the sandstones in term of porosity and permeability; the limited amount of smectite, illite-smectite, and silica cementation had less control on the sandstone's properties in this particular case study.

## **Conclusions**

1. Diagenetic processes may be related to some extent to the development of specific sequence stratigraphic surfaces. Subaerial unconformities in fluvial settings are particularly prone to control the distribution of diagenetic minerals within the sequence. The nature of the diagenetic minerals below the sequence boundary may in turn depend on the climatic conditions during the formation of the subaerial unconformity.

2. The upper sequence boundary of the Coalspur Formation (i.e., a subaerial unconformity) is underlain by a thick zone of kaolinite/dickite in the sandstones. The precipitation of kaolin minerals below the sequence boundary may be related to flushing of meteoric water and dissolution of unstable minerals during the formation of the subaerial unconformity. Following burial, most of the original kaolinite was transformed into dickite.

3. The occurrence of authigenic kaolin minerals within the Coalspur sequence may be interpreted to reflect the influence of humid climatic conditions on the groundwater chemistry at the time of sedimentation, as well as during subsequent uplift and subaerial erosion. Humid climate conditions are also indicated by the presence of thick coal seams within the upper Coalspur Formation.

4. The observed pattern of distribution of early authigenic clay minerals within a fluvial succession may be used to infer the position of 'cryptic' nonmarine sequence boundaries,

which lack an evident lithological expression. Integration of diagenesis and sequence stratigraphy also allows for better prediction of reservoir quality in nonmarine sequences.

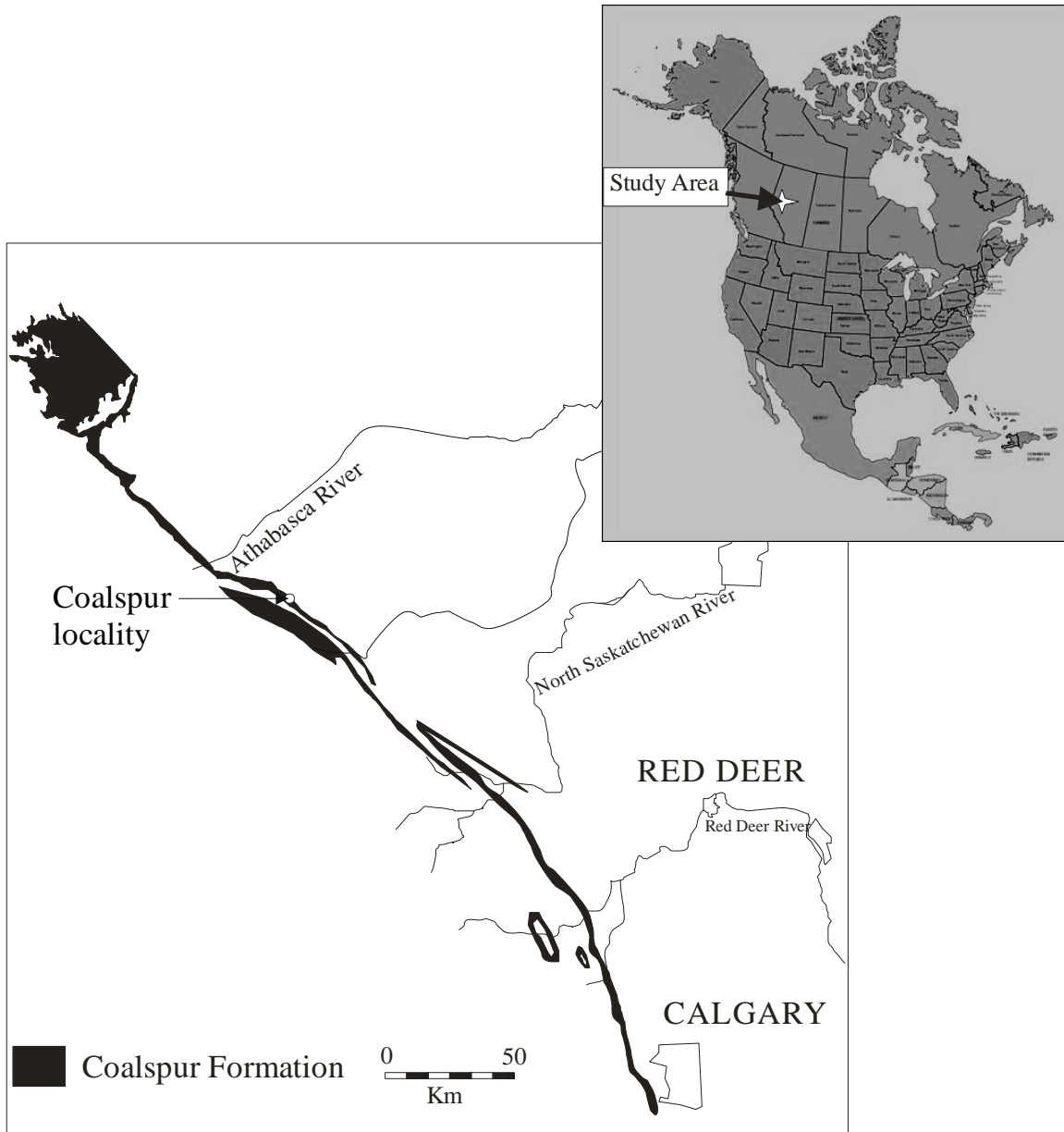


Figure 1. Outcrop distribution of the Coalspur Formation in Alberta, and the location of the studied outcrop section.

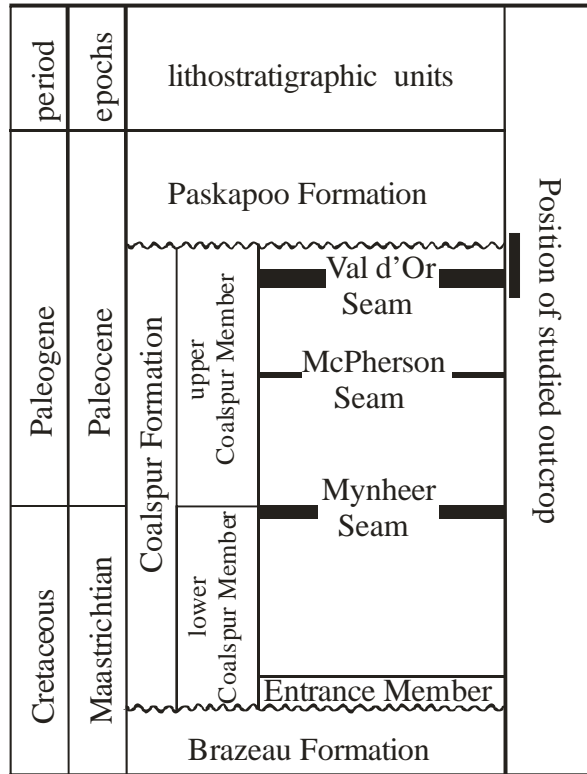


Figure 2. Generalized chart of the late Maastrichtian-Paleocene stratigraphy of west-central Alberta, showing the position of the upper Coalspur Formation and its main coal seams.

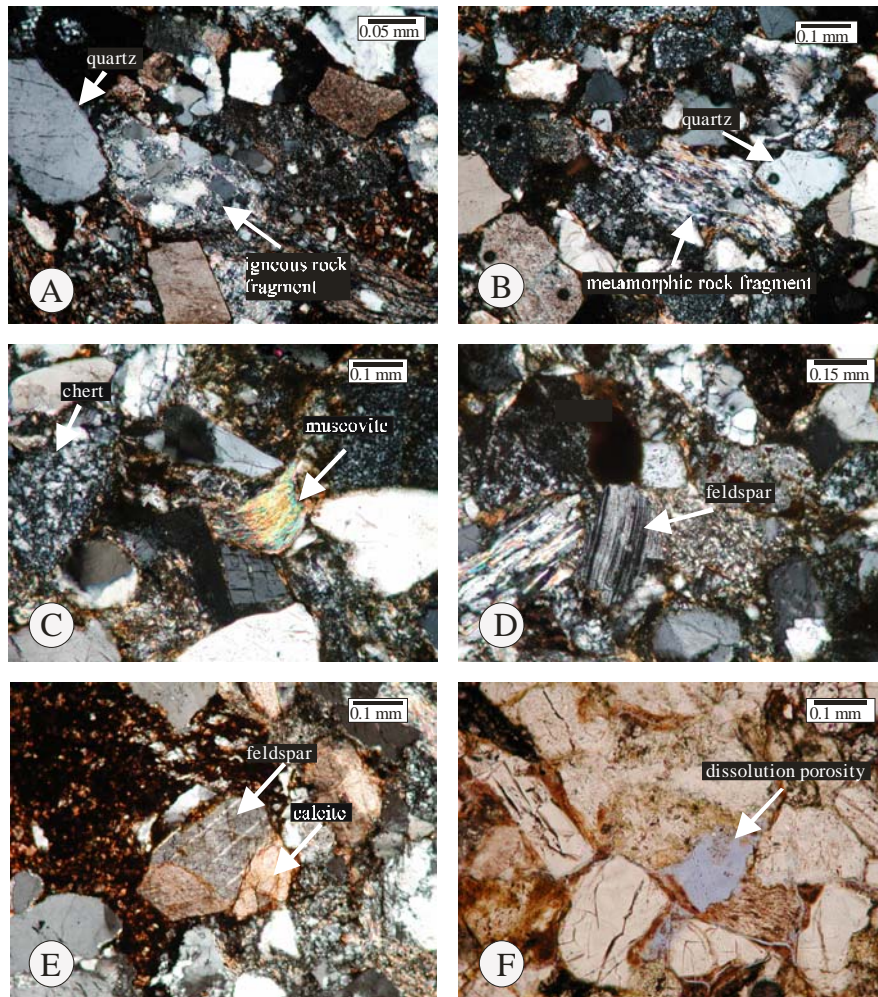


Figure 3. Thin-section photomicrographs: (A) – litharenite with igneous rock fragments and quartz grains. (sample 1, upper Coalspur Formation, Coalspur locality); (B) – detrital grain of metamorphic origin (sample 3, upper Coalspur Formation, Coalspur locality); (C) – detrital chert of sedimentary origin and muscovite grain. Note the uniform microcrystalline quartz with no visible relict texture. (sample 2, upper Coalspur Formation, Coalspur locality); (D) – twinned plagioclase feldspar grain (sample 1, upper Coalspur Formation, Coalspur locality); (E) – feldspar grain and calcite cement filling the pore-space (arrow) (sample 6, upper Coalspur Formation, Coalspur locality); (F) – secondary porosity resulting from dissolution of probable feldspar grain (arrow) (sample 8, upper Coalspur Formation, Coalspur locality).

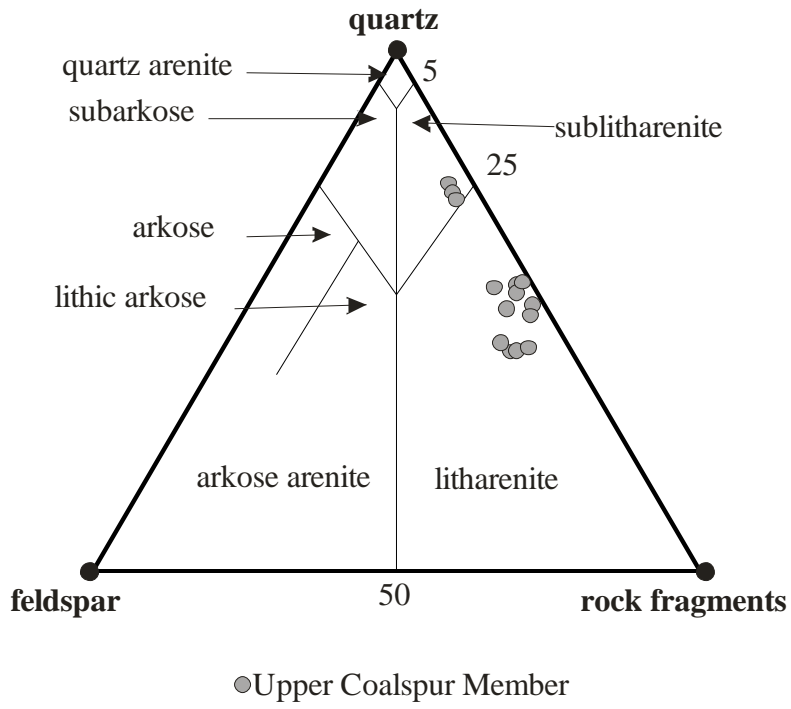


Figure 4. Classification of the upper Coalspur Formation sandstones (after Pettijohn et al., 1987).



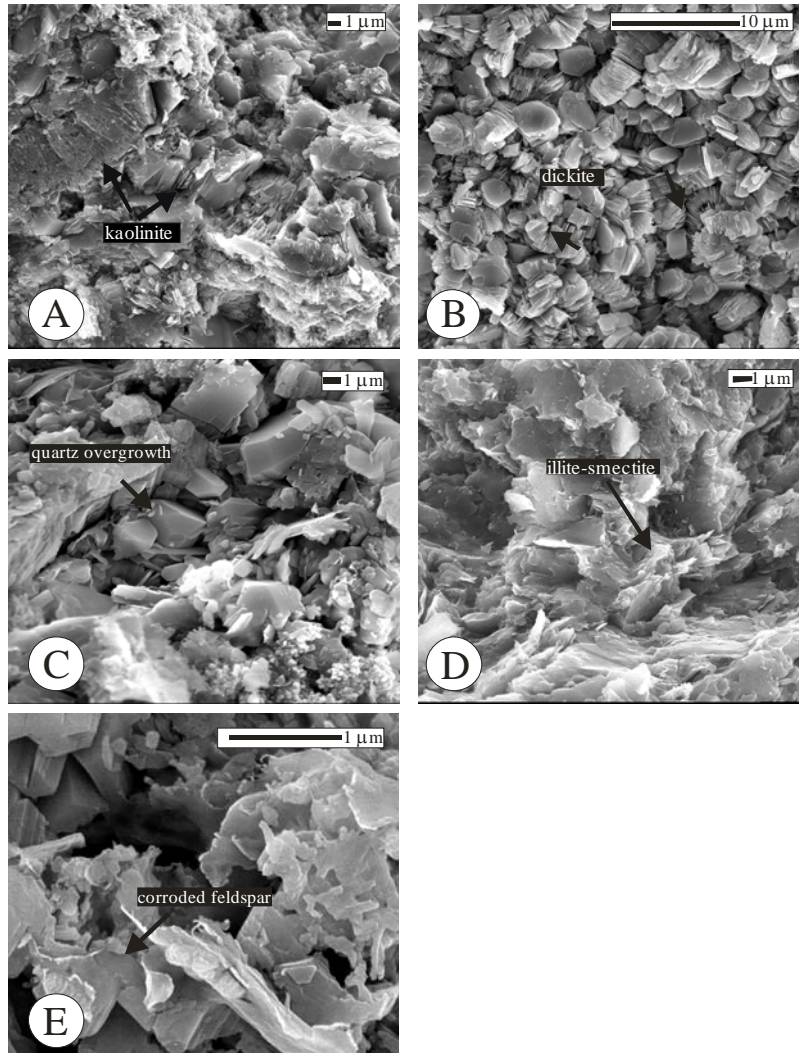


Figure 5. SEM photomicrographs: (A) – authigenic kaolinite formed as pore-filling clay probably from meteoric water flushing during Tertiary uplift (sample 5, upper Coalspur Formation, Coalspur locality); (B) – vermicular aggregates of euhedral crystals of authigenic dickite formed as pore filling cement below the sequence boundary (sample 2, upper Coalspur Formation, Coalspur locality); (C) – quartz overgrowth in sandstone (sample 3, upper Coalspur Formation, Coalspur locality); (D) – smectite and smectite-illite mixed layers (sample 1, upper Coalspur Formation, Coalspur locality); (E) – corroded feldspar and formation of secondary porosity (sample 6, upper Coalspur Formation, Coalspur locality).

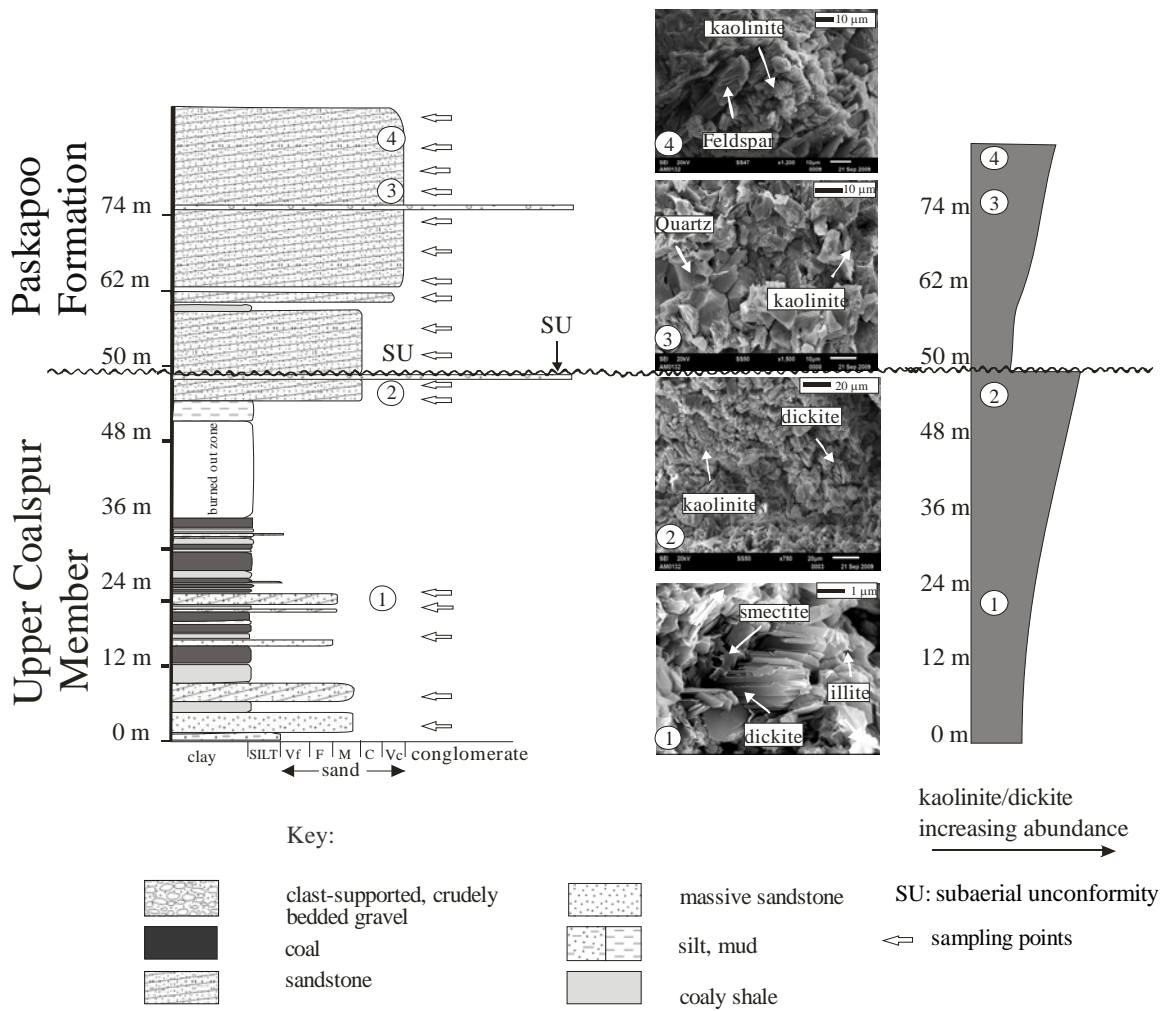


Figure 6. Vertical lithologic profile for the Coalspur locality section, showing the occurrence and abundance of authigenic kaolin minerals in relation to the sequence boundary as indicated by SEM analyses. Please note that the horizontal scale of studied outcrop is about six meter wide.

## References

Aitken, J.F. and Flint, S.S., 1995. The application of high-resolution sequence stratigraphy to fluvial systems: a case study from the Upper Cretaceous Breathitt Group, eastern Kentucky, USA. *Sedimentology*, v. 42, p. 3– 30.

Bjorlykke, K., 1984, Formation of secondary porosity: how important is it?, in McDonald, D.A., and Surdam, R.C., eds., *Clastic Diagenesis: American Association of Petroleum Geologists, Memoir 37*, p. 277-286.

Catuneanu, O., 2006. *Principles of Sequence Stratigraphy*. Elsevier, Amsterdam, 375 pp.

Catuneanu, O., Sweet, AR, and Mial, AD. 2000. Reciprocal stratigraphy of the Campanian-Paleocene Western Interior of North America. *Sedimentary Geology*, V. 134, p. 235-255.

Catuneanu, O. and Sweet, A.R. 1999. Maastrichtian-Paleocene foreland basin stratigraphies, Western Canada: A reciprocal sequence architecture. *Canadian Journal of Earth Sciences*, v. 36, p. 685-703.

Csoma, A.E., Goldstein, R.H., Mindszenty, A. and Simone, L. 2004. Diagenetic salinity cycles and sea level along a major unconformity, Monte Camposauro, Italy. *Journal of Sedimentary Research*, v. 6, p. 889-903.

Dawson, F.M., Kalkreuth, W.D. and Sweet, A.R. 1994. Stratigraphy and coal resource potential of the Upper Cretaceous to Tertiary strata of northwestern Alberta. Geological Survey of Canada Bulletin 466.

Dutta, P. 1992. Climatic influence on diagenesis fluvial sandstones, In: Diagenesis, III. Developments in sedimentology, 47, Wolf, K. and Chillingrain, G. (eds.), 674p.

Ehrenberg, S.N., Aagaard, P., Wilson, M.J., Fraser, A.R., and Duthie, D.M.L. 1993. Depth-dependent transformation of kaolinite to dickite in sandstones of the Norwegian continental shelf. Clay Minerals, v. 28, p. 325–352.

Emery, D., Myers, K.J., and Young, R., 1990, Ancient subaerial exposure and freshwater leaching in sandstones: Geology, v. 18, p. 1178-1181.

Garcia, A.J.V. 2000. Pre-Aptian unconformity in the Sergipe-Alagoas Basin (northeastern Brazil); an important control on the pre-rift reservoir sandstone porosity evolution. Brazil 31st international geological congress; abstracts volume.

Grim, R. E. 1953. Clay mineralogy, McGraw-Hill Series in Geology, 377p.

Jerzykiewicz, T. 1997. Stratigraphic framework of the upper Cretaceous to Paleocene strata of the Alberta Basin. Geological Survey of Canada Bulletin 510, 121p.

Jerzykiewicz, T. and Langenberg, W. 1983. Structure, stratigraphy and sedimentology facies of the Paleocene and Lower Cretaceous coal-bearing strata in the Coalspur and Grande Cache areas, Alberta. Canadian Society of Petroleum Geologists Conference, The Mesozoic of Middle North America, Field Trip Guidebook, No. 9, 63p.

Jerzykiewicz, T. and Mclean, J.R. 1980. Lithostratigraphical and sedimentological framework of coal-bearing Upper Cretaceous and Lower Tertiary strata, Coal Valley area, central Alberta Foothills. Geological Survey of Canada, Paper 79-12, 47 p.

Jerzykiewicz, T. and Sweet, A.R. 1986. The Cretaceous-Tertiary boundary in the central Alberta Foothills. In; Stratigraphy. Canadian Journal of Earth Science, v. 23, p. 1356-1374.

Jerzykiewicz, T. and Sweet, A.R. 1988. Sedimentological and palynological evidence of regional climatic changes in the Campanian to Paleocene sediments of the Rocky Mountain Foothills, Canada. Sedimentary Geology, v. 59, p. 29-76.

Jerzykiewicz, T., Lerbekmo, J.F. and Sweet, A.R. 1984. The Cretaceous-Tertiary boundary, central Alberta Foothills. 1984 Canadian Paleontology and Biostratigraphy Seminar, Programme with Abstracts, p.4.

Ketzer, J.M., Morad, S., Evans, S., Al-Aasm, I.S., 2002. Distribution of diagenetic alterations in fluvial, deltaic, and shallow marine sandstones within a sequence

stratigraphic framework: evidence from the Mullaghmore Formation (Carboniferous), NW Ireland. *J. Sediment. Res.* V. 72, 760–774.

Ketzer, J.M., Holz, M., Morad, S., Al-Aasm, I.S., 2003a. Sequence stratigraphic distribution of diagenetic alterations in coalbearing, paralic sandstones: evidence from the Rio Bonito Formation (early Permian), southern Brazil. *Sedimentology* 50, 855– 877.

Ketzer, J.M., Morad, S. and Amorosi, A. 2003b. Predictive diagenetic clay-mineral distribution in siliciclastic rocks within a sequence stratigraphic framework. In: *Clay Mineral Cements in Sandstones*, International Association of Sedimentologists Special Publication 34, R.H. Worden and S. Morad (eds.), Blackwell Publication, Oxford, p. 43-61.

Lerbekmo, J.F. and Sweet, A.R. 2008. Magnetobiostratigraphy of the continental Paleocene upper Coalspur and Paskapoo formations near Hinton, Alberta. *Bulletin of Canadian petroleum Geology*. V. 56, No.2, p. 118-146.

Longiaru, S., 1987, Visual comparators for estimating the degree of sorting from plane and thin sections: *J. Sediment. Petrology*, v. 57, p. 791-794.

Luebking, G, Longman, M. and Carlisle, J. 2001. Unconformity related chert/ dolomite production in the Pennsylvanian Amsden Formation, and the utilization of the drillstem

test in finding hydrocarbons. Annual Meeting Expanded Abstracts, American Association of Petroleum Geologist. Pp. 121.

McCarthy, P.J. and Plint, A.G. 1998. Recognition of interfluvial sequence boundaries: integrating paleopedology and sequence stratigraphy. *Geology*, v. 26, p. 387– 390.

Miall, A.D. 1997. *The Geology of Stratigraphic Sequences*. Springer, Berlin.

Morad, S., Ketzer, J.M., De Ros, L.F., 2000. Spatial and temporal distribution of diagenetic alterations in siliciclastic rocks: implications for mass transfer in sedimentary basins. *Sedimentology*, v. 47, p. 95– 120. (Suppl. 1).

Nurkowski, J.R. 1984. Coal quality, coal rank variation and its relation to reconstructed overburden, Upper Cretaceous and Tertiary plains coals, Alberta, Canada. *American Association of Petroleum Geologists Bulletin*, v. 68, p. 285-295.

Pettijohn, F. J., Potter, P.E. and Siever, R. 1987, *Sand and sandstone*, 2nd (ed.). Springer-Verlag, New York, 553 pp.

Posamentier, H. W., Jervey, M.T. and Vail. 1988. Eustatic controls on clastic deposition I- Conceptual framework. In: C.K. Wilgus, B.S. Hastings, C.G.St.C. Kendall, H.W. Posamentier, C.A. Ross. and J.C. Van Wagoner, (eds.), *Sea level change: an integrated approach*: SEPM Special Publication 42, p. 109-124.

Posamentier, H. W. and Vail. 1988. Eustatic controls on clastic deposition II- Sequence and systems tract models. In: C.K. Wilgus, B.S. Hastings, C.G.St.C. Kendall, H.W. Posamentier, C.A. Ross. And J.C. Van Wagoner, (eds.), Sea level change: an integrated approach: SEPM Special Publication 42, p. 125-154.

Robert, C. and Chamley, H. 1991. Development of early Eocene warm climates, as inferred from clay mineral variations in oceanic sediments. *Palaeogeogr. Palaeoclimatol. Palaeoecol.* v. 89, p. 315-31.

Shanley, K.W. and McCabe, P.J. 1994. Perspectives on the sequence stratigraphy of continental strata. *American Association of Petroleum Geologists Bulletin*, v. 78, p. 544-568.

Shanmugam, G., 1990, Porosity prediction in sandstones using erosional unconformities, in Meshri, I.D., and Ortoleva, P.J., eds., *Prediction of Reservoir Quality through Chemical Modeling*: American Association of Petroleum Geologists, Memoir 49, p. 1-23.

Shanmugam, G., and Higgins, J.B., 1988, Porosity enhancement from chert dissolution beneath Neocomian unconformity, Ivishuk Formation, North Slope, Alaska: *American Association of Petroleum Geologists, Bulletin*, v. 72, p. 523-535.



Shutov, V.D., Aleksandrova, A.V., and Losievskaya, S.A. 1970. Genetic interpretation of the polymorphism of the kaolinite group in sedimentary rocks. *Sedimentology*, v. 15, p. 69–82.

Suttner J, and Dutta, K. 1986. Alluvial sandstone composition and paleoclimate, II. Authigenic Mineralogy. *Journal of Sedimentary Petrology*, v. 56, p. 346- 358.

Tardy, Y., 1971, Characterization of the principal weathering types by the geochemistry of waters from some European and African crystalline massifs: *Chemical Geology*, v. 7, p. 253-271.

Velde, B. 1985. Clay minerals, a physico-chemical explanation of their occurrence: *Developments in Sedimentology*, v. 4, New York, Elsevier, 427 p.

Weaver, C.E. 1989. Clays, Muds, and Shales. *Developments in Sedimentology*, v. 44, Elsevier, Amsterdam, 819pp.

Wilson, M.D. and Pittman, E.D. 1977. Authigenic clays in sandstones: recognition and influence on reservoir properties and paleoenvironmental analysis. *Journal of Sedimentary Petrology*, v. 47, p. 3-31.

Wu, Y., Shouan, Z. and Ai, H. 1998. Unconformity types and their relationship to oil/ gas

reservoirs in the Tarim Basin, Xinjiang, China. *Xinjiang Petroleum Geology*. 19; v. 2, p. 101-105.

## Chapter 5

*A version of this chapter has been submitted for publication. Khidir, A. and Catuneanu, O. 2010. Bulletin of Canadian Petroleum Geology.*

### **Diagenesis of the Cretaceous-Tertiary Willow Creek Sandstones, Southwestern Region of Alberta**

#### **Introduction**

The Willow Creek Formation, which accumulated during the late Maastrichtian to early Paleocene time in the southwest of Alberta, is composed of a fully nonmarine succession of irregular red, green, brown and purple bentonic shales and sandy shales interbedded with lenticular green-grey, fine-grained, argillaceous and minor calcareous sandstones. The sandstones increase in thickness towards the top of the formation, and the shaly beds almost disappear. The Willow Creek Formation consists of meandering river deposits: sandstones in point bars, crevasse splays, and mudstones in the floodplain. Abundance of trough and planar-tabular cross bedding, all suggest a generally fluvial environment of deposition. The most remarkable characteristic of this formation is the common occurrence of pedogenic caliche and the presence of the Cretaceous-Tertiary (K-T) boundary within it (Jerzykiewicz and Sweet, 1986a, 1988; Sweet et al., 1990; Jerzykiewicz, 1992). Based on the position of the K-T boundary, two informal members were recognized, the upper member and lower member. Both members contain caliche horizons as a result of the arid climate in this region (Jerzykiewicz and Sweet, 1986b; Jerzykiewicz and Sweet, 1988). Although this formation has been subjected to numerous sedimentological and palynological studies (Lerbekmo, 1985; Jerzykiewicz and Sweet,

1988; Greg and Jerzykiewicz, 1989; Lerbekmo, 1989; Dawson et al., 1994, Lerbekmo, and Sweet, 2000), the sandstone diagenetic history has received less attention. In southern Alberta, only a few wells encountered gas in the Willow Creek sandstone (e.g. 02/16-16-11-25W4, 00/6-16-22-20W4, and 00/06-25-22-20W4). The purpose of the present study is to investigate the characteristics of the different diagenetic processes affecting reservoir quality of the Willow Creek sandstones. This, in turn may assist in better delineating other areas of potential reservoir for similar age fluvial deposits occurring in the subsurface such as the Scollard and Coalspur Formations in southern and southwestern Alberta.

### **Geological Background**

Early geological studies of the Willow Creek Formation were conducted by Dawson (1886), Williams and Dyer (1930), Russell (1932), Allan and Rutherford (1934), Hages (1943), Douglas (1950), Tozer (1953), and Carrigy (1971). Dawson (1883) identified the Willow Creek Formation based on its red coloration. Dawson (1884) defined the formation at the mouth of Willow Creek and the adjacent part of the Oldman River. Williams and Dyer (1930) recorded the best exposures of the formation on the Oldman River east of Fort Macleod. Douglas (1950) described most of the lower part of the formation, whereas Tozer (1956) described the formation on both sides of the Alberta Syncline. A representative section of the formation on the Crowsnest River near Cowley was described thoroughly by Jerzykiewicz and Sweet (1986b, 1988). This formation was also studied by Jerzykiewicz (1997) and Lerbekmo and Sweet (2000).

The Willow Creek Formation in southern Alberta (Fig. 1) is underlain by the St. Mary River Formation and overlain by thick sandstone beds of the Porcupine Hills Formation

(Fig. 2). The lower contact, which is correlated with the sub-Entrance unconformity (Jerzykiewicz, 1997), is unconformable, whereas the upper contact is gradational (Lerbekmo and Sweet, 2000).

### **Tectonic and Burial History**

The Willow Creek Formation is part of the Western Canada foredeep fill and accumulated in a predominantly fluvial environment during late Cretaceous to early Paleocene time (Smith and Putnam, 2005). Deposition of this formation was tightly linked to tectonic processes. Tectonic activity and the downwarping of the western half of the foreland basin during late Maastrichtian time resulted in deposition of the formation (Jerzykiewicz and Labonte, 1991). At the time, the basin subsidence resulted in higher sedimentation rates giving rise to the thick successions of the Willow Creek Formation (Jerzykiewicz and Labonte, 1991). Subsidence was controlled initially by tectonic loading of thrust sheets and later by sediment loading (Jordan, 1981). Sedimentation continued until the beginning of Eocene time. At the beginning of the Eocene epoch, subsidence of the foreland basin was replaced by isostatic uplift resulting in the erosion of more than 1000 m of post-Paleocene sediments from the foreland basin (Hacquebard, 1977; Nurkowski, 1984; Bustin, 1992, Dawson, et. al., 1994). Therefore, the Willow Creek Formation was subject to deep burial followed by significant uplifting. The Willow Creek Formation was probably buried deeper than 1.5 km prior to Paleocene time. The complicated tectonic and burial history of the formation resulted in its complex diagenetic history.

The formation has been deformed in an asymmetrical synclinal structure, with gently dipping beds along the Oldman and Crowsnest Rivers. The average thickness of this

formation is approximately 1250 m. Carrigy (1971) recorded a thickness of 1006 m close to the axis, whereas on the west side of the Alberta Syncline the thickness is about 1375 m (Tozer, 1956).

## **Methods**

Fieldwork included detailed logging of seven stratigraphic sections and collection of 70 sandstone samples (Fig. 3). Fifty thin sections were cut and impregnated with blue epoxy in order to highlight the porosity. The petrographic modal analyses of the 50 samples was based on point-counts of 400 medium sand (0.025–0.50 mm) grains were conducted, using both the Gazzi-Dickinson (GD) and the traditional (T) counting methods (Dickinson 1970; Suttner et al. 1981). A scanning electron microscope with an energy-dispersive, X-ray analyzer was used on 70 sandstone samples in order to characterize the habits of authigenic minerals and to determine their paragenetic relationships. Helium porosity tests of 24 selected samples were performed. The permeability of the sandstone samples was measured by using a Pressure Decay Profile Permeameter.

Calcite samples for mass spectrometric analyses were collected under a binocular microscope by using a dental pick to cleave individual cements from polished thin sections. Samples averaging about 80  $\mu\text{g}$  were transferred to reaction vessels. Oxygen isotopic compositions were calculated by using a phosphoric acid- $\text{CO}_2$  fractionation factor of 1.011025 at 25°C for calcite. The reaction of calcite cement with 100% phosphoric acid at 25°C liberates  $\delta^{18}\text{O}$  of carbon dioxide and is a standard procedure for separating the  $\delta^{18}\text{O}$  (Wachter and Hayes, 1985). The oxygen and carbon isotope data are reported in the normal  $\delta$  notation relative to the Standard Mean Ocean Water (SMOW) for oxygen and the PeeDee Belemnite (PDB) standard for carbon. The reproducibility of

duplicate analyses is generally better than  $\pm 0.14\text{‰}$  for each oxygen and carbon isotope measurement. To determine stages of calcite cementation, an acid solution of potassium ferricyanide which imparts a blue stain to rich iron calcite was used (Dickson, 1966; Lindholm and Finkleman, 1972).

### **Detrital Composition**

Petrographic investigation of the Willow Creek sandstones revealed that their framework grains are rock fragments and quartz with a minor amount of feldspar (Table 1). Their present sandstone composition is slightly different from their composition at the time of deposition due to extensive diagenesis. The total of secondary pores plus primary pores filled with cement averages 10%. This value suggests that feldspar and other detrital grains have been partially or completely dissolved. If these dissolved grains are disregarded, the sandstones are now mainly lithic arenite (Pettijohn et al., 1987), with an average composition of Q<sub>44</sub>, R<sub>49</sub>, F<sub>7</sub> (Fig. 4).

The sandstones contain average 44% monocrystalline quartz (Fig. 5 A) and 8.8% polycrystalline quartz (Fig. 5 B). Three types of lithic components are observed in the sandstones: sedimentary, igneous, and metamorphic. Sedimentary rock fragments, which include chert, carbonate, and shale, are the most dominant rock fragments (Fig. 5A) and average 55.5% of the total rock fragments. Igneous rock fragments, which are mostly of volcanic origin (Fig. 5 C), compose about 21.5% of the total lithic components. Metamorphic detritals including polycrystalline quartz (Fig. 5 D) average 23% of the rock fragments.

Feldspar is present in amounts ranging from 1.8% to 14.4% and averaging 7% of the total framework grains (Fig.5 E). Although plagioclase is the dominant feldspar, orthoclase is also present. Muscovite was observed as well (Fig. 5 F).

The grain size, which decreases from the lower to the upper Willow Creek sandstones, averages 0.15 mm. The grain shapes are subrounded to subangular. The sandstones are moderately- to well - sorted according to the definition of Longiaru (1987). The sandstones are characterized by a general lack of matrix, with an average of 1% (range 0-3%).

The sandstones of the Willow Creek Formation were derived primarily from sedimentary, volcanic and metamorphic source areas (Mack and Jerzykiewicz, 1989). A sedimentary source is indicated by the abundance of detrital chert (Fig. 4 A) and carbonate rock fragments. A volcanic source is shown by the presence of volcanic rock fragments, which contain plagioclase and display microlitic or lathwork textures (Fig. 5 C), whereas the existence of polycrystalline quartz and foliated quartz and mica signifies a metamorphic source (Fig. 5 D).

### **Clay Minerals**

Both authigenic and non-authigenic clays were observed in the Willow Creek sandstones. The non-authigenic clays are irregular and oriented parallel to the grain surface (Fig. 6 A) and show features characteristic of mechanical infiltration. Infiltrated clay coatings typically show the smooth surface texture of smectite when examined under the SEM (Fig. 6 A). In contrast, authigenic clay minerals occur as grain coatings or pore-filling cements of pseudo-hexagonal and fibrous crystals oriented perpendicular to the grain surface (Fig. 6 B) or as euhedral plates 5-10  $\mu\text{m}$  wide and 7-20  $\mu\text{m}$  long in both primary



and secondary pores (Fig. 6 A). The sandstones generally contain a diversity of authigenic clay minerals including smectite, kaolinite, dickite, illite, and chlorite.

### ***Smectite***

Smectite, one of the dominant clay minerals in the sandstones, occurs as crenulated crystals that coat framework grains (Fig. 6 B).

Abundant smectite in the sandstones plays a major role in controlling reservoir quality (Primmer et al., 1997). Authigenic smectite in the sandstones is also regarded as a potential source material for other diagenetic processes such as illitization, chloritization, and silica cementation.

### ***Source of smectite***

Smectite probably formed from weathering products. Climatic aridity during the deposition of the Willow Creek Formation (Jerzykiewicz and Sweet, 1988), likely controlled water chemistry (Velde, 1985), and coupled with the relatively high volcanoclastic content (Fig. 5A), favoured smectite formation. SEM studies indicate that smectite was also formed from feldspar grains by weathering processes (Fig. 6 C).

### ***Kaolin***

Kaolin crystals, widely varying in size and morphology, occur as pore-filling cement, pseudomorphic replacement of feldspars, and clay. Most of the kaolin clay minerals are authigenic in origin. The authigenic origin of the kaolin polytype is determined based on its morphology and crystal habit (Fig. 6 E). Two forms of authigenic kaolin polytypes have been recognized: kaolinite (Fig. 5 D) and dickite (Fig. 6 E).

Kaolinite, characterized by its vermicular and booklet-like shape, occurs as pore-filling cement. Generally, kaolinite forms at shallow burial depths less than 1400 m (Bjørlykke, 1998). During deep burial, most kaolinite transfers into a more blocky shape. The dickite (Fig. 6 A) most likely replaced the kaolinite, as indicated by the presence of remnant kaolinite crystals within the dickite (Fig. 6 A). Generally, dickite replaces kaolinite within a burial depth ranging from 2500-5000 m (Hurst and Irwin, 1982; Ehrenberg, et al., 1993; Osborne et al., 1994). In deeply buried sandstones, kaolinite-to-dickite transformation proceeds by continuous structural changes associated with crystal coarsening and progresses from booklet to blocky morphology (Lanson, et al., 2002). As burial depth reaches greater than 4000 m, the dickite transforms into more isometric blocky crystals (Beaufort et al. 1998). The presence of the blocky dickite (Fig. 6 E) may suggest that the sandstones were buried deeper than 2 km. This finding is consistent with the burial and tectonic history of the sandstones.

#### *Source of kaolinite*

The distribution pattern of kaolinite is controlled by the availability of unstable grains such as feldspar and mica, and by the availability of a great amount of meteoric water (Bjørlykke, 1998). During wetter climatic conditions, the action of low-pH ground waters on detrital aluminosilicate minerals such as feldspar and/or mica result in kaolinite precipitation (Bjørlykke, 1998).

#### *Illite*

Illite, one of the most abundant authigenic clay minerals in the sandstones (Fig. 6 F and 7 A), occurs as wispy authigenic crystals lining pore spaces. Illite is formed by the

weathering or hydrothermal alteration of aluminum-rich minerals such as smectite, kaolinite, k-feldspar and mica during the different stages of diagenesis. Illite also forms as an intermixed layer with smectite (Fig. 6 F).

#### *Source of illite*

In this study, smectite is regarded as one of the main sources of illite precipitation, as indicated by the presence of a significant amount of a mixed layer of illite-smectite (Fig. 7 B and Fig. 6 F), whereas the presence of a significant amount of kaolinite with a relatively lower degree of illitization suggests that kaolinite was not the major source of the authigenic illite.

#### *Chlorite*

Authigenic flakes and rosettes of chlorite (Fig. 6 F) occur in the sandstones as thin coating clay. Chlorite grain coating is typically the dominant clay in lithic sandstones with abundant unstable rock fragments such as volcanic lithic grains (Rabin and Lerbekmo, 1977). The main processes for chlorite formation in sandstones are replacement of unstable grains, replacement of authigenic clays, and direct precipitation of chlorite from pore fluids (Anjos et al., 2003; Chang et al., 1986). Chlorite distribution, however, varied typically in relation to depth, suggesting an increasing authigenesis with deep burial. The timing of the chlorite formation was either contemporaneous with or after the quartz overgrowth precipitation (Fig. 7 F).

#### *Source of chlorite*

In the Willow Creek sandstones, the alteration of volcanic rock fragments was clearly a significant source for chlorite precipitation, as indicated by the abundant volcanic lithic

components (Fig. 5 A). Another possible source for the formation of chlorite is the late diagenetic chloritization of smectite. The presence of mixed layers of chlorite-smectite supports this finding (Fig. 7 C).

### **Quartz Cement**

Quartz cement, the authigenic cement most responsible for the destruction of sandstone porosity in deeply buried reservoirs (Blatt, 1979; Lerbekmo, 1961), commonly occurs as an euhedral overgrowth on detrital grains. In the Willow Creek sandstones, most of the quartz overgrowths are unaltered, even though the detrital quartz grains show indications of corrosion during the later diagenetic regime (Fig. 7 D).

The distribution of silica cement in the sandstones is variable. This study finds that the lowest concentrations of quartz are in samples tending to contain pore-lining clay (Fig. 7 F). This finding suggests that the pore-lining clays controlled silica cementation in the Willow Creek sandstones.

### *Source of Quartz Cement*

The probable sources of silica cementation in the sandstones are the dissolution of feldspar grains and the illitization of smectite or kaolinite (Fig. 7 A and B). Due to the higher Si/Al ratio in feldspar than in the clay minerals, the dissolution of feldspar is regarded as the most probable source of silica cement (Fig. 8 A). Pressure dissolution, which is an important source for silica cementation in many sandstone reservoirs (Lerbekmo and Platt, 1962). The chert grains may consider one of the sources of silica cement that generated through pressure solution (Lerbekmo and Platt, 1962). The timing of the silica cementation is uncertain. Silica cementation probably started early after

feldspar dissolution and continued during burial from alteration of authigenic minerals (Fig. 7 E and F).

### **Calcite Cement**

Calcite cement, the most dominant cement in the Willow Creek sandstones, occurs in amounts ranging from traces to 45 %, and averages 15% of the total cement. Calcite cement is present as either poikilotopic spar with individual crystals reaching several millimeters in diameter, or as micrite (Fig.5 A and D). Calcite fills the primary or secondary pores and replaces the framework grains, mainly the feldspars. Most of the calcite cement formed in the vadose zone, as indicated by the presence of vadose features such as rhizcretions and glaebules (Jerzykiewicz and Sweet, 1986a; Esteban and Klappa, 1983).

#### *Source of Calcite Cement*

In the Willow Creek sandstones, the probable sources of the calcite cement are the dissolution of volcanic rock fragments and Ca-feldspar, and the illitization of smectite. However, the dissolved carbonate, which was brought in solution from the thrust-fold belt by fluvial systems, may also be regarded as an additional source for the calcite cement.

#### *Isotope Geochemistry of Calcite Cement*

Calcite cement in the Willow Creek sandstones has a range of  $\delta^{13}\text{C}$  values between  $-4.5$  and  $+0.4$  ‰ PDB, (Table 2). The higher  $\delta^{13}\text{C}$  values may be attributed to a significant involvement of carbon from soil-derived bicarbonate (Morad et al., 1993).

The oxygen isotope values of  $\delta^{18}\text{O}_{\text{water}}$  show a range from  $-17.6$  to  $-7.9$  ‰ (Table 2). The negative isotopic composition of the  $\delta^{18}\text{O}$  is consistent with the precipitation of calcite cement from meteoric waters (Beckner and Moszley, 1998). Carbonates deposited from meteoric water show a wide range of isotopic compositions, depending on the isotopic composition of rainfall, the temperature, the rate of evaporation, the relative humidity, and biological productivity (Hoefs, 2004). However, the reaction from mixing oxygen values from meteoric waters with those derived from the dissolution of detrital constituents, predominantly  $^{18}\text{O}$ -rich minerals such as volcanic rock fragments and feldspar (Fig. 8A), may cause a decrease in the  $\delta^{18}\text{O}$  values of the calcite cement. During deep burial, a thermally driven exchange between fluids and carbonate cement occurs (Longstaffe and Ayalon, 1987). This increase in temperature may cause a decrease in the  $\delta^{18}\text{O}$  values of the calcite cement (Longstaffe, 1989).

### **Porosity and Permeability of the Willow Creek Sandstones**

The present porosity of the Willow Creek sandstones is both primary and secondary in origin (Fig. 8 A and B). Different factors caused the decrease in the primary porosity of the sandstones, including compaction, calcite cementation, and authigenic clay mineral formation (Fig. 5 A and F; Fig 7 A and B).

The recognition of secondary porosity is based on petrographic and scanning electronic microscope studies (Schmidt and McDonald, 1979). The sandstones are characterized by several types of secondary porosity, including grain moldic porosity (Fig. 7A) and the partial dissolution of calcite cement (Fig. 8 B). Dissolution is the main process that enhances porosity during shallow and deep burial. The sandstone's porosity ranges from 4% to 11% and averages 9.4% (Fig. 9, Table 3). Examination of permeability versus

porosity plot (Fig. 9) indicates that two general trends are present. The upper Willow Creek generally plots on a higher permeability trend than the lower Willow Creek.

The sandstones generally have low permeability, ranging between 0.3 mD to 6.0 mD and averaging 5 mD (Table 3). Authigenic clay mineral and quartz cementation are the main control on the sandstone permeability. Clay and quartz cementation between the pores resulted in the plugging of the pore throats, hence reducing the permeability (Fig. 7).

## **Discussion**

### **Diagenetic Sequence**

The relative timing of the major diagenetic sequence of the sandstones, which has been determined from thin-section slides and SEM examination, is based on texture relationships (Fig. 10).

Diagenesis, as recognized in the Willow Creek sandstones, resulted from several processes including infiltration of clay, compaction, feldspar and rock fragment dissolution, and dissolution and transformation of authigenic minerals. Due to the complicated diagenetic interaction of these processes, the precise timing of the main diagenetic events cannot be completely defined. However, the diagenetic regimes of the Willow Creek Formation combine several processes related to three stages of diagenesis: eodiagenesis after deposition, mesodiagenesis during burial, and telodiagenesis after uplift. These diagenetic stages are adopted from Schmidt and McDonald (1979).

## **Eodiagenesis**

Climatic conditions and sandstone facies may play a significant role in controlling the nature of eogenetic (early) cements (Walker et al., 1978). In order for the climate to control the authigenic clay minerals in sandstones, the minerals must form relatively early and at shallow depths where the interstitial waters are mostly of meteoric origin (Suttner and Dutta, 1986). The arid to semiarid climatic conditions during the deposition of the Willow Creek sandstones (Jerzykiewicz and Sweet, 1986a, 1988; Sweet et al., 1990; Jerzykiewicz, 1992) had a strong control on the meteoric water, sandstone mineralogy, chemistry of pore fluids, and the nature of the early cement.

The diagenetic processes that are attributed to the eogenetic regime of the Willow Creek sandstones are early calcite cementation, infiltration, the dissolution of unstable grains, clay mineral formation, early silica cementation, and initial mechanical compaction.

Early calcite cement represents the first diagenetic event encountered in the studied samples. The evidence of the eogenetic origin of the calcite cementation in the sandstones is their low Fe content, loose grain packing, and the presence of undeformed ductile grains within calcite-cemented areas (Fig. 11 A).

The detrital silicate minerals are subject to dissolution and replacement by clay. The dissolution of feldspar and clay replacement become significant after deposition due to meteoric water flushing. Leaching occurs along the cleavages, which are the zones of weakness in the grains (Fig. 8A). SEM study showed that leaching of feldspar resulted in the precipitation of authigenic smectite and/or kaolinite (Fig. 6 C). The authigenic characteristic of clay minerals is indicated by the nature of the grain-clay textures (Wilson and Pittman, 1977).



Smectite, the dominant clay mineral during the early and intermediate stages of sandstone weathering (Chesworth, 1977), can form as a weathering product during arid to semiarid climatic conditions. The minimal throughput of water during arid to semiarid climatic conditions resulted in increased cation concentrations (Ca, Mg, Na, K, etc.) in the groundwater (Velde, 1985) and caused the precipitation of smectite. Generally, smectite has a higher occurrence than kaolinite in the studied sandstone samples. The occurrence of kaolinite in the Willow Creek sandstones is probably due to short seasonal humidity and is linked to increased ground water flow through the fluvial sandstones. Mechanical compaction occurred shortly after deposition, as shown by the abundance of deformed soft-grain minerals in some samples (Fig. 5 F). The amount of mechanical compaction is controlled primarily by the sandstone's mineralogy.

### **Mesodiagenesis**

Along with sandstone's provenance and depositional fabric, the diagenetic processes characterizing shallow burial (eodiagenesis) are an extremely important stage for later diagenetic reactions (mesogenesis) (Berner, 1980). During mesogenesis, the diagenetic modifications in the sandstones are chemical compaction, deformation of ductile grains, calcite and quartz cementation, continuous dissolution of unstable grains such as feldspar, mica, and rock fragments, and clay replacement.

Compaction is a continuous process throughout shallow and burial diagenesis, as indicated by the deformation of ductile grains and the presence of long, concavo-convex and sutured contacts between quartz grains (Fig. 11 B). The compaction effect on the sandstone's properties was controlled by the variation in the amount and pattern of calcite

cement (Fig. 5 F). Abundant calcite cementation inhibited the later mechanical compaction of the sandstones, thus preserving the unfilled part of the primary porosity.

Calcite cementation, the most volumetrically important, continued throughout mesodiagenesis. The main source of mesogenetic calcite was probably the local dissolution-reprecipitation of early calcite cement and carbonate intraclasts, smectite dissolution, and Ca-feldspar dissolution (Fig. 8A).

The next most important mesodiagenetic cement in the sandstones is quartz overgrowth (Fig. 7 D). Its presence suggests that the sandstones were buried deeper than 2.5 km, corresponding to a temperature greater than 70 °C. This is in agreement with findings by other authors who investigated different sedimentary basins (McBride, 1989; Giles et al., 1992; Worden and Morad, 2000; Salem, et al., 2000). The main controls on the amount of mesodiagenetic silica cement are the availability of silica ions, eogenetic cementation, and the amount of authigenic clay coating. The lack of quartz overgrowths in some samples of the Willow Creek sandstones is probably due to the process of grain coating via the precipitation of authigenic calcite or clay minerals (Fig. 11 C and D). Grain coating is considered to be an important diagenetic mechanism controlling quartz cementation during burial (Heald and Larese, 1974; Pittman and Lumsden, 1968).

The mesogenetic clay minerals in the sandstones are illite, chlorite, and dickite. Illite typically begins to form during burial at temperatures that exceed 70 °C (Bjørlykke, 1998), and strongly increases in sandstones buried deeper than 3.8 - 4 km equal to 120 – 140 °C (Bjørkum and Gjelsvik, 1988; Ehrenberg and Nadeau, 1989; Bjørlykke and Aagaard, 1992; Ehrenberg, 1990; Giles et al., 1992). As was previously suggested, the main source of illite is smectite. The transformation of smectite to illite requires a supply

of potassium and the privation of silica at the expense of aluminium. A supply of potassium was probably transferred locally from the simultaneous dissolution of potassium feldspar (Fig. 7 B). Illitization potentially releases considerable amounts of  $Mg^{2+}$  and  $Fe^{2+}$  ions that could be used in chlorite formation during later diagenetic reactions within the same rock.

Chlorite forms by the diagenetic transformation of smectite grain coatings (Fig 7 C). The formation of a mixed layer of chlorite-smectite suggests that Mg-rich clay minerals, which are abundant in the sandstones, were preferentially altered to a mixed-layer composition during progressive burial and increased temperature. The mesogenetic origin of chlorite has been suggested by Hillier et al. (1996) and Worden and Morad (2000) studies. These researchers indicated that the transformation of Mg-rich clay minerals to chlorite via a mixed layer chlorite-smectite occurred at a depth greater than 3 km, which evidently occurred during mesogenesis.

Dickite, another mesogenetic clay mineral, is formed by a progressive increase in burial depth from 2-3 km, or at a depth corresponding to a temperature between 70 and 90°C (Worden and Morad, 2003). At a depth greater than 4.5 km most of the kaolinite transfers into more blocky dickite (Cassagnabere, 1998). The main source of blocky dickite (Fig. 6 E) in the Willow Creek sandstones was eogenetic kaolinite (Fig. 7 E). The transformation of the kaolinite into dickite is probably enhanced by an increase in the acidity of the pore water, or a decrease in the  $aK^+/aH^+$  ratio (Worden and Morad, 2003). The timing of the dickite formation was probably before that of the illite because illite forms overgrowths and envelopes the edges of dickite (Fig. 7 B).

### **Telodiagenesis**

The telogenesis regime is characterized by the displacement of formation water by meteoric water during a phase of tectonic uplift and erosion, promoting the infiltration of meteoric water into the sandstones. Generally, meteoric water is very dilute, oxidizing, saturated with dissolved CO<sub>2</sub>, and therefore acidic (Worden and Morad, 2003). This characteristic of meteoric water leads to the alteration of detrital grains and the formation of authigenic clay minerals. However, the main telogenetic processes during this stage are leaching of feldspar grains, (Fig. 5 C, Fig. 8 A, and B), precipitation of kaolinite (Fig. 6 D) and dissolution of calcite cement. It is likely that late, topographically driven, meteoric recharge during basin uplift is responsible for the dissolution of calcite and feldspar and the formation of kaolinite.

### **Diagenetic Control on Reservoir Properties**

The reservoir properties (porosity and permeability) of the Willow Creek sandstones show considerable heterogeneity (Table 3). This heterogeneity was probably induced by the sandstones' complex diagenetic history, which resulted in various types of diagenetic alterations that controlled the sandstones' porosity and permeability. The upper Willow Creek plots on a somewhat higher permeability trend than the lower Willow Creek (Fig. 9) probably due grain size differences between the upper Willow Creek sandstones and the lower Willow Creek sandstones. Size does affect permeability; the finer the sand, the lower the permeability.

During eogenesis, most of the deterioration in both porosity and permeability resulted from calcite cementation, authigenic clay-mineral precipitation, and the infiltration of

clay. Early calcite cementation reduced the primary porosity by filling the pore space between the grains. The precipitation of authigenic smectite and the infiltration of clay reduce the porosity and permeability in the sandstones because of their depositional structure, which causes the pore systems to have a very high surface-area-to-volume ratio (Almon, 1979). The smectite also changed the pore diameter and resulted in reduced permeability.

Eogenetic processes produced a minor portion of the secondary porosity by initial framework-grain dissolution. Petrographic evidence suggests that lithic fragments and feldspar grains were the most abundant types of grains dissolved in the sandstones (Fig. 5 D). The dissolution-porosity development is probably a continuous process during mesodiagenesis.

The influence of diagenetic alteration on the reservoir quality continued during mesogenesis. The mesogenetic processes that had an impact on porosity and permeability include calcite precipitation, compaction, clay mineral alteration and feldspar dissolution. In most sandstone samples, calcite cementation thoroughly filled the space between grains, resulting in a reduction in porosity and, thus, poor reservoir properties. Poor reservoir quality characterizes the sandstones that show evidence of mechanical and chemical compaction (Fig. 5 F). Sandstones that contain a mixture of minerals other than quartz, such as rock fragments and ductile minerals, respond differently to pressure. The softer grains are deforming more readily and accommodating much of the increase in load, resulting in porosity reduction. Compaction continued in the sandstones and stopped when the sandstones were cemented completely by calcite.

The mesogenic clay minerals such as chlorite and illite are important controls on the porosity and the permeability of the sandstones where the clays bridge or fill pores. Thin chlorite pore-linings helped to preserve porosity by inhibiting quartz overgrowth and/or pressure dissolution (e.g., Pittman and Lumsden, 1968; Heald and Larese, 1974; Dutton, 1977; Pittman et al., 1992; Ehrenberg et al., 1993; Hillier, 1994; Ryan and Reynolds, 1996; Anjos, et al., 2003). The thicker chlorite grain coatings resulted in decreasing permeability and an increase in the irreducible water saturation, hence resulting in a poor sandstone reservoir. Illite pore-linings on the other hand, are not as effective as chlorite in stopping quartz cementation (Morad, et al., 1994; De Rose et al., 2000), but illite appears to increase intergranular pressure dissolution, which causes an increase in quartz cementation and, hence, decreased reservoir quality. The reservoir quality of the sandstones also decreased due to the microporous nature of the authigenic illite, which work as solid overgrowths that divide the pore spaces into a large number of very thin channels, causing increased tortuosity.

During mesogenesis, most of the secondary porosity was created by the leaching of unstable grains such as lithics, feldspar and eogenetic carbonate (Fig. 5 D).

During telogenesis, the formation of kaolinite and the dissolution of feldspar grains and calcite cement also exerted control on reservoir quality (Fig. 8 A and B). Kaolinite, which consumed a large part of the original pore space, reduced the porosity and resulted in poor reservoir quality, whereas the leaching of unstable grains and the dissolution of calcite cement resulted in the development of secondary porosity.

## Conclusion

1. The Willow Creek sandstones in the southern Foothills region of west-central Alberta are classified as sublitharenites and lithic arenites.
2. Three diagenetic stages have been recognized in the Willow Creek sandstones: eodiagenesis, mesodiagenesis, and teleodiagenesis. Eogenetic evolution resulted primarily in clay infiltration, the formation of authigenic smectite, cementation by calcite, and the initial dissolution of unstable framework grains. The mesogenesis stage was characterized by chemical compaction, deformation and bending of ductile grains, calcite and quartz cementation, continued dissolution of feldspar, mica, and rock fragment grains, illitization and/or chloritization of smectite, and the transformation of kaolinite into dickite. The diagenetic processes exerted during teleodiagenesis are calcite and feldspar dissolution and kaolinite precipitation.
3. The diagenetic processes that occurred during progressively increasing burial and subsequent uplifting, have exerted an important control on reservoir heterogeneity in the predominantly fluvial Late Maastrichtian - Early Paleocene Willow Creek sandstones. Generally, the reservoir heterogeneity of the sandstones can be attributed to variations in the amount of calcite cement, and the occurrence of several events of calcite cementation.
4. This study may assist in better delineating other areas of potential reservoir for similar age fluvial deposits occurring in the subsurface such as Scollard and Coalspur formations in southern and southwestern Alberta.

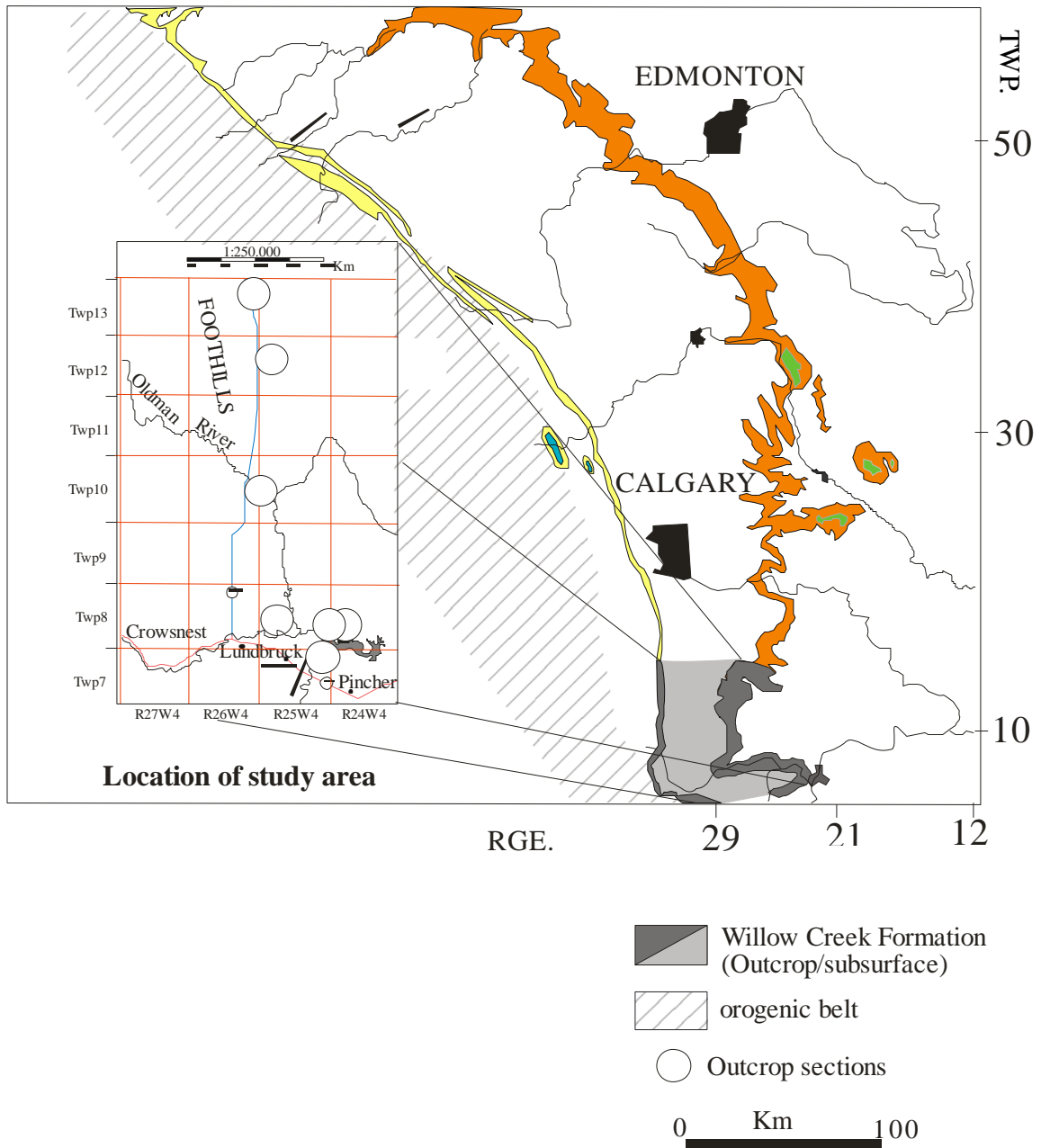


Figure 1. Outcrop distribution of the Willow Creek Formation in southwestern Alberta, and the location of the studied outcrop sections.



Southern Foothills	
Age	Formation
Paleocene	Porcupine Hills Formation
	Willow Creek Formation
	upper Willow Creek
Maastrichtian	lower Willow Creek
	St. Mary River Formation
Campanian	Bearpaw Formation
	Belly River Group

Figure 2. Generalized chart of the late Campanian to Paleocene stratigraphy of southwestern Alberta, showing the position of Willow Creek Formation.

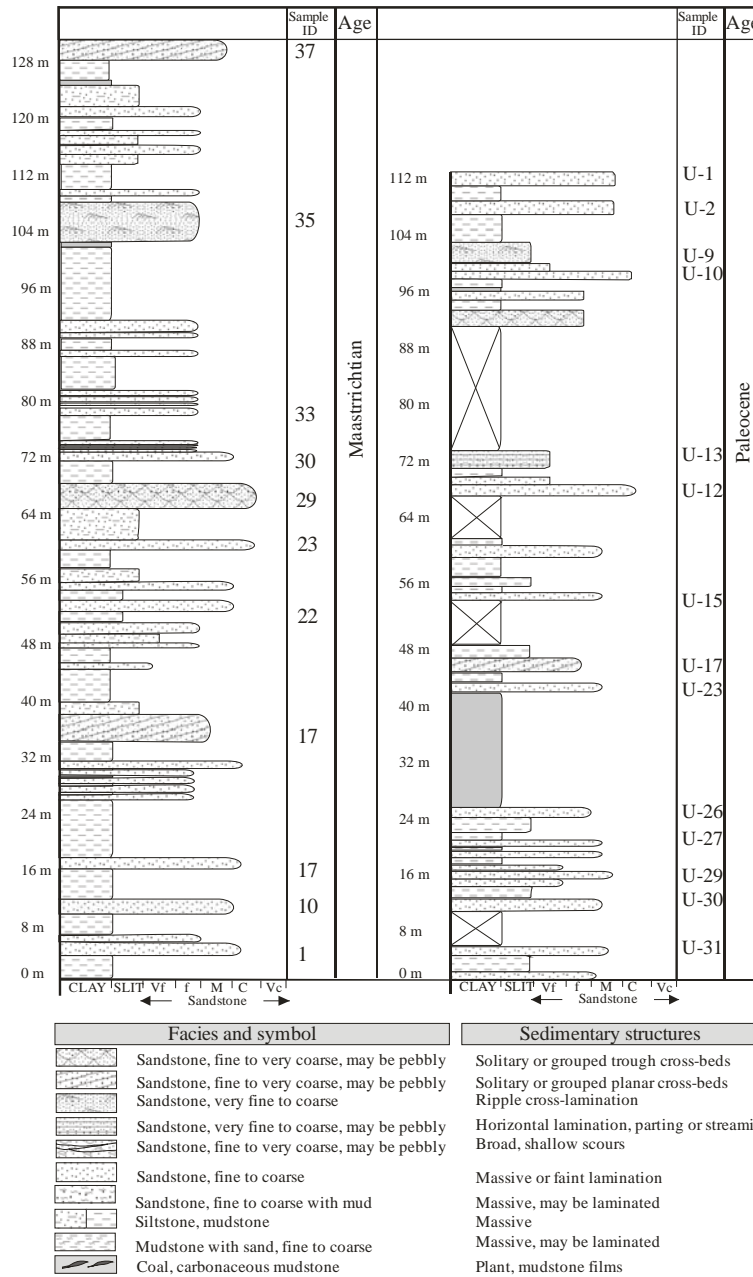


Figure 3. Vertical profiles for the Oldman River locality, upper Willow Creek Formation (Paleocene) and Oldman River Dam Reservoir, lower Willow Creek Formation (Maastrichtian). The table shows the locations of the samples analyzed in the study area the . Zero datum is the base of the outcrop section.

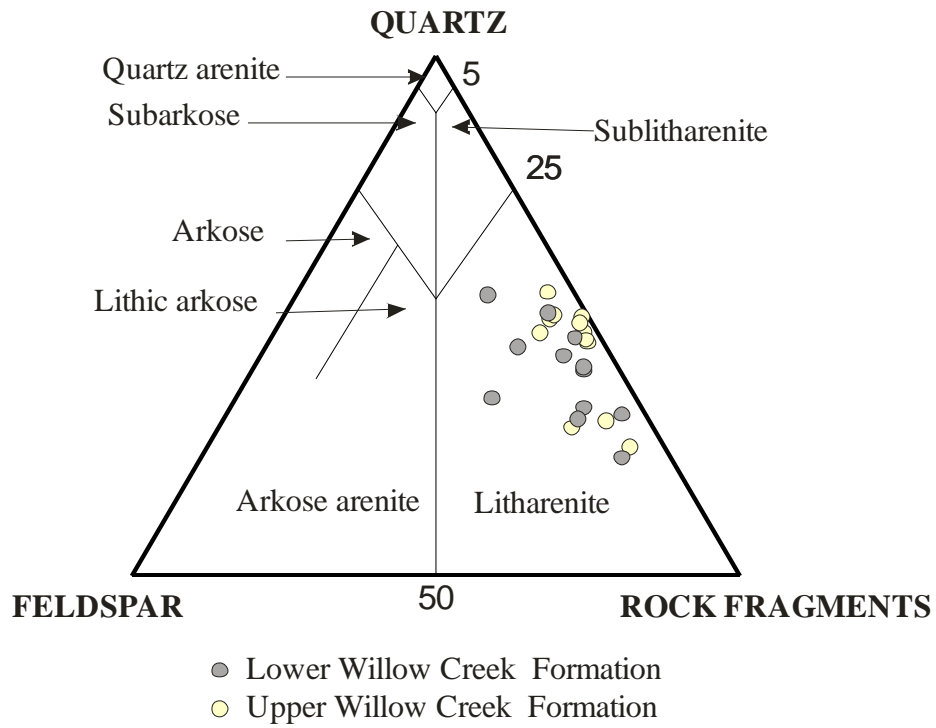


Figure 4. Classification of Willow Creek Formation sandstones (after Pettijohn et al., 1987).

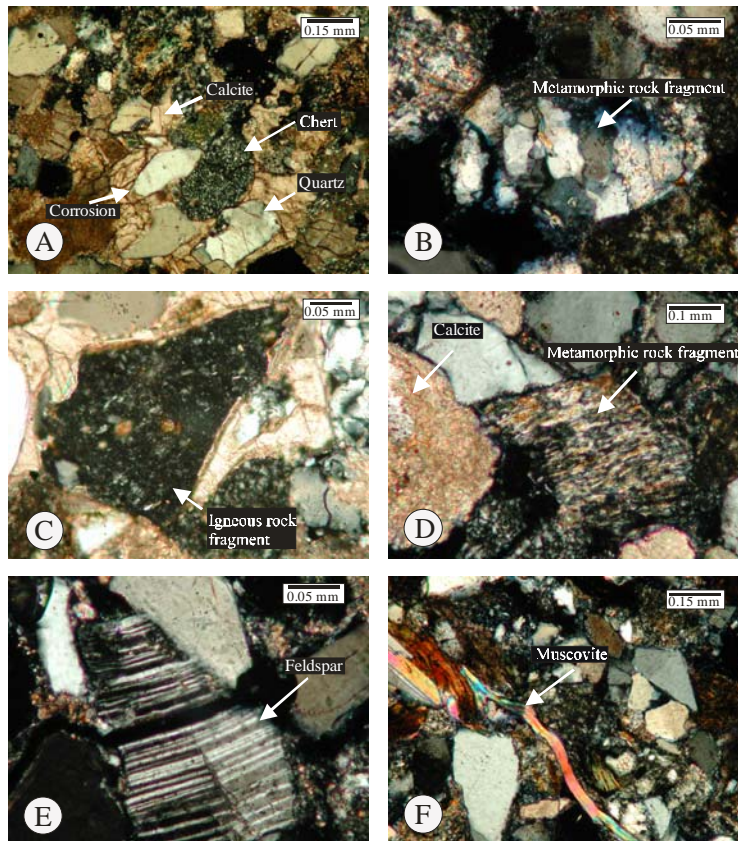


Figure 5. Thin section photomicrographs were taken under cross-polarizers.: (A) – quartz and chert grains “floating” in calcite cement. Note the corrosion of quartz grain by calcite cement which occurred during late diagenesis (sample 10, lower Willow Creek Formation, Oldman River Dam Reservoir); (B) – polycrystalline quartz grain of metamorphic origin consists of numerous elongate quartz crystals welded together (sample 1, lower Willow Creek Formation, Oldman River Dam Reservoir); (C) – igneous rock fragment probably of volcanic origin. Note the small laths of feldspar and very fine crystallinity (sample C4, lower Willow Creek Formation, Oldman River Dam Reservoir); (D) – high rank metamorphic rock fragment. Note the partial dissolution of the metamorphic rock fragments and development of secondary porosity (sample 12, lower Willow Creek Formation, Oldman River Dam Reservoir); (E) – unaltered feldspar grain (sample 1, lower Willow Creek Formation, Oldman River Dam Reservoir); (F) – deformed muscovite by compaction mechanism. Note the effect of mechanical compaction on porosity (sample C12, lower Willow Creek Formation, Oldman River Dam Reservoir).

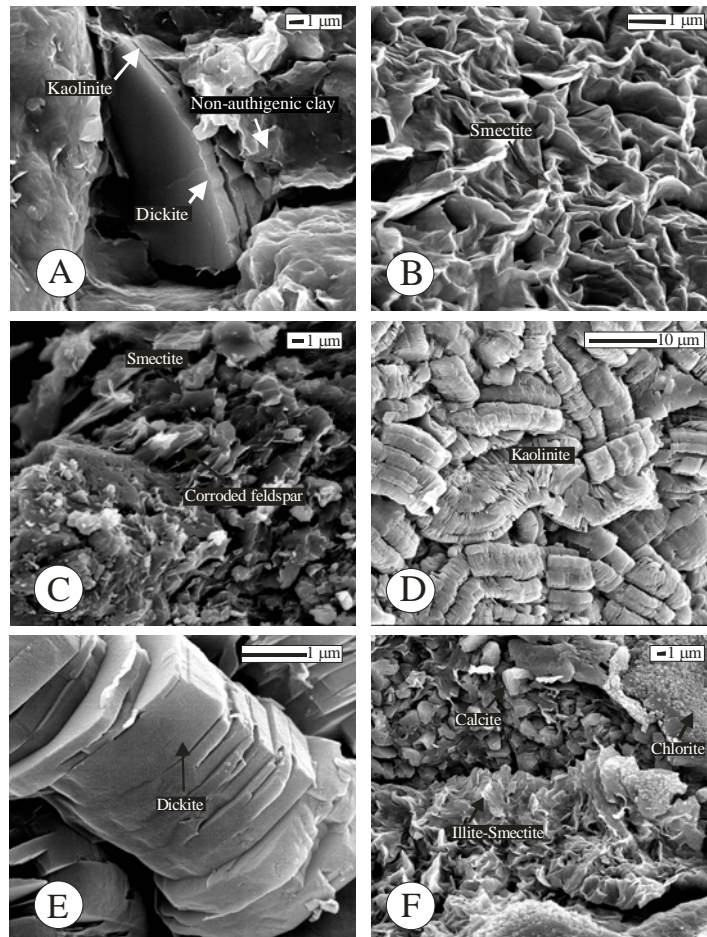


Figure 6. SEM photomicrographs: (A) – smectite and authigenic dickite pore-filling. Note the remnant of authigenic kaolinite between dickite crystals (sample C12, lower Willow Creek Formation, Oldman River Dam Reservoir); (B) – authigenic smectite formed as pore-lining clay (sample 3, lower Willow Creek Formation, Oldman River Dam Reservoir); (C) – alteration of feldspar grain and formation of smectite (sample 3, upper Willow Creek Formation, Oldman River Dam Reservoir); (D) – vermicular aggregates of euhedral crystals of authigenic kaolinite formed as a pore-filling clay that reduced the porosity (sample C 5, lower Willow Creek Formation, Oldman River Dam Reservoir); (E) – vermicular aggregates of euhedral crystals of authigenic dickite. Note the blocky shape of the dickite crystals (sample C 3, lower Willow Creek Formation, Oldman River Dam Reservoir); (F) – authigenic pore-filling illite-smectite and late diagenetic chlorite. Note that illite-smectite postdate calcite cement and predate chlorite (sample B 13, upper Willow Creek Formation, Oldman River Dam Reservoir).



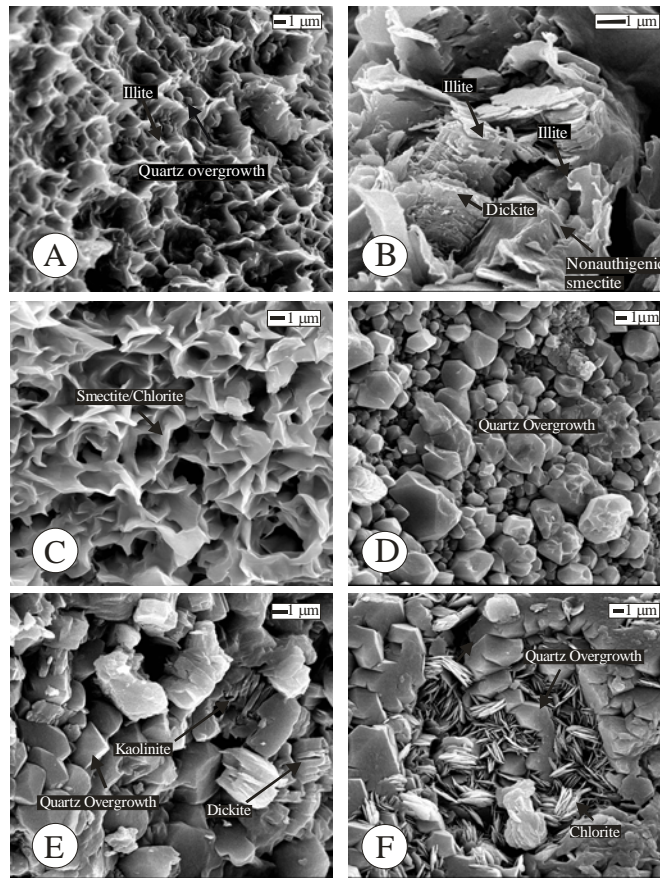


Figure 7. SEM photomicrographs. (A) – authigenic illite and minute amount of quartz overgrowth. Note the role of illite coating on silica cementation (sample B 12, upper Willow Creek Formation, Oldman River Dam Reservoir); (B) – illitization of kaolin minerals and smectite. Note that the timing of dickite formation was before illite because illite forms overgrowths and envelopes the edges of dickite (sample B 10, upper Willow Creek Formation, Oldman River Dam Reservoir); (C) – authigenic smectite/chlorite mixed layers (sample B 2, upper Willow Creek Formation, Oldman River Dam Reservoir); (D) – quartz overgrowth formed during mesogenesis. Note the intense quartz cementation and the absence of authigenic clay minerals (sample C 4, lower Willow Creek Formation, Oldman River Dam Reservoir); (E) – Authigenic dickite and quartz overgrowth both formed during mesogenesis (sample K-T B 9, lower Willow Creek Formation, highway 22 locality); (F) – Authigenic chlorite engulfed by quartz overgrowth (sample C 4, lower Willow Creek Formation, Oldman River Dam Reservoir).

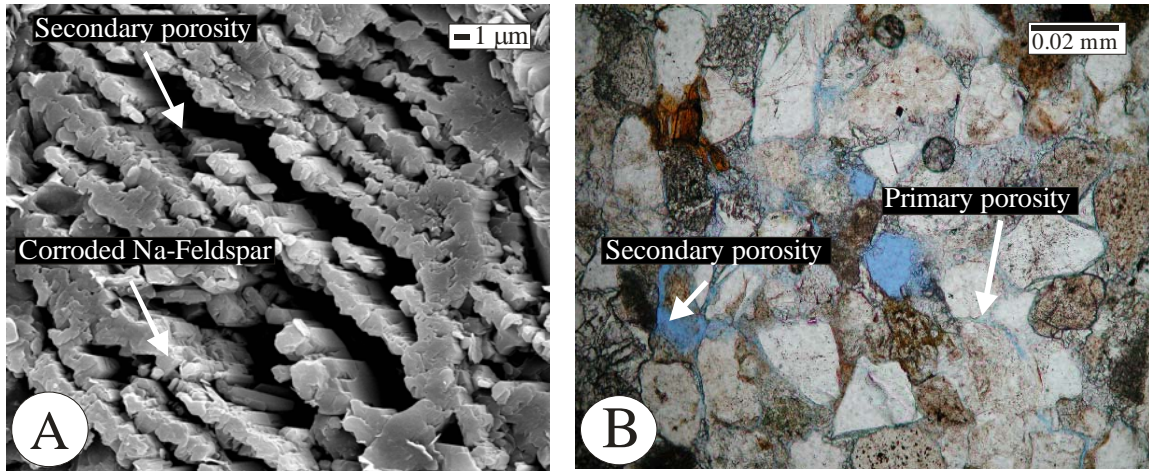


Figure 8. SEM and thin section photomicrographs was taken under plane light (A) – Secondary leaching of plagioclase feldspar and development of secondary porosity (sample C 4, lower Willow Creek Formation, Oldman River Dam Reservoir); (B) – preserved unfilled part of the primary porosity by early calcite cementation and the dissolution of calcite cement and development of secondary porosity (sample B 10, upper Willow Creek Formation, Oldman River Dam Reservoir).

### Permeability VS Porosity of the Willow Creek Formation

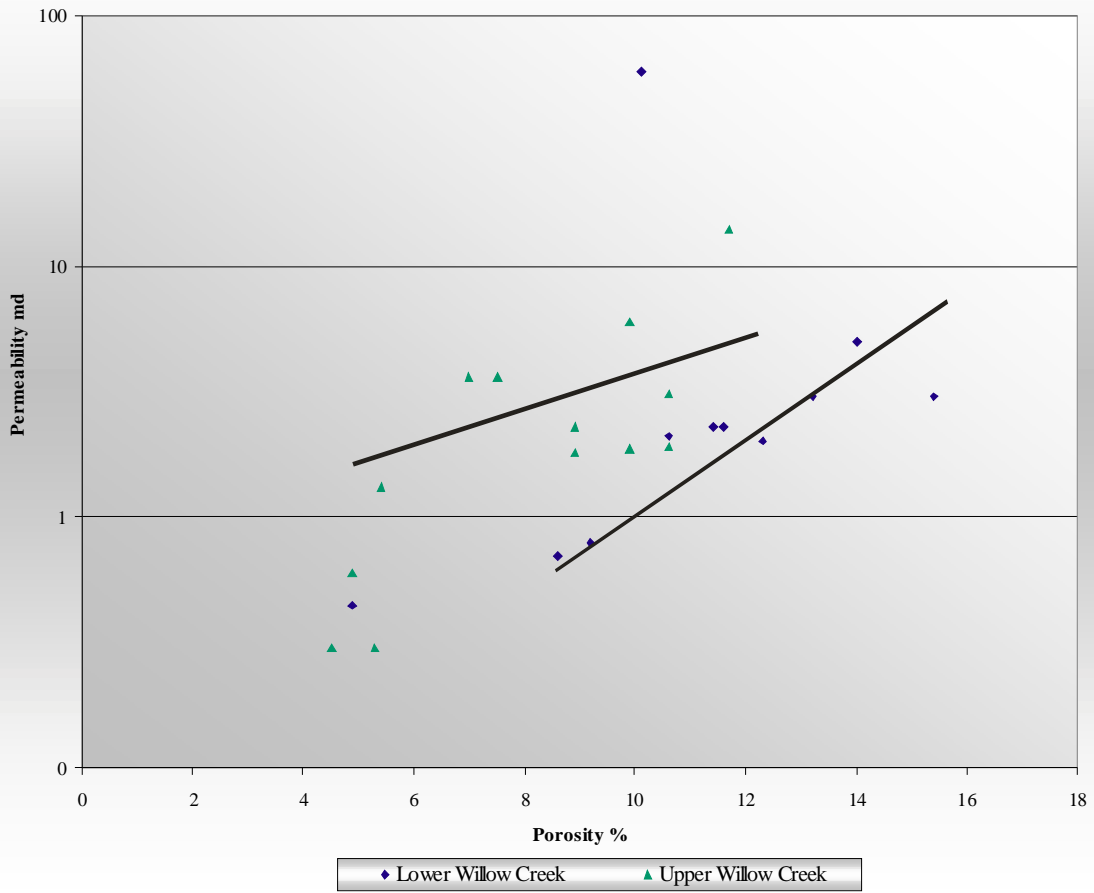


Figure 9. Plot showing sandstone permeability mD versus porosity (vol.%) from outcrop samples, Willow Creek sandstones.



Diagenesis sequence	Eodiagenesis	Mesodiagenesis	Telodiagenesis
Compaction	<u>Mechanical</u>	<u>Chemical</u>	
Calcite cementation	—————	—————	- - - - - ?
Dissolution of feldspar and volcanic fragments	—————	—————	
Quartz overgrowth	—————	—————	- - - - - ?
Smectite pore fill	—————	- - - - -	—————
Kaolinite pore fill	—————	—————	
Formation of dickite		—————	
Formation of illite		—————	- - - - - ?
Formation of chlorite		—————	- - - - - ?
Calcite dissolution			—————
Quartz dissolution			- - - - - ? ———

Figure 10. Generalized diagenetic sequence for the Willow Creek Formation.

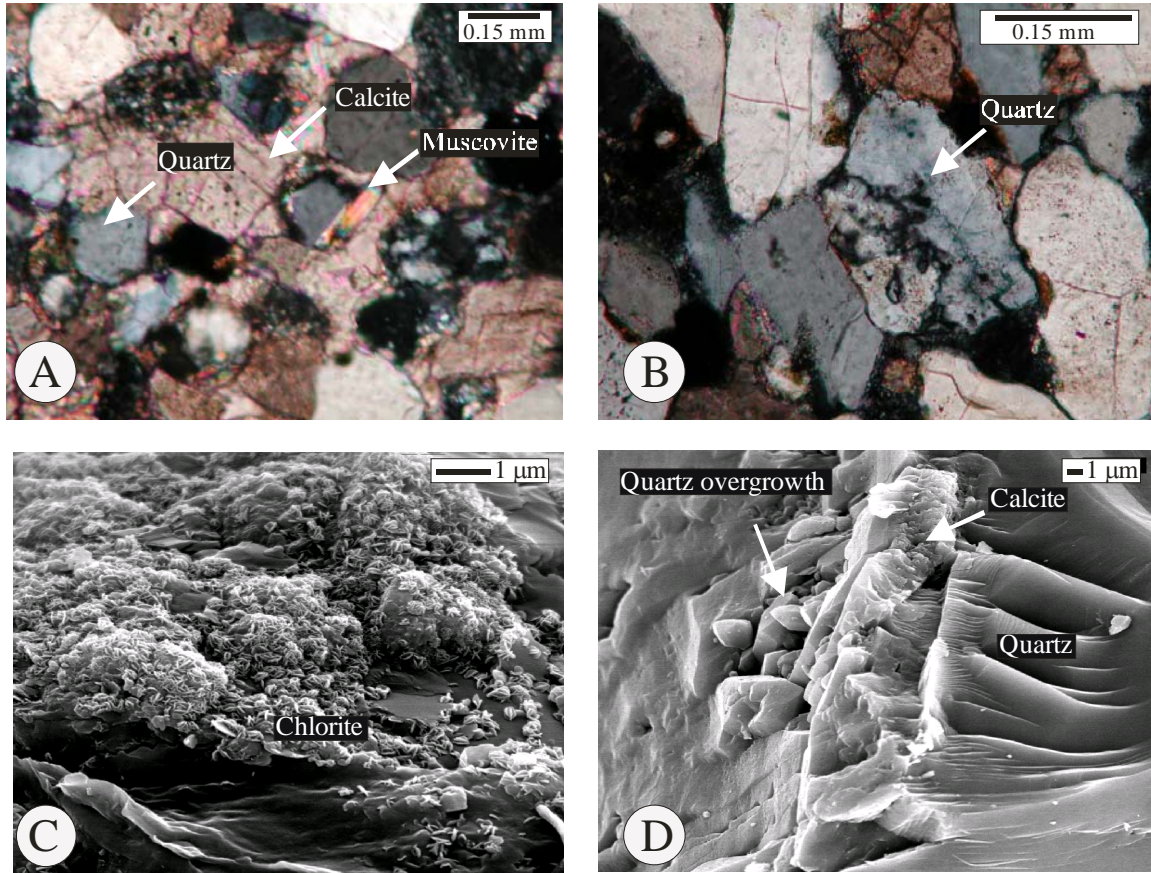


Figure 11. SEM and thin section photomicrographs (A) – quartz grains “floating” in calcite cement. Note the loose grain packing and undeformed muscovite grain (sample 17, lower Willow Creek Formation, Oldman River Dam Reservoir); (B) – quartz grains. Note the presence of long, concavo-convex and sutured contacts between quartz grains (sample 17 B, upper Willow Creek Formation, Oldman River Dam Reservoir); (C) – authigenic chlorite coating (sample B 4, upper Willow Creek Formation, Oldman River Dam Reservoir); (D) – quartz overgrowth and calcite cement-coated quartz grain. Note that calcite coating inhibited further silica cementation (sample 3, lower Willow Creek Formation, Oldman River Dam Reservoir).

Sample ID	Formation Name	Mono-Quartz %	Poly-Quartz %	Feldspar %	Chert %	Carbonate %	Volcanic Lithics%	Meta. Lithics %	Grain Size mm
-1-	Lower Willow Creek	48	6	5.6	19	6.4	10	5	0.1
-10-	Lower Willow Creek	57.1	4.6	6.1	12.3	4.6	10.7	4.6	0.1
-17-	Lower Willow Creek	38	4.2	14	19	4.9	9.1	10.8	0.1
-22-	Lower Willow Creek	40	2.5	7	20.6	7.5	11.4	11	0.15
-23-	Lower Willow Creek	37.2	2.7	6.2	33	2	13.5	5.4	0.2
-29-	Lower Willow Creek	34	3.5	5.5	34	1.8	16	5.2	0.2
-30-	Lower Willow Creek	38	0	7.1	26.1	8.6	11.9	8.3	0.1
-31-	Lower Willow Creek	40	3.5	4	27	3.5	11	11	0.15
-33-	Lower Willow Creek	42.5	0	1.8	25.9	9.2	16.6	4	0.1
-35-	Lower Willow Creek	31	5.8	7	25.5	5.8	17.6	7.3	0.15
-37-	Lower Willow Creek	40.6	5.2	3.7	33.4	2.2	10.5	4.4	0.2
U-1	Upper Willow Creek	35	5.4	5.5	28.6	4	9	12.5	0.2
U-2	Upper Willow Creek	46.7	1.6	3	28	2	13.4	5.3	0.2
U-9	Upper Willow Creek	53.1	4	6	15.6	8.2	8.1	5	0.1
U-10	Upper Willow Creek	41	5.8	9.8	18.1	6.8	11.7	6.8	0.2
U-13	Upper Willow Creek	49	7.2	7.2	16.3	5.5	9	5.8	0.05
U-12	Upper Willow Creek	39	6.5	3.2	27	2.5	12	9.8	0.15
U-15	Upper Willow Creek	41.6	6	14.4	17	4	11	6	0.15
U-17	Upper Willow Creek	57.2	5.3	7.1	12.2	1.7	9.4	7.1	0.07
U-23	Upper Willow Creek	57	2.8	9.6	18	3.3	5.6	3.7	0.1
U-26	Upper Willow Creek	57	2.8	9.6	18	3.3	5.6	3.7	0.07
U-27	Upper Willow Creek	37.4	11.4	14.2	20	2.8	5.5	8.7	0.1
U-29	Upper Willow Creek	52	7.4	8.6	24.6	1.3	2.4	3.7	0.15
U-30	Upper Willow Creek	43	2	10	17	8	8	12	0.1
U-31	Upper Willow Creek	58	0	8.8	17.6	3.2	5.1	7.3	0.1

Table 1. Detrital mineralogy of the Willow Creek sandstones in the southern Foothills of Alberta.

Sample Number	13/12-C	18/16-O	VSMOW
1	-2.511	-13.199	15.211
6	-1.701	-9.814	18.596
10	-2.688	-15.056	13.354
11	-4.58	-13.129	15.281
12	-7.492	-10.607	17.803
13	-2.106	-10.889	17.521
14	-1.119	-7.928	20.482
16	-0.879	-9.644	18.766
18	-2.297	-15.191	13.219
19	-1.56	-10.422	17.988
20	-2.555	-8.968	19.442
25A	-3.354	-8.915	19.495
26	-0.78	-9.998	18.412
29	-1.79	9.922	38.332
31	-3.687	-12.496	15.914
33	-3.011	-13.904	14.506
34	-1.64	-8.771	19.639
37	-0.473	-9.735	18.675
KT1	-3.192	-17.63	10.759

Table 2. Oxygen and carbon isotopic compositions of calcite cement from the Willow Creek sandstones.

Formation Name	Sample ID	Porosity %	Permeability md	Calcite cement %
Lower Willow Creek	-1-	15.4	3	7
Lower Willow Creek	-10-	4.9	0.44	25
Lower Willow Creek	-17-	9.2	0.79	10
Lower Willow Creek	-22-	10.6	2.1	8
Lower Willow Creek	-23-	13.2	3	7
Lower Willow Creek	-29-	10.1	59.4	4
Lower Willow Creek	-30-	11.4	2.3	5
Lower Willow Creek	-31-	11.6	2.3	5
Lower Willow Creek	-33-	8.6	0.7	10
Lower Willow Creek	-35-	12.3	2	4
Lower Willow Creek	-37-	14.0	5	3
Upper Willow Creek	U-1	4.5	0.3	30
Upper Willow Creek	U-2	11.7	14	3
Upper Willow Creek	U-9	10.6	1.9	1
Upper Willow Creek	U-10	8.9	1.8	10
Upper Willow Creek	U-13	9.9	1.86	11
Upper Willow Creek	U-12	9.9	6	8
Upper Willow Creek	U-15	8.9	2.3	13
Upper Willow Creek	U-17	10.6	3.1	5
Upper Willow Creek	U-23	4.9	0.6	25
Upper Willow Creek	U-26	7.5	3.6	40
Upper Willow Creek	U-27	7.0	3.6	40
Upper Willow Creek	U-29	5.3	0.3	40
Upper Willow Creek	U-30	5.4	1.32	45

Table 3. Porosity and permeability of selected Willow Creek sandstones.

## References

Allan, J.A. and Rutherford, R.L. 1934. Geology of central Alberta. Research Council of Alberta, Geology Division, Report 30.

Almon, W. R. 1979. Sandstone diagenesis as a factor in stimulation design. Preceeding of the 24<sup>th</sup> Annual Southwest Petroleum Short Course, Lubbock, Texas.

Anjos, S.M.C., De Ros, L.F. and Silva, C.M.A. 2003. Chlorite authigenesis and porosity preservation in the Upper Cretaceous marine sandstones of Santos Basin, offshore eastern Brazil. International Association of Sedimentologist, Special Publication, v. 34, p. 291-316.

Beaufort, D., A. Cassagnabere, S. Petit, B. Lanson, G. Berger, J. C. Lacharpagne, and H. Johansen, 1998. Kaolinite-to-dickite reaction in sandstone reservoirs, Clay Minerals, v. 33, p. 297-316.

Beckner, J.R. and Moszley, P.S. 1998. Origin and spatial distribution of early vadose and phreatic calcite cements in the Zia Formation, Albuquerque Basin, New Mexico, USA. Special Publication of International Association of Sedimentologists, v. 26, p. 2-51.

Berner, R.A. 1980. Early Diagenesis: A theoretical Approach. Proceton University Press, New Jersey, 241p.

Bjørlykke, K. 1998. Clay mineral diagenesis in sedimentary basins – a key to the prediction of rock properties. Example from the North Sea Basin. *Clay Minerals*, v. 33, p. 15-34.

Bjørlykke, K. and Aagaard, P. 1992. Clay mineral in North Sea sandstones. In: *Origin, diagenesis, and petrophysics of clay minerals in sandstone* (Houseknecht, D.W. and Pittman, E.D. eds). SEPM Special Publication 47, p. 65-80

Bjørkum, P.A. and Gjelsvik, N. 1988. An isochemical model for formation of authigenic kaolinite, k-feldspar, and illite in sediments. *Journal of Sedimentary Petrology*, v. 58, p. 506-511.

Blatt, H. 1979. Diagenesis Processes. In: *Aspect of diagenesis*. (Scholle, P.A. and Schluger, P.R. eds). Society of economic and Paleontologists and Mineralogists. Special Publication 26.

Bustin, R.M. 1992. Organic maturation of the Western Canadian Sedimentary Basin. *International Journal of Coal Geology*, v. 19, p. 319-358.

Carrigy, M.A. 1971. Lithostratigraphy of the uppermost Cretaceous (Lance) and Paleocene strata of the Alberta plains. *Research Council of Alberta Bulletin* 27, 161p.

Cassagnabere, A. 1998. Caractérisation et interpretation de la transition kaolinite-dickite dans les réservoirs a hydrocarbunres de Froy et Rind (Mer du Nord), Norvège. PhD thesis, University of Poitiers, pp. 238.

Chang, H.K., Mackenzie, F.T. and Schoonmarker, J. 1986. Comparison between the diagenesis of decahedral and trioctahedral smectite, Brazilian offshore basins. *Clays and Clay Minerals*, v. 34, p. 407-423.

Chesworth, W. 1977. Weathering stages of the common igneous rocks, index minerals and mineral assemblage at the surface of the earth. *Journal of Soil Science*, v. 28, p. 490-497.

Dawson, F.M., Evan, C. G., Marsh R., and Richardson, R. 1994. Uppermost Cretaceous and Tertiary of the Western Canada Sedimentary Basin. *In: Geological Atlas of the Western Canada Sedimentary Basin*. G.D. Mossop and I. Shetsen (comps.), Calgary. Canadian Society of Petroleum Geologists and Alberta Research Council, p. 387-406.

Dawson, G.M. 1886. Preliminary report on the physical and geological features of that portion of the Rocky Mountains between the latitude 49 degrees and 51 degrees 30 minutes. *Geological Survey of Canada, Annual Report, 1885*, v. 1, part B, 169 p.

Dawson, G. M. 1884. Report on the region in the Vicinity of the Bow and Belly Rivers, North West Territory; *Geological Survey of Canada, Rept. of Prog. 1882-83-84*, pt. C.



Dawson, G. M. 1883. Preliminary Report on the Geology of the Bow and Belly River Region, North West Territory, with Special Reference to the Coal Deposits. Geological Survey of Canada, Rept. of Prog. 1880-82, pt. B.

De Rose, L.F., Morad, S., Broman, G., Césero, P. and GomezGras, D. 2000. Influence of uplift and magmatism on distribution of quartz illite cementation: evidence from Siluro-Devonian sandstones of the Paraná Basin, Brazil. In: Quartz cementation in sandstones, (Worden R.H. and Morad, S., (eds.), International Association of Sedimentologist Special Publication 29, Blackwell Science, Oxford, p. 231-252.

Dickinson, W.R., 1970, Interpreting detrital modes of greywacke and arkose: *Journal of Sedimentary Petrology*, v. 40, p. 695–707.

Dickson, J.A.D., 1966. Carbonate identification and genesis as revealed by staining. *Journal of Sedimentary Petrology*, v. 36, p. 491-505.

Douglas, R.I.W. 1950. Callum Creek, Longford Creek, and Gap map-areas, Alberta. Geological Survey of Canada, Memoir 255.

Dutton, S.P. 1977. Diagenesis and porosity distribution in deltaic sandstones. Strawn Series (Pennsylvanian), North-central Texas. *Trans. Gulf Coast Assoc. Geol. Soc.*, v. 27, p. 272-277.

Ehrenberg, S.N. 1990. Relationship between diagenesis and reservoir quality in sandstone. *Bulletin of American Association of Petroleum Geologists*, v. 74, p. 1538-1559.

Ehrenberg, S.M., Aagaard, P., Wilson, M.J., Fraser, A. R. and Duthie, D.M.L. 1993. Depth-dependent transformation of kaolinite to dickite in sandstones of Norwegian continental shelf. *Clay Minerals*. v. 28, p. 325-352.

Ehrenberg S.N. and Nadeau P.H. 1989. Formation of diagenetic illite in sandstones of the Garn formation, Haltenbanken area, mid-Norwegian continental shelf. *Clay Minerals*, 24, p. 233-253.

Esteban, M. and Klappa, C. F. 1983. Subaerial exposure environment. *In* P. A. Scholle, D. C. and Moore (eds.) *Carbonate depositional environments: American Association of Petroleum Geologist Memoir 33*, p. 1- 54.

Giles, M. R., Syevenson, S., Martin, S. V., Cannon, S.J. C., Hamilton, P.J., Marshall, J.D. and Samways, G.M. 1992. The reservoir properties and diagenesis of Brent Group: a regional perspective. *In*, *Geology of Brent Group*, Morton, A.C., Haszeldine, R.S., Giles, M.R. and Brown, S., *Geological Society Special Publication 61*, p. 289-327.

Greg, H.M. and Jerzykiewicz, T. 1989. Provenance of post-Wapiabi sandstones and its implications for Campanian to Paleocene tectonic history of southern Canada Cordillera. *Canadian Journal of Earth Science*, v. 26, p. 665-676.

Hacquebard, P.A. 1977. Rank of coal as index of organic metamorphism for oil and gas in Alberta, Canada. *American Association of Petroleum Geologists Bulletin* 61; v. 5, p. 791.

Hages, C.O. 1943. Cowley map-area, Alberta. *Geology Survey of Canada Paper* 43-1.

Heald, M. and Larese R. 1974. Influence of coatings on quartz cementation. *Journal of Sedimentary Petrology*, v. 44, no. 4, p. 1269-1274.

Hillier, S. 1994. Pore-lining chlorite in siliciclastic reservoir sandstones: electron microprobe SEM and XRD data, and implications for their origin. *Clay Mineral.*, v. 29(4), p. 664-679.

Hillier, S., Fallick, A.E. and Matter, A. 1996. Origin of pore-lining chlorite in Aeolian Rotliegend of northern Germany. *Clay Minerals*, v. 31, p. 153-171.

Hoefs, J. 2004. *Stable isotope geochemistry*. Springer- Verlag Berlin Heidelberg New York, pp. 244.

Hurst, A., and Irwin, H. 1982. Geological modeling of clay diagenesis in sandstones, *Clay Minerals*, v. 17, p. 5-22.

Jerzykiewicz, T. 1997. Stratigraphic framework of the upper Cretaceous to Paleocene strata of the Alberta Basin. *Geological Survey of Canada Bulletin* 510, 121p.

Jerzykiewicz, T. 1992. Controls on the distribution of coal in the Campanian to Paleocene post-Wapiabi strata of the Rocky Mountain Foothills, Canada. *Geological Society of America, Special Paper* 267, p. 139-150.

Jerzykiewicz, T. and Labonte, M. 1991. Representation and statistical analysis of directional sedimentary structures in the uppermost Cretaceous-Paleocene of the Alberta foreland basin. In: *Current Research, Part B, Geological Survey of Canada, Paper* 91-1B, p. 47-49.

Jerzykiewicz, T. and Sweet, A.R. 1988. Sedimentological and palynological evidence of regional climatic changes in the Campanian to Paleocene sediments of the Rocky Mountain Foothills, Canada. *Sedimentary Geology*, v. 59, p. 29-76.

Jerzykiewicz, T. and Sweet, A.R. 1986a. The Cretaceous-Tertiary boundary in the central Alberta Foothills. I: Stratigraphy. *Canadian Journal of Earth Science*, v. 23, p. 1356-1374.

Jerzykiewicz, T. and Sweet, A.R. 1986b. Caliche and associated impoverished palynological assemblages: an innovative line of Paleoclimate research onto the uppermost Cretaceous and Paleocene of southern Alberta. *In* Current Research, Part B. Geological Survey of Canada, Paper 86-1B, p. 653-663.

Jordan, T.E. 1981. Thrust loads and foreland basin evolution, Cretaceous, western United State. *American Association of Petroleum Geologist*, v. 14, p. 75-99.

Lanson, B., Beaufort, D., Berger, G., Bauer, A., Cassaganbere, A. and Meunier, A. 2002. Authigenic kaolin and illite minerals during burial diagenesis of sandstones: a review. *Clay Minerals*, v. 37, p. 1-22.

Lerbekmo, J.F. 1989. The stratigraphic position of the 33-33r polarity chron boundary in southeastern Alberta. *Bulletin of Canadian Petroleum Geology*, v. 37, p. 43-47.

Lerbekmo, J.F. 1985. Magnetostratigraphic and biostratigraphic correlations of Maastrichtian to Early Paleocene strata between south-central Alberta and southwest Saskatchewan. *Bulletin of Canadian Petroleum Geology*, v. 33, p. 213-226.

Lerbekmo, J.F. and Plantt, R.L. 1962. Promotion of pressure-solution of silica in sandstones. *Journal of Sedimentary petrology*, v. 32, No. 3, p. 514-519.

Lerbekmo, J.F. 1961. Porosity reduction in Cretaceous sandstones of Alberta. *Journal of Alberta Society of petroleum geologists*, v. 9, No. 6, p. 192-199.

Lerbekmo, J.F. and Sweet, A.R. 2000. Magnetostratigraphy and biostratigraphy of the continental Paleocene in the Calgary area, southwestern Alberta. *Bulletin of Canadian Petroleum Geology*, v. 48; no.4, p. 285-306.

Lindholm, RC. and RB Finkleman, 1972, Calcite staining semi quantitative determination of ferrous iron. *Journal of Sedimentary Petrology*. v. 42, p. 239-242.

Longiaru, S. 1987. Visual comparators for estimating the degree of sorting from plane and thin section. *Journal of sedimentary petrology*, v. 57, p. 791-794.

Longstaffe, F. J. (1989) Stable isotopes as tracers in clastic diagenesis. *In* Hutcheon, I. E. (ed) *Short Course in Burial Diagenesis*, Mineralogical Association of Canada, Montreal, pp. 201-277.

Longstaffe, F. J. & Ayalon, A. (1987) Oxygen-isotope studies of clastic diagenesis in the Lower Cretaceous Viking Formation, Alberta; implications for the role of meteoric water. *In Diagenesis of Sedimentary Sequences*. Marshall, J. D., (ed), Geological Society Special Publication, Liverpool, p. 277-296.

Mack, G.H. and Jerzykiewicz, T. 1989. Provenance of post-Wapiabi sandstones and its implications for Campanian to Paleocene tectonic history of the southern Canadian Cordillera. *Canadian Journal of Earth Sciences*, v. 26, p. 665-676.

McBride, E. F. 1989. Quartz cementation in sandstones: a review, *Earth Science Reviews*, v. 26, p. 69-112.

Morad, C.I., Fastovsky, D.E. and Driese, S.G. 1993. Geochemistry and stable isotopes of paleosols. University of Tennessee Department of Geology Sciences. Studies in Geology, 65 p. no. 3, p. 346-358.

Morad, S., Ben Ismail, H., Al-Aasm, I.S. and De Ros, L.F. 1994. Diagenesis and formation-water chemistry of Triassic reservoir sandstones from southern Tunisia. *Journal of Sedimentology*, v. 41, p. 1253-1272.

Nurkowski, J.R. 1984. Coal quality, coal rank variation and its relation to reconstructed overburden, Upper Cretaceous and Tertiary plains coals, Alberta, Canada. *American Association of Petroleum Geologists, Bulletin*, v. 68, p. 285-295.

Osborne, M., Haszeldine, R. S., and A. E., Fallick, 1994. Variation in kaolinite morphology with growth temperature in isotopically mixed pore-fluids, Brent Group, UK North Sea, *Clay Minerals*, v. 29, p. 591-608.

Pettijohn, F. J., Potter, P.E. and Siever, R. 1987, *Sand and sandstone*, 2nd (ed.). Springer Verlag, New York, 553 p.

Pittman, E.D., Larese, R.E. and Heald, M.T. 1992. Clay coats: occurrence and relevance to preservation of porosity in sandstones. In: *Origin, Diagenesis, and Petrophysics of Clay Minerals in Sandstones*. Society of Economic Paleontologists and mineralogists

Special Publication 47, (Houseknecht, D. W. and Pittman, E.D., (eds.), Tulsa, OK, p. 241-265.

Pittman, E. and Lumsden, D.N. 1968. Relationship between chlorite coating on quartz grain and porosity, Spiro Sand, Oklahoma. *Journal of Sedimentary Petrology*, v. 38, p. 668-670.

Primmer, T.J., Cade, C.A., Avans, I. J. 1997. Global patterns in sandstone diagenesis: application to reservoir quality prediction for petroleum exploration. *American Association of Petroleum Geologists. Memoir 69*. p. 61-78.

Rabin, G.C. and Lerbekmo, J.F. 1977. A seminar on diagenesis. A home Oil Company Limited Publication, Calgary, Alberta. 56 p.

Russell, L.S. 1932. The Cretaceous-Tertiary Transition of Alberta. *Royal Society of Canada transitions*, v.26, p. 121-156.

Ryan, P.G. and Reynolds, R. G. 1996. The origin and diagenesis of grain-coating serpentine-chlorite in Tuscaloosa Formation, United States Gulf Coast. *American Association of Mineralogists*, v. 81, p. 213-225.

Salem, M. A., Morad, S., Mato, F. L. and Al-Asam, I. S. 2000, Diagenesis and reservoir-quality of fluvial sandstones during progressive burial and uplift: Evidence from the



Upper Jurassic Biopeda Member, Recôncavo Basin, Northeastern Brazil. *Bulletin of American Association of Petroleum Geologists*, v. 84, No. 7, p. 1015-1040.

Schmidt, V. and McDonald, D. A. 1979. The role of secondary porosity generation in the course of sandstone diagenesis. In P. A. Scholle and P. R. Schulger, eds., *Aspects of diagenesis*. SEPM Special publication 26, p. 175-207.

Smith, D.G. and Putnam, P. 2005. Fluvial architecture of the Lower Tertiary Paskapoo-Willow Creek formations, southwest Alberta. Field trip no. 11, 2005 AAPG annual convention.

Suttner, L.J. and Dutta, K. 1986. Alluvial sandstone composition and paleoclimate. II. Authigenic Mineralogy. *Journal of Sedimentary Petrology*, v. 56, no.3, p. 346- 358.

Suttner, L.J., Basu, A., and Mack, G.H., 1981, Climate and the origin of quartz arenites: *Journal of Sedimentary Petrology*, v. 51, p. 1235–1246.

Sweet, A.R., Braman, D.R. and Lerbekmo, J.F. 1990. Palynofloral response to K/T boundary events: A transitory interruption within a dynamic system. In: *Global catastrophes in Earth history*, V.L. Sharpton and P.D. Ward (eds.). Geological Society of America, Special Paper 247, p. 457-469.

Tozer, E. T. 1956. Uppermost Cretaceous and Paleocene non-marine molluscan faunas of Western Alberta. Geological Survey of Canada, Memoir 280, p. 1-125.

Tozer, E.T. 1953. The Cretaceous-Tertiary transition in southwestern Alberta. Third annual Field Conference and Symposium, Alberta Society of Petroleum Geologists, p. 23-31.

Velde, B. 1985. Clay minerals, a physico-chemical explanation of their occurrence. *Developments in Sedimentology*, v. 4, Elsevier, New York, 427 p.

Wachter, E. A. and Hayes, J. M. 1985. Exchange of oxygen isotopes in carbon dioxide-phosphoric acid systems *Journal of Chemical Geology: Isotope Geoscience section*, v 52, Issues 3-4, 15, p. 365-374.

Walker, T.R., Waugh, B. and Crone, A. J. 1978. Diagenesis in first-cycle desert alluvium of Cenozoic age, southwestern United States and northwestern Mexico: *Geological Society of America Bulletin*, v. 89, p. 19-32.

Wilson, M.D. and Pittman, E.D. 1977. Authigenic clays in sandstones: recognition and influence on reservoir properties and paleoenvironmental analysis. *Journal of Sedimentary Petrology*, v. 47, p. 3-31.

Williams, M. Y., and Dyer, W. S. 1930. *Geology of Southern Alberta and Southwestern Saskatchewan*; Geol. Surv., Canada, Mem. 163. Ziegler, W.H. 1969. The development of sedimentary basins in western and Arctic Canada. Alberta Society of Petroleum Geologists.

Worden, R.H. and Morad, S. 2003. Clay in sandstones: controls on formation, distribution and evolution. In: Clay mineral cement in sandstones: Special Publication of the International Association of Sedimentologists, Worden, R.H. and Morad, S. (eds.), v. 34, p. 3-41.

Worden, R. H. and Morad, S. 2000. Quartz cementation in oil field sandstones: a review of the key controversies. In: Quartz cementation in sandstones: Special Publication of the International Association of Sedimentologists, Worden, R.H. and Morad, S. (eds.), v. 29, p. 1-20.

## Chapter 6

### **Petrography and diagenesis of the Paleocene Coalspur sandstones in west-central Alberta: implications for the reservoir properties of fluvial facies**

#### **Introduction**

The Coalspur Formation is part of the Western Canada foredeep fill, and accumulated in fluvial-lacustrine environments during the late Maastrichtian to the early Paleocene. Deposition of this formation was tightly linked to tectonic processes in the adjacent Cordilleran belt (Catuneanu and Sweet, 1999).

This study focuses on the upper Coalspur Formation, of early Paleocene age, which outcrops in numerous localities in western Alberta (Fig. 1). An economically significant amount of high-quality thermal coal associated with floodplain facies occurs within the upper part of the formation (Jerzykiewicz and Mclean, 1980). The upper Coalspur Formation and its coal zones have been described and studied from numerous drillholes, test pits, and other outcrop sections in western Alberta (Kramers and Mellon, 1972; McLean and Jerzykiewicz, 1978; Dawson et al., 1994). To date, however, examinations of the diagenetic history of the sandstones and their reservoir characteristics have received less attention. In this paper we investigate the diagenetic history and reservoir quality of these early Paleocene sandstones of the Coalspur Formation in two main locations, the Red Deer River sections and the Coalspur locality (Fig. 1), through detailed outcrop and laboratory work.

## **Geological Background**

The Coalspur Formation (Jerzykiewicz and McLean, 1980) consists of interbedded mudstone, siltstone and fine-grained sandstone with minor coarser-grained sandstone beds and channel lags (Jerzykiewicz and McLean, 1980). This formation overlies the upper massive sand of the Brazeau Formation and is overlain by the Paskapoo Formation (Fig. 2). Both the lower and the upper contacts are represented by unconformities (Jerzykiewicz, 1992).

The Coalspur Formation consists of two informal members. The upper Coalspur member is characterized by extensive development of numerous coal zones and fine-to-medium-grained buff-colored sandstones, which lie above the coal-barren sediments of the lower Coalspur member. In the Foothills region, the upper Coalspur Formation reaches a thickness greater than 250 m, while in the Plains the correlative upper Scollard Formation thins to less than 50 m in the outcrops along the Red Deer Valley (Jerzykiewicz, 1992). The lithology of the upper Coalspur Formation changes significantly between the Coalspur locality in the northwest and the Red Deer River sections (about 35 km southwest of Sundre) (Jerzykiewicz, 1992). Coals observed in the Coalspur locality sandstones are almost missing in the Red Deer River sections (Figs. 4 and 5). These facies differences are attributed to paleoclimatic and tectonic influences (Jerzykiewicz and Sweet, 1988, Catuneanu and Sweet, 1999). The detail study of Jerzykiewicz and Sweet (1988) revealed evidence of paleoclimatic variations during the latest Cretaceous to earliest Tertiary in the Rocky Mountain Foothills region. They concluded that the climate during early Paleocene was more humid in the central part of the Foothills and

relatively drier in the southern part of the Foothills. Climatic differences were probably due to orographic topographic controls combined with atmospheric circulation.

### **Data Base and Methodology**

Fieldwork was performed in the Foothills of central Alberta (Fig. 1). Outcrop sections were studied in detail, including thickness measurements and facies analysis. Figure 3 shows the facies codes used for the description of all outcrop sections (Figs. 4, 5 and 6). The localities studied in the Foothills of central Alberta include the Red Deer River section 1 (Fig. 4), the Red Deer River section 2 (Fig. 5), and the Coalspur locality (Fig. 6). The studied outcrop sections are positioned in the upper part of the upper Coalspur Formation, above the Silkstone coals (Fig. 2). Thirty two core samples and a total of 20 sandstone beds within the studied area were described and analyzed. Thin sections prepared from fresh outcrop samples were examined with a standard petrographic microscope and the specimens were impregnated with blue epoxy resin to highlight their porosity. Two hundred points were counted for each slide. The mineralogy of authigenic cements was established by X-ray diffraction. In order to study the diagenetic processes that affected the evolution of the sandstone beds, samples with the same grain sizes were examined by using a JEOL JSM 6400 scanning electron microscope (SEM) equipped with an energy-dispersive x-ray analyzer.

The oxygen and carbon isotope data are presented in usual  $\delta$ -notation relative to Standard Mean Ocean Water (SMOW) for oxygen (Craig, 1961) and the belemnite *Belemnitella Americana* from the PeeDee Formation (PDB) for carbon (Craig, 1957). Carbon and oxygen isotopic analyses were performed by using the extraction method of McCrea

(1950). Samples were powdered and weighted prior to reaction, and the weight percent of calcite was determined manometrically. The powdered rock samples were reacted with anhydrous phosphoric acid at 25°C. 'Calcite' gas was extracted after 2 hours of reaction. An oxygen-isotope CO<sub>2</sub>-H<sub>2</sub>O fractionation factor of 1.0412 at 25°C was used to calibrate the mass spectrometer reference gas. Oxygen isotopic compositions were calculated by using a phosphoric acid-CO<sub>2</sub> fractionation factor of 1.011025 at 25°C for calcite (Wachter and Hayes, 1985). The reproducibility of repeat analyses was better than ± 0.16‰ PDP for each oxygen and carbon isotope measurement.

### **Thin Section Petrography of the Upper Coalspur Sandstones**

The upper Coalspur Formation is composed predominantly of sandstones and coal beds. The sandstone consists mainly of quartz, rock fragments, and feldspar grains, with percentages varying from one locality to another (Figs. 4, 5 6). Accessory minerals such as muscovite have also been recognized. The grains, which are subrounded to subangular, range from fine-to medium-grained and display moderate sorting. Based on Pettijohn's et al. (1987) classification, the upper Coalspur sandstones are defined as litharenites to sublitharenites (Fig. 7).

#### *Rock Fragments*

The predominant types of rock fragments in the upper Coalspur sandstones are polycrystalline quartz of metamorphic origin and chert, an argillaceous group (including shale, slate, phyllite and schist) and lithics of igneous origin. The majority of rock fragments range in size from 0.09 to 0.2 mm in diameter, with an average size of 0.1 mm,

and are subrounded. The dominant lithoclasts are sedimentary rock fragments, which make up 45% of lithoclasts, and are composed mainly of chert (Fig. 8 A), shale and carbonates. Metamorphic rock fragments are also relatively abundant, making up 35% of lithoclasts (Fig. 8 B). Fine-grained metamorphic fragments include slate/phyllite and fine-grained schist. Igneous rock fragments are recognized by their almost isotropic groundmass, feldspar microlites and phenocrysts (Fig. 8 C). Igneous lithic components are generally well rounded, semi-spherical in shape, and compose 20% of the lithic grains. Rock fragment fractions in the sandstones make up 20-50% (average of 42%) of the framework grains.

#### *Monocrystalline Quartz*

Monocrystalline quartz averages 53% (range 30-75%) of the framework grains. The original shape of the monocrystalline quartz is difficult to define with a petrographic microscope in some of the upper Coalspur sandstones because of the precipitation of overgrowths (Fig. 8 D). Generally, monocrystalline quartz grain shapes range from subangular to subrounded. Some of the detrital quartz shows well-rounded nucleus grains outlined by a thin envelope of clay and iron oxides on the surface (Fig. 8 E). The majority of monocrystalline quartz ranges in size from 0.1 to 0.2 mm in diameter, with an average size of 0.15 mm. Fractured grains are common and some contain inclusion vacuoles or embayments. Partial replacement by calcite is seen in the upper Coalspur sandstones (Fig. 8 D).



### *Feldspar*

Feldspar is averaging 8% (range 2-20%) of the framework grains. Both plagioclase feldspar and potassium feldspar are present in the upper Coalspur sandstones. Plagioclase feldspar, which exhibits a size range similar to that of quartz, is less common in the finer fraction and forms a significant part of the coarse fraction only. Much, but not all, feldspar shows multiple twinning (Fig. 9 A). Corrosion of grain edges by calcite is common. Detrital grains of plagioclase show considerable alteration, mainly sericitization (Fig. 9 B) probably due to role of surface weathering.

Potassium feldspars are also observed (usually less than 3% of framework components). Two varieties of K-feldspar are present, orthoclase and microcline. Microcline makes up only about 1% of the total feldspar components and is distinguished by spindle shape polysynthetic twinning.

### **Authigenic Minerals**

Authigenic minerals observed within the sandstones include kaolinite, dickite, pore-lining smectite, calcite, authigenic quartz, chlorite, chlorite-smectite grain-coating, and illite.

### *Calcite*

Calcite cement ranges in abundance from trace amounts to 20% in the upper Coalspur sandstones. The early calcite cements display drusy, blocky and poikilotopic attributes (Fig. 10 A) (Jacka, 1970; Folk, 1974; Burns and Matter, 1995). The presence of poikilotopic and blocky calcite cements (Fig. 10 B) suggests that precipitation occurred

in the phreatic zone (Jacka, 1970; Folk, 1974). An early stage of carbonate precipitation can be inferred when crystals of carbonate are embayed by closely packed quartz grains (Fig. 10 C). In these cases, the space between grains was thoroughly filled, and therefore the primary porosity of the sandstone was lost. Introduction of carbonate does not involve a volumetric expansion but, rather, corrosion and replacement of quartz grains (Fig. 10 A, and D). The late diagenetic calcite cement typically post-dates quartz overgrowths, as is indicated by the corroded boundaries between overgrowths and calcite cement (Fig. 10 E). Calcite can also be seen replacing and corroding fresh detrital feldspars (Fig. 10 F). The presence of early and late calcite cementation suggested that calcite cementation probably continued during diagenesis.

#### *Sources of calcite cement*

Volcanoclastic detrital fragments in sandstones could provide significant amounts of calcium (Morad and De Ros, 1994). Thus, the abundance of volcanic rock fragments in the sandstones suggests that volcanic rock fragments may be considered as one of the sources of calcite cement in this formation. Carbonate rock fragments derived from the sedimentary strata in the Rocky Mountain Front Ranges represent possible potential source of calcite cement in the upper Coalspur sandstones.

#### **Clay Minerals**

Identification of clay minerals was performed by using X-ray diffractometry and SEM. The authigenic clay minerals constitute 7 to 8% from total rock volume of the upper Coalspur sandstones. Authigenic minerals include chlorite, chlorite-smectite, smectite,

kaolinite, dickite, and illite. An authigenic origin is attributed to the clay rims that form coats around detrital sand grains and grow perpendicularly to grain surface (Wilson and Pittman, 1977). SEM and petrographic observations showed that the clay coatings are generally homogenous in thickness and that clay mineral growth is perpendicular to the grain surface (Fig. 11 A).

### *Chlorite*

Chlorite is one of diagenetic clay mineral in the sandstones of the upper Coalspur Formation. Chlorite occurs as pore linings (rims) composed of crystals oriented perpendicular to grain surfaces (Fig. 11 A) and locally evolves into complete pore fillings. In thin sections, chlorite is recognized by its homogeneous-green to brownish-green color. Under the SEM, authigenically formed chlorite commonly appears as rosettes of pseudo-hexagonal crystals or honeycombs (Fig. 11 B). The latter growth consists of plates arranged in a cellular pattern analogous to a honeycomb. The crystals are attached to the edges of the detrital sand grains and commonly curve and intersect to form the distinctive cellular pattern. XRD analysis indicates the presence of both magnesium- and iron-rich types of chlorite.

### *Source of Chlorite*

The precipitation of chlorite requires a source of Fe and Mg. Possible sources of Fe and Mg are clastic biotite, mafic rock fragments or early diagenetic Fe minerals. For the upper Coalspur sandstones, the probable source of chlorite is the late diagenetic transformation of smectite, which requires an elevated  $\text{Fe}^{+2}/(\text{OH}^+)^2$  ratio in the pore water

(Chang et al., 1986). Thus, the chlorite likely tends to occur in the sedimentary layers enriched in detrital Fe-silicates and Fe-oxides. The presence of mixed layers of chlorite-smectite coatings supports this hypothesis. The chemical composition of authigenic chlorite exhibits a definite temperature dependence (Jahren and Aagaard, 1989), indicating temperatures ranging from >100-130° C (Velde, 1975). According to the synthetic work of Nelson and Roy (1958) normal chlorite needs considerably higher temperatures to be synthesized, a process which might occur during late diagenesis.

Chlorite crystals become coarser grained with increasing burial depth (Fig. 11 B) as a result of crystal growth (Jahren and Aagaard, 1989). Detailed study of these crystals provides insight into the dynamic nature of chlorite growth during burial diagenesis. The amount of authigenic chlorite is relatively higher in coarse-grained sandstones. Spötl et al. (1994) have described the same correlation between grain size and the occurrence of chlorite in the sandstones of the Arkoma foreland basin, USA. These data suggest that chlorite formation within the upper Coalspur sandstones is controlled by initial mineralogical composition, burial depth and the grain size of framework constituents.

#### *Chlorite/Smectite (C-S)*

Chlorite-smectite clay minerals have been identified in the sandstones and are clearly authigenic, occurring in individual crystals oriented perpendicular to grain surfaces (Fig. 11 C). Chlorite/smectite occurs as a pore-lining and pore-filling clay, which is commonly associated with hypersaline and/or lacustrine environments (Fisher, 1988).

### *Source of Chlorite/Smectite*

The parent material for chlorite/smectite may have been detrital clay or partially degraded mica (Plamer, 1987; Fisher, 1988). However, there are no transitions from detrital mica to the chlorite/smectite observed, or chlorite/smectite occurring in individual laminae, which might suggest that the chlorite-smectite formed from a pre-existing detrital mica. The morphology and chemistry of chlorite/smectite in the upper Coalspur Formation, which were observed by SEM and XRD studies, suggest that chlorite/smectite formed from detrital smectite enriched in Mg and Fe by the dissolution of detrital ferromagnesian minerals during burial (Velde, 1985).

### *Smectite*

Smectite, which forms at lower temperatures in sandstones with a relatively high content of volcanoclastics, is a widely distributed clay in the upper Coalspur sandstones, occurring as coating rims (Fig. 11 D), altered detrital fragments, and pore-filling interstitial fibrous cement. Authigenic smectite in the sandstones has a highly crenulated, honeycombed crystal shape, with wavy plate or sheet-like architecture.

### *Source of Smectite*

Ca-feldspar and alteration of volcanic rock fragments and volcanic glass are possible sources of smectite formation in the upper Coalspur sandstones, as indicated by SEM photomicrographs (Fig. 11 E). A pore-water chemistry controlled by an arid climate also favors smectite development (Velde, 1985).

### *Kaolinite and Dickite*

Kaolinite and dickite are the predominant diagenetic clay minerals in the upper Coalspur sandstones (Fig. 12 A). Kaolinite abundance is highly variable, with most kaolinite occurring close to the coal zones. Kaolinite occurs as fine-grained crystals of booklet- or vermiform-shape, or as lath-shaped pseudo-hexagonal crystals (Fig. 12 A). It is abundant as pore-filling cement and replaces feldspar and micas. Kaolinite's authigenic origin is documented by using petrographic and SEM techniques (Fig. 12 A).

### *Source of Kaolinite*

Kaolinitization may be related to climate and feldspar alteration (Bjørlykke, 1998). Besides the transformation of K-feldspar, vermiform aggregates of kaolinite plates are also associated with the replacement of muscovite grains (Bjørkum and Gjelsvik, 1988).. They require the removal of silica and/or potassium so that the  $K^+/H^+$  ratio and the silica concentration remain inside the kaolinite stability field (Garrels and Christ, 1965). The release of organic acid from organic matter may decrease the  $K^+/H^+$  ratio. According to Bjørlykke (1994), important kaolinite formation during the early stage of diagenesis, consequential from the alteration of K-feldspar and muscovite, is a function of meteoric water flux through the sediment. Because of the fluvio-lacustrine nature of the upper Coalspur sandstone units, the presence of meteoric water during early diagenesis is most likely. Such meteoric water is often slightly acidic due to dissolved  $CO_2$  and organic acids produced in the soil profile (Giles and DeBoer, 1990). At low pH values, little silica would be in solution, and kaolinite is likely to be in its stable form (Grim, 1953). The abundance of kaolinite might also be related to meteoric water chemistry, which is

controlled by climate. Kaolinite is usually abundant where there is active drainage and no marked dry season (e.g., Sieffermann et al., 1968; Chamley 1968; Quatin et al., 1975).

Texturally, dickite (Fig. 12 B), which was observed in the sandstones, can be distinguished from kaolinite by its more blocky habit (Ehrenberg et al., 1993). Osborne et al. (1994) suggested that kaolinite morphologies are related to the depth of burial; precipitation of vermiform kaolinite occurs at shallow depth while at great depths, blocky kaolinite precipitates. The blocky morphology has been reported in deeply buried sandstone reservoirs (Hurst and Irwin, 1982; Osborne et al., 1994). We therefore infer that the diagenetic vermiform kaolinite (Fig. 12 A) precipitated during shallower burial at low temperatures, under conditions of low supersaturation in ionic concentration. During deeper burial (higher temperature), increased rates of feldspar dissolution resulted in higher degrees of supersaturation, and more blocky kaolinite precipitated into the open pore-space (Fig. 12 B). The kaolinite-dickite cement in the studied outcrop sections typically has a fresh appearance (Fig. 12 A) and post-dates the quartz cement. Precipitation of kaolinite continued throughout the late diagenetic history, probably from meteoric water influx during the Tertiary uplift.

### *Illite*

The upper Coalspur sandstones in the study areas have less authigenic illite.

### *Source of Illite*

The possible source of illite within the sandstones is smectite (Fig. 12 C), which tends to transform to illite with deeper burial due to a decrease in stability with higher temperatures (Bjørlykke, 1998).

### *Quartz*

Authigenic quartz is present as euhedral overgrowths (Fig. 11 B). In the sandstones, quartz cement commonly postdates pore-filling, grain-coating and pore-lining clays. Generally, siliceous cement is abundant in the upper Coalspur sandstones, with the exception of where sandstone samples are dominated by authigenic clay minerals and/or chert, probably because grain-coatings tend to inhibit silica cementation (Heald and Larese, 1974).

### *Influence of grain-coating on silica cement development*

Grain coating in quartz-rich sandstones has been recognized as an important porosity-preserving constituent during medium-to-deep burial diagenesis (Heald and Larese, 1974; Lerbekmo, 1961). The process of grain coating, via the precipitation of authigenic clay minerals, is an important diagenetic mechanism that controls the precipitation of silica cement during deep burial (Pittman and Lumsden, 1968; Heald and Larese, 1974). The higher burial temperatures, may be important factors in controlling silica precipitation. Increasing temperature with increased burial depth enhances kaolinite and/or smectite-to-illite transformation. These chemical alterations, which release Si, are considered important sources of authigenic quartz formation (Bjørlykke, 1983).



Well-developed clay coats, particularly chlorite, are commonly effective physical barriers that prevent silica from nucleating on detrital quartz grains under medium-to-deep burial conditions (Fig. 12 E). This mechanism is effective for preserving primary intergranular porosity in sublitharenites, while clay coatings are not as critical in lithic arenites with 45% or more lithic material, because of the low quartz content. When the coating is discontinuous and thin, authigenic quartz may still be able to connect with the lattice of the detrital grains.

In addition to clay minerals, grain coating by calcite may also prevent the development of silica cements. In the case of the upper Coalspur sandstones however, the isolated patches of calcite cement covering the detrital quartz grains are not abundant enough to effectively stop the precipitation of silica cements.

#### *Sources of quartz cement*

The precipitation of quartz cements is generally related to (1) a release of silica during the kaolinitization of feldspar (Bjørlykke, 1983), (2) pressure solution (Pettijohn et al., 1972), (3) dissolution of volcanic fragments or (4) release of silica during smectite illitization (Hower et al., 1976; Boles and Frank, 1979). Dissolution of volcanic fragments and pressure solution are the main source for silica release of this formation. Kaolinitization of feldspars by meteoric water may also have played a role in silica formation in this particular case study, as indicated by the abundance of authigenic kaolinite (Fig. 12 A). In contrast, the limited smectite illitization in the studied sandstones suggests that smectite illitization was unessential in the supply of silica in the upper Coalspur Formation.

## **Porosity of the Upper Coalspur Sandstones**

The present porosity of the upper Coalspur sandstones is both primary (Fig. 12 F) and secondary in origin (Fig. 10 A). Most of the secondary porosity in the sandstones is intergranular and was formed by the dissolution of pore filling and replacive cements. The timing of secondary porosity generation is uncertain. The deformation of ductile grains and relict clay coatings or rims may suggest early primary porosity reduction, possibly shortly after compaction. The dissolution of unstable detrital grains most likely was a continuous process throughout burial, which also caused a slight increase in secondary porosity. The porosity determined from thin sections ranges from 1% to 8% and averages 6%. Secondary porosity, which is generated by dissolution of unstable framework grains (especially feldspars), makes about 70% of the total porosity.

The porosity of the Coalspur sandstones measured in 32 core samples ranges from 4% to 24% and averages 17%. Core permeability ranges from 0.01 mD to 78 mD and averages 22 mD (Table 1). The reservoir quality tends to improve in the subsurface.

## **Stable Isotopes**

The oxygen isotope values ( $\delta^{18}\text{O}$ ) of the early calcite cement in the upper Coalspur Formation vary from  $-11.00$  to  $-5.17\text{‰}$  <sub>water</sub> and the carbon isotopic composition ( $\delta^{13}\text{C}$ ) of the same cement ranges from  $-0.41$  to  $-5.61\text{‰}$  <sub>PDB</sub> (Table 2). The low  $\delta^{18}\text{O}$  values suggest that the calcite cement is controlled to a large extent by the relatively light isotopic composition of meteoric water (Longstaffe, 1994). These low  $\delta^{18}\text{O}$  values most likely originated under colder climatic conditions (Longstaffe, 1994; Tang et al., 1997).

The wide range of carbon isotopic compositions (Table 2) may result from the isotopic exchange between calcite cement and pore water during subsequent stages of diagenesis. However, the  $\delta^{13}\text{C}$  values of most samples are from  $-2$  to  $-0.4\%$ , values typical of  $\text{CO}_2$  derived mainly from carbonate of abiotic origin (Ayalon and Longstaff, 1988). One sample has low  $\delta^{13}\text{C}$  value ( $-5.6\%$ ), which can be derived from various reactions involving organic matter during a deep stage of diagenesis (Irwin and Coleman, 1977).

## **Discussion**

### *The petrographic composition of sandstones*

Chemical weathering influences the detrital composition of sand size sediment from source to depositional areas. Rock fragments are most sensitive to chemical degradation. Therefore, their relative abundance is a good indicator of cumulative weathering effects (Mann and Cavaroc, 1973; Young et al., 1975; Basu, 1976, 1985; Mack and Suttner, 1977; Dutta and Suttner, 1984; Suttner and Dutta, 1986; Grantham and Velbel, 1988; Jermy and Michael, 1988; Corcoran et al., 1999). Under humid climatic conditions the percentage of rock fragments is significantly lower because of the extensive chemical weathering which results in partial and/or complete dissolution of lithic grains (Suttner and Dutta, 1986; Grantham and Velbel, 1988; Jermy and Michael, 1988; Corcoran, et al., 1999).

The climatic signature on the detrital framework of the upper Coalspur sandstones may be inferred from the modal percentages of rock fragments (Figs. 4, 5, 6). The petrographic composition of sandstones may also be controlled by topographic gradients, and provenance variability (Basu, 1985).

### *Distribution of Authigenic Minerals*

The formation of authigenic clay minerals in sandstones involves nucleation and growth from a supersaturated aqueous solution and, consequently, occurrences have thermodynamic and kinetic constraints. Kinetic constraints may stop precipitation from a supersaturated solution. The saturation state of a mineral, at a specified pressure and temperature, is determined by the chemical composition of co-existing porewater. Growth rates and the nucleation of authigenic minerals also depend on the degree of supersaturation as well as temperature (Mclean, 1965; Ridley and Thompson, 1986). In addition, the porewater composition influences the mineral-water interface properties, which are important for growth and nucleation.

### *Climatic influence on authigenic clay mineral distribution*

Climate variability may control the nature of early diagenetic cements via the influence of meteoric water (Walker et al., 1978; Suttner and Dutta, 1986; Tebbens et al., 1998). Formation of cation-rich clays such as smectite takes place in drier climate conditions when ionic concentration in the groundwater is high (Velde, 1985). In a humid and warm climate, authigenic kaolinite is abundant as a result of decreasing ionic concentration of the groundwater (Dutta, 1992). The upper Coalspur sandstones include a diversity of early authigenic minerals (Figs. 4, 5, 6), whose relative amounts vary significantly from one bed to another. These shifts in the pattern of distribution of early authigenic clays may indicate corresponding climatic fluctuations during syn-depositional or early diagenetic times.

Humid climatic conditions (Jerzykiewicz and Sweet, 1988) and pore fluid chemistry controlled the occurrence of kaolinite in the upper Coalspur sandstones; in contrast, the presence of smectite suggests less efficient chemical weathering and more arid conditions. As such, several cycles of climate shift may be inferred during the deposition of the upper Coalspur Formation. With increased burial depth, most of the vermicular kaolinite transformed to more blocky dickite while smectite converted to chlorite via chlorite/smectite phase as indicated by the presence of chlorite/smectite mixed layers (Fig. 11 C). In a number of samples smectite also transformed to illite. Cycles of climate shift may therefore be inferred from the alternation of kaolinite/dickite- and smectite/chlorite/illite-bearing layers.

#### *Diagenetic Sequence*

The upper Coalspur sandstones in the study area exhibit a complex diagenetic history that strongly influenced their porosity and permeability in terms of both loss and enhancement. The sequence of diagenetic events of the sandstones is inferred from thin-section slides and SEM studies (Fig. 13).

Compaction is occur as an early diagenetic event (Fig. 11 D), which is significant for sediments with high clay content and grains like mica. The rate of compaction of sediments decreases through time, as diagenetic cementation of sandstones stabilizes the grain framework. Early diagenesis after initial mechanical compaction includes dissolution of volcanic fragments together with early dissolution of detrital plagioclase feldspars, calcite cementation (Fig. 10 B), and formation of pore-fillings of early kaolinite and development of clay coatings, such as rims of smectite. The ground water

chemistry and the flow rate of meteoric water at this stage of shallow depths has great influence on later authigenesis by controlling the cement type

During middle-to-late diagenetic stages, rim chlorite grows perpendicular to quartz grain surfaces and appears to be intergrown with the quartz cements (Fig. 11 B). Additionally, middle-to-late diagenetic stages in the upper Coalspur Formation in the study areas consist of (1) continuing dissolution of feldspar grains (Fig. 9 B), (2) formation of chlorite/smectite pore filling (Fig. 11 C), (3) formation of illite; (4) formation of dickite pore filling (Fig. 12 B), (5) alteration of mica and other iron bearing minerals; (6) authigenic quartz precipitation (Fig. 8 D), (7) precipitation of chlorite; (8) precipitation of calcite cement, and (9) corrosion and dissolution of quartz grains and authigenic silica (Fig. 10 E).

#### *Reservoir Heterogeneity*

Reservoir heterogeneity on the scale of meters to tens of meters is related diagenetic alterations. The main diagenetic processes that had important impact on porosity and/or permeability of the upper Coalspur sandstones are compaction and formation of calcite, quartz and clay minerals cement.

Mechanical compaction plays a strong role in reducing primary porosity of the sandstones due to abundance of ductile grains, such as muscovite. The reduction of primary porosity in the sandstones began rapidly after deposition and early burial, as is indicated by the existence of deformed ductile grains (Fig. 10 D). The primary porosity of the sandstones also decreased due to the precipitation of silica cement (Fig. 8 D). Silica cement was probably derived from pressure solution at the points of contact between

quartz grains. Calcite and clay cements exerted an important control on reservoir heterogeneity owing to variations in the amount of calcite and authigenic clay minerals in the sandstones. The presence of pore-filling authigenic clays such as kaolinite consumed a large part of the original pore space, resulting in reduced porosity. Pore-filling interstitial fibrous smectite and/or chlorite (Fig. 11 C and D) also resulted in porosity and permeability reduction because of their very high surface area to volume ratio (Almon, 1979). Microscopic recovery efficiency (microporosity) in chlorite-rich sandstones tends to be higher than in mixed-layer-rich sandstones. The difference in reservoir quality between subsurface and outcrop samples is likely due to the influence of weathering on outcrops.

## **Conclusions**

1. The upper Coalspur sandstones in the Foothills region of west-central Alberta are classified as sublitharenites and lithic arenites.
2. The composition of the framework grains in the upper Coalspur sandstones is controlled mainly by paleoclimate and source area. Climate is considered to be the important factor affecting maturity because source rocks were similar and remained relatively unchanged throughout deposition of framework grains.
3. The main controls on the distribution of early authigenic minerals in the upper Coalspur sandstones are climate, pore fluid chemistry, and the detrital composition of the sediment. The distribution of late authigenetic clay minerals is controlled by burial

pressure and temperature, type of early authigenic clay minerals and the nature of pore water fluids.

4. The diagenetic sequence in the upper Coalspur sandstones was reconstructed based on the relationships observed between the framework constituents and the diverse types of authigenic minerals.

The early diagenesis of the upper Coalspur sandstones is characterized by (1) initial mechanical compaction, (2) calcite cementation, (3) early dissolution of detrital feldspars along with dissolution of volcanic fragments, and (4) formation of clay coatings, rims, pore-linings, early kaolinite and smectite pore fills. Burial diagenesis consists of (1) continuing dissolution of feldspar grains, (2) alteration of pore-filling kaolinite, and smectite, (3) formation of chlorite/smectite pore filling, (4) formation of illite, (5) formation of dickite pore-filling, (6) alteration of mica and other iron-bearing minerals, (7) authigenic quartz precipitation, (8) precipitation of chlorite, (9) precipitation of late calcite cement, and (10) corrosion and dissolution of quartz grains and authigenic silica.

5. This study demonstrates the role of burial, climate, and pore-water chemistry in controlling the diagenetic processes. During burial the pore water is in equilibrium with respect to the minerals. At a give time there is very little solids dissolved in the pore water compared to what is in the minerals.

The study also shows the value of petrographic and SEM analyses in the assessment of porosity in fluvial reservoirs. Both primary and secondary porosity have been observed in the upper Coalspur sandstones. Such a study may be used as an analogue for the



assessment of other fluvial-lacustrine reservoirs in the subsurface of the Western Canada Sedimentary Basin.

6. The porosity and permeability of the sandstones tends to be improved in the subsurface relative to the outcrop equivalents, due to the influence of weathering on outcrop samples.

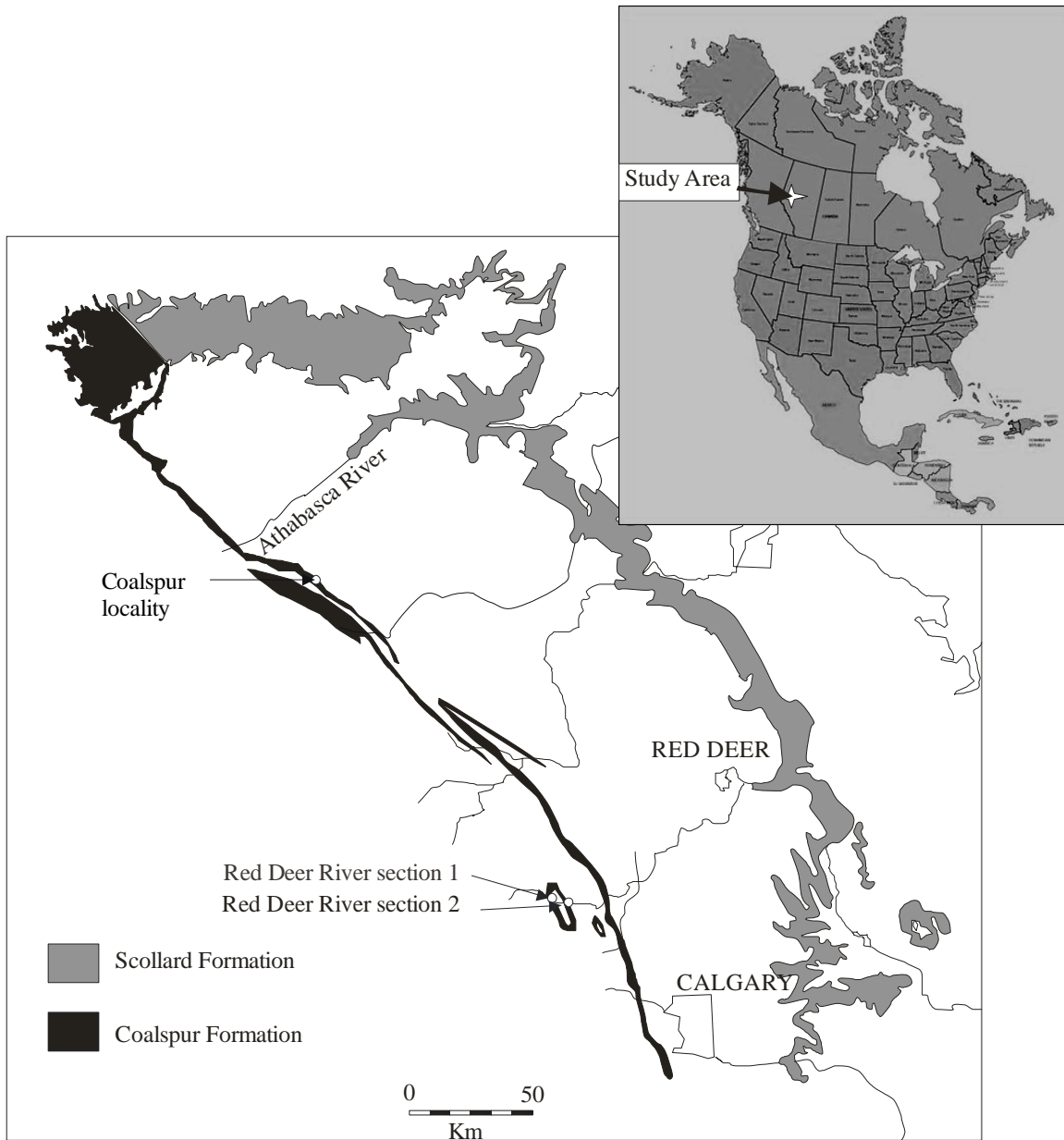


Figure 1. Outcrop distribution of the Scollard and Coalspur formations in Alberta, and the location of the studied outcrop sections.

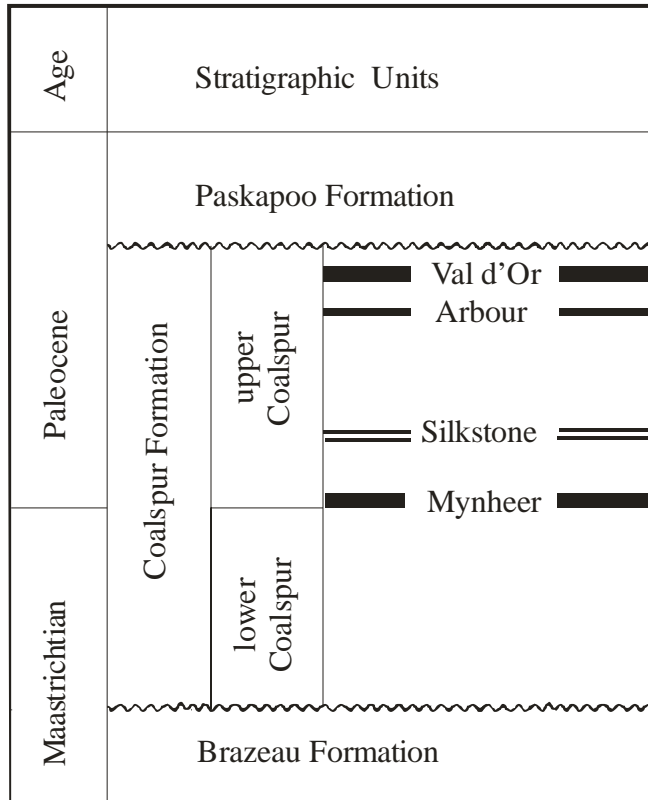


Figure 2. Generalized chart of the late Maastrichtian-Paleocene stratigraphy of west-central Alberta, showing the position of the upper Coalspur Formation and its major coal seams.

Facies	Facies code and symbol	Sedimentary structures	
Gh		Clast-supported, crudely bedded gravel	Horizontal bedding, imbrication
St		Sandstone, fine to very coarse, may be pebbly	Solitary or grouped trough cross-beds
Sp		Sandstone, fine to very coarse, may be pebbly	Solitary or grouped planar cross-beds
Sr		Sandstone, very fine to coarse	Ripple cross-lamination
Sh		Sandstone, very fine to coarse, may be pebbly	Horizontal lamination, parting or streaming lineation
Sl		Sandstone, very fine to coarse, may be pebbly	Low-angle (<15°) cross-beds
Ss		Sandstone, fine to very coarse, may be pebbly	Broad, shallow scours
Sm		Sandstone, fine to coarse	Massive or faint lamination
Sb		Sandstone, fine to very coarse, may be pebbly	Ball-and-pillow structure, may show internal lamination
Sf		Sandstone, fine to coarse with mud	Massive, may be laminated
Fl		Sandstone, siltstone, mudstone	Fine lamination, very small ripples
Fsm		Siltstone, mudstone	Massive
Fp		Mudstone with pebbles	Vague laminated mudstone with floating, isolated clasts
Fs		Mudstone with sand, fine to coarse	Massive, may be laminated
Fb		Mudstone, siltstone	Ball-and-pillow structure, may show internal lamination
Fm		Mudstone, siltstone	Massive, desiccation cracks
C		Coal, carbonaceous mudstone	Plant, mudstone films

Figure 3. Facies types used to describe the sedimentological characteristics of the studied outcrop sections (Figs. 4-6).

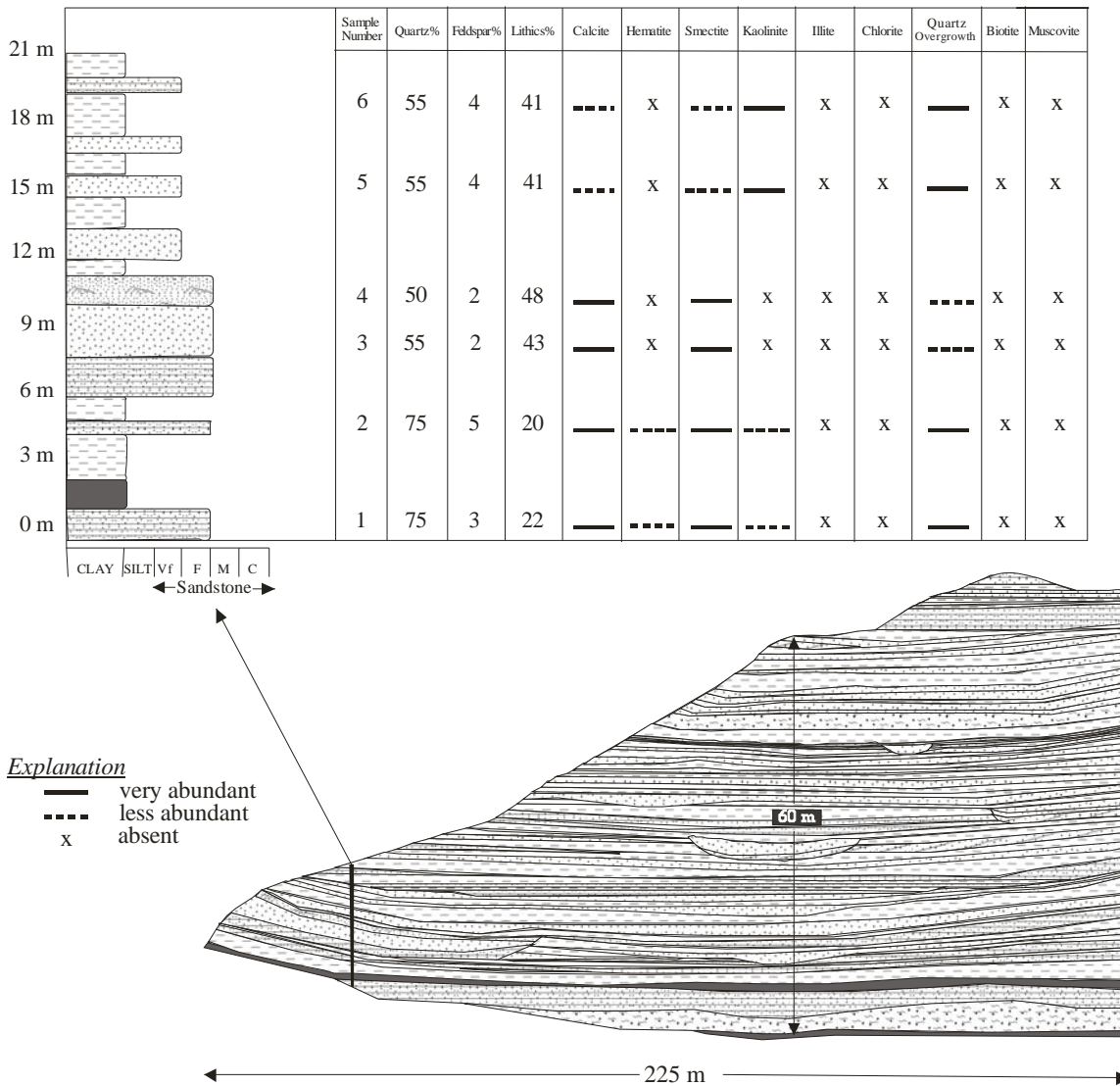


Figure 4. Outcrop sketch and vertical profile for the Red Deer River section 1. This section is located at a roadcut in the Red Deer River valley about 35 km southwest of Sundre. The table shows the sandstone composition in terms of detrital constituents and authigenic minerals. The relative percentages of the three main framework constituents (quartz, feldspars, lithoclasts), out of 100%, are used to classify the sandstones (Fig. 7). See Figure 3 for facies codes.

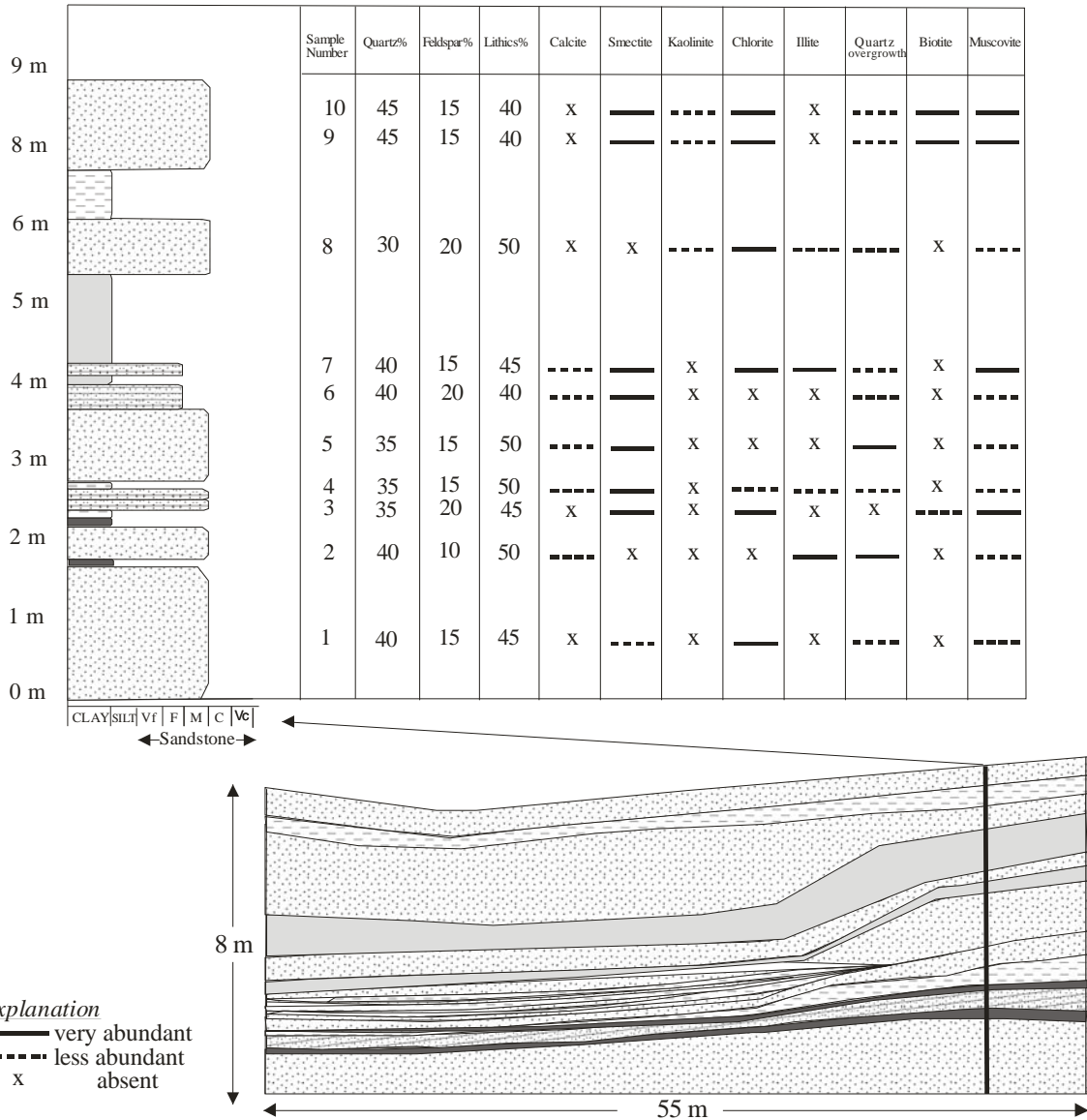


Figure 5. Outcrop sketch and vertical profile for the Red Deer River section 2. This section is located at the Red Deer River valley along the River about 35 km southwest of Sundre. Stratigraphic location of this section is below section 1 of the same locality. The table shows the sandstone composition in terms of detrital constituents and authigenic minerals. The relative percentages of the three main framework constituents (quartz, feldspars, lithoclasts), out of 100%, are used to classify the sandstones (Fig. 7). See Figure 3 for facies codes.

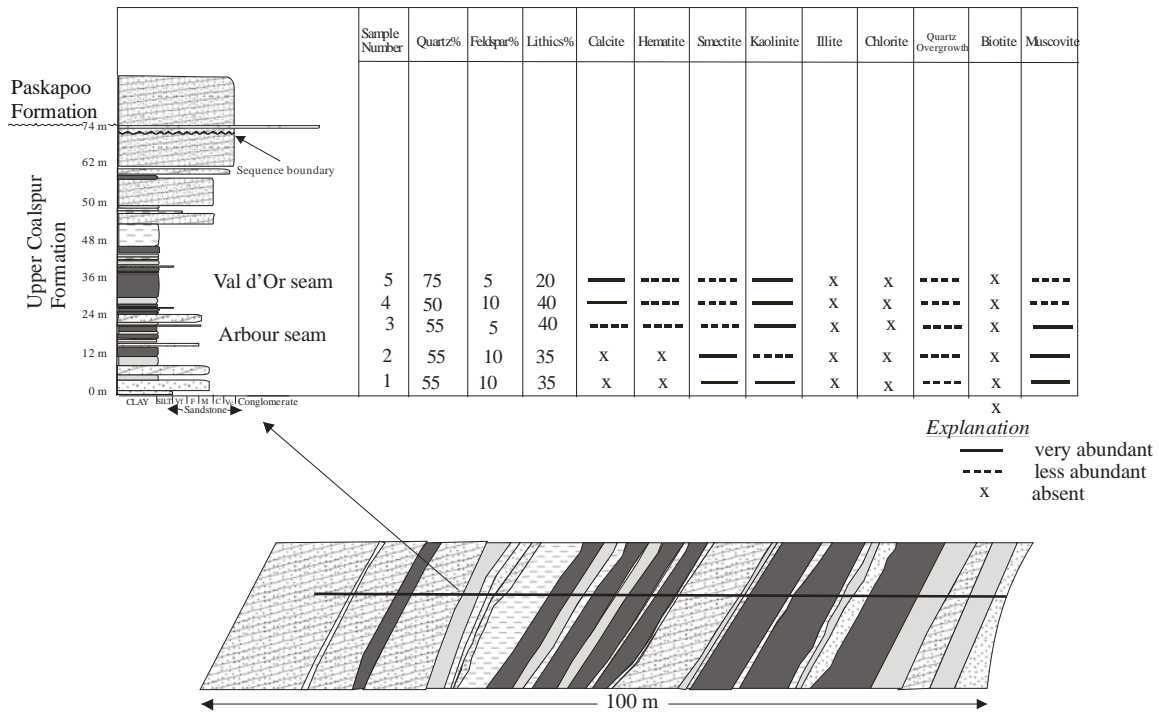


Figure 6. Outcrop sketch and vertical profile for the Coalspur locality in a roadcut along Highway No. 47. The table shows the sandstone composition in terms of detrital constituents and authigenic minerals. The relative percentages of the three main framework constituents (quartz, feldspars, lithoclasts), out of 100%, are used to classify the sandstones (Fig. 7). See Figure 3 for facies codes.

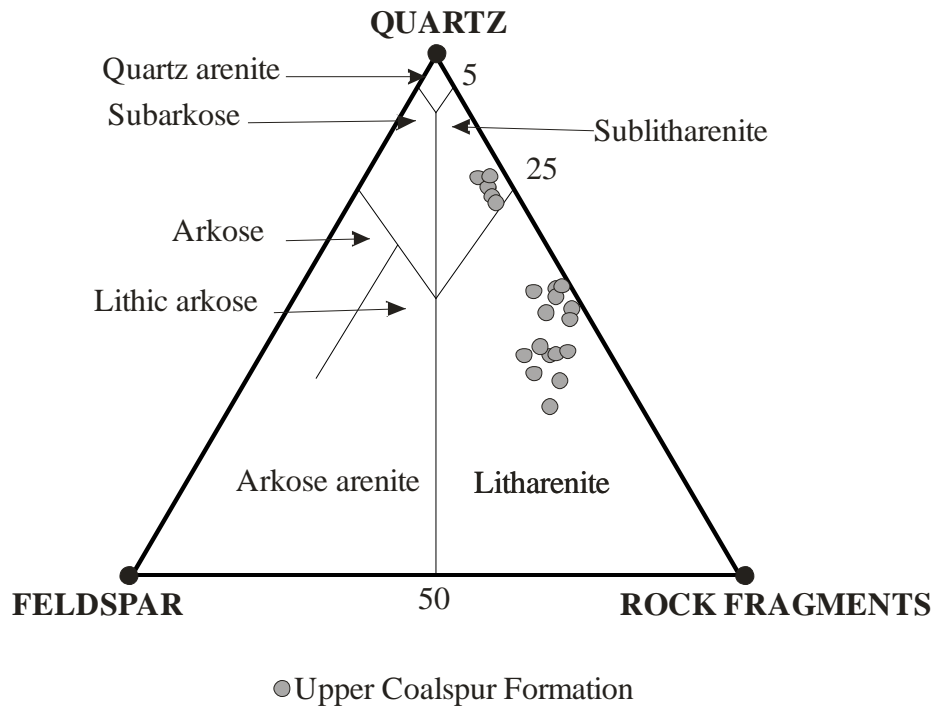


Figure 7. Classification of the upper Coalspur Formation sandstones (after Pettijohn et al., 1987).



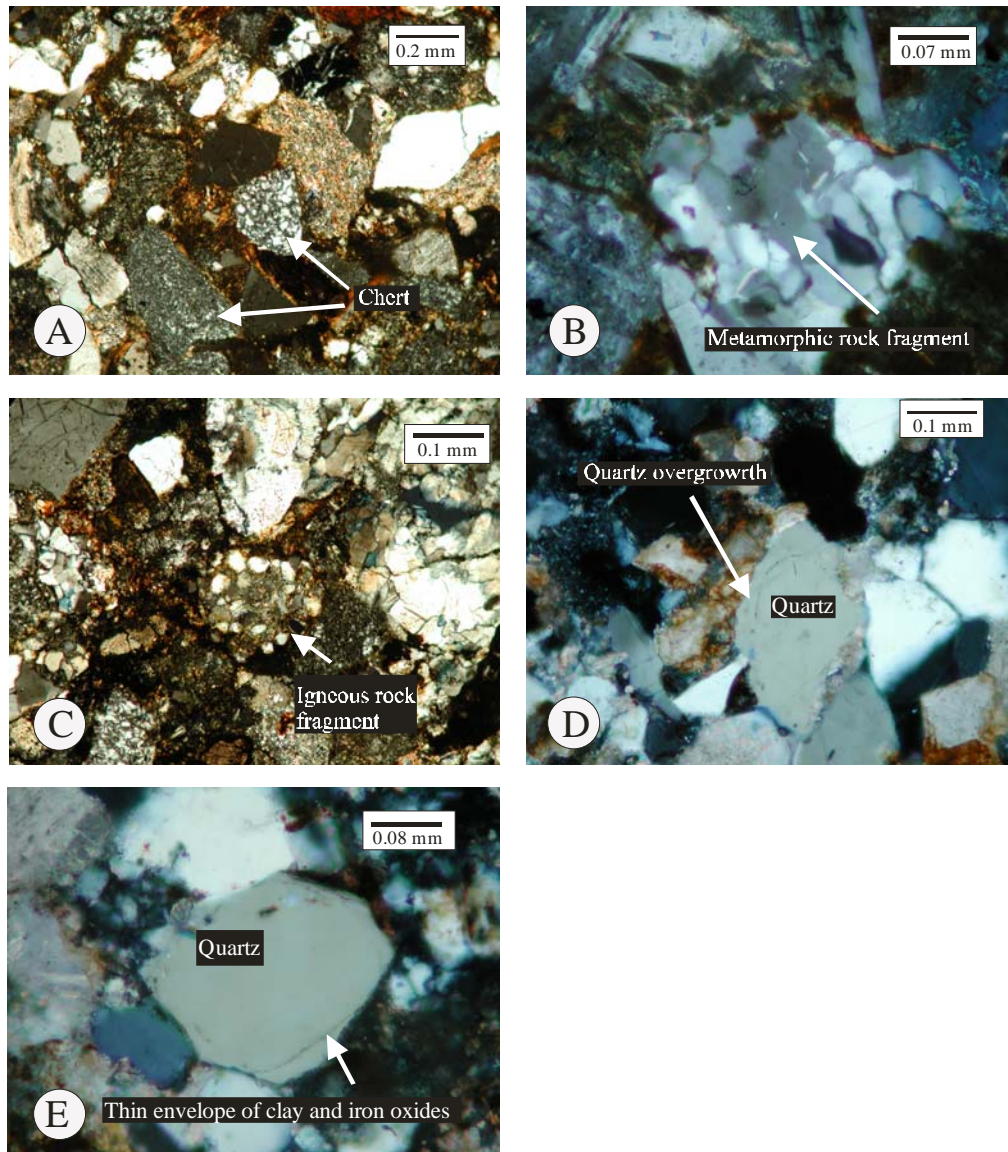


Figure 8. Thin-section photomicrographs: (A) – litharenite with chert lithoclasts. Note the uniform microcrystalline quartz with no visible relict texture, (sample -1, upper Coalspur Formation, Coalspur locality); (B) – detrital grain of polycrystalline quartz of metamorphic origin (sample 3, upper Coalspur Formation, Red Deer River section 1); (C) – detrital grains of igneous origin (sample 2, upper Coalspur Formation, Coalspur locality); (D)– quartz overgrowth (arrow) associated with quartz grains (sample 1, upper Coalspur Formation, Red Deer River section 1); (E) – thin envelope of clay and iron oxides associated with quartz overgrowth (arrow) (sample 2, upper Coalspur Formation, Red Deer River section 1).

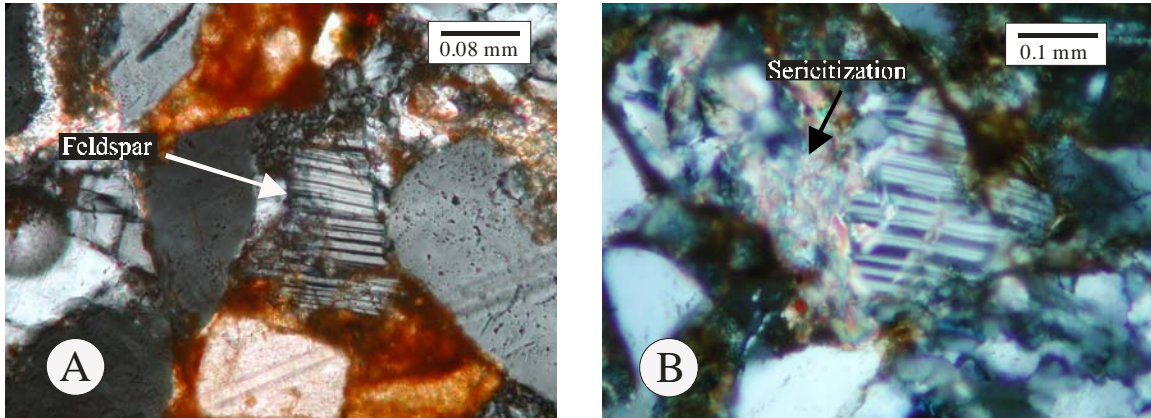


Figure 9. Thin-section photomicrographs: (A) – feldspar shows multiple twinning, (sample -2, upper Coalspur Formation, Coalspur locality); (B) – plagioclase detrital shows considerable alteration, mainly vacuolization and sericitization (sample 4, upper Coalspur Formation, Red Deer River section 2).

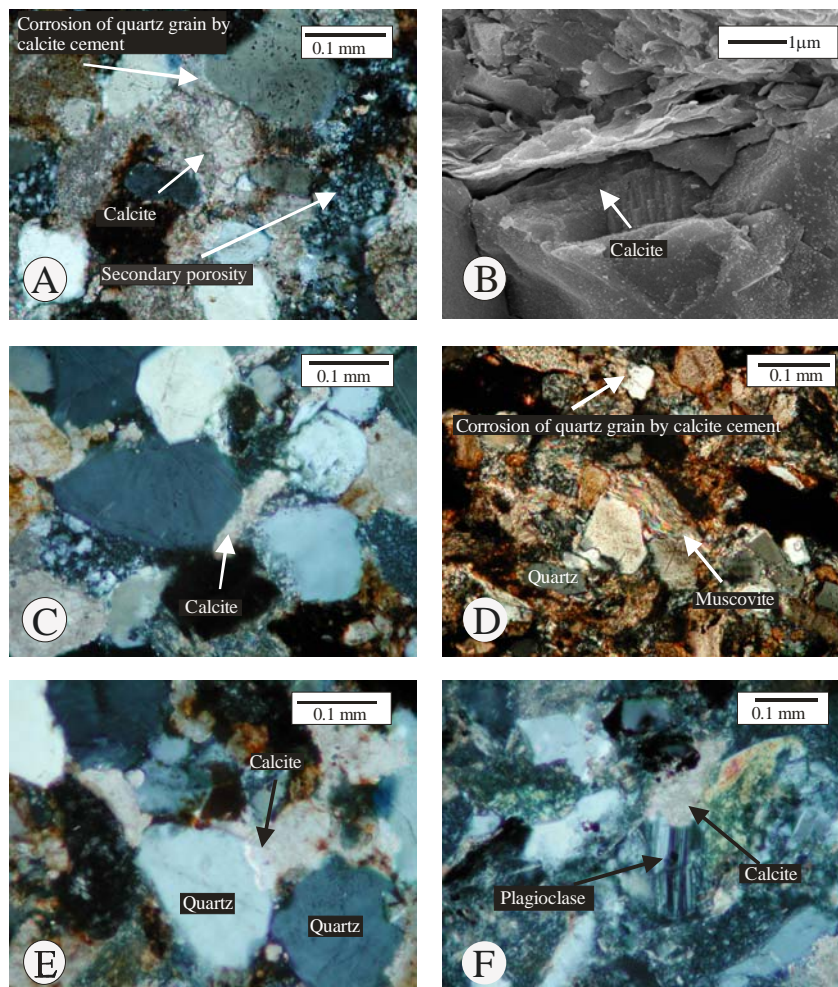


Figure 10. Thin-section photomicrographs and scanning electron photomicrograph: (A) – poikilotopic calcite (arrow) cement (sample 3, Upper Coalspur Formation, Red Deer River section 1); (B) – early blocky calcite cement (sample 5, upper Coalspur Formation, Red Deer River section 1); (C) – An early stage of carbonate precipitation can be recognized by crystals of carbonate which are embayed by closely packed quartz grains (sample 1, upper Coalspur Formation, Red Deer River section 1); (D) – Deformed muscovite grain by compaction and corroded quartz grain by early calcite cement (sample 4, upper Coalspur Formation, Coalspur locality); (E) – quartz grain corroded by early poikilotopic calcite cement (sample 3, upper Coalspur Formation, Red Deer River section 1); (F) – detrital plagioclase showing alteration, vacuolization and sericitization. Note the early calcite cement altered the detrital feldspar (sample 2, upper Coalspur Formation, Red Deer River section 2).



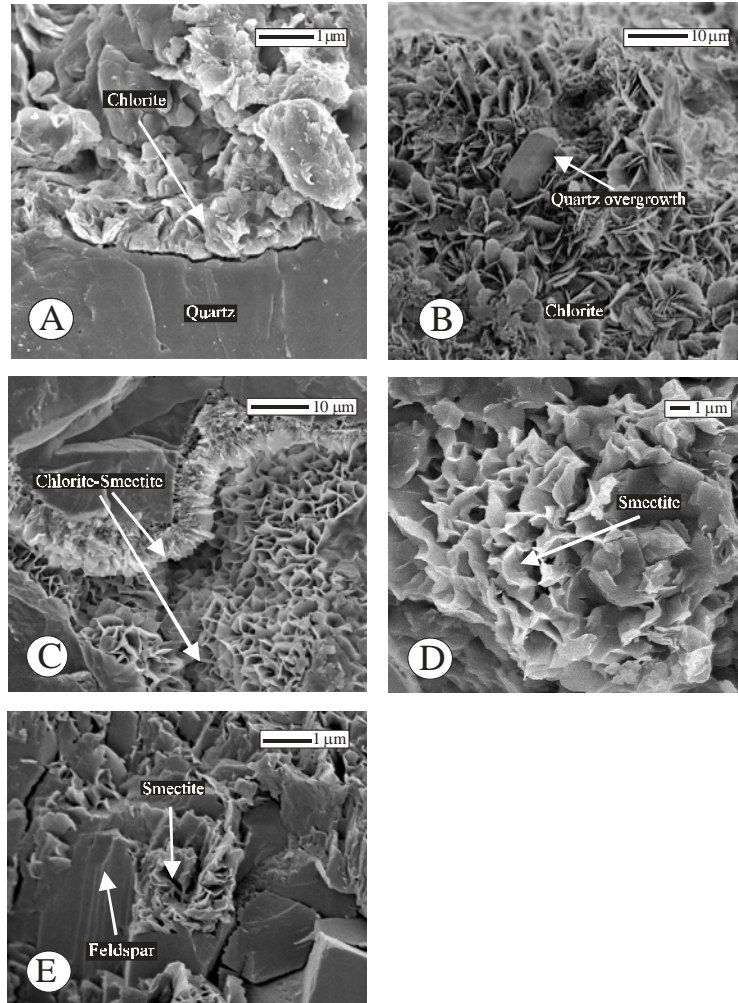


Figure 11. Scanning electronic photomicrographs: (A) – chlorite appears as pore linings (rims) composite crystals perpendicularly oriented to grain surface (arrow) of quartz grain (sample 10, upper Coalspur Formation, Red Deer River section 2); (B) – authigenically formed chlorite (arrow) appears as rosettes of pseudo-hexagonal crystals. Note quartz overgrowth restricted by chlorite cement (sample 9, upper Coalspur Formation, Red Deer River section 2); (C) – authigenically formed chlorite-smectite (arrows) appears as composite of crystals perpendicularly oriented to grain surface (sample 3, upper Coalspur Formation, Red Deer River section 2); (D) – authigenic smectite showing highly crenulated, honeycombed, and interlocking crystal shapes (sample 8, upper Coalspur Formation, Red Deer River section 2); (E) – feldspar alteration into smectite (sample 5, upper Coalspur, Coalspur locality).

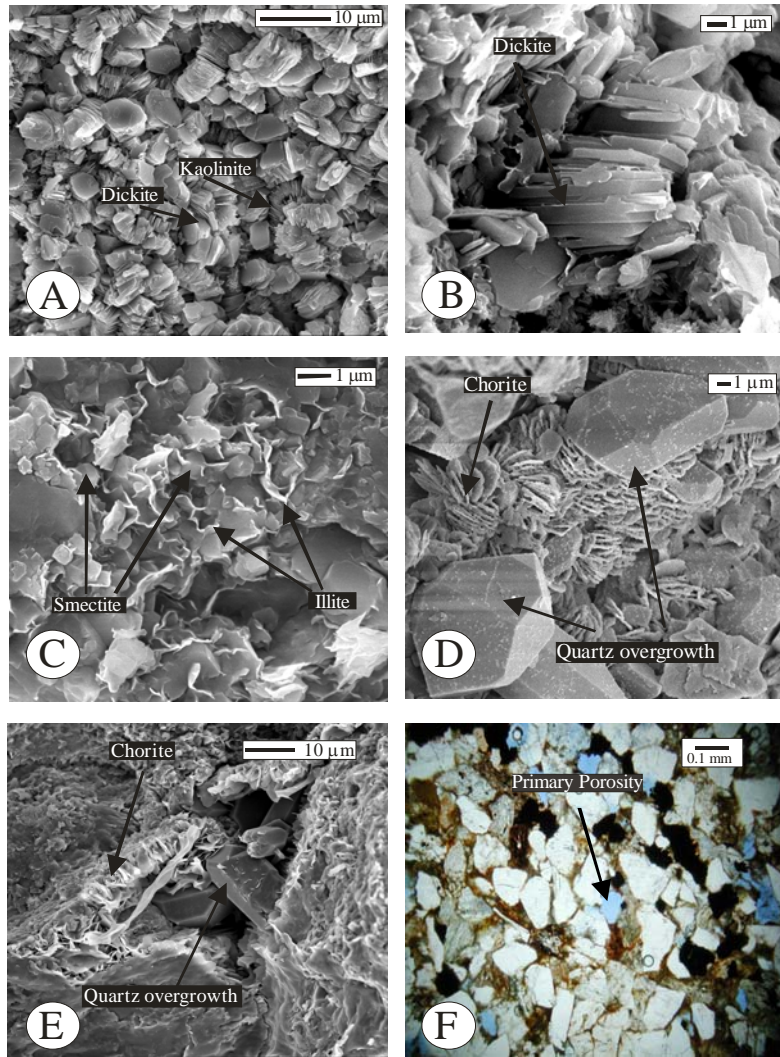


Figure 12. Scanning electronic photomicrographs and thin-section photomicrograph: (A) – vermicular aggregates of euhedral crystals of authigenic kaolinite and dickite (arrows) (sample 1, upper Coalspur Formation, Coalspur locality); (B) blocky kaolin (dickite). Note the thickness and blocky habit of the crystals (sample 3, upper Coalspur Formation, Coalspur locality); (C) alteration of smectite grain coating to illite (arrows) (sample 1, upper Coalspur Formation, Red Deer River section 2); (D) - euhedral quartz overgrowth (sample 13, upper Coalspur Formation, Red Deer River section 1); (E) – silica overgrowths postdated by pore-filling chlorite (sample 10, upper Coalspur Formation, Red Deer River section 2); (F) – preserved primary porosity in sandstone (sample 3, upper Coalspur Formation, Coalspur locality).

Diagenesis sequence	Early <span style="display: inline-block; width: 80%; border-bottom: 1px solid black;"></span> Late
Compaction	<u>Mechanical</u> <u>Chemical</u>
Calcite cementation	—————?
Dissolution of feldspar and volcanic fragments	—————
Smectite pore fill	—————?
Kaolinite pore fill	—————?
Formations of smectite-chlorite pore fill	.....? —————?
Chlorite formation	—————
Quartz overgrowth	.....? —————?
Formation of dickite	—————
Formation of illite	.....? —————
Quartz dissolution	.....? —————
Mica alteration	.....? —————?

Figure 13. Generalized diagenetic sequence of the upper Coalspur sandstones in the Foothills region of west-central Alberta.

Location	Sample Top (m)	Sample Base (m)	Sample forms	KMax (mD)	Porosity	Grain Density (kg/m3)
00/14-07-030-04W5/0	486	486.05	Coalspur Fm	22.8	0.15	2660
00/14-07-030-04W5/0	504	504.05	Coalspur Fm	0.04	0.056	2660
00/14-07-030-04W5/0	591	591.05	Coalspur Fm	0.73	0.1	2680
00/14-07-030-04W5/0	631	631.05	Coalspur Fm		0.036	2680
00/14-07-030-04W5/0	712	712.05	Coalspur Fm	0.09	0.062	2680
00/14-07-030-04W5/0	824	824.05	Coalspur Fm	0.51	0.13	2690
02/16-12-041-05W5/0	617.43	618.17	Coalspur Fm	1.96	0.173	2690
02/16-12-041-05W5/0	618.17	618.88	Coalspur Fm	0.39	0.173	2710
02/16-12-041-05W5/0	618.88	619.63	Coalspur Fm	65	0.22	2670
02/16-12-041-05W5/0	619.63	620	Coalspur Fm	26	0.241	2660
02/16-12-041-05W5/0	620	620.39	Coalspur Fm	0.01	0.043	2700
02/16-12-041-05W5/0	620.39	620.62	Coalspur Fm	0.02	0.056	2710
02/16-12-041-05W5/0	620.62	621.06	Coalspur Fm	0.5	0.131	2690
02/16-12-041-05W5/0	621.06	621.69	Coalspur Fm	83.7	0.216	2670
02/16-12-041-05W5/0	621.69	622.25	Coalspur Fm	12.8	0.247	2660
02/16-12-041-05W5/0	622.25	622.56	Coalspur Fm	0.63	0.138	2690
02/16-12-041-05W5/0	622.56	622.95	Coalspur Fm	53.5	0.219	2670
02/16-12-041-05W5/0	622.95	623.46	Coalspur Fm	28.3	0.215	2680
02/16-12-041-05W5/0	623.46	623.76	Coalspur Fm	3.84	0.188	2680
02/16-12-041-05W5/0	623.76	624.14	Coalspur Fm	5.35	0.195	2680

Table 1. Well location, sample top and sample base, permeability (mD), Porosity fraction, average grain-size measurements (mm), gain density of 32 selected core samples from Coalspur sandstones.

Sample Number	Carbon PDB	Oxygen water	SMOW Oxygen	Locality	upper Coalspur Formation
S-1	-0.839	-8.31	20.10	Red Deer River sections	
S-2	-0.417	-10.40	18.01		
S-3	-2.130	-10.95	17.46		
S-4	-1.165	-9.10	19.31		
S-5	-1.883	-11.01	17.40		
3	-1.377	-8.21	20.20	Coalspur locality	
4	-1.377	-8.21	20.20		
5	-5.616	-5.17	23.24		

Table 2. Oxygen and carbon isotopic compositions from the upper Coalspur Formation (the Red Deer River valley sections and Coalspur locality).



## References

Ayalon, A. and Longstaffe, F. 1988. Oxygen isotopes studies of diagenesis and pore-water evaluation in the Western Canada Sedimentary basin: Evidence from the Upper Cretaceous Basal Belly River sandstone, Alberta. *Journal of Sedimentary Petrology*, v.58, no.5, p. 489-505.

Basu, A. 1976. Petrology of Holocene sands derived from plutonic source rocks; implications to the paleoclimatic interpretation. *Journal of Sedimentary Petrology*, v. 46, p. 694- 709.

Basu, A. 1985. Influence of climate and relief on compositions of sands released at source areas. In: *Provenance of Arenites*. G.G.Zuffa (ed.). Reidel, Holland, p. 1-18.

Bjørlykke, K. 1983. Diagenesis reaction in sandstones. In: *Sediment Diagenesis*. A. Parker and B.W.Sellwood (eds.). Reidel, Holland, p. 169-213.

Bjørlykke, K. and Gjelsvik, N. 1988. An isochemical model for formation of authigenic kaolinite, K-feldspar, and illite in sediments. *Journal of Sedimentary Petrology*, v. 58, p. 506-511.

Bjørlykke, K. 1994. Fluid-flow processes and diagenesis in sedimentary basin. In: *Geofluid: Origin, Migration and Evolution of fluid in sedimentary basins*. J. Parnell (ed.). p. 127-140.

Bjørlykke, K. 1998. Clay mineral diagenesis in sedimentary basins - a key to the prediction of rock properties. Examples from the North Sea Basin. *Clay Minerals*, v. 33, p. 15–34.

Boles, J.R. and Franks, S.G. 1979. Clay diagenesis in Wilcox sandstones of southwest Texas: Implication of smectite diagenesis on sandstone cementation. *Journal of Sedimentary Petrology*, v. 49, p. 55-70.

Burns, S.J. and Matter, A. 1995. Geochemistry of carbonate cement in surficial alluvial conglomerates and their paleoclimatic implications, Sultanate of Oman. *Journal of Sedimentary Research*, A65 (1), p. 170-177.

Craig, H. 1961. Isotopic variations in meteoric waters. *Science*, New York, v. 133, p. 1702-3.

Craig, H. 1957. Isotopic standards for carbon and oxygen and correction factors for mass-spectrometric analysis of carbon dioxide. *Geochemistry Cosmochemistry Acta*, v. 12, p. 133-49.

Catuneanu, O. and Sweet, A.R. 1999. Maastrichtian-Paleocene foreland basin stratigraphies, Western Canada: A reciprocal sequence architecture. *Canadian Journal of Earth Sciences*, v. 36, p. 685-703.

Chamley, H. 1968. La sedimentation argileuse actuelle en Mediterranée nord-occidentale. Bulletin Societé Geologique de France, v. 10, p. 75-88.

Chang, H.K., Mackenzie, F.T. and Schoonmarker, J. 1986. Comparison between the diagenesis of decahedral and trioctahedral smectite, Brazilian offshore basins. Clays and Clay Minerals, v. 34, p. 407-423.

Corcoran, P.L., Mueller, W.U. and Padgham, W.A. 1999. Influence of tectonism and climate on lithofacies distribution and sandstone and conglomerate composition in the Archean Beaulieu Rapids Formation, Northwest Territories, Canada. Precambrian research 94, v. 3-4, p. 175-204.

Dawson, F.M., Kalkreuth, W.D. and Sweet, A.R. 1994. Stratigraphy and coal resource potential of the Upper Cretaceous to Tertiary strata of northwestern Alberta. Geological Survey of Canada Bulletin 466.

Dutta, P. 1992. Climatic influence on diagenesis of fluvial sandstones. In: Diagenesis, III. K. Wolf and G. Chillingrain (eds.). Developments in sedimentology, v. 47, 674 p.

Dutta, P.K. and Suttner, L.J. 1984. Alluvial sandstone composition and paleoclimate, II. Authigenic mineralogy. Journal of Sedimentary Petrology, v. 56, p. 346-358.

Ehrenberg, S.M., Aagaard, P., Wilson, M.J., Fraser, A. R. and Duthie, D.M.L. 1993. Depth-dependent transformation of kaolinite to dickite in sandstones of Norwegian continental shelf. *Clay Minerals*. v. 28, p. 325-352.

Fisher, R.S. 1988. Clay minerals in evaporite host rocks, Palo Duro Basin, Texas Panhandle. *Journal of Sedimentary Petrology*, v. 58, p. 836-844.

Folk, R.L. 1974. The nature history of crystalline calcium carbonate: effect of magnesium contact and salinity. *Journal of Sedimentary Petrology*, v. 44, p. 40-53.

Garrels, R.M. and Christ, C.L. 1965. *Solutions, Minerals and Equilibria*. Harper and Row, New York.

Giles, M.R. and DeBoer, R.B. 1990. Origin and significance of redistributinal secondary porosity. *Mineral Petrology Geology*, v. 7, p. 378-397.

Grantham, J.H. and Velbel, A. 1988. The influence of climate and topography on rock-fragments abundance in modern fluvial sands of the Southern Blue Ridge Mountain, North Carolina. *Journal of Sedimentary Petrology*, v. 2, p. 219-227.

Grim, R.E. 1953. *Clay mineralogy*. McGraw-Hill Series in Geology, 377 p.

Heald, M. and Larese, R. 1974. Influence of coatings on quartz cementation. *Journal of Sedimentary Petrology*, v. 44, no.4, p. 1269-1274.

Hower, J., Eslinger, W.V., Hower, M. and Perry, E.A. 1976. Mechanical of burial metamorphism of argillaceous sediments I. Mineralogical and chemical evidence. *Geological Society of America Bulletin*, v. 87, p. 725-737.

Hurst, A. and Irwin, H. 1982. Geological modeling of clay diagenesis in sandstones. *Clay Minerals*, v. 17, p. 5-22.

Irwin, H., and Coleman, M. 1977. Isotopic evidence for source of diagenetic carbonates formed during burial of organic-rich sediments. *Nature*, v.269, p. 209-213.

Jacka, A.D. 1970. Principles of cementation and porosity-occlusion in the Upper Cretaceous sandstone, Rocky Mountain Region. In: *Wyoming Geological Association Guidebook, Twenty-second Annual Field Conference*, p. 265-268.

Jahren, J.S. and Aagaard, P. 1989. Compositional variations in diagenetic chlorites and illites, and relationships with formation water chemistry. *Clay Minerals*, v. 24, p. 157-170.

Jerzykiewicz, T. 1992. Controls on the distribution of coal in the Campanian to Paleocene post-Wapiabi strata of the Rocky Mountain Foothills, Canada. Geological Society of America, Special Paper 267, p. 139-150.

Jerzykiewicz, T. and Mclean, J.R. 1980. Lithostratigraphical and sedimentological framework of coal-bearing Upper Cretaceous and Lower Tertiary strata, Coal Valley area, central Alberta Foothills. Geological Survey of Canada, Paper 79-12, 47 p.

Jerzykiewicz, T. and Sweet, A.R. 1988. Sedimentological and palynological evidence of regional climatic changes in the Campanian to Paleocene sediments of the Rocky Mountain Foothills, Canada. Journal of Sedimentary geology, v.59, p. 26-76.

Jerzykiewicz, T. 1997. Stratigraphic framework of the upper Cretaceous to Paleocene strata of the Alberta Basin. Geological Survey of Canada Bulletin 510, 121p.

Jermy, G. and Michael, A. 1988. The influence of climate and topography on rock-fragment abundance in modern fluvial sands of the Southern Blue Ridge Mountains, North Carolina. Journal of Sedimentary Petrology, v. 58. No. 2, p. 219-227.

Keith, M.L. and Weber, J.N. 1964. Carbon and oxygen isotopic composition of selected limestones and fossils. Geochimica et Cosmochimica Acta, v. 28, p. 1787-1816.

Kramers, J.W. and Mellon, G.B. 1972. Upper Cretaceous-Paleocene coal-bearing strata, northwest central Alberta Plains. In: Proceedings of the First Geological Conference on Western Canadian Coal. G.B. Mellon, J.W. Kramers and E.J. Seagel (eds.). Research Council of Alberta, Information Series 60, p. 109-124.

Longstaffe, F.J. 1994. Stable isotopic constraints on sandstone diagenesis in the Western Canada sedimentary basin. In: Quantitative diagenesis: recent developments and applications to reservoir geology. A. Parker and B.W. Sellwood (eds.). Dordrecht, Kluwer Academic Publishers, p. 223-274.

Mack, H and Jerzykiewicz, T. 1989. Detrital modes of sand and sandstone derived from andesitic rocks as a paleoclimatic indicator. *Journal of Sedimentary Geology*, v. 65, p. 35-44.

Mack, H., and Suttner, L. 1977. Paleoclimatic interpretation from petrographic composition of Holocene Sands and the Fountain Formation (Pennsylvanian) in the Colorado Front Range. *Journal of Sedimentary Petrology*, v. 47, no.1, p. 89-100.

McCrea, J.M. 1950. On the isotopic chemistry of carbonates and a paleotemperature scale. *Journal of Chemistry physics*, v. 18, p. 849-857.

Mann, W.R. and Cavaroc, V. 1973. Composition of sands released from three source areas under humid, low relief weathering in the North Carolina piedmont. *Journal of Sedimentary Petrology*, v. 43, p. 870- 881.

Mclean, J.R. and Jerzykiewicz, T. 1978. Cyclicality, tectonics and coal: some aspects of fluvial sedimentology in the Brazeau- Paskapoo Formations. Coal valley area, Alberta, Canada. In: fluvial Sedimentology, E. Miall (ed.). Canadian Society of Petroleum Geologists Memoir 5, p. 441-468.

Mclean, D.D. 1965. The science of metamorphism. Edinburgh, Oliver and Boyd, p. 103-108.

Morad, S. and De Rose, L.F. 1994. Geochemistry and diagenesis of stratabound calcite cement layers within the Rannoch Formation of the Brent Group, Murchison field, North Viking Graben (North Sea)- Comment. Journal of Sedimentary Geology, v. 93, p. 135-141.

Mullis, A.M. 1992. A numerical model for porosity modification in a sandstone-mudstone boundary by quartz pressure dissolution and diffuse mass transfer. Sedimentology, v. 39, p. 99-107.

Nelson, B.W. and Roy, R. 1958. Synthesis of the chlorites and their structure and chemical constitution, American Mineralogy, v. 43, p. 707-725.

Osborne, M., Haszeldine, R.S. and Fallick, A.E. 1994. Variation in kaolinite morphology with growth temperature in isotopically mixed pore-fluids, Brent Group, UK North Sea. Clay Minerals, v. 29, p. 591-608.



Pettijohn, F.J., Potter, P.E. and Siever, R. 1987, Sand and sandstone, 2nd Edition. Springer-Verlag, New York, 553 p.

Pettijohn, F.J., Potter P.E. and Siever, R. 1972. Sand and sandstones, Springer- Verlag, Berlin, 618 p.

Pittman, E.D. 1963. Uses of zoned plagioclase as an indicator of provenance. Journal of Sedimentary Petrology, v. 33, p. 380-386.

Pittman, E. and Lumsden, D.N. 1968. Relationship between chlorite coating on quartz grain and porosity, Spiro Sand, Oklahoma. Journal Sedimentary Petrology, v. 38, p. 668-670.

Plamer, D.P. 1987. A saponite and chlorite-rich clay assemblage in Permian evaporite and red bed strata, Palo Duro Basin. Texas Panhandle, University of Texas Bureau of Economic Geology Circular 87-3, 21p.

Quatin, P., Badaut-Trauth, D. and Weber, F. 1975. Mise en evidence de mineraux secondaires, argiles et hydroxides, dans les andolosoles des Nouvelles-Hebrides, après la deferrification par la method de Endrey. Bulletin du Groupe d' Argiles de France, v. 27, p. 51-67.

Ridley, J. and Thompson, A.B. 1986. The role of mineral kinetics in the development of metamorphic microtextures. In: *Metamorphic reaction: Kinetics Texture and Deformation*. A.B. Thompson and D. C. Rubie (eds.). *Advances in Physical Chemistry*, v. 4, p. 154-193.

Sieffermann, G., Jehl, G. and Millot, G. 1968. Allophanes et minéraux argileux des alterations récentes des basaltes du Mount Cameroun. *Bulletin du Groupe d' Argiles de France*, v. 20, p. 109-129.

Spötl, C., Houseknecht, D.W. and Longstaffe, F. I. 1994. Authigenic chlorite in sandstones as indicators of high-temperature diagenesis, Arkoma Foreland Basin, USA. *Journal Sedimentary Research*, A64, v. 3, p. 553-566.

Suttner, L.J. and Dutta, K. 1986. Alluvial sandstone composition and paleoclimate. II. Authigenic Mineralogy. *Journal of Sedimentary Petrology*, v. 56, no.3, p. 346- 358.

Tang, Z., Parnell, J. and Longstaffe, F.J. 1997. Diagenesis and reservoir potential of Permian-Triassic fluvial/lacustrine sandstones in the southern Junggar Basin, northwestern China. *American Association of Petroleum Geologists Bulletin*, v. 81, no.11, p. 1843-1865.

Tebbens, L.A., Veldkamp, A. and Kroonenberg, S.B. 1998. The impact of climate change on the bulk and clay geochemistry of fluvial residual channel infillings: the Late

Weichselian and Early Holocene river Meuse sediments (The Netherlands). *Journal of Quaternary SCI* 13, v. 4, p. 345-356.

Velde, B., Raoult, J.F. and Leikine, M. 1975. Metamorphosed berthierine pellets in mid-Cretaceous rocks from northeast Algeria. *Journal of Sedimentary Petrology*, v. 39, p. 1249-1516.

Velde, B. 1985. Clay minerals, a physico-chemical explanation of their occurrence. *Developments in Sedimentology*, v. 4, Elsevier, New York, 427 p.

Wachter, E.A. and Hayes, J.M. 1985. Exchanges of oxygen isotopes in carbon dioxide-phosphoric acid systems. *Chemical Geology*, v. 52, p. 356-74.

Walker, T.R., Waugh, B. and Crone, A. 1978. Diagenesis in first cycle desert alluvium of Cenozoic age, southern U. S. and northwest Mexico. *Geological Society of America Bulletin*, v. 89, p. 19-32.

Wilson, M.D. and Pittman, E.D. 1977. Authigenic clays in sandstones: recognition and influence on reservoir properties and paleoenvironmental analysis. *Journal of Sedimentary Petrology*, v. 47, p. 3-31.

Young, S., Basu, A., Suttner, J., Mack, G. and Darnell, N. 1975. Use of size composition trends in Holocene soil and fluvial sand derived from paleoclimate interpretation.

Proceedings the IX International Sedimentary Congress, Nice, France, Theme 1, p. 201-209.

## Chapter 7

### **Concluding Remarks**

This dissertation presents six studies that examine the diagenesis, porosity and permeability, burial history, isotope geochemistry, and sedimentology of the Upper Cretaceous-Lower Tertiary fluvio-lacustrine sandstones of the Scollard, Coalspur, and Willow Creek formations, via detailed outcrops and laboratory work. As well, the intention of this thesis is to combine the study of sandstone diagenesis, reservoir characterization with the methods of sequence stratigraphy.

Chapter 2 presents a study of reservoir characterization of Scollard-age fluvial sandstones, Alberta foredeep. The sandstones are predominantly litharenites and sublitharenites. The porosity of the sandstones is both depositional and diagenetic in origin. Laboratory analyses indicate that porosity in sandstones with less than 5% calcite cement averages 15%, with a mean permeability of 79 mD. In contrast, sandstones with greater than 5% calcite cement average 8% porosity, with a mean permeability of 1.3 mD. Cementation coupled with compaction had an important effect in the destruction of porosity after sedimentation. The sandstone properties are also severely reduced where the pore-lining clays are abundant (>15%). The potential of a sandstone to serve as a reservoir for producible hydrocarbons is strongly related to the sandstone's diagenetic history. Three diagenetic stages are identified: eodiagenesis before effective burial, mesodiagenesis during burial, and telodiagenesis during exposure after burial. Eodiagenesis resulted in mechanical compaction, calcite cementation, kaolinite and smectite formation, and dissolution of chemically unstable grains. Mesodiagenesis

resulted in chemical compaction, precipitation of calcite cement, quartz overgrowths, chlorite, dickite, and illite formation. Finally, telodiagenesis seems to have had less effect on reservoir properties, even though it resulted in the precipitation of some kaolinite and the partial dissolution of feldspar. This study shows the importance and limitations of outcrops as a source of data for understanding the characterization of subsurface sandstone reservoirs.

Chapter 3 presents basin scale distribution of clay minerals in late Maastrichtian-Early Paleocene fluvial strata of Alberta foredeep and their implication for burial depth. The distribution of authigenic clay minerals, as well as the degree and history of diagenetic alteration within the late Maastrichtian-early Paleocene sandstones vary with the geographic location across the Alberta foredeep. The Scollard sandstones were buried to a depth of less than 1.5 km, corresponding to a burial temperature of no more than 70° C. This conclusion is supported by the limited conversion of smectite to illite; the absence of authigenic dickite; and the weak albitization of K-feldspar coupled with limited precipitation of silica cements. The abundance of blocky dickite, illite and chlorite suggest that the Willow Creek and Coalspur sandstones were buried deeper than 3 km. The morphological characteristics of dickite, chlorite, and illite crystals suggest a maximum burial depth of approximately 3 – 4 km, corresponding to 90 – 120° C. This conclusion is also supported by the albitization of K-feldspar and by the development quartz overgrowths within the sandstones. The diversity in the distribution of the authigenic clay minerals in the region is follows basin-scale trends that reflect the burial depth history of these strata.

Chapter 4 presents the predictive diagenetic clay-mineral distribution in siliciclastic rocks within a nonmarine sequence stratigraphic framework. The study of upper Cretaceous - lower Tertiary fluvial deposits of the Coalspur Formation in the Foothills region of west-central Alberta reveals that the distribution of early authigenic kaolinite is not only dependent on paleoclimatic conditions, but also has a well-defined relation to the sequence stratigraphic framework. In this context, it has been observed that kaolin mineral content increases in sandstones lying in the vicinity of subaerial unconformities, which mark the most significant stratigraphic hiatuses and hence the sequence boundaries in fully fluvial successions. This study therefore suggests that the change in clay mineral assemblages and the clay's chemistry in the stratigraphic section is strongly dependant on the position of the analyzed sandstone samples relative to the sequence boundaries. In a larger context, this method of delineating depositional sequences in nonmarine successions based on authigenic clays needs to be adapted on a case-by-case basis, as the diagnostic early diagenetic minerals underlying the sequence boundary may change as a function of paleoclimate and also as a function of late diagenetic processes. The observed pattern of distribution of early authigenic clay minerals within a fluvial succession may be used to infer the position of sequence boundaries.

Chapter 5 presents the sedimentology and diagenesis of the Willow Creek Formation of the southwestern region of Alberta. This dissertation indicates that the sandstones are fine to medium-grained, are moderate to well-sorted litharenite, and have undergone a complicated diagenetic history. The diagenetic regimes of the sandstones combine several processes related to three stages of diagenesis: eodiagenesis after deposition, mesodiagenesis during burial, and telodiagenesis after uplift. The diagenetic processes recognized during eogenesis include compaction, cementation (calcite, clay minerals), and the dissolution of feldspar grains. The extensive occurrences of early calcite cement suggest that the calcite was a main control on the porosity. Intense calcite cementation, which precipitated from porewater with a significant meteoric component as the  $\delta^{18}\text{O}$  data indicate, however, inhibited the later mechanical compaction of the sandstones, thus preserving an unfilled part of the primary porosity. The most important mesogenesis processes that controlled reservoir quality were the illitization and chloritization of smectite followed by dickite formation. The pore-filling illite and chlorite resulted in a considerable loss of porosity, whereas the pore-lining chlorite may have helped in retaining the porosity by preventing the precipitation of quartz overgrowths. During telogenesis dissolution of calcite cement created secondary porosity, whereas the precipitation of kaolinite caused a reduction in porosity. This study may perhaps help enhance the understanding of the role of diagenetic controls on the sandstone quality of the fluvial reservoir, and may also provide an analogue for the same type of fluvial sandstone in the subsurface.

Chapter 6 investigates the diagenetic history and reservoir quality of these early Paleocene sandstones of the Coalspur Formation in two main locations, the Red Deer



River sections and the Coalspur locality, through detailed outcrop and laboratory work. This study demonstrates the role of burial, climate, and pore-water chemistry in controlling the diagenetic processes. The study also shows the value of petrographic and SEM analyses in the assessment of porosity in fluvial reservoirs. Both primary and secondary porosity have been observed in the upper Coalspur sandstones. Such a study may be used as an analogue for the assessment of other fluvial-lacustrine reservoirs in the subsurface of the Western Canada Sedimentary Basin. The porosity and permeability of the sandstones tends to be improved in the subsurface relative to the outcrop equivalents, due to the influence of weathering on outcrop samples.

In occlusion, this study demonstrates the value of the study of authigenic minerals and their distributions in assessment of burial depth, sequence boundary, diagenesis history, reservoir qualities and paleoclimate in fluvial reservoir.

There are a few limitations in these studies such as the use of outcrop samples for reservoir assessment. Outcrop samples could show clear recent pore destruction. Upon exposure, the pore system of the sedimentary rocks could be destroyed by sediment infill, by weathering product such as iron oxide and clays, and by surface to near surface cementation. Because of this limitation, samples from subsurface core, which have not been affected by surface weathering, were used for comparison.

The method of relating the distribution pattern of authigenic minerals to the burial history of the basin does present another significant limitation. No precise geothermal gradient data during the time of deposition can be used for accurate burial depth construction. One way to overcome this limitation and to confirm the accuracy of our results is to compare our finding with results from other methods. Our study suggests about 1 to 3 km of

sediments have been removed from the Western Canada sedimentary basin during Tertiary uplift. This conclusion has been based on the pattern of authigenic minerals distribution in our study area. Other studies demonstrate the same conclusion by using different methods. For example, the study of coal quality and its relation to reconstructed overburden and burial depth of Cretaceous and Tertiary Plains Coal of Alberta by Nurkowski (1984) indicated erosion had removed between 900 and 1.900 m of sediment, with greatest amount of removal occurring in west-southwest direction. This finding closely matches our finding.

Construction of the burial depth and identification of the sequence boundary using the distribution of authigenic minerals is the key finding of this research. Using subsurface data from different Formation to confirm these same results will be the subject of future research.

## Appendix A

<u>Locality</u>	<u>Latitude / Longitude</u>
4- the Knudsen's Farm locality	51.914°N / 112.967° W
5- the Buffalo Jump Provincial Park locality	51.945667°N / 112.9635° W
6- the Ardley locality	52.914997°N / 112.967° W
7- the Griffith's Farm locality	51.914°N / 112.967° W
8- the Kneehills Creek locality	51.584°N / 112.826° W
9- the Hummer Hills locality	51.127°N / 113.408° W
10- the Bow River locality	50.879°N / 113.232° W
11- the Sundre locality	51.747°N / 114.803° W
12- the Red Deer River Valley section1	51.732°N / 114.809° W
13- the Red Deer River Valley section 2	51.728°N / 114.813° W

14- the Coalspur locality	53.187°N / 117.018° W
15- the old roadcut near Highway 22	50.873°N / 114.302° W
16- the Oldman River	49.593°N / 114.178° W
17- the Oldman River Dam Reservoir	49.603°N / 114.087° W
18- the Oldman River locality	49.583°N / 113.983° W

Appendix B

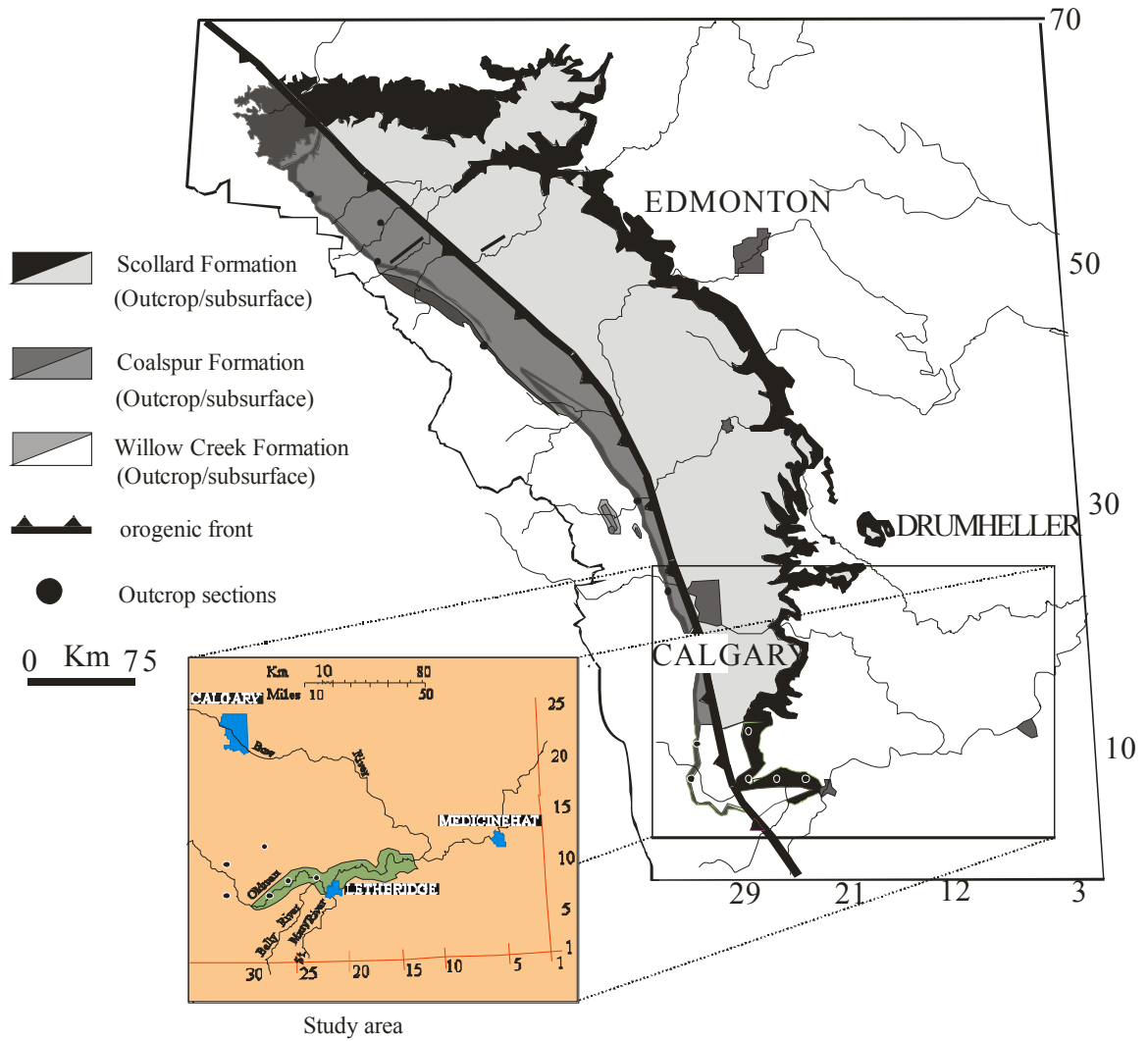
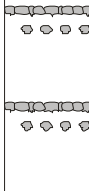
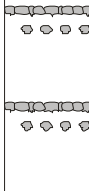
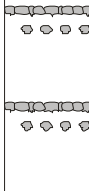


Figure 1. Outcrop distribution of the Willow Creek Formation in Alberta, and the location of the studied outcrop sections.

Southern Foothills					
Age	Formation				
Paleocene	Porcupine Hills Formation				
	Willow Creek Formation				
Maastrichtian	<table border="1"> <tr> <td>upper Willow Creek</td> <td></td> </tr> <tr> <td>lower Willow Creek</td> <td>  </td> </tr> </table>	upper Willow Creek		lower Willow Creek	
	upper Willow Creek				
lower Willow Creek					
	ST. Mary River Formation				
	Bearpaw Formation				
Campanian	Belly River Group				

 Caliche facies

Figure 2. Generalized chart of the late Maastrichtian-Paleocene stratigraphy of the south Foothills region Alberta, showing the position of the Willow Creek Formation and its major caliche horizons.

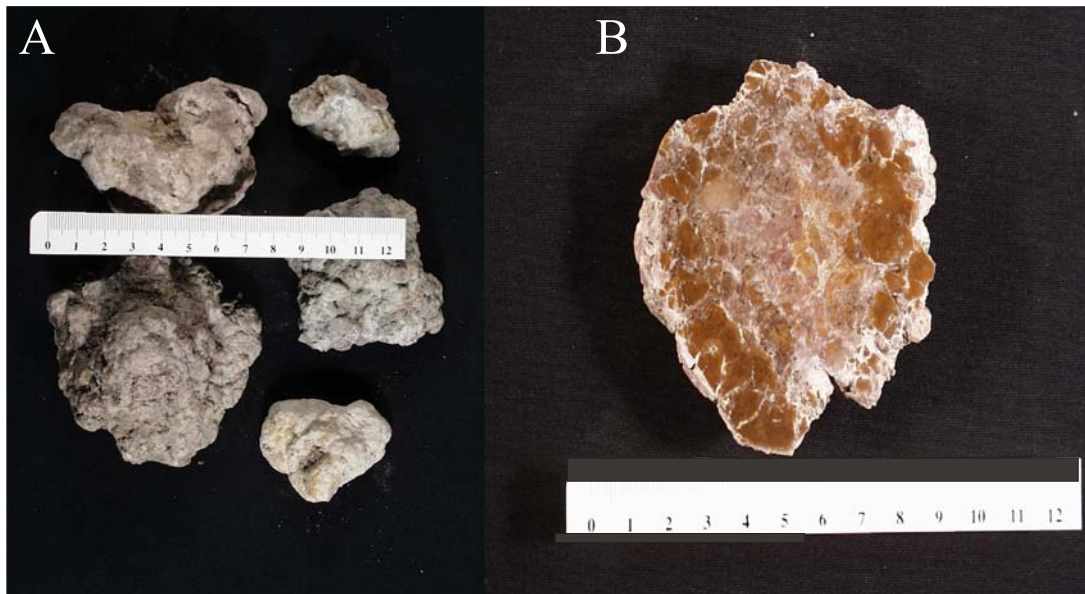


Figure 3. Caliche glaebules from the lower Willow Creek Formation. A. External surface of calcrete nodules. B. Internal structure of nodule. Note sparitic veins are cutting across the nodules randomly.

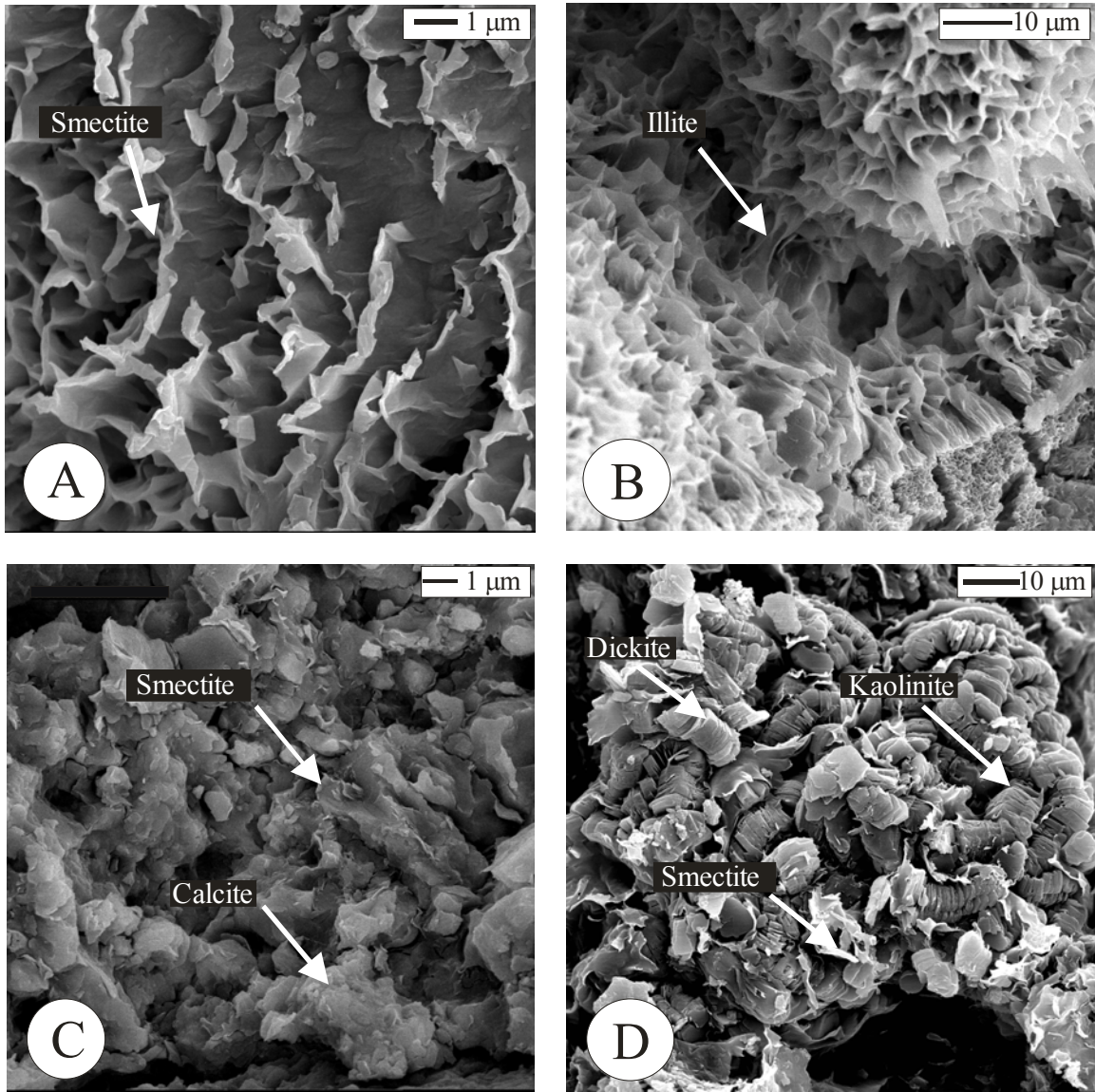


Figure 4. Scanning electron photomicrographs of authigenic clay minerals associated with calcrete facies: (A) and (C) – authigenic smectite (sample L3, lower Willow Creek Formation, along Oldman River); (B) – authigenic illite (sample 9, lower Willow Creek Formation, along Crowsenest River); (D) – authigenic kaolinite, dickite and smectite (sample 25 A, lower Willow Creek Formation, along Crowsenest River).



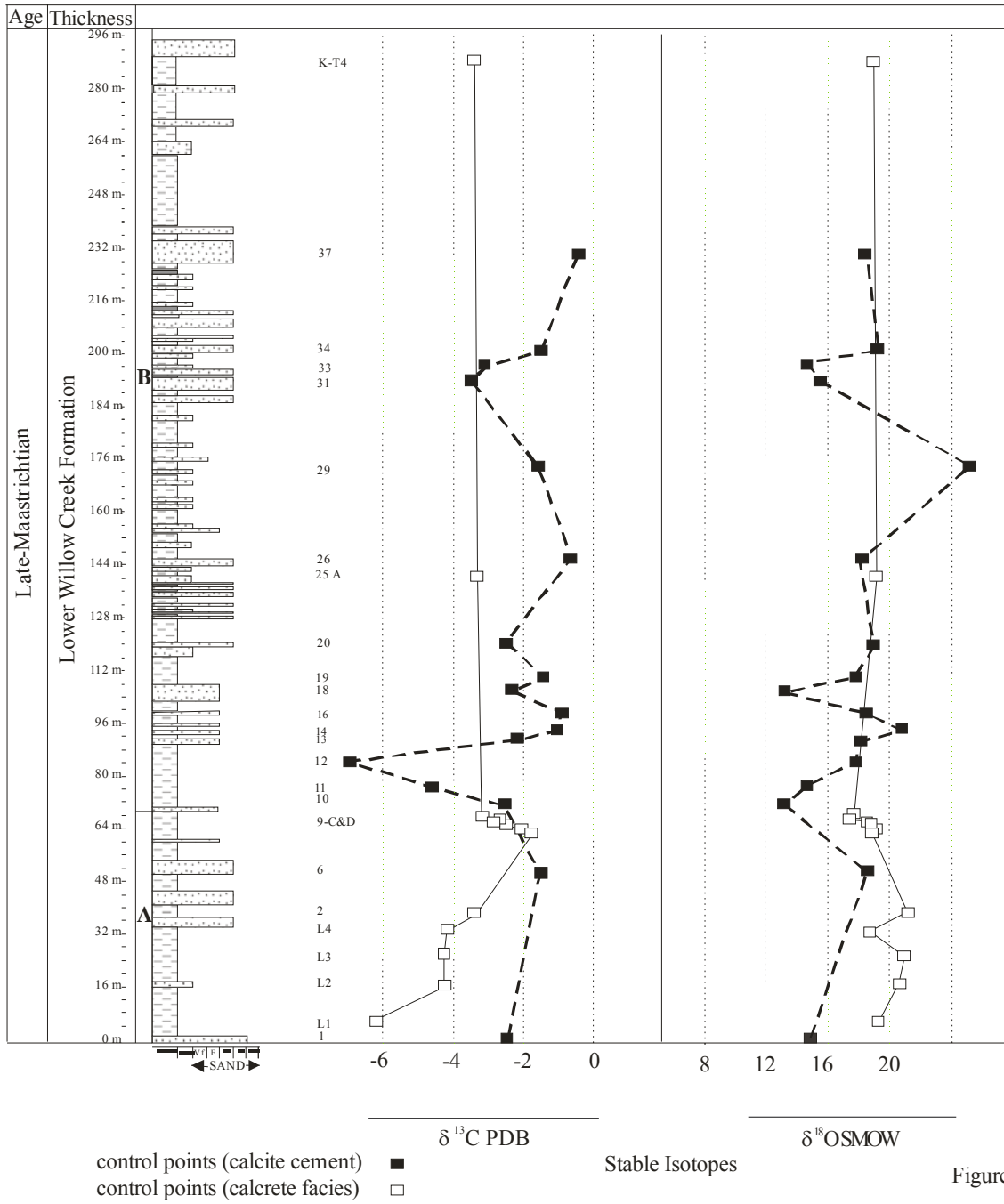


Figure 5. Stratigraphic profile of the lower Willow Creek Formation showing the position of the calcrete and calcite samples.